A Study Of The P2X7 Purinoceptor And Vascular ATP Metabolic Pathways In Chronic Kidney Disease-Associated Arterial Calcification

Richard Stephen Fish

2014

A thesis submitted to University College London in fulfilment of the requirement for the degree of Doctor of Philosophy

This work is kindly supported by a clinical research training fellowship awarded by Kidney Research UK

DECLARATION

I, Richard Stephen Fish, confirm that the work presented in this thesis is my own. Where information has been derived from other sources, I confirm that this has been indicated in the thesis.

Date: **November 2014**

Richard Stephen Fish

ABSTRACT

The risk of cardiovascular-related death is several-fold higher in patients with chronic kidney disease (CKD) compared with the general population. Arterial calcification (AC) is extremely common in patients with CKD and strongly associates with cardiovascular-related mortality, however, there are currently no specific treatments to prevent its development and/or progression. Abundant evidence now suggests that AC is cell-mediated and actively-regulated, involving mechanisms linked to bone homeostasis, production of calcification inhibitors and vascular smooth muscle cell (VSMC) function.

The P2X7 receptor (P2X7R) is an ATP-sensitive cation channel which has been implicated in several biological processes, in non-vascular contexts, thought to be important in the aetiology of AC. In addition, disruption to the normal function of some enzymes involved in ATP metabolism has been shown to contribute to AC, although little is known about their role in CKD-related arterial calcium deposition.

The work in this thesis tested the primary hypothesis that P2X7R contributes to the pathogenesis of CKD-associated AC. Preliminary work was also conducted to examine the expression of components of the ATP-metabolising system in this clinical setting.

P2X7R expression was confirmed in human and rodent vascular smooth muscle but was un-affected by calcification. *In vitro*, the P2X7R-specific antagonist, A438079, did not influence calcium deposition occurring in the presence of human VSMCs or segments of rat aorta exposed to 'calcification-promoting' medium. Calcification of cultured rat aorta was also not influenced by a second P2X7R-specific antagonist, A839977, or by BzATP (a receptor agonist). Aortic rings from mice deficient in P2X7R calcified to a similar extent to wild-type controls *in vitro*.

A novel, adenine-based mouse model was developed to evaluate the effect of P2X7R gene deficiency on CKD-associated AC *in vivo*. However, the number of mice exhibiting AC in the final experiment was too low to draw any firm conclusion. Therefore, rats were fed an adenine-containing, high phosphate diet for 4 weeks (to

induce CKD and AC) and administered a selective P2X7R antagonist, twice daily, throughout this period. Pharmacological blockade of P2X7R did not influence the magnitude of aortic calcification in this model.

Quantification of mRNA performed on tissue obtained from the *in vivo* rat experiment suggested that VSMC-specific markers are down-regulated in calcified arteries, although VSMC osteogenic transformation, which is widely reported in the literature to occur in the context of AC, was not detected. Expression of the apoptosis marker, caspase-3, was increased in calcified arteries *in vivo*. P2X7R blockade did not influence any of these changes in mRNA expression.

Expression of mRNA for ENPP-1, an ATP-metabolising enzyme responsible for the generation of the calcification inhibitor, pyrophosphate (PPi), was significantly increased in calcified arteries from CKD rats. Functional activity of ENPP-1 was also increased in these vessels. The expression of mRNA for other components of the ATP-metabolising system was also in keeping with an attempt by VSMCs to generate more PPi, possibly as an adaptive, defensive response to uraemic, calcification-promoting factors. Furthermore, an increase in ENPP-1 mRNA expression was detected in calcified inferior epigastric arteries from patients with end-stage renal disease (extracted at the time of kidney transplantation).

In summary, P2X7R does not appear to contribute to the pathogenesis of CKD-associated AC, although this should be confirmed in experimental models which more closely simulate human disease. Arterial expression of enzymes involved in the metabolism of ATP does seem to change in AC. Future work should therefore focus on gauging the clinical relevance of this in order to better understand the mechanisms underlying the disease and potentially develop new therapeutic interventions.

ACKNOWLEDGEMENTS

I am grateful to Kidney Research UK for awarding my Clinical Research Training Fellowship which made this work possible.

I would also like to thank my supervisors, Dr Jill Norman, Dr Frederick Tam, Professor David Wheeler and Professor Robert Unwin, for their guidance and help.

The P2X7R antagonist, AZ11657312, employed during the rat *in vivo* experiment, was kindly provided by AstraZeneca (coordinated by Dr Peter Gilmour) as part of a grant, jointly funded with the Medical Research Council, awarded to my supervisors.

Many thanks to Dr Richard Weaver for performing the *in vivo* P2X7R antagonist pharmacokinetic studies, Dr Tertius Hough for the routine biochemical analysis of serum and urine and Ms Mahrokh Nohadani for Pircosirius red staining of kidney sections. Obtaining ethical approval for the collection of human tissues was coordinated by Dr Rukshana Shroff and the transplant surgery and collection of arteries from patients was performed by Mr Ben Lindsey, Mr Bimbi Fernando, Mr Neal Banga and Mr Colin Forman.

I am also thankful to the following individuals for their invaluable help and teaching which enabled me learn and perform the techniques employed during this work: Mr Mark Neal, Ms Alison O'Hara, Mr Duncan Moore, Mrs Michelle Murphy, Dr Joanne (*in vivo* procedures), Dr Annette Schumacher (animal diets), Professor Tim Arnett and Dr Isabel Orriss (micro-CT scanning and purinergic system expertise), Dr John Booth (P2X7 and qPCR expertise), Professor Alan Salama (experimental advice), Dr Ben Caplin (human tissue work and statistics), Dr Siobhan Moyes and Dr Johanna Donovan (*in vitro* work, Western blotting, immunofluorescence and imaging), Dr Patricia DeWinter (qPCR) and Dr Nathan Davies (PPi assay).

Finally, throughout this project, my wife, Ruth, has provided me with an unwavering and tireless source of support and encouragement. I am, as always, grateful for her understanding, perspective, companionship and love.

TABLE OF CONTENTS

LIST OF FIGURES

LIST OF TABLES

ABBREVIATIONS

28S	28S Ribosomal RNA
2D	2-Dimensional
3D	3-Dimensional
α-SMA	Alpha-Smooth Muscle Actin
ABCC-6	ATP Binding Cassette-6
AC	Arterial Calcification
ADHR	Autosomal Dominant Hypophosphataemic Rickets
ADP	Adenosine Di-Phosphate
ADPKD	Autosomal Dominant Polycystic Kidney Disease
ALP	Alkaline Phosphatase
ALT	Alanine Transaminase
AMP	Adenosine Mono-Phosphate
ANCA	Anti-Neutrophil Cytoplasmic Antibody
ANK	Ankylosis Protein
ANOVA	Analysis Of Variance
ApoE	Apolipoprotein E
APRT	Adenine Phosphoribosyltransferase
APS	Ammonium Persulfate
ARHR2	Autosomal Recessive Hypophosphataemic Rickets Type 2
ATP	Adenosine Tri-Phosphate
BCA	Bicinchoninic Acid
BMD	Bone Mineral Density
BMP	Bone Morphogenetic Protein
bp	Base Pair
BSA	Bovine Serum Albumin

BzATP	2,3-(Benzoyl-4-Benzoyl)-ATP
cAMP	Cyclic AMP
CD39	synonymous with Ecto-Nucleoside Triphosphate Diphosphohydrolase-1 (NTPDase-1)
CD73	synonymous with Ecto-5'-Nucleotidase
cDNA	Complementary DNA
CKD	Chronic Kidney Disease
CKD-MBD	Chronic Kidney Disease-Mineral Bone Disorder
CT	Computerised Tomography
DAPI	4',6-Diamidino-2-Phenylindole
DMEM	Dulbecco's Modified Eagle Medium
DMSO	Dimethyl Sulfoxide
DNA	Deoxyribonucleic Acid
dNTP	Deoxynucleotide
DTT	Dithiothreitol
ECM	Extraellular Matrix
EDTA	Ethylenediaminetetraacetic Acid
ELISA	Enzyme-Linked Immunosorbent Assay
ENPP	Ecto-Nucleotide Pyrophosphatase/Phosphodiesterase
ERK	Extracellular-Signal-Regulated Kinase
ESRD	End-Stage Renal Disease
FGF-23	Fibroblast Growth Factor-23
GACI	Generalised Arterial Calcification Of Infancy
GAPDH	Glyceraldehyde 3-Phosphate Dehydrogenase
GFR	Glomerular Filtration Rate
GSK	Glaxo
H & E	Haematoxylin & Eosin

HmD	Haemodialysis
HEPES	4-(2-Hydroxyethyl)-1-Piperazineethanesulfonic Acid
HPMC	Hydroxypropyl Methylcellulose/0.1% Tween80
HPRT	Hypoxanthine-Guanine Phosphoribosyltransferase
HRP	Horseradish Peroxidase
hVSMC	Human Vascular Smooth Muscle Cell
IEL	Internal Elastic Lamina
IHD	Ischaemic Heart Disease
IL	Interleukin
ip	Intraperitoneal
KDIGO	Kidney Disease Improving Global Outcomes
KO	Knockout
KW	Kruskal Wallis
LDLR	Low-Density Lipoprotein Receptor
LPS	Lipopolysaccharide
MeATP	Methylene ATP
MGP	Matrix Gla Protein
M-MLV	Moloney-Murine Leukemia Virus
MMP	Matrix Metalloproteinase
MMW	Mean Molecular Weight
mRNA	Messenger RNA
MRS	Magnetic Resonance Spectroscopy
MV	Matrix Vesicle
MWU	Mann-Whitney U
NBF	Neutral Buffered Formalin
NLRP3	Nacht Domain-,Leucine-Rich Repeat-,and PYD-Containing Protein-3

NS	Nephrotic Syndrome
NT5E	5'-nucleotidase, Ecto (gene encoding ecto-5'-nucleotidase (CD73))
NTPDase	Ecto-Nucleoside Triphosphate Diphosphohydrolase (CD39)
P2X7R	P2X7 Receptor
PAGE	Polyacrylamide Gel Electrophoresis
PBS	Phosphate-Buffered Saline
PCR	Polymerase Chain Reaction
PD	Peritoneal Dialysis
PFA	Para-Formaldehyde
pNP-TMP	Thymidine 5’-Monophosphate p-Nitrophenyl Ester Sodium Salt
PPADS	Pyridoxalphosphate-6-Azopheny-2’,4’-Disulfonate
PPi	Inorganic Pyrophosphate
PTH	Parathyroid Hormone
PWV	Pulse Wave Velocity
qPCR	Quantitative Polymerase Chain Reaction
RIN	RNA Integrity Number
RIPA	Radioimmunoprecipitation Assay
RNA	Ribonucleic Acid
RPL13a	Ribosomal Protein L13a
RRT	Renal Replacement Therapy
RT	Reverse Transcription
Runx-2	Runt-Related Transcription Factor-2
rVSMC	Rat Vascular Smooth Muscle Cell
SD	Standard Deviation
SDHA	Succinate Dehydrogenase Complex, Subunit A
SDS	Sodium Docecyl Sulphate

SM-22	Smooth Muscle-22
SMMHC	Smooth Muscle Myosin Heavy Chain
SNP	Single Nucleotide Polymorphism
TAE	Tris-Acetate-EDTA
TBS	Tris-Buffered Saline
TBS/T	Tris-Buffered Saline/Tween
TEM	Transmission Electron Microscopy
TEMED	Tetramethylethylenediamine
TNAP	Tissue Non-Specific Alkaline Phosphatase
TNF-α	Tumour Necrosis Factor Alpha
TP	Transplant
Tris	Tris(hydroxymethyl)aminomethane
tRNA	Transfer RNA
UDP	Uridine-5'-Di-phosphate
Up_4A	Uridine Adenosine Tetraphosphate
UTP	Uridine-5'-Tri-phosphate
UUO	Unilateral Ureteric Obstruction
UV	Ultraviolet
VSMC	Vascular Smooth Muscle Cell
WT	Wild-type
YWHAZ	Tyrosine 3-Monooxygenase/Tryptophan 5-Monooxygenase Activation Protein Zeta

CHAPTER 1 – INTRODUCTION

PART 1 - Chronic Kidney Disease-Associated Arterial Calcification

1.1 Chronic Kidney Disease Is Associated With Increased Cardiovascular Risk

Chronic Kidney Disease (CKD) is a global health problem with an estimated prevalence of 12% in developed countries (Levey *et al* 2011, Levey & Coresh 2012). Cardiovascular events are the leading cause of death in patients with CKD (Angelantonio *et al* 2010) and those on renal replacement therapy (RRT) (Pruthi *et al* 2014). Moreover, renal impairment is associated with a marked increase in cardiovascular risk compared with the general population (Tonelli *et al* 2006) and this risk continues to increase as glomerular filtration rate (GFR) declines (Go *et al* 2004). Scoring systems which use traditional 'Framingham' risk factors (Dawber *et al* 1957, Dawber *et al* 1959) to predict the likelihood of a cardiovascular event consistently produce underestimates in patients with CKD (Weiner *et al* 2007) and accordingly the concept of 'renal specific' risk factors has emerged. A number of these non-traditional risk factors have been proposed (Baigent *et al* 2000) and include chronic inflammation, volume overload, elevated parathyroid hormone (PTH), anaemia, 'uraemic toxins', hyperhomocysteinaemia, hyperphosphataemia and, perhaps most importantly, arterial calcification (AC).

1.2 Arterial Calcification In Patients With Chronic Kidney Disease

AC is highly prevalent in patients with CKD and can occur in the intimal or medial layers of the vessel wall (Amann 2008). Intimal calcification occurs in the context of atherosclerotic disease in a fashion identical to that seen in the general population and is associated with the numerous, well-established risk factors known to promote this process (Dawber *et al* 1957, Dawber *et al* 1959). Calcification of the arterial media is much more specific, although not unique, to patients with CKD (Amann 2008).

AC is linked to adverse health outcomes and numerous studies have shown that the severity of AC predicts survival, with higher calcification scores associated with increased mortality in both dialysis (London *et a*l 2003) and pre-dialysis patients (Chiu *et al* 2010). In the case of intimal calcification this observation is hardly surprising given that it is directly related to atherosclerotic disease. However, medial

AC leads to decreased arterial compliance, an increase in pulse-wave velocity (PWV) and an associated increase in cardiac afterload (London *et al* 2003, Sigrist *et al* 2007, Sutliff *et al* 2011), which may also contribute to this increase in cardiovascular risk.

AC also contributes to profound morbidity in patients with end-stage renal disease (ESRD). AC of the iliac vessels frequently precludes successful kidney transplantation because of the difficulty posed in forming donor-recipient arterial anastomoses and, similarly, creation of arterio-venous fistulae can be complicated in patients requiring haemodialysis (HmD). In addition, AC contributes to the devastating and often fatal condition calciphylaxis (calcific uraemic arteriolopathy) (Adrogue *et al* 1981).

1.3 The Aetiology Of Arterial Calcification

Calcification of the arterial intima, as discussed above, is associated with atherosclerosis. The pathogenesis of this form of vascular disease is relatively well established and known to involve lipid accumulation, inflammatory cell infiltration and plaque formation (Weber & Noels 2011). In contrast, the mechanisms contributing to arterial medial calcification are much less well understood but seem to be different to those involved in atheroma because lipid and inflammation are consistently absent in these lesions and calcification can occur independently at this site (Shanahan *et al* 1999, Shroff *et al* 2008). This form of disease is the focus of this thesis and all subsequent reference to AC relates to calcium deposition within the medial layer of the vessel wall.

1.3.1 AC is not simply the result of passive mineral deposition.

The traditionally held view was that AC occurred in patients with CKD when the circulating concentrations of calcium and phosphate were elevated to such a degree so as to 'supersaturate' serum, with the consequent passive deposition of both in the walls of blood vessels. However, AC is frequently seen in patients with 'normal' circulating levels of these ions such as in the setting of diabetes (Shanahan *et al* 1999) and/or aging (Allison *et al* 2004), and not all patients with hyperphosphataemia develop AC (Parfitt 1969, Amann 2008). Therefore intuitively

the pathogenesis must be more complex than the explanation offered by this simple 'passive-deposition' model.

The 'passive-deposition' theory also falls down when one considers the normal process of bone formation. In this tissue, on-going mineralisation manifesting as hydroxyapatite deposition (which is also the most common form of mineral detected in AC (Schliper *et al* 2010)), occurs in an organised fashion without the requirement of elevated serum calcium and phosphate concentrations. This suggests that conditions and/or adaptations in the local environment, rather than the absolute concentration of the relevant circulating ions, determine whether calcification develops. In addition, there are now several described genetic disorders that result in abnormal calcification of the vasculature without disturbances in serum calcium and phosphate balance (Rutsch *et al* 2003, St Hilaire *et al* 2011, Nitschke *et al* 2012, Eytan *et al* 2013).

The implication from these observations is that 'non-passive' factors must contribute to the pathogenesis of AC. As will now be reviewed, this concept has led to a recent explosion of research into the possible factors governing the development and progression of ectopic arterial calcium deposition.

1.4 Methods Used To Study Arterial Calcification

Before discussing the current theories pertaining to the pathogenesis of AC it is important to outline the various experimental systems employed to study the disease. *In vitro* and *in vivo* models have been developed, each with distinct advantages and drawbacks.

1.4.1 Cell and tissue culture models.

As expanded upon below, the vascular smooth muscle cell (VSMC) has emerged as a 'key player' in the development of AC and *in vitro* models used frequently involve the culture of this cell type. In culture, VSMCs are described to form nodules which spontaneously calcify over a number of weeks (Proudfoot *et al* 1998). When the concentration of phosphate and/or calcium of the culture medium is increased, calcification is reported to occur more rapidly and in association with matrix vesicles (MVs) released from the cell (Reynolds *et al* 2004).

Although VSMCs in culture can secrete matrix (Underwood & Whitelock 1998, Reynolds *et al* 2004), they lack their normal extracellular architecture. In particular, the elastic lamina is absent *in vitro,* which *in vivo* is the initial site of medial AC (Lanzer *et al* 2014). *Ex vivo* arterial ring culture models offer an alternative approach to overcome this issue (Lomashvili *et al* 2004, Shroff *et al* 2010). Here, segments of artery are removed from either animals or humans and cultured in a similar fashion to VSMCs. Owing to the fact that tissue is intact in this system, it is thought to better simulate 'real life' conditions. Furthermore, when VSMCs are placed in culture they lose their contractile properties usually present *in vivo* and simultaneously change expression profiles of some genes (Nakano-Kurimoto *et al* 2009). Ring culture models are thought to also minimise this effect (Lomashvili *et al* 2004).

1.4.2 Rat models.

In rats, AC can be induced by CKD-independent or -dependent mechanisms. For investigating CKD-associated AC there are 3 main rat models in common use – the 5/6th nephrectomy model, the Cy/+ rat and the adenine nephropathy model. A brief account of the non-CKD models will first be given before expanding upon these CKD-dependent systems.

1.4.2.i Non-CKD rat models.

In the absence of renal injury AC has successfully been induced by the administration of warfarin (Price *et al* 1998), owing to its antagonism of vitamin K, which is required to activate the calcification inhibitor matrix gla-protein (MGP) (Hao *et al* 1995) (see section 1.5.3.ii). High-dose vitamin D can also be injected into rats with the effect of causing widespread AC (Fleisch *et al* 1965). A more invasive method of producing AC was described by Basalyga *et al* (2004) whereby the aorta was surgically exposed and calcium chloride directly applied for 15 minutes using a pre-soaked gauze.

1.4.2.ii The 5/6th nephrectomy model.

The 5/6th nephrectomy model usually involves a two-stage surgical procedure whereby a partial nephrectomy of one kidney is performed, followed by a contralateral total nephrectomy some days later (Chauntin & Ferris 1932). This reduction in functional renal mass is enough to induce the serum biochemical

changes of CKD such as elevations in creatinine, urea and phosphate, but rarely leads to arterial calcium deposition (Shobeiri *et al* 2010). AC can be induced in this model by the addition of a high phosphate diet. The normal dietary phosphate content for rats is around 0.5% (Haut *et al* 1980). If this is increased to at least 0.9%, some rats, but not all, will develop AC over 3-6 months (Neven & D'Haese 2011). Additional daily administration of vitamin D to animals on this regime has been reported to bring calcification rates closer to 100% (Haffner *et al* 2005).

1.4.2.iii The Cy/+ rat.

The heterozygous Cy/+ rat develops autosomal dominant polycystic kidney disease (ADPKD) and by around 9 months of age displays all the biochemical features of advanced CKD (Kaspareit-Rittinghausen *et al* 1990). AC was induced in this model by Moe *et al* (2008). These investigators fed a 0.7% phosphate-containing diet to male Cy/+ rats and observed high-turnover bone disease and AC in 60% of these animals at 38 weeks. Interestingly, no calcification was observed at 34 weeks.

1.4.2.iv The adenine nephropathy model.

The third rat model involves the dietary administration of adenine. This model closely resembles the human disease, adenine phosphoribosyltransferase (APRT) deficiency - a rare, autosomal recessive disorder which can result in ESRD if untreated (Bollee *et al* 2010). Adenine is usually metabolised by the enzyme APRT to generate adenosine mono-phosphate (AMP) (Hori & Henderson 1966). As a consequence of this reaction the concentration of circulating adenine is usually maintained at a very low level. However, if present in sufficiently high amounts, (a diet containing 0.75% adenine is commonly administered), the excess load will cause the enzyme to become saturated. Under these circumstances adenine is metabolised by xanthine oxidase to yield the product 2,8-dihydroxyadenine which is relatively insoluble at urinary pH and therefore precipitates out in the tubular lumen causing obstruction, fibrosis and ultimately advanced renal impairment (Yokozawa et al 1986, Okada *et al* 1999). High-turnover bone disease is also a feature of this model (Katsumata *et al* 2003).

If used in combination with a high phosphate diet, some rats fed this regime will develop AC over 4 weeks (Shobeiri *et al* 2010, Neven & D'Haese 2011). However,

many of the early studies that employed this model reported high variability with some animals developing extensive AC but calcium deposition undetectable in others. In this regard a major advance was made by Price *et al* (2006) who combined the 0.75% adenine/high phosphate regime with a low (2.5%) dietary protein content. This had the unexpected effect of inducing extensive aortic calcification in all animals. The mechanism underlying this observation is unclear but may involve a higher bioavailability of phosphate due to less of the ion being bound to protein (Neven & D'Haese 2011).

1.4.3 Mouse models.

1.4.3.i Non-CKD models.

A number of murine models of AC are described in mice with targeted genetic deletions. Examples include animals with a specific knockout (KO) of genes encoding apolipoprotein E (apoE) (Jawein *et al* 2004), low-density lipoprotein receptor (LDLR) (Ishibashi *et al* 1994), MGP (Luo *et al* 1997), ecto-nucleotide pyrophosphatase/phosphodiesterase-1 (ENPP-1) (Sali *et al* 1999) and fetuin A (Schafer *et al* 2003). The *apoE* and *LDLR* KO animals actually develop atherosclerotic calcification and are therefore less useful for studying medial disease. The others have deletions in genes encoding calcification inhibitors (see section 1.5.3).

1.4.3.ii CKD model.

To investigate AC due to CKD, only one mouse model has been described to date (El-Abbadi *et al* 2009). This involves a two-stage surgical reduction of renal mass ($5/6^{th}$ nephrectomy) in adult, female, DBA/2 mice, followed by an extended period of high phosphate feeding. In the original report by El-Abbadi *et al* (2009) the majority of mice exhibited extensive medial aortic calcification with typical biochemical features of advanced renal disease after 3 months. Interestingly, these authors reported that female mice developed aortic calcification much more readily than males, hence the exclusive use of this gender. These investigators have also shown that high-turnover bone disease occurs in this model (Lau *et al* 2012a).

The DBA/2 strain of mouse used in this model appears to be critical as it is prone to cardiovascular calcification whereas other commonly employed strains such as the

C57Bl/6 are reported to be resistant (Eaton *et al* 1978). The mechanism underlying this strain difference has been partially elucidated. Using quantitative trait locus analysis, a number of relevant loci have been mapped with the major contributor (*Dyscalc1)* located on chromosome 7 (Ivandic *et al* 2001). The causative gene was subsequently found to be Abcc6 (which encodes the ATP-binding cassette transporter ABCC-6). Mice prone to calcification display reduced levels of this protein (Meng *et al* 2007).

1.5 The Pathogenesis Of Arterial Calcification

There is now overwhelming evidence to indicate that AC involves the non-passive deposition of mineral and that it is a cell-mediated and regulated process. A number of mechanisms have been implicated in the pathogenesis and those which have been consistently advanced in the literature are now discussed. It should be noted however that for the majority of these pathways much controversy and divided opinion still exists within the scientific community regarding their relevance and role in mediating AC. A summary of these mechanisms is shown in Figure 1.1.

1.5.1 The role of the VSMC.

1.5.1.i Links with bone formation.

Although a number of cell types have been shown to contribute to AC (Shanahan *et al* 2011), the VSMC is now considered to be fundamentally important. VSMCs are of mesenchymal origin and display a continuum of plasticity in their phenotype, ranging from a contractile state at one end to a synthetic entity at the other. This latter state is characterised by the ability of the cell to proliferate and secrete growth factors and extracellular matrix (ECM) (Rensen *et al* 2007).

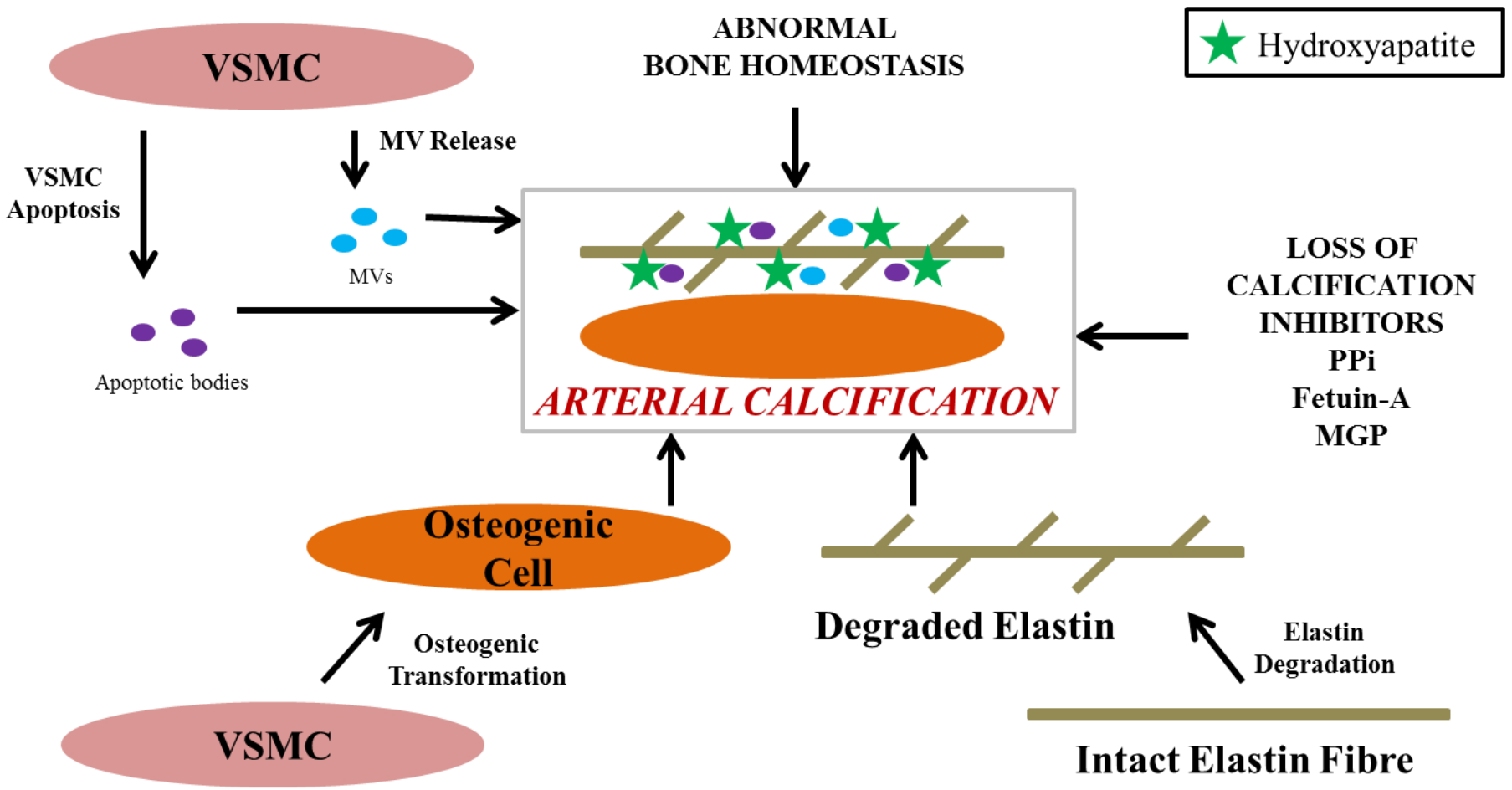

Figure 1.1. Pathogenic Mechanisms of CKD-Associated AC. Many pathways are described to contribute to AC which ultimately manifests as hydroxyapatite deposition on elastin fibres running between layers of VSMCs. VSMCs can undergo a change in phenotype, taking on the characteristics of osteogenic cells thereby promoting AC. VSMCs can alternatively undergo apoptosis or secrete matrix vesicles (MVs). Apoptotic bodies and MVs are able to act as nucleation sites for hydroxyapatite growth. Abnormal bone homeostasis and decreased levels calcification inhibitors are both observed in CKD and are closely linked to AC. Degradation of elastin also promotes mineral binding and subsequent expansion of mineralisation. PPi: inorganic pyrophosphate; MGP: matrix gla protein.

Techniques such as transmission electron microscopy (TEM) (Schlieper *et al* 2010) and magnetic resonance spectroscopy (MRS) (Duer *et al* 2008) have revealed that in man, arterial mineral deposits frequently take the form of hydroxyapatite in a structure that very closely resembles the architecture of bone. In keeping with these observations, a number of *in vitro* studies (reviewed in Shanahan *et al* 2011) have reported that, when cultured in calcification-promoting (high phosphate) conditions, VSMC phenotype switches from the contractile state to take on characteristics more typically associated with bone-forming, (i.e. synthetic and secretory), osteoblast-like cells. This so called 'osteogenic transformation' is usually inferred by detecting a decrease in messenger ribonucleic acid (mRNA) and/or protein for VSMC-specific markers such as alpha-smooth muscle actin (α-SMA) and smooth muscle-22 (SM-22) (Proudfoot & Shanahan 2012) in association with an increase in osteogenic transcription factors such as runt-related transcription factor-2 (runx-2) (Komori *et al* 1997, Ducy *et al* 1997) and osterix (Nakashima *et al* 2002) and/or other bone-related proteins including bone morphogenetic protein (BMP) -2 (Celil *et al* 2005).

Similar findings have also been reported by some groups using *in vivo* models. For example, using immunohistochemistry to assess aortas taken from $5/6^{th}$ nephrectomised mice, Pai *et al* (2011) reported decreased and increased staining in calcified vessels for SM-22 and runx-2, respectively. In humans, increased staining for runx-2 and other bone-related proteins has been reported in calcified vessels taken from patients with ESRD (Moe *et al* 2002, Shroff *et al* 2008).

It is thought that phosphate plays a key role in mediating VSMC osteogenic transformation. *In vitro* studies have suggested that VSMCs up-regulate runx-2 when cultured in high phosphate conditions and that this occurs in a dose-dependent manner (Jono *et al* 2000). Intracellular uptake of phosphate through the sodium-dependent co-transporters PiT-1 and PiT-2 is thought to be vital to this pathway because cell and animal studies in which these proteins were knocked-down showed suppression of both runx-2 expression and calcium deposition (Li *et al* 2006, Crouthamel *et al* 2013).

How phosphate brings about these cellular changes is unknown. One group have implicated activation of extracellular-signal-regulated kinase (ERK) 1/2 as a possible mechanistic pathway because up-regulation of runx-2 occurred in parallel with

increased phosphorylation of this protein in murine VSMCs exposed to high phosphate *in vitro*. Inhibition of ERK1/2 phosphorylation prevented this effect (Speer *et al* 2009). Other potential phosphate-induced mechanisms include increasing SM-22 methylation (Montes de Oca *et al* 2010) and an elevation in reactive oxygen species (Zhao *et al* 2011).

1.5.1.ii VSMC apoptosis and release of MVs.

Some studies have implicated apoptosis as an important mechanism in driving the development of AC. Cultured VSMCs undergo apoptosis in calcification-promoting conditions and apoptotic bodies are thought to act as nucleation sites for mineral attachment and crystal expansion (Proudfoot *et al* 2000). Increased apoptosis has been demonstrated in calcified arteries taken from patients with CKD (Shroff *et al* 2008) and apoptosis inhibitors have been shown to reduce AC in an *ex vivo* model (Shroff *et al* 2010).

Elevated extracellular calcium is thought to be an important driver of apoptosis in this context. VSMCs undergo enhanced apoptosis when cultured in an elevated concentration of calcium and the apoptotic bodies formed calcify to a greater extent when the environment is rich in this ion (Proudfoot *et al* 2000). In this study by Proudfoot *et al*, phosphate appeared to exert a synergistic effect in mediating apoptosis. This may be due to phosphate-induced suppression of the anti-apoptotic factor, growth arrest-specific protein 6 (Son *et al* 2006).

Another early event in the development of AC is thought to be the release of MVs by VSMCs. MVs are membrane-bound sacs containing pre-formed hydroxyapatite which, in a similar fashion to apoptotic bodies, can serve as nucleation sites for hydroxyapatite growth (Reynolds *et al* 2004). In non-calcified states VSMCs still seem to contain MVs but here the vesicles are loaded with calcification inhibitors such as fetuin A (Reynolds *et al* 2005). The combination of suppressed inhibitor levels (see section 1.5.3) and elevated extracellular calcium appear to confer the property of 'calcification-competence' on these MVs.

1.5.2 AC is related to bone health.

Over recent years a number of studies have consistently reported an inverse relationship between bone health and AC. In both the general population and in those with osteoporosis, bone mineral density (BMD) has been shown to negatively correlate with extra-osseous mineralisation (see Persy & D'Haese 2009). A connection with rarer bone disorders such as Paget's disease has also been suggested (Laroche & Delmotte 2005). A similar association seems to exist in CKD, although as detailed below, the spectrum of bone disease is more complex in this clinical setting, encompassing more than isolated alterations in BMD.

In recognition of the fact that in a number of observational studies investigating patients with renal impairment, disturbances in mineral homeostasis were closely linked not only to bone health, but also to arterial disease in the form of ectopic calcification, in 2006 the Kidney Disease Improving Global Outcomes (KDIGO) group coined the term 'Chronic Kidney Disease-Mineral Bone Disorder' (CKD-MBD) (Moe *et al* 2006). This is defined as the presence, in a patient with CKD, of at least one of the following:

1. Abnormalities in serum phosphate, calcium, PTH or vitamin D.
2. Abnormalities of bone turnover, mineralisation, volume, linear growth or strength.
3. Vascular or other soft tissue calcification.

Although the paradigm of CKD-MBD has now been adopted by the renal community it must be borne in mind that a definitive link between bone and AC has yet to be proven (Persy & D'Haese 2009).

As implied by the second component of the CKD-MBD definition above, several elements of normal bone homeostasis can be disturbed in patients with renal dysfunction. Which of these processes is most closely related to AC is unknown. Low bone turnover has been found to associate with AC by some groups (London *et al* 2004, Tomiyama *et al* 2010) whilst others have found a link with both high- and low-turnover states (Barreto *et al* 2008, Asci *et al* 2011). Experimentally, correction of the low-turnover state in CKD mice, achieved by administration of BMP-7,

resulted in an attenuation of AC (Davies *et al* 2005). The study by Tomiyama *et al* (2010) also reported an inverse relationship between AC and bone density and volume. Other groups have also found AC to negatively correlate with bone volume (Barreto *et al* 2008, Adragao *et al* 2009).

1.5.3 Inhibitors of calcification.

A number of calcification inhibitors are produced *in vivo* to protect against unwanted ectopic mineral deposition in sites such as the cardiovascular system. Possibly the one that has received most attention is inorganic pyrophosphate (PPi) which is discussed in depth in Part 2 of this chapter. Other inhibitors that have been studied in some detail include fetuin A and MGP.

1.5.3.i Fetuin A.

Fetuin A is a protein synthesised in the liver and is present in extracellular tissue as well as in high concentrations in plasma. The molecule strongly binds calcium and phosphate and is thought to act as a scavenger of these ions to prevent calcification (Jahnen-Dechent *et al* 2011). In keeping with this theory, fetuin A KO mice display widespread extra-skeletal mineral deposits (Schafer *et al* 2003, Jahnen-Dechent *et al* 2011).

Serum fetuin A appears to be suppressed in patients with ESRD (Ketteler *et al* 2003) but not early stages of CKD (Ix *et al* 2006). In a cross-sectional study of dialysis patients Ketteler *et al* (2003), found an association between lower circulating fetuin A and cardiovascular mortality. Whether this finding is related to inhibition of calcification is not clear, however some studies have found an inverse correlation between plasma fetuin A levels and AC in patients with CKD (Moe *et al* 2005, Koos *et al* 2009).

1.5.3.ii MGP.

MGP is a vitamin K-dependent protein present in bone and the vasculature (Hao *et al* 1995). As noted above, rodents treated with the vitamin K antagonist, warfarin, develop AC (Price *et al* 1998) and MGP KO mice exhibit widespread ectopic mineral deposition (Luo *et al* 1997). In humans, a mutated form of MGP occurs in Keutal's syndrome (Munroe *et al* 1999), a rare autosomal recessive disorder in

which AC is a feature, albeit relatively mild (Meier *et al* 2001). MGP is reported to be up-regulated in calcified arteries taken from uraemic rats, possibly as a protective response, although the exact mechanism through which it inhibits AC remains uncertain (Lomashvili *et al* 2011). Patients with CKD are vitamin K-deficient (Holden *et al* 2010) and treatment with vitamin K reduces AC in uraemic rats (McCabe *et al* 2013). Together these findings suggest that CKD is, in effect, a state of functional MGP deficiency.

1.5.4 Degradation and remodelling of the ECM.

Microscopic evaluation of the early stages of AC has indicated that mineral deposition initially occurs on elastin fibres in the ECM (Lanzer *et al* 2014, O'Neill & Adams 2014). Elastin has a propensity to bind calcium and phosphate (Urry 1971) and increasing evidence suggests that integral and structural disruption of this molecule within the ECM contributes to AC (Pai & Giachelli 2010).

Matrix metalloproteinases (MMPs) -2 and -9 and cathepsin S are enzymes capable of degrading elastin (Chow *et al* 2007). *In vivo* studies have indicated that genetic deficiency of any of these proteins can protect against arterial calcium deposition (Basalyga *et al* 2004, Aikawa *et al* 2009). Using the Cy/+ rat model, Chen *et al* (2011) showed an increase in activity of both MMP-2 and MMP-9 in CKD and that blocking enzyme activity pharmacologically reduced calcification in an *ex vivo* model. Up-regulation of MMP-2 was also detected in arteries taken from patients with CKD compared with controls (Ada *et al* 2009) and this correlated with both the degree of elastin fibre disorganisation and detectable calcification. In the murine model of CKD-associated AC, fragmentation and disruption of elastin were seen to occur prior to the onset of calcification (Pai *et al* 2011).

Interestingly some authors have also shown that elastin fragments can induce VSMC osteogenic transformation *in vitro* even in the absence of increased phosphate (Simionescu *et al* 2005). When high phosphate conditions are present, calcification is accelerated in the presence of elastin degradation products (Hosaka *et al* 2009).

1.6 Current Treatment Options For Arterial Calcification

At present there are no treatments available to specifically prevent or attenuate the progression of AC. Cholesterol-lowering agents are of proven efficacy for reducing atherosclerosis-related mortality in those at risk in the general population (Baigent *et al* 2005) and this benefit seems to be maintained in patients with CKD (Baigent *et al* 2011) although probably not in those on dialysis (Wanner *et al* 2005, Fellstrom *et al* 2009). The utility of these agents in kidney transplant (TP) recipients is currently uncertain (Palmer *et al* 2014). Beta-blockers and agents that inhibit the renin-angiotensin-aldosterone system may also confer some cardiovascular protection in selected patients with CKD although large, randomised, prospective studies using patient-centred outcomes are lacking (Kidney Disease: Improving Global Outcomes (KDIGO) CKD Work Group 2013).

Although AC is not simply a function of circulating concentrations of phosphate and calcium, as demonstrated experimentally in the studies discussed previously (section 1.5), these ions are clearly able to contribute to ectopic mineralisation. These observations, coupled with the apparent link between bone health and AC, have led many to investigate whether correcting phosphate and calcium biochemistry in patients with CKD will influence the development and/or progression of arterial calcium deposition.

Phosphate-binding agents are commonly prescribed to patients with ESRD in an attempt to limit intestinal absorption of this ion and a number of studies have evaluated the influence of these compounds on AC. Phosphate-binders can be either calcium-containing or non-calcium-containing and a major issue that has recently come to light is the excess calcium burden caused by administration of the former class of compound. Many studies have indicated that calcium-containing binders lead to a more rapid progression of AC compared with non-calcium-containing agents (Chertow *et al* 2002, Block *et al* 2005, Russo *et al* 2007) and moreover, a recent meta-analysis demonstrated that calcium-containing compounds were also associated with a higher mortality rate (Jamal *et al* 2013).

In fact, whether phosphate-binders are beneficial at all is uncertain. No prospective trial has ever been performed to determine whether these agents confer a survival

benefit compared with placebo. A prospective trial which evaluated both calcium-based and non-calcium-based phosphate binders in patients not yet on RRT suggested that whilst these agents do lower serum phosphate, they may actually lead to *increased* AC (Block *et al* 2012). It should be noted that progression of AC was not the primary outcome in this study and patient numbers were relatively small. In addition, the greatest risk for AC seemed to be in the group taking calcium-based drugs. However, the findings highlight the urgent need for trials addressing patient-level outcomes. At present most clinicians would still advocate the use of phosphate-binders for patients with hyperphosphataemia although it is likely that prescriptions of calcium-based agents will now fall.

Calcimimetic drugs such as cinacalcet, effectively reduce serum PTH and also suppress calcium and phosphate levels (Quarles *et al* 2003, Block *et al* 2004). These agents have been shown to reduce AC in rats with CKD (Kawata *et al* 2008, Henley *et al* 2009). The ADVANCE trial (Raggi *et al* 2011) compared the effect of cinacalet plus low dose vitamin D with vitamin D therapy alone, on the progression of AC in patients on HmD. The primary outcome measure in this trial was progression in density of AC and this did not reach statistical significance. However, when AC was measured volumetrically, cinacalcet retarded progression. In the EVOLVE trial (Chertow *et al* 2012), cinacalcet led to a non-significant reduction in the primary composite end-point of cardiovascular events and death compared with placebo. The effect reached statistical significance after correcting for baseline characteristics.

A number of other interventions which aim to minimise phosphate and/or calcium loading are currently recommended by KDIGO (Kidney Disease: Improving Global Outcomes (KDIGO) CKD–MBD Work Group 2009). Logically they would all seem to be beneficial, although none have been evaluated in long-term, randomised, controlled trials. Suggested measures include restricting dietary intake of phosphate, optimising dialytic phosphate removal, minimising dialysate calcium concentrations and avoiding excessive vitamin D therapy.

Despite theoretical advantages of these interventions they remain non-specific to AC and whilst some may possibly slow progression of the disease, there is currently no way of inhibiting the process altogether. Based on what is known about the pathogenesis of AC a number of potential therapeutic agents are currently in the

early stages of investigation. Examples of these include vitamin K (Krueger *et al* 2013) and sodium thiosulphate (Adirekkiat *et al* 2010). As will now be discussed, there are a number of reasons to consider evaluating various components of the purinergic system as potential targets for therapy.

PART 2 - Adenosine Tri-Phosphate And Arterial Calcification

1.7 An Overview Of The Purinergic System

The ability of adenosine tri-phosphate (ATP) to exert physiological effects in the mammalian heart, in addition to its role as the main cellular energy source, was first recognised almost a century ago in the seminal work of Drury and Szent-Gyorgi (1929). The extracellular ATP receptor system, known collectively as the purinergic system, was first predicted by Burnstock in the 1970s and is now well-characterised (Burnstock 2006, Burnstock 2012). It has been implicated in a number of biological processes and disease states, well illustrated by the therapeutic role of the P2Y12 antagonist, clopidogrel, in the treatment of myocardial infarction (Sabatine *et al* 2005).

Two broad categories of purinergic receptors have been identified on a wide range of cells (see Burnstock 2012 for an in-depth review and historical perspective). P1 receptors are G protein-coupled and respond primarily to adenosine. Four subtypes have been described to date, A1, A2A, A2B and A3. P2 receptors are principally activated by tri- and di-nucleotides and are classified as either P2X or P2Y. P2X receptors are ion-gated channels consisting of 3 subunits, 7 subtypes are currently recognised (P2X1-7). P2Y receptors are G protein-coupled with 8 subtypes currently known (P2Y1, 2, 4, 6, 11-14). Receptors are numbered according to the order in which they were discovered. The dis-continuous P2Y numbering system is because some receptors were initially assigned to this group but subsequently identified as either species homologues or as belonging to an alternative receptor family.

The availability of extracellular nucleotides for activation of these receptors is tightly regulated by a number of enzymes, the ecto-nucleotidases, which catalyse the metabolism of ATP and related molecules (Figure 1.2) (Zimmermann *et al* 2012). There are 4 broad categories of enzymes in this class. Ecto-nucleoside triphosphate diphosphohydrolases (NTPDases), of which there are 8, including CD39 (NTPDase-

1), hydrolyse ATP to yield AMP plus 2 phosphates (Kaczmarek *et al* 1996). In contrast, the ecto-nucleotide pyrophosphatase/phosphodiesterases (ENPPs), of which there are 7 with ENPP-1 being the best characterised and studied (Terkeltaub 2001, Mackenzie *et al* 2012), generate AMP plus inorganic PPi from hydrolysis of ATP.

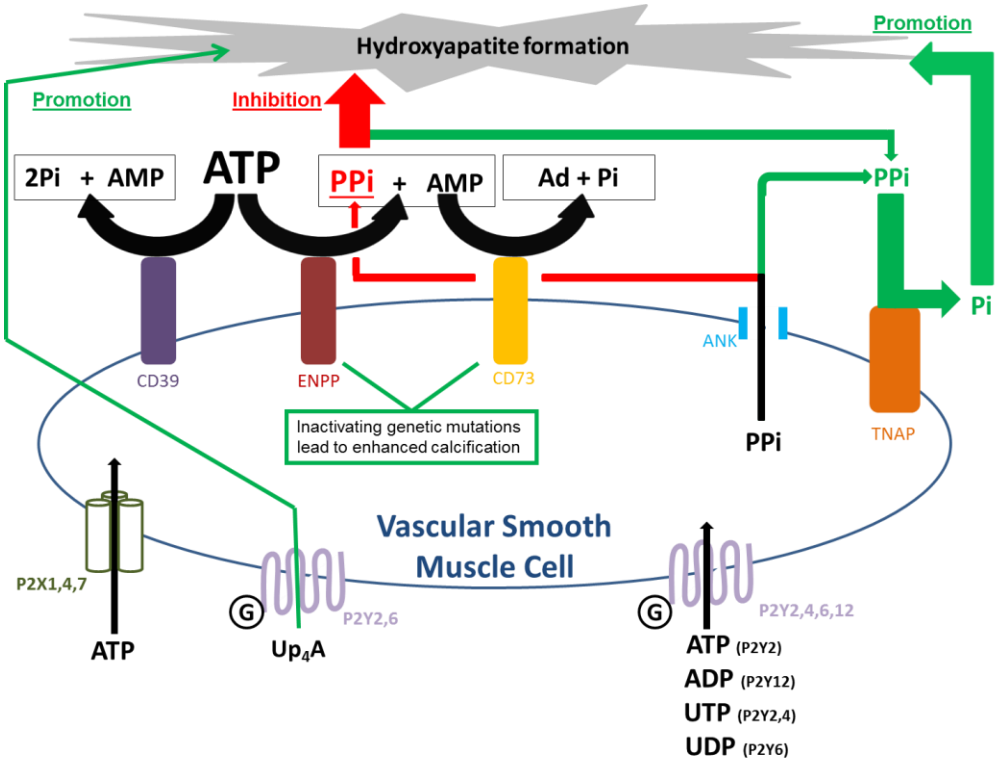

Figure 1.2. The Purinergic System and its Regulation of AC in VSMCs.

P2X receptors are ion channels composed of 3 subunits and P2Y receptors are G-protein coupled. The expression of P2X receptors 1, 4 and 7 and P2Y receptors 2, 4, 6 and 12 has been demonstrated on VSMCs and the preferred agonists for these receptors are shown. Additionally, Up_4A has recently been implicated to promote arterial calcification via signalling through P2Y2 and P2Y6 receptors. VSMCs also express adenosine A2 receptors (not shown).

ATP and other ligands for P2X and P2Y receptors gain access to the extracellular space in a number of ways (see text). ATP is hydrolysed by either CD39 (ecto-nucleoside triphosphate diphosphohydrolases (NTPDases)) into AMP plus 2 phosphates (Pi), or by ecto-nucleotide pyrophosphatase/phosphodiesterases (ENPPs) into AMP plus inorganic pyrophosphate (PPi). AMP is hydrolysed into adenosine (Ad) and Pi by CD73 (ecto-5'-nucleotidase). PPi can also reach the extracellular space from within the cell through the putative membrane transporter ANK (ankylosis) protein. PPi is subsequently hydrolysed into Pi by tissue non-specific alkaline phosphatase (TNAP).

PPi is a potent inhibitor of calcification, however it is also the substrate for generation of Pi by TNAP and subsequent hydroxyapatite formation. The balance between ENPP1 and TNAP activity is therefore critical in determining whether calcification pursues. Autosomal recessive mutations in ENPP1 cause arterial calcifications in infancy and autosomal recessive mutations in CD73 cause arterial calcifications in adulthood.

UTP: Uridine-5'-tri-phosphate; UDP: Uridine-5'-di-phosphate.

This family of enzymes can alternatively hydrolyse ATP to generate adenosine di-phosphate (ADP) and subsequent AMP with phosphate side-products, although this reaction occurs much less readily than that of PPi generation. PPi is a potent inhibitor of hydroxyapatite formation (Fleisch *et al* 1965), and thus tissue calcification, but can be converted to phosphate by the action of the enzyme tissue non-specific alkaline phosphatase (TNAP) (Murshed *et al* 2005), thereby promoting mineralisation. Intracellular PPi may also be secreted via the ankylosis protein (ANK) (Terkeltaub 2001). AMP is converted to adenosine by the action of ecto-5'-nucleotidase (CD73), which also generates one phosphate molecule (Arch & Newsholme 1978).

1.7.1 Potential sources of extracellular ATP.

ATP release from erythrocytes (Bergfeld & Forrester 1992) and perivascular nerves (Lew & White 1987) has been described. With respect to the cardiovascular system specifically, studies have shown that endothelial cells (Bodin & Burnstock 1996) and VSMCs (Katsuragi *et al* 1991) are able to contribute directly to extracellular ATP levels. Proposed mechanisms of release from these cells include vesicular exocytosis, ATP-binding cassettes, and connexin and pannexin hemi-channels. In addition, direct cell surface synthesis of ATP by F_1/F_0-ATP synthase has been proposed (Lohman *et al* 2012).

1.8 Purinergic Receptor-Mediated Calcification

The expression of P2 receptors in VSMCs has been investigated and the presence of P2X1, P2X4 and P2X7 has been demonstrated, along with P2Y2, P2Y4, P2Y6 and P2Y12. Of the P1 sub-family, A2 receptors are the main receptors present in the arterial media (Wang *et al* 2002, Wang *et al* 2003, Erlinge & Burnstock 2008, Burnstock 2009, Schuchardt *et al* 2011) (Figure 1.2).

1.8.1 P2Y receptors.

P2Y receptors have been directly implicated in the process of AC. Schuchardt and colleagues (2012) were able to show enhanced calcification of both cultured rat VSMCs and the medial layer of rodent aortic rings on exposure to calcification medium (culture medium supplemented with 10mM β-glycerolphosphate) with the addition of uridine adenosine tetraphosphate (Up_4A). This molecule, released from

endothelial cells under conditions such as hypoxia or exposure to shear stress is able to activate a number of P2X and P2Y receptors (Matsumoto *et al* 2011). The authors went on to identify P2Y2 and P2Y6 as potential mediators of AC in experiments using VSMCs exposed to specific receptor antagonists and also aortic rings from P2Y2 KO mice. Furthermore, this study found that Up_4A is elevated in patients with CKD.

Of interest, Erlinge and colleagues (1998) have linked P2Y2 receptors to a switch in VSMC phenotype from contractile to synthetic in experiments showing that the expression of mRNA for this receptor is upregulated in rodent VSMCs in long-term culture (representing cells in the synthetic state) compared with rodent aortic medial cells (VSMCs in the contractile state). P2Y2 receptor agonists have also been shown to increase TNAP activity in human heart valve interstitial cells (Osman *et al* 2006), which was interpreted by the authors to indicate a pro-mineralising function.

However, the situation is clearly complex, since in contrast to these findings, experiments by Cote and colleagues (2012a) provoked cultured human aortic valve interstitial cells to calcify using medium containing 2-5 mM phosphate and exposed them to either suramin (a general purinergic receptor antagonist), iso-pyridoxalphosphate-6-azopheny-2',4'-disulfonate (iso-PPADS) (P2X receptor antagonist) or CGS15943 (adenosine receptor antagonist). They found that only suramin increased mineralisation, whereas the other agents had no effect. They concluded that this was consistent with an inhibitory effect of P2Y on valve calcification. They went on to show that treatment of cells with 2-thioUTP, a P2Y2 agonist, reduced mineralisation, and that P2Y2 knockdown increased mineral deposition. With further experiments, the authors implicated inhibition of apoptosis by P2Y2 as the underlying mechanism that seemed to protect against calcification.

1.8.2 Other purinergic receptors.

Although controversial, adenosine has been linked to AC through *in vitro* experiments attempting to explain the mechanism whereby genetic deficiency of the enzyme CD73 leads to calcium deposition in peripheral arteries (St Hilaire *et al* 2011) (see section 1.10.2.ii). To date, there are no reports of studies investigating the role of P2X receptors in this context. However, as will now be discussed, one

member of this sub-family – the P2X7 receptor (P2X7R), has several links to processes implicated in the biology of arterial calcium deposition, making it worthy of exploration as a potential player in the pathogenesis and as a possible therapeutic target.

1.9 The P2X7 Receptor

1.9.1 Structural properties.

The basic structure of P2X7R is the same as the other 6 P2X receptors, i.e. an oligomer, composed of 3 subunits, each possessing intracellular N- and C- termini and two membrane-spanning domains separated by an extracellular loop (Burnstock 2006). However, P2X7R has several important unique properties which distinguish it from other members of the P2X sub-family. These include a markedly higher ATP requirement for activation, a substantially (200 amino acids) longer intracellular C-terminus and the ability to generate a large 'pore-like' structure within the cell membrane (Suprenant *et al* 1996).

Mathematical modelling has been used to predict the possible 'cascade of events' involved in the production of this transmembrane pore (Yan *et al* 2010, Pelegrin 2011), which is thought to be key in mediating many biological actions of P2X7R (Wiley *et al* 2011). Following binding of one ATP molecule, P2X7R undergoes a conformational change and the affinity for ATP is reduced. Attachment of a second ATP molecule induces further architectural disruption and the opening of a low-conductance channel, permitting the transmembrane movement of small cations. ATP affinity is further reduced. Addition of a third ATP molecule to this complex causes a conformational shift back to a symmetrical shape. This is associated with formation of the high-conductance pore which is permeable to molecules up to 900kDa in size.

P2X7R in the cell membrane is usually anchored to non-muscle myosin and disassociation from this protein is thought to be important in the final step of pore formation. The C-terminus may well regulate this process as disruption to the normal structure of this region of the protein does not affect the ion-channel function of P2X7R but does impact on large molecule transmembrane flux (i.e. pore formation) (Adinolfi *et al* 2010).

1.9.2 Tissue distribution.

Originally P2X7R was thought to be exclusively expressed on haemopoietic cells. However, it has now been shown to have a fairly ubiquitous distribution in the human body although levels of expression differ widely between tissues (Burnstock & Knight 2004). In keeping with the known pro-inflammatory role of P2X7R (discussed in section 1.9.4), the receptor is most abundant in macrophages and other mononuclear peripheral blood cells. Interestingly neutrophils only show intracellular expression (Gu *et al* 2000, Wiley *et al* 2011).

In the vascular system, the expression of P2X7R has not been very well characterised. However, presence of the receptor has been demonstrated in human umbilical cord artery and vein (Piscopiello *et al* 2013), as well as on human endothelial cells (Wilson *et al* 2007), smooth muscle in veins (Cario-Toumaninatz *et al* 1998) and arterial adventitia in rats (Lewis & Evans 2001). P2X7R protein expression in arterial VSMCs has not previously been reported although the presence of mRNA has been detected (Wang *et al* 2002, Schuchardt *et al* 2011). With relevance to the possible link between AC and bone, the presence of P2X7R has been demonstrated in both osteoblasts (Gartland *et al* 2001) and osteoclasts (Jorgensen *et al* 2002).

1.9.3 Agonists and antagonists.

1.9.3.i Receptor agonists.

Compared with other P2X receptors, P2X7R requires much higher concentrations of ATP for activation (EC_{50} > 80–100μM at P2X7R) (Suprenant *et al* 1996). The most potent receptor agonist is the ATP analogue 2,3-(benzoyl-4-benzoyl)-ATP (BzATP) for which EC_{50} = 7μM (Suprenant *et al* 1996). It should be noted however that BzATP is not a specific P2X7R agonist as it is able to activate many other P2X and some P2Y receptors (Bianchi *et al* 1999, Michel *et al* 2001). BzATP is followed, in order of decreasing affinity, by ATP, 2-methylthio-ATP, adenosine-(γ-thio)-triphosphate and ADP (North 2002).

1.9.3.ii Receptor antagonists.

A number of molecules capable of inhibiting P2X receptors have been used in research for many years. Examples of these general P2X antagonists include suramin, oxidised ATP and PPADS (Wiley *et al* 2011). KN-62 is a relatively specific antagonist of P2X7R in humans and mice but does not inhibit the receptor in rats (Donnelly-Roberts *et al* 2007).

Specific antagonists to P2X7R have only become commercially-available over the last few years and have greatly facilitated research into the characteristics and functions of the receptor. One of the most commonly used agents is A438079 – a tetrazole-based compound originally developed by the Abbott Laboratory (Nelson *et al* 2006). This has an IC_{50} value of 0.1 and 0.3μM for BzATP-induced Ca^{2+} influx through human and rat P2X7Rs respectively (Donnelly-Roberts *et al* 2007). A438079 has been widely used for *in vitro* studies and has also successfully been employed in rodent studies to modulate nociception (McGaraughty *et al* 2007) and ameliorate experimental glomerulonephritis (Taylor *et al* 2009a). Other commercially-available specific P2X7R antagonists include A740003, AZ11645373 and A839977. Early phase human clinical trials in conditions such as rheumatoid arthritis have indicated that pharmacological blockade of P2X7R is well tolerated and safe (Keystone *et al* 2012, Stock *et al* 2012).

1.9.4 Receptor functions and potential links to CKD-associated AC.

The best characterised function of P2X7R is its role in mediating assembly of the Nacht Domain-, Leucine-Rich Repeat-, and PYD-Containing Protein-3 (NLRP3) inflammasome (Di Virgilio 2007). In macrophages primed by stimulants such as bacterial-derived lipopolysaccharide (LPS) or inflammatory cytokines such as tumour necrosis factor-alpha (TNF-α), P2X7R orchestrates the release of interleukin (IL) 1-beta and IL-18 along with caspase-1 activation by inducing inflammasome assembly. These events seem to be dependent upon a fall in intracellular potassium brought about by ion transit through the P2X7R-associated pore (Booth *et al* 2012). P2X7R therefore appears to function as a ‘damage sensor’ in these circumstances, acting to induce a local inflammatory response (Di Virgilio 2007).

As reviewed in Part 1 of this introduction (section 1.3), despite a clear role in atherosclerosis, inflammatory cells are consistently reported to be absent in medial AC lesions (Shanahan *et al* 1999, Shroff *et al* 2008). Some authors have shown that inflammatory cytokines such as TNF-α can exacerbate VSMC-associated calcification *in vitro* (Tinut *et al* 2000) and one recent report has linked the NLRP3 inflammasome itself to calcium deposition (Wen *et al* 2013). However, a definitive contribution of these and associated inflammatory processes in the pathogenesis of AC requires confirmation.

Whilst the role of inflammatory-related mechanisms in AC awaits verification there are a number of other known functions of P2X7R which would seem to have a more relevant and direct association with what is currently known about the pathogenesis of AC. These potential links are outlined below and form the basis upon which the primary hypothesis of this thesis is made.

1.9.4.i P2X7R and bone.

Early work examining the bone phenotype of mice with a genetic deficiency of P2X7R ($P2X7^{-/-}$ mice) indicated a functional role for the receptor in this tissue but yielded contrasting results. Studies by Ke *et al* (2002) suggested that $P2X7^{-/-}$ animals had a marked decrease in bone mineral content and bone formation and increased bone resorption compared with controls. However, work by Gartland *et al* (2003a) found no difference in BMD and an *increase* in cortical bone. Importantly, 2 lines of $P2X7^{-/-}$ mice have been developed. The Pfizer KO (Solle *et al* 2001) was produced by the insertion of a neomycin cassette into exon 13 resulting in disruption of the C-terminus. This animal was used by Ke *et al* (2002). The Gartland group (2003a), in contrast, studied the Glaxo (GSK) KO. This mouse was originally generated by the insertion of a lacZ transgene into exon 1 (procedure described by Chessell *et al* 2005). Subsequent studies have indicated that a functional splice variant, $P2X_7$-k, which is expressed in some tissues in the GSK model, escapes inactivation and therefore may explain the differences seen between the 2 lines (Nicke *et al* 2009). An alternative splice variant has been described in the Pfizer model but this is non-functional (Taylor *et al* 2009b). The implication from these observations is that findings in the GSK mouse should be interpreted with caution.

Data obtained from *in vitro* studies have been equally inconclusive. Experiments have been conducted examining the role of P2X7R in both osteoblasts and osteoclasts but the functional effect of the receptor in both cell types remains uncertain. Panupinthu *et al* (2008) reported a stimulatory effect of P2X7R on bone formation which was suggested to occur through osteoblast receptor-mediated production of lysophosphatidic acid, a promoter of osteogenesis (Sims *et al* 2013). In contrast, using an armoury of antagonists and agonists, Orriss *et al* (2012) found that P2X7R exerted an inhibitory influence on osteoblast function resulting in suppressed bone formation. These authors highlighted a number of methodological differences between these two studies to potentially explain the disparate findings.

In osteoclasts, P2X7R may have an inhibitory effect (prevention of bone resorption), as deficiency of the receptor has been shown to suppress apoptosis of mouse osteoclasts (Gartland *et al* 2003b). However, paradoxically, inhibition of the receptor using antagonists and a monoclonal antibody has been shown to limit the *generation* of multi-nucleated osteoclasts from precursor cells which would also theoretically lead to a net decrease in bone resorption (Agrawal *et al* 2010). Interestingly, one group have reported that P2X7R is required to actually release ATP, which is in turn metabolised to adenosine, which signals through P1 receptors to drive giant osteoclast formation (Pellegatti *et al* 2011). Deficiency of P2X7R prevented this process and inhibited resorption of bone.

The exact role of P2X7R in the skeletal system remains elusive, however, there is irrefutable evidence to indicate that in some way, the receptor is involved in bone homeostasis. Worthy of particular note are the observations that in man, loss-of-function P2X7R single nucleotide polymorphisms (SNPs) have been associated with an increased risk of developing osteoporosis (Gartland *et al* 2012) and fracture (Ohrlendorff *et al* 2007).

1.9.4.ii P2X7R and apoptosis.

Exposure to ATP can result in cell death by P2X7R-mediated mechanisms (Franceschi *et al* 1996). This may be a function of the P2X7R ion-channel as relatively a brief exposure to ATP (insufficient to permit pore formation) triggers apoptotic death in mast cells (Bulanova *et al* 2005). However, the pore-forming

capacity of P2X7R also seems to be important in causing cell death as it appears to lead to osmotic shifts and consequent cytolysis (Suprenant *et al* 1996).

P2X7R-mediated apoptosis has been shown in a number of cell types including skin epithelia (Gröschel-Stewart *et al* 1999), astrocytes (Zheng *et al* 1991), dendritic cells (Coutinho-Silva *et al* 1999), macrophages (Suprenant *et al* 1996) and, with respect to the vascular system, porcine aortic endothelial cells (von Albertini *et al* 1998). This functional role for the receptor appears to be clinically relevant. In experimental glomerulonephritis in mice, P2X7R co-localised with glomerular cells positive for the apoptotic marker, caspase-3 (Turner *et al* 2007) and genetic deficiency of P2X7R ameliorated renal injury in this model (Taylor *et al* 2009a).

With relevance to the possible pathogenesis of AC, P2X7R is thought to enhance apoptosis of human osteoblasts (Gartland *et al* 2001). As discussed above, P2X7R-mediated apoptosis of osteoclasts has also been reported (Gartland *et al* 2003b), however other groups have suggested a suppressed apoptotic effect (Grol *et al* 2009). Whether P2X7R is also involved in apoptosis of VSMCs is currently unknown.

1.9.4.iii P2X7R and ECM degradation.

Release of ECM-degrading enzymes from mononuclear cells represents a further mechanism potentially linking P2X7R and AC. Work studying this cell type in culture demonstrated P2X7R-dependent release of MMP-9 following exposure to ATP. This effect was lost when cells were also treated with P2X7R antagonists (Gu & Wiley 2006). In addition, another group were able to show P2X7R-dependent release of cathepsins from macrophages in concentrations sufficient to degrade a collagen matrix (Lopez-Castejon *et al* 2010).

1.9.4.iv P2X7R and renal disease.

All causes of kidney injury, if unresolved for a prolonged period of time, have the potential to result in fibrosis of the renal interstitium. The extent of this fibrosis is known to correlate well with declining renal function (i.e. progression of CKD) (Bohle *et al* 1991, Nangaku 2004). P2X7R has been implicated in the aetiology of a number of specific renal pathologies including glomerulonephritis (Taylor *et al* 2009a), polycystic kidney disease (Chang *et al* 2011) and diabetic nephropathy

(Vonend *et al* 2004). However, more relevant to the development of AC is a reported link between the receptor and tubulointerstitial fibrosis.

Using the unilateral ureteric obstruction (UUO) model, Goncalves *et al* (2006) demonstrated after 14 days, that kidneys from $P2X7^{-/-}$ mice showed less collagen deposition and macrophage infiltration. In addition, significantly fewer myofibroblasts were detected in the medulla. Furthermore, *in vitro* studies have revealed a possible P2X7R-mediated cross-talk between renal epithelial cells and fibroblasts (Ponnusamy *et al* 2011) and receptor inhibition has also been shown to ameliorate fibrosis in non-renal models (Riteau *et al* 2010).

1.10 The ATP-Metabolising System And Calcification

1.10.1 ATP metabolism and PPi generation: the roles of ENPP-1 and ANK.

Data implicating direct signalling by purine receptors in the process of AC is just beginning to emerge, however more is known about the roles played by the enzymes involved in the hydrolysis of ATP (Figure 1.2) and the associated metabolites, in particular PPi. The ability of PPi to inhibit ectopic calcification was demonstrated almost half a century ago using subcutaneous injections in rats exposed to high doses of vitamin D (Fleisch *et al* 1965). The mechanism whereby this is achieved seems to be the chemisorption of PPi onto the surface of hydroxyapatite, preventing attachment of further calcium and phosphate, and thus inhibiting crystal growth (Francis 1969). More recent work has provided further experimental evidence of the importance of PPi in preventing AC. For example, cultured rodent aortic rings exposed to an elevated phosphate concentration will calcify following PPi removal using alkaline phosphatase (Lomashvili *et al* 2004). Treatment with intraperitoneal (ip) PPi also reduces AC induced in uraemic rats (O'Neill *et al* 2011) and also in ApoE KO mice (Riser *et al* 2011). In the setting of CKD in man, PPi levels inversely correlate with the degree of AC (O'Neill *et al* 2010), and reduced levels are seen in dialysis patients irrespective of dialysis modality, inflammation or nutritional status, when compared with control subjects (Lomashvili *et al* 2005).

1.10.1.i Clinical manifestations of genetic mutations in ENPP-1 - generalised AC of infancy and autosomal recessive hypophosphataemic rickets type 2.

As previously discussed (section 1.7), ENPP-1 generates PPi (and AMP) following the hydrolysis of ATP and alterations in this reaction are clinically relevant. One of the earliest and most significant discoveries in this respect was that autosomal recessive mutations leading to inactivation of ENPP-1 result in the condition of generalised AC of infancy (GACI) (Rutsch *et al* 2003). This disorder is characterised by increased hydroxyapatite deposition within the elastic laminae of arteries, with associated stenosis and mortality. The ectopic calcification seen in this disease is presumably due to reduced PPi production and availability. Indeed treatment with bisphosphonates, which are analogues of PPi, have been shown to improve the prognosis of the condition (Rutsch *et al* 2008). Subsequent genetic studies have demonstrated that inactivating mutations of the *ENPP-1* gene can also cause autosomal recessive hypophosphataemic rickets type 2 (ARHR2) (Levy-Litan *et al* 2010, Lorenz-Depiereux *et al* 2010). Moreover, the *ENPP-1* inactivating K121Q (rs1044498) polymorphism is associated with increased AC scores in dialysis patients (Eller *et al* 2008).

1.10.1.ii Murine models of ENPP-1 deficiency - correlation with human disease.

The potential importance of ENPP-1 in disorders of calcification was initially discovered from work studying the 'tiptoe walking' (ttw/ttw) mouse. This mouse, originally developed in Japan in 1978 (Hosoda *et al* 1981), is characterised by ectopic calcification most marked in peripheral and intervertebral joints (Sakamoto *et al* 1994), leading to progressive ankylosis. The phenotype was shown to result from a nonsense mutation in the *ENPP-1* gene (Okawa *et al* 1998). Subsequently an *ENPP-1* KO mouse was developed (Sali *et al* 1999), the phenotype of which has been investigated in detail.

These animals show spontaneous calcification of the coronary arteries and aorta (Mackenzie *et al* 2012) and markers of bone formation are demonstrable in the aortic media (Zhu *et al* 2011). Decreased serum calcium and phosphate concentrations are present compared with wild-type (WT) mice (Mackenzie *et al* 2012). Of interest, these mice also show increased levels of the phosphaturic hormone fibroblast growth factor 23 (FGF-23) (Mackenzie *et al* 2012), as has also been reported in ARHR2

(Levy-Litan *et al* 2010, Lorenz-Depiereux *et al* 2010): FGF23 has been linked to AC in patients with CKD (Desjardin *et al* 2012) and FGF23 mutations that resist degradation are the cause of autosomal dominant hypophosphataemic rickets (ADHR) (White *et al* 2000).

The bones of *ENPP-1* KO mice show abnormal mineralisation and architecture, probably due to decreased PPi availability for conversion to inorganic phosphate by TNAP (Anderson *et al* 2005). It is interesting to note that while the *ENPP-1* KO mouse biochemical and bone phenotype is similar to that of patients with ARHR2, these patients do not seem to develop AC. Conversely patients with GACI, while exhibiting the same vascular changes as *ENPP-1* KO mice, do not tend to show the same skeletal and biochemical abnormalities.

1.10.1.iii ENPP-1 regulation at the cellular level.

Limited information is available on the regulation of ENPP-1 expression and function in VSMCs. Using early passage rat VSMCs, Prosdocimo and colleagues (2010) showed a decrease in ENPP-1 mRNA expression under calcification conditions *in vitro*, growing cells in 5mM phosphate and 1µM forskolin (used to activate adenylate cyclase and thus elevate cyclic AMP (cAMP)) for 10 days. Of note, the authors were not able to demonstrate a significant decrease in mRNA expression when cells were grown in 5mM phosphate alone, implicating an important role for cAMP in the calcification pathway. These authors also assessed ENPP-1 protein expression and functional activity, and suggested that while both 5mM phosphate and 1µM forskolin could independently reduce protein expression after 10 days, functional activity was the same as at baseline, as shown by no change in methylene ATP (MeATP) metabolism, a specific substrate.

In contrast to this study, Huang and colleagues (2008), using later passage murine aortic VSMCs, showed an increase in ENPP-1 expression following exposure to 25µM forskolin and 5mM β-glycerolphosphate for 7 days in culture. In addition, Mathieu's group, using human valve cells, found an increase in ENPP-1 expression with increasing concentrations of phosphate in the culture medium (Cote *et al* 2012a). Furthermore, this group generated data suggesting that non-specific

inhibition of ecto-nucleotidases could attenuate AC in rats treated with warfarin (Cote *et al* 2012b).

It should be noted that this group used a different strain of rodent than Prosdocimo *et al* (2010) and the subtypes of ecto-nucleotidases detected in aortas were markedly different between the two laboratories. The regulation of ENPP-1 expression and activity is clearly complex and negative feedback mechanisms involving TNAP-regulated ENPP-1 expression and activity, described in experiments using bone cells (Johnson *et al* 2000) is an added complication. The regulation of ENPP-1 in the setting of CKD is currently unknown but worthy of investigation.

1.10.1.iv The role of ANK.

Another important player implicated in the generation of extracellular PPi is ANK, a transmembrane protein that may mediate intracellular PPi efflux from cells (Ho *et al* 2000, Terkeltaub 2001). Autosomal dominant inherited mutations in the gene encoding ANK have been demonstrated to cause two different calcification disorders: craniometaphyseal dysplasia (Nurnberg *et al* 2001) and autosomal dominant familial calcium PPi dihydrate deposition (Williams *et al* 2002). Furthermore, aortas taken from *Ank* KO mice calcify more readily than those from WT mice when exposed to an elevated phosphate concentration *in vitro* (Villa-Bellosta *et al* 2011a) and *Ank* KO mice fed a high phosphate diet develop AC (Murshed *et al* 2005). Intriguingly, Villa-Bellosta *et al* (2011a) have suggested that ANK might be able to transport ATP from the intra- to the extracellular compartment.

1.10.2 Roles played by other ecto-nucleotidases.

1.10.2.i TNAP.

The availability of PPi is not only dependent on its generation, but also on its metabolism which is controlled by the enzyme TNAP. This protein is present on most cell types, including VSMCs, and catalyses the conversion of PPi to inorganic phosphate, thereby promoting mineralisation (Murshed *et al* 2005). The human condition, hypophosphatasia, is caused by missense loss-of-function mutations in the *TNAP* gene. This inherited trait is considered to be an autosomal dominant negative, although recessive inheritance patterns have also been described (Mornet 2007).

TNAP serum levels are reduced in these patients, PPi concentrations increased, and bone mineralisation impaired (Russell *et al* 1971). *TNAP* KO mice die before weaning and exhibit a similar phenotype to the human disease (Fedde *et al* 1999).

TNAP has been linked to AC. Elegant experiments from O'Neill's group (Lomashvili *et al* 2008) used two rodent CKD models to demonstrate that both the expression and activity of TNAP are increased in uraemic conditions, suggesting this as a potential mechanism for the increased prevalence of AC in patients with CKD. While the exact pathway mediating the observed increase in TNAP was not elucidated, mRNA expression was not increased, but when aortic rings were isolated and incubated with uraemic serum, an increase in TNAP activity was detected, indicating that an as yet unidentified circulating factor may be responsible for up-regulating enzyme activity. The authors suggest that this factor is probably not phosphate or PTH, because of the low concentrations likely to have been present *in vitro*.

1.10.2.ii Mutations in NT5E in patients with calcification of arteries and joints.

Another significant finding arose recently from genetic studies of 3 families exhibiting extensive calcification of lower limb vessels in adulthood (St Hilaire *et al* 2011). These patients showed autosomal recessive homozygous or compound heterozygous mutations in the 5'-nucleotidase, ecto (*NT5E)* gene, which encodes the CD73 protein, an enzyme responsible for the conversion of AMP to adenosine (Arch & Newsholme 1978) (Figure 1.2).

To investigate the potential mechanism behind these findings the investigators examined skin fibroblasts from affected individuals and demonstrated a marked increase in TNAP activity and calcification when cells were incubated with β-glycerolphosphate compared with fibroblasts from healthy controls. These effects *in vitro* could be reversed by administration of either adenosine or rescue by transfection with a CD73-encoding vector.

The authors hypothesise that the calcification seen in individuals with CD73 mutations is due to decreased inhibition of TNAP secondary to reduced levels of adenosine. However, as pointed out by some commentators (Robson *et al* 2011), the expression profile of ecto-nucleotidases on fibroblasts is different to that on VSMCs;

moreover, *CD73* KO mice do not seem to exhibit ectopic calcification. Therefore the exact mechanism underlying these intriguing observations remains a subject for further investigation.

1.10.2.iii The potential involvement of CD39 in AC.

CD39 or NTPDase-1 has not, at present, been linked to AC directly, despite being highly expressed by VSMCs (Robson *et al* 2006). It is of interest that this enzyme, in its nucleotide hydrolyzing capacity, has been linked to other important roles within the vasculature, including modulation of thrombosis and inflammation (Robson *et al* 2005) and regulation of vascular tone (Kauffenstein *et al* 2010a). In addition, of all the ecto-nucleotidases, CD39 has the most evidence linking it directly to regulation of signalling through purine receptors (Kauffenstein *et al* 2010b). CD39 could potentially limit the availability of ATP for conversion to PPi by ENPP-1 and so it would be of interest to examine the expression and regulation of this enzyme in the context of AC.

PART 3 - Hypotheses, Rationales, Aims and Objectives

1.11 Primary Hypothesis

The work in this thesis tested the primary hypothesis that P2X7R contributes to the pathogenesis of CKD-associated AC.

1.11.1 Rationale.

As reviewed above (section 1.9.4), a large body of evidence links P2X7R, in non-vascular contexts, to many biological processes thought to be important in mediating CKD-associated AC. The potential mechanisms implicated in AC which could possibly involve P2X7R, and might therefore be disrupted by receptor inhibition, are summarised in Figure 1.3.

P2X7R is expressed on osteoblasts and reported by some groups to promote bone formation. VSMCs are described to convert to osteoblast-like cells (osteogenic transformation) during the process of AC where they contribute to ectopic

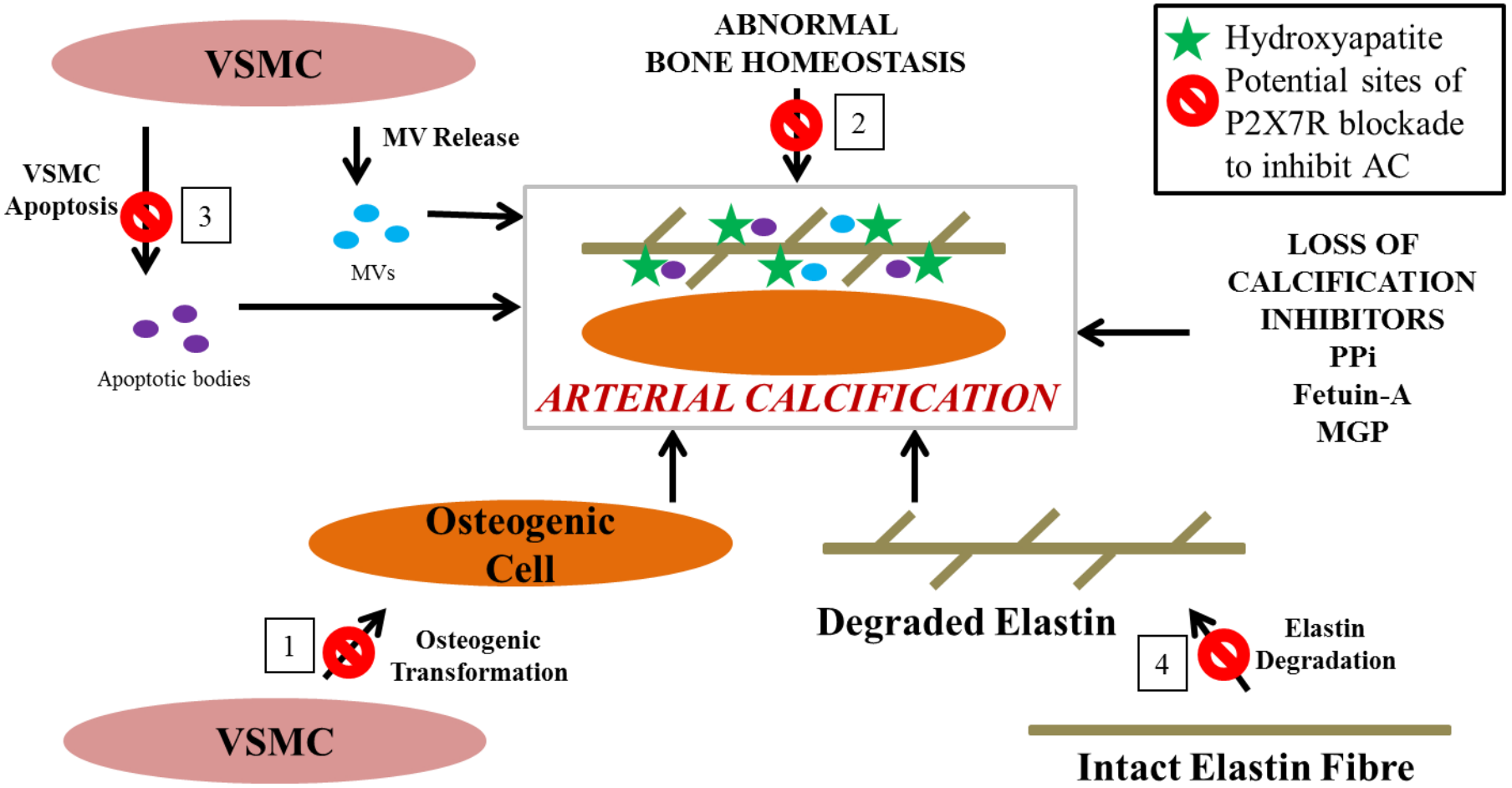

Figure 1.3. Pathogenic Pathways of AC Potentially Modifiable by P2X7R Blockade. Blockade of P2X7R might potentially attenuate AC by: 1. Inhibiting VSMC osteogenic transformation. 2. Maintaining systemic bone health. 3. Preventing VSMC apoptosis. 4. Limiting elastin degradation. In addition P2X7R blockade might prevent the progression of CKD in general (not shown, see text). PPi: inorganic pyrophosphate; MGP: matrix gla protein

mineralisation in a fashion resembling bone formation. Blockade of P2X7R might therefore inhibit this process. Alternatively, other studies have suggested that P2X7R may *suppress* bone formation. Disruption of normal bone homeostasis is associated with AC and therefore, conversely, inhibiting P2X7R might ameliorate arterial calcium deposition through *maintaining* systemic bone health.

In contexts unrelated to bone, AC is closely linked to VSMC apoptosis. Apoptosis is mediated by P2X7R in a number of non-vascular cell types and might potentially play a similar role in VSMCs. P2X7R is also known to contribute to release of enzymes capable of degrading ECM such as MMPs. ECM degradation is thought to be an important step in the development of AC and P2X7R blockade might limit this process. Finally, there is some evidence to suggest that P2X7R may contribute to the progression of CKD in general by promoting renal fibrosis.

To date, no previous studies have examined whether P2X7R plays a role in the development and/or the progression of AC. In addition, despite the adverse impacts on health conferred by AC, no specific treatments are currently available. The main goal of this project was therefore to determine if P2X7R is implicated in the aetiology of AC and whether the receptor might potentially be a future therapeutic target.

1.11.2 Experimental aims and objectives.

1. *To assess the role of P2X7R in AC in vitro using an optimised model.*

Specific objectives:

a) Confirm the expression of P2X7R in VSMCs.

b) Optimise an *in vitro* model of AC.

c) Examine the effects of P2X7R-specific antagonists and agonists on AC *in vitro*.

d) Study the effect of P2X7R deficiency on AC *in vitro* using genetically manipulated cells and/or tissue.

2. *To examine the impact of P2X7R gene deletion on AC in vivo.*

Specific objectives:

a) Develop and optimise a non-surgical mouse model of CKD-associated AC.

b) Determine the effect of P2X7R gene deletion on AC using this model.

3. *To evaluate the effect of pharmacological P2X7R blockade on AC in vivo.*

Specific objectives:

a) Optimise a rat model of CKD-associated AC.

b) Determine the expression of P2X7R in normal and calcified rodent arteries.

c) Investigate the effect of pharmacological P2X7R antagonism on AC in rats.

d) Assess the influence of pharmacological P2X7R antagonism on AC-related cellular pathways *in vivo.*

e) Examine the impact of pharmacological P2X7R antagonism on architectural changes in rodent bone caused by CKD.

1.12 Supplementary Hypothesis

This project also sought to test the hypothesis that the expression profiles of arterial ATP-metabolising enzymes are altered in CKD-associated AC.

1.12.1 Rationale.

As reviewed in Part 2 of this introduction, several components of the ATP-metabolising system have links with calcification. However, with the exception of TNAP, these ecto-nucleotidases have not been specifically assessed in the setting of CKD-associated AC. Uraemia has been shown to alter the activity of TNAP. Similar induced functional changes in companion ATP-related proteins could potentially impact on the production of molecules known to influence AC, in particular PPi. Knowledge of any such regulation would firstly increase the understanding of the pathogenesis of AC and secondly, potentially provide novel targets for therapeutic interventions.

Therefore whilst not the primary goal of this thesis, and not intended to be an exhaustive investigation, the work performed in relation to this supplementary hypothesis (Chapter 6) strived to generate preliminary data pertaining to the expression profiles of the constituents of the arterial ATP-metabolising system. Attention centred on ENPP-1 given its capacity to generate PPi.

1.12.2 Experimental aims and objectives.

1. *To examine the expression of ENPP-1 and associated enzymes responsible for ATP metabolism in normal and calcified arteries.*

   Specific objectives:

   a) Compare the expression of ENPP-1, CD39, CD73, TNAP and ANK in arteries of CKD rats with those from control animals.

   b) Analyse the functional activity of ENPP-1 in arteries taken from CKD rats and control animals.

   c) Assess the expression of ENPP-1 in calcified and un-calcified arteries taken from humans with ESRD.

CHAPTER 2 - MATERIALS AND METHODS

2.1 Reagents And Materials

Unless stated otherwise, all reagents were purchased from Sigma (Poole, UK). Tissue culture plasticware was manufactured by Corning (New York, USA). Microcentrifuge tubes were manufactured by Eppendorf (Hamburg, Germany). Dissection equipment was purchased from Thermo Fisher Scientific (Loughborough, UK) with the exception of scalpels which were obtained from Scientific Laboratory Supplies (SLS) (Nottingham, UK). All experimental diets were produced by SSNIFF (Soest, Germany). Suppliers of specific reagents and equipment are detailed in the relevant sections below. All water (H_2O) used for making reagents and for wash steps was molecular biology grade (resistivity 18.2MΩ).

2.2 Studies With Human Tissue

2.2.1 Ethical considerations.

The collection of, and all subsequent research undertaken with human arteries described in this thesis were approved by a Committee from the National Research Ethics Service. All patients provided prior written consent permitting the removal, (at the time of kidney transplantation), and subsequent use for research of, a short segment of one inferior epigastric artery.

2.2.2 Tissue collection, processing and storage.

Patients admitted to the Royal Free London NHS Foundation Trust in order to receive a kidney TP (from a live or a deceased donor), were eligible for inclusion. During the TP operation, following the routine surgical division of the inferior epigastric artery, a short segment of this vessel (typically 1-2cm in length) was removed and immediately placed into a vial containing Medium-199 supplemented with 0.1mg/ml streptomycin and 100U/ml penicillin. The sample was then stored at 4ºC for a maximum of 24 hours before processing.

A short segment from the end of the vessel was fixed in 10% Neutral-Buffered Formalin (NBF) for 24 hours, washed 3 times in Phosphate-Buffered Saline (PBS) and embedded in paraffin. The remaining vessel had as much adventitia removed as possible following which a transverse cut was made to divide it into 2 equal

segments. One half was snap-frozen in liquid nitrogen and stored at -80ºC. The other half was put into RNAlater (Qiagen, Manchester, UK) and stored at -20ºC until required.

2.3 Animal Husbandry

All *in vivo* work was approved by the Home Office Science Unit and performed under personal license 70/24024 and project license 70/7344 (Dr Jill Norman). Animals were housed and experimental work performed in the Comparative Biology Unit, UCL Medical School, Royal Free Campus. Rats and mice were maintained on a 12 hour light-dark cycle and given free access to food and water at all times. Animals were fed a standard maintenance diet (Special Diets Services, Essex, UK) until such time as dietary manipulation was commenced (see relevant experiments for details). Maximum cage occupancy for experiments was 4 for rats and 5 for mice. All rats used were adult, male Wistars, aged approximately 10-12 weeks and weighing approximately 400g (Charles River, Margate, UK). Genders, strains and ages of mice are described in the relevant sections. All animals fed experimental diets were weighed weekly with daily visual monitoring of clinical wellbeing.

2.4 Experiments To Develop A Murine Model Of Chronic Kidney Disease-Associated Arterial Calcification

2.4.1 Administration of folic acid to mice.

2.4.1.i Reagents and diets.

Folic acid powder was dissolved in 0.3M $NaHCO_3$ solution (vehicle) to obtain the required concentration, filtered through a 0.2µM filter and protected from light. The concentration of folic acid solution was such that the administered volume was consistently between 240-360µl irrespective of the dose received. Solutions were always made up fresh and administered within one hour of being prepared.

The experimental diet used in this study contained 1% (high) phosphate. All other constituents were present at normal levels (diet A, Table 2.1).

Constituent	DIET A	DIET B	DIET C	DIET D	DIET E	DIET F	DIET G
Adenine (%) [0]	0	**0.25** or 0	**0.20 or 0.25**	**0.75** or 0	**0.25**	0	**0.75**
Phosphate (%) [0.5]	**1.0**	**0.92**	**0.92**	**0.92**	**0.92**	0.50	0.50
Calcium (%) [0.7]	0.6	**1.0**	**1.0**	**1.0**	**1.0**	0.71	0.71
Crude Protein (%) [17.8]	17.8	**2.5 or 7.5**	**2.5**	**2.5**	**2.5**	**2.5**	**2.5**
Crude Fat (%) [4.6]	4.6	**7.6**	**7.6**	4.6	4.6	4.6	4.6
Chocolate Flavour	-	-	+	-	-	-	-
Vitamin D3 (IU/kg)	1000	1000	2000	1000	1000	1000	1000
Vitamin K3 (mg/kg)	4	4	4	4	4	4	4
Crude Fibre (%)	5.0	5.0	5.0	5.0	5.0	5.0	5.0
Crude Ash (%)	5.3	6.3	6.3	6.2	6.3	3.7	3.7
Starch (%)	29.8	34.4 or 28.7*	34.4	37.3	38.2	38.5	38.5
Sugar (%)	12.8	26.7	26.7	26.8	26.7	26.0	26.0

Table 2.1. Animal Diets. Summary of the main ingredients contained in experimental animal diets. Figures in bold depict the manipulated components of each formulation (i.e. those which differ substantially from physiological levels). Values in square brackets represent approximate 'normal' levels of the adjusted constituents in rodent diets (personal communications with SSNIFF scientists). Studies which employed each diet are as follows (in order as they appear in the thesis): Diet A – Mouse experiments involving folic acid, also used to 'pre-condition' some mice for consuming a synthetic diet (see Chapters 2 and 4). Diet B – Pilot studies involving adenine-feeding to mice (both protein levels employed), final mouse experiment examining effect of P2X7R gene deletion on AC (2.5% protein diet only, zero adenine contained in control diet for this study). C – Pilot studies to optimise mouse adenine-diet. D – First pilot rat study (control diet contained zero adenine), diet administered to rats in 'V' and 'HD' groups in main experiment assessing the use of a P2X7R antagonist on AC *in vivo*. E – second pilot study in rats. F – Control diet fed to rats in the 'N' group in the P2X7R antagonist experiment. G – Fed to rats in the 'A' group in the P2X7R antagonist experiment, also fed to 3 mice in pilot studies optimising adenine administration. *28.7% starch in diet containing 7.5% protein.

2.4.1.ii Study protocol.

DBA/2 mice were obtained from Harlan (Bicester, UK) and an in-house breeding colony was established. Females exclusively were used for this study. Mice of approximately 20 weeks of age received an ip injection of either folic acid or vehicle whilst under mild reversible isofluorane anaesthesia. The following day the high phosphate diet was started and continued for 20 weeks at which time mice were sacrificed. Blood was sampled at baseline, (before folic acid administration), and at subsequent time-points (detailed in Chapter 4).

2.4.2 Pilot studies to examine the effect of feeding adenine-containing diets to mice.

2.4.2.i Diets.

Diets B and C (Table 2.1) were principally used for these experiments. These diets contained 0.9% (high) phosphate, 1% (high) calcium and 7.6% fat. The fat content was elevated slightly from the standard 4.6% in order to try and make the pellets softer and more palatable for the mice. Diet C had chocolate flavouring added and a slightly elevated (but still physiological) vitamin D3 level (2000 IU/kg). The adenine and protein contents of these diets were adjusted as described in Chapter 4. Diet A (high phosphate only, Table 2.1) was fed to some mice for a week before the adenine-containing feed was started in order to 'pre-condition' the animals for eating a synthetic diet (see Chapter 4). The effect of 0.75% adenine was examined in 3 mice (see Chapter 4).

2.4.2.ii Study animals.

Mice used in these experiments were aged 10-12 weeks. A number of pilot studies using adenine-containing feed were performed (see Chapter 4). The first pilot study involved male and female WT DBA/2 mice taken from the in-house breeding colony. Subsequent studies assessed C57Bl/6 males (obtained from Charles River, Margate, UK) and backcrossed WT male mice of the 5^{th} generation (described in section 2.5).

2.4.2.iii Administration of diets.

Test diets were fed to mice for 6 weeks unless they were poorly tolerated and had to be withdrawn early. For the early experiments, diets were administered in the form of both pellets and powder, however powder tended to be scuffed out into bedding and that remaining in feeding bowels found wet. As such, pellets only were used for the later studies.

2.5 Backcrossing Of P2X7$^{-/-}$ Mice Onto The DBA/2 Background

2.5.1 Background: original generation of P2X7$^{-/-}$ mice.

Pfizer P2X7$^{-/-}$ mice were originally generated by inserting a neomycin cassette into exon 13 and deletion of nucleotides 1527-1607 (Solle *et al* 2001) and ultimately maintained on the Bl/6 background. All P2X7$^{-/-}$ mice used in this thesis are the Pfizer model.

2.5.2 Backcrossing procedure.

The aim of backcrossing was to transfer the P2X7$^{-/-}$ (on the C57Bl/6, calcification resistant background) onto the DBA/2 (calcification prone) background (Eaton *et al* 1978). To obtain at least 97% of the DBA/2 background it was calculated that a minimum of 5 backcrossings would be required. Initially 3 adult male P2X7$^{-/-}$ mice (Pfizer, New York, New York, USA) were kindly donated by Dr Frederick Tam (Imperial College, London, UK) and bred with 3 WT female DBA/2 mice (Harlan, Bicester, UK). Male offspring identified by genotyping as heterozygous were backcrossed with WT DBA/2 females to produce the subsequent generation. Initially, male offspring were bred with the original 3 WT female mice, however, after generation 3 it was necessary to obtain new, younger females to continue with backcrossing. Backcrossing was stopped when the 5th generation had been reached, and 5th generation heterozygous mice were then bred to produce WTs and P2X7$^{-/-}$. Mice used in the final experiment to assess the effect P2X7R gene deletion on AC (see section 2.6 and Chapter 4) were either offspring from these breeding pairs or offspring of subsequent WT and KO pairs that were set up. However, as no further backcrossing occurred after the 5th generation, all mice were of the same background. All mice were genotyped before entry into an experiment.

2.5.3 Genotyping of mice.

Ear punches were obtained under mild, reversible isofluorane anaesthesia. Tissue samples were digested and deoxyribonucleic acid (DNA) liberated using an adapted 'HotShot' protocol (Truett *et al* 2000). This method works on the principle that NaOH will denature double-stranded DNA by causing hydrogen bonds between nitrogenous bases to loosen. Tris(hydroxymethyl)aminomethane (Tris)-Cl is included to maintain pH.

2.5.3.i Solutions.

Stock solutions (50x) were made up:

Solution 1 contained 1.25M NaOH, 10mM ethylenediaminetetraacetic acid (EDTA), pH≈12, made by dissolving 50g NaOH and 2.9g EDTA into ≈900ml H_2O which was then made up to 1L.

Solution 2 contained 2M Tris-Cl, pH≈5, made by dissolving 315.2g Tris-Cl in ≈900ml H_2O which was then made up to 1L.

2.5.3.ii Genotyping procedure.

Fresh 1x aliquots of solutions 1 and 2 were made by adding 1470µl polymerase chain reaction (PCR) -grade water to 30ul of each 50x solution. 75µl of solution 1 was put into each 0.2ml PCR tube and earclips were then added (one per tube). Samples were incubated on a GeneAmp PCR System (Applied Biosystems) at 95°C for 30 minutes followed by a 4°C hold. Samples were then removed and 75µl of solution 2 was added to each. Samples were mixed and then, if not analysed immediately, stored at -20°C.

To run the genotyping reaction, 2µl DNA was added to 23µl of a 'mastermix 'of reagents, the contents and relative proportions of which were the following:

- 12.5µl REDTaq ReadyMix.
- 1µl of each primer (4 primers were required – see Table 2.2).
- PCR grade water to make up to 23µl.

The PCR steps and conditions for genotyping were as follows:

1. 3 min at 94°C
2. 30 seconds at 94°C
3. 1min at 60°C
4. 1min at 72°C.

   Steps 2-4 were repeated for 35 cycles.
5. 2 min at 72°C
6. Hold at 10°C

The PCR run was performed using the same machine as that used for DNA extraction. PCR products, along with a 100 base-pair (bp) marker ladder (Thermo Fisher Scientific), were then electrophoresed on a 2% agarose gel made with 1x TAE (Tris-Acetate-EDTA) containing 0.04ul/ml ethidium bromide at 80V for 40min. 1x TAE was made by diluting a 50x TAE solution (containing 2M Tris acetate and 0.05M EDTA at pH 8.2) in H_2O.

Bands were observed under ultraviolet (UV) light in a UV lightbox (Biorad, Hemel Hempstead, UK). A single band at 363bp indicated WT; a single band at 280bp indicated P2X7$^{-/-}$; double bands indicated heterzygous mice (Figure 2.1).

Wild Type Forward	TGG ACT TCT CCG ACC TGT CT
Wild Type Reverse	TGG CAT AGC ACC TGT AAG CA
Mutant Forward	CTT GGG TGG AGA GGC TAT TC
Mutant Reverse	AGG TGA GAT GAC AGG AGA TC

Table 2.2. Primers used for P2X7 Genotyping of Mice.

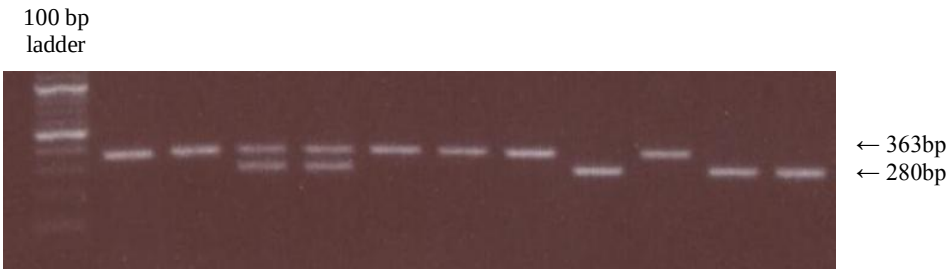

Figure 2.1. Genotyping of Mice. PCR products were run on a 2% agarose gel and visualised under UV light. A single band at 363bp indicated WT; a single band at 280bp indicated P2X7$^{-/-}$; double bands indicate heterzygous mice. A 100 bp reference ladder is shown in the left-hand land.

2.6 Experiment To Determine The Effect Of P2X7R Gene Deletion On Arterial Calcification

2.6.1 Study animals.

Male WT and P2X7$^{-/-}$ mice aged 10-14 weeks were entered into the study. The generation and background of these mice is described in section 2.5. Where possible, mice were caged in pairs, although by necessity a few triplet and singleton cages were set up. These were comparable in number for WTs and KOs. Baseline blood was taken in the week prior to dietary manipulation.

2.6.2 Study protocol.

Mice were divided into 4 groups: WT and P2X7$^{-/-}$ controls (WTC, n=8, and KOC, n=8) and WT-adenine and P2X7$^{-/-}$-adenine groups (WTA, n=11, and KOA, n=10). Mice were fed a diet containing 0.9% phosphate, 1% calcium, 7.6% fat and 2.5% protein with the addition of adenine (0.25%) as appropriate (Diet B, Table 2.1). Animals were fed test diets for 6 weeks before sacrifice.

2.7 Experiment To Assess The Influence Of A Selective P2X7R Antagonist On Arterial Calcification In Rats

2.7.1 Pilot studies examining the effects of administering adenine-containing diets to rats.

Small pilot studies were first undertaken to optimise the *in vivo* model for use in the final experiment. In the first of these, rats were divided into 2 groups (n=4 per group). All were fed a diet containing 0.92% phosphorus, 1% calcium and 2.5% protein for 4 weeks. 0.75% adenine was added for 4 animals (Diet D, Table 2.1).

A second pilot study was performed whereby a further 4 rats were fed a similar diet but with an adenine content of 0.25% (Diet E, Table 2.1) for 6 weeks. This regime was not as successful for inducing AC as Diet D hence 0.75% adenine was employed in the final experiment (see below and Chapter 5 for details).

2.7.2 Group and dietary assignments for final experiment.

Rats were divided into 5 groups and fed test diets for 4 weeks. The ‘control’ group (N, n=10), received a diet containing a normal amount of phosphate (0.5%) and calcium (0.7%) and a low (2.5%) protein content (Diet F, Table 2.1). The ‘adenine

alone' group (A, n=6), received a similar diet but with the addition of 0.75% adenine (Diet G, Table 2.1). The 'vehicle-treated' (V, n=9), 'low-dose P2X7R antagonist-treated' (LD, n=7) and 'high-dose P2X7R antagonist-treated' (HD, n=8) groups were fed a similar diet to the A group, but with elevated levels of phosphate and calcium (0.92% and 1% respectively), i.e. the diet from the pilot experiments which resulted in the most consistent AC (Diet D, Table 2.1).

2.7.3 Preparation and administration of the selective P2X7R antagonist.

For the duration of the 4 weeks, animals in the V, LD and HD groups received twice daily oral gavage of either the P2X7R antagonist AZ11657312 (AstraZeneca, Cheshire, UK) (LD and HD groups) or vehicle alone (0.5% hydroxypropyl methylcellulose/0.1% Tween80) (HPMC) (AstraZeneca) (V group). LD rats received 20mg/kg per dose, the HD group received 60mg/kg. These doses were selected based upon previous data (held by AstraZeneca), showing biological effects of the higher dose in other, (non-vascular related), *in vivo* experimental rat models. Owing to practical and logistical restrictions, the N and A groups were not gavaged and were run either side, (A group before, and N group after), of the period during which gavaging of the other 3 groups took place.

AZ11657312 was provided as a powder and the manufacturer advised that the compound would be soluble in HPMC for up to 2 weeks at ambient temperature, in the dark at pH 6.5. In general, fresh batches were made up on a weekly basis. The required mass of powder was weighed out and placed into a sterile receptacle marked with accurate volume indicators. Approximately 75% of the required vehicle volume was then added before briefly vortexing to wet the compound. The pH was then brought up to 6.5 with the drop-wise addition of 0.1M NaOH and vehicle added to make up to the final required volume. Aliquots of 10ml were made and stored at room temperature in the dark (wrapped in aluminium foil). All stocks of the vehicle were also brought up to pH 6.5 by the drop-wise addition of 0.1M NaOH and stored similarly.

2.7.3.i Compound administration by oral gavage.

Oral gavaging was performed at 8am and 4pm daily throughout the study period. Animals were scruffed, and a metal gavage cannula, connected to a 5ml syringe

containing the appropriate volume of study agent, was passed down the oesophagus into the stomach prior to administration. Animals were immediately returned to their cage and observed for signs of distress. On occasion, usually due to severe resistance in passing the gavage cannula, dosing was not attempted (detailed in Chapter 5).

2.7.4 Determination of serum levels of AZ11657312.

To assess whether adequate serum concentrations of antagonist were maintained for a sufficient length of time, blood samples were taken from rats in the HD group. 4 rats had blood withdrawn from the tail vein on the first day of study at 2 hours post first dose (peak), and immediately before the second dose (trough). Further blood samples were taken on day 14 (trough level) and at sacrifice (trough). In addition, day 14 peak samples were taken from the other 4 HD rats. Serum drug concentrations were measured *post hoc* by liquid chromatography-tandem mass spectrometry (Xenogesis, Nottingham, UK).

2.7.5 Collection of biological samples.

On day 14 of study, rats had 500µl blood withdrawn from a tail vein for assessment of renal and liver function. On the penultimate day of study, immediately following the morning gavage, rats were put into individual metabolic cages for 24 hours where they were provided with free access to study diet and water. The following morning they were weighed and returned to their home cage. The urine volume was measured before snap freezing 5 x 1ml aliquots, and the water intake determined. Rats were then sacrificed and tissue collected.

2.8 Blood Sampling From Rodents

Blood samples from live mice were obtained from either the tail or saphenous veins. Blood from deceased mice was obtained via cardiac puncture using a 25G needle. Mouse blood was collected in 250µl lithium-heparin containing microvettes (Sarstedt, Leicester, UK). Following collection, blood was centrifuged at 400xg for 20 minutes at room temperature. Serum was then removed, aliquotted out, and stored at -80ºC.

Blood samples from live rats were taken from the tail vein using a ‘butterfly’ needle, collected into the same type of receptacle, and processed in the same way, as mouse

samples. The exception to this was for samples taken for measurement of drug levels which were collected into EDTA-containing vials (Sarstedt). Blood samples from deceased rats were taken via cardiac puncture using a 23G needle, and collected into 6ml, lithium-heparin containing vials (Sarstedt). Following collection, blood was centrifuged at 400xg for 20 minutes. Serum was then collected, aliquotted, and stored at -80ºC.

2.9 Harvesting And Storage Of Rodent Tissue

Mice and rats were individually sacrificed by exposure to an elevated CO_2 concentration. Death was confirmed by cervical dislocation. The ventral surface was then sprayed with 70% ethanol and a midline incision made, starting over the lower abdomen and working up until the diaphragm was punctured. This was then divided, the rib cage reflected, and blood drawn from the right ventricle.

Liver, spleen, bowel and lungs were removed, following which both kidneys were dissected out and weighed. For rats, a transverse incision was made to divide the left kidney into upper and lower halves. A transverse slice was taken from the cut surface of the upper half and fixed in 4% paraformaldehyde (PFA) (TAAB, Aldermaston, UK) for 24 hours before washing 3 times in PBS. Specimens were kept at 4ºC in PBS until processing for histological assessment. The remaining left upper pole was cut in half longitudinally. One half was snap-frozen in liquid nitrogen and stored at -80ºC, the other half was stored at -20 ºC in RNAlater (Qiagen, Manchester, UK). For mice, the top half of the left kidney was fixed in 4% PFA (TAAB) and subsequently processed as described above. The lower half was snap-frozen.

Following harvesting of kidney tissue, a cut was made through the right iliac artery and the aorta flushed through with ice-cold PBS. Aortas were then dissected out and cleaned of excess connective tissue. Rat aortas were divided into 3 sections – arch, thoracic and abdominal. The first 2cm of thoracic and abdominal aorta, and the aortic arch from the root to the brachiocephalic branch, were all placed into PBS for subsequent quantitative analysis of calcium content. The next 2mm from each segment was fixed in 4% PFA (TAAB) for histological assessment (subsequent handling was as described for kidney tissue above). The remaining arch and thoracic

aorta were snap-frozen in liquid nitrogen and stored at -80ºC. A small segment of abdominal aorta was snap-frozen and stored in a similar way, however the majority of remaining abdominal aorta was stored in RNA later (Qiagen) at -20ºC. For mouse aortas, a thin slice was taken from the proximal arch and fixed for histological processing and the rest of the arch (until just distal to the third branch) was put into PBS for subsequent assessment of calcium content. The remaining aorta was all placed into RNAlater (Qiagen) except for a thin slice taken at the level of the diaphragm for histological processing as above.

Finally, the right femur (rats) was dissected out, quickly cleaned and fixed in 10% NBF for 48 hours, before being moved into 70% ethanol at room temperature for medium-term storage.

2.10 Biochemical Analysis Of Serum And Urine

2.10.1 Routine biochemistry.

All routine serum and urine biochemical analysis was performed at MRC Harwell, Oxfordshire, UK. The majority of analytical techniques involved colourimetric quantification of analytes following a reaction with specific reagents (all detailed in Hough *et al* 2002). Creatinine was analysed using the enzymatic method and urea using the urease/glutamate dehydrogenase method. Calcium and phosphate were analysed using arsenazo III and molybdate respectively. Alkaline phosphatase (ALP) was measured using 4-nitrophenylphosphate and albumin using bromocresol green. Cholesterol analysis employed cholesterol oxidase and peroxidase and alanine transaminase (ALT) measurement utilised a modified technique without pyridoxyl phosphate. Urinary protein was determined photometrically.

2.10.1.i Calculation of corrected calcium.

Corrected calcium was determined by the following formula:

Corrected calcium = measured total calcium - ((measured albumin - 30) x 0.017)

This is based on the assumption that there is 0.017 mmol/l calcium per g/l albumin and that average albumin = 30g/l (Stechman *et al* 2010).

2.10.2 PTH Enzyme-Linked Immunosorbent Assay (ELISA).

2.10.2.i General principle.

The PTH concentration in rat serum was measured using the Rat Intact PTH ELISA Kit (Immutopics Inc, San Clemente, California, USA). This kit utilises the 'sandwich' ELISA principle whereby samples are incubated in a streptavidin-coated well together with 2 PTH antibodies (a biotinylated capture antibody and a horseradish peroxidase (HRP) -conjugated antibody respectively) to form a complex. Following the incubation period and a series of wash steps, a substrate solution is applied to the residual complex bound to the well and incubated. The colour intensity produced by the resultant reaction is directly proportional to the amount of PTH present and this can be measured spectrophotometrically.

2.10.2.ii Method.

Serum samples were slowly thawed on ice and then centrifuged at 400xg at 4ºC for 1 minute in order to pellet off any fibrin strands or cellular debris. Samples, positive controls and standards (all 25µl) were pipetted out in duplicate into test wells (positive controls and standards were provided in the kit). A solution (100µl) containing both antibodies was then applied to all wells which were incubated at room temperature for 3 hours in the dark with gentle rocking. An additional volume of one sample was run without antibody added as a negative control.

Following this incubation step wells were washed 5 times with 350µl wash solution before applying 150µl ELISA HRP substrate for 30 minutes (incubation carried out at room temperature in the dark with gentle rocking). Absorbance was then read at 620nm. ELISA Stop Solution (100µl) was then immediately added to each well and mixed for 1 minute. The absorbance was then read at 450nm on a microplate reader (EZ Read 400; Biochrom Ltd, Cambridge, UK). Final PTH concentrations were calculated using the standard curve. The standards provided in the kit were such that the working range for the assay was 0 – 3160 pg/ml.

2.10.3 PPi assay.

To assess relative differences in PPi content between serum samples, the 'Pyrophosphate Assay Kit II' was used (Abcam, Cambridge, UK). This kit uses a

proprietary fluorogenic PPi sensor which has a fluorescence intensity proportional to the concentration of PPi present.

Initially, 20µl of each serum sample was added to 80µl PBS and the absorbance profile read in order to assess for scatter and any potential absorbance within the range of emission wavelengths relevant for the measurement of PPi fluorescence. No major absorbance peaks were detected around 470nm for any sample, and in general the degree of scatter was similar for all.

For PPi measurement, 50µl serum was incubated with 50µl PPi sensor at room temperature in the dark for 10 minutes before reading the fluorescence at Ex/Em = 370/470nm using a FLUOstar Omega plate reader (BMG Labtech, Ortenberg, Germany). Test samples were run in duplicate, and in addition, a further 50µl volume of each was analysed without the presence of PPi sensor in order to control for background autofluorescence. The final results were calculated as the mean of duplicate samples and expressed in arbitrary fluorescence units.

2.11 Assessment Of ENPP-1 Activity In Arterial Tissue

ENPP-1 activity was assessed by colourimetrically measuring the hydrolysis of the synthetic substrate thymidine 5'-monophosphate p-nitrophenyl ester sodium salt (pNP-TMP) (Nam *et al* 2011, Lomashvili *et al* 2011). This reaction liberates p-nitrophenylate which causes the reaction solution to turn yellow, the optical density of which can be measured at 405nm. It should be noted that this assay is not specific for ENPP-1 as pNP-TMP is also a substrate for other ENPPs. However, as ENPP-1 has been shown to be the dominant ENPP in both cultured VSMCs and in-tact arterial tissue (Villa-Bellosta *et al* 2011a) this system represents a reasonable method for evaluating its activity.

Arterial tissue was taken from storage at -80ºC and slowly thawed on ice in isotonic buffer (PBS containing 1mM $CaCl_2$). Volumes of reaction solution (200µl), consisting of 180µl buffer and 20µl pNP-TMP (5mM final concentration), were pipetted into a 96 well-plate and baseline optical density readings were taken. Arterial segments had any residual blot clot removed and were divided in 2 in order to run samples in duplicate. These were then placed into the reaction solution-containing wells and incubated at room temperature in the dark for 1 hour. Wells

containing only reaction solution and/or isotonic buffer (without tissue) were run as negative controls. Rings were removed from their wells, dried overnight and weighed. The final optical density of each individual reaction was recorded and the mean taken of replicate samples. Results were expressed as change in optical density (arbitrary units) per mg tissue.

2.12 Micro-Computerised Tomography (CT) Analysis Of Bone

All work involving micro-CT technology was performed in collaboration with Professor Tim Arnett (UCL, London).

2.12.1 General principles.

Examination of an object by micro-CT enables information to be obtained about its 3-dimensional (3D) structure in a convenient and relatively quick manner. Test objects are held in place on a high-precision stage and rotated. Two-dimensional X-ray shadows are obtained from a number of angular viewpoints and these are used to reconstruct cross-sectional images of the object using a well-defined cone-beam algorithm originally described by Feldkamp *et al* (1984). Ultimately this information generates a 3D representation of the internal micro-structure of the object under examination.

2.12.2 Micro-CT scanning.

Femurs were taken from storage (in 70% ethanol), wrapped in cling-film (to prevent drying out and movement artefact during scanning), and mounted on the stage of the scanner (SKYSCAN 1172, Brucker, Kontich, Belgium). Scanning conditions consisted of a 0.5mm aluminium filter, an X-ray voltage of 40kV, an X-ray current of 250µA and a camera resolution of 2000x1048. The rotation step was set a 0.4º. Scans typically lasted an hour in length. Upon completion of the scan, cross-sectional images were reconstructed as outlined above.

2.12.3 Data analysis.

In order to analyze trabecular and cortical bone parameters it was first necessary to define a ‘reference point’ on each femur to ensure measurements were standardised across samples. This point was determined using the reconstructed images and moving up slice by slice, starting at the growth plate, until the first ‘broken bridge’

of primary spongiosa was seen (Figure 2.2A). For each femur, the trabecular bone was examined in a 1mm long segment starting 3mm above the reference point, and cortical bone was examined in a 1mm long segment starting 6.5mm above the reference point.

The areas containing trabecular and cortical bone to be analyzed were defined in the respective 1mm segments on each femur by digitally drawing round the 'region of interest' every 10 slices (Figures 2.2B and C). Slices in between were automatically interpolated by the computer programme. Regions of interest were then converted into binary images and processed by SKYSCAN software to generate measurements of bone parameters.

2.13 Tissue Culture

2.13.1 Specific reagents.

The P2X7R antagonists A438079 and A839977 were both purchased from Tocris (Bristol, UK). BzATP and A438079 were made up in sterile H_2O. A839977 was made up in dimethyl sulfoxide (DMSO). Corresponding volumes of these vehicular agents were added to control medium for experiments.

For experiments using elastase, porcine pancreatic elastase was bought as lyophilised powder and reconstituted with sterile H_2O. This was then aliquotted and stored at -20ºC. For experiments, the required volume of thawed elastase solution was added directly to culture medium.

For experiments using alkaline phosphatase, calf intestinal alkaline phosphatase (Invitrogen, Paisley, UK) was purchased as a solution and stored at -20ºC until

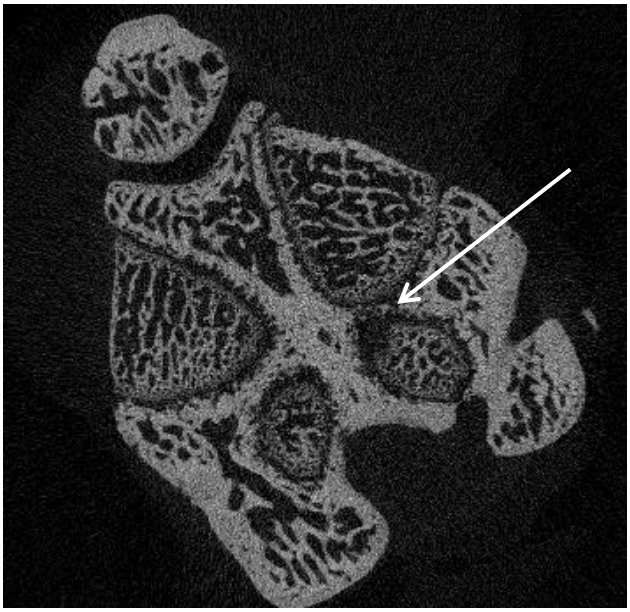

A

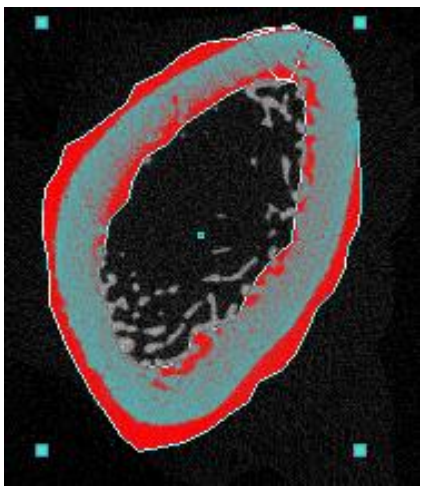

B

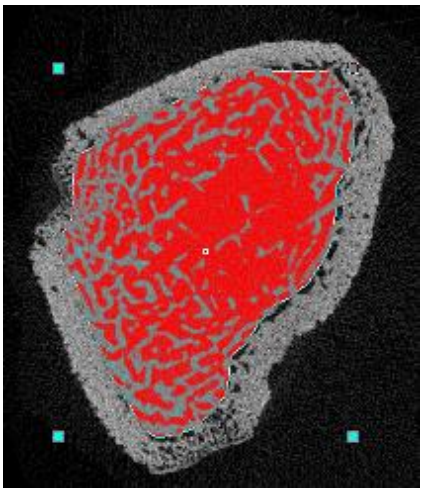

C

Figure 2.2. Micro-CT Analysis of Bone. A: Identification of Reference Point. The 'reference point' on each femur was determined by moving up slice by slice, starting at the growth plate, until the first 'broken bridge' of primary spongiosa was seen (arrow). For each femur, the trabecular bone was examined in a 1mm long segment starting 3mm above the reference point, and cortical bone was examined in a 1mm long segment starting 6.5mm above the reference point. B: Cortical Bone Region of Interest. A line was digitally drawn around the whole cross-sectional image followed by a second line within the central portion of the image in order to exclude any trabecular bone. The area selected for analysis was then highlighted red. C: Trabecular Bone Region of Interest. A single line was digitally drawn in the centre of the image in order to separate the cortical and trabecular bone. The area selected for analysis was then highlighted red.

required. It was then added directly to culture medium to obtain the required concentration.

To increase the pH of tissue culture medium, drops of sterile 10M NaOH were added to basal medium. Following mixing, the pH of a 3ml aliquot was taken immediately using a pH probe.

2.13.2 *In vitro* culture of human VSMCs.

Primary human VSMCs (hVSMCs) (TCS Cell Works, Buckingham, UK) were grown at 37°C and 5% CO_2 in cell culture flasks containing medium M199 (Lonza, Slough, UK) supplemented with growth factors (smooth muscle cell growth supplement, (TCS Cell Works)), 5% fetal calf serum (as part of the growth supplement), 4mM L-glutamine (Invitrogen), 25ug/ml gentamicin and 50ng/ml amphotericin. At approximately 80% confluence cells were trypsinised and passaged at no greater than 1:3 split using warmed 1X 0.05% trypsin-EDTA (Invitrogen). For experiments, cells were used at passage 6-10 and plated at an approximate density of $1x10^4$ cells per ml. Cells were counted using a haemocytometer and non-viable cells were stained with trypan blue.

At 50-60% confluency cells were serum-starved overnight and then exposed to experimental medium. 'Calcification-promoting medium' was made by supplementing basal medium with small volumes of either 3M CaCl and/or 3M NaH_2PO_4 to obtain the required concentration of calcium and phosphate respectively. In all experimental medium (control or calcification-promoting) serum was supplemented to 4% unless otherwise indicated and contained gentamcin, amphotericin and L-glutamine at the same concentrations as detailed above. Experiments ran for the time courses indicated (see Chapter 3). Medium was changed every 2-3 days.

2.13.3 Generation of rodent VSMCs.

To reduce the number of animals used, aortas of Sprague-Dawley rats taken from control arms of experiments were kindly donated from others in our group. Aortas were cleaned of blood, fat and connective tissue under a dissecting microscope and cut into rings approximately 1mm in depth. Rings were then cultured in identical conditions as those described for hVSMCs. It was usual to observe outgrowths of

cells after 2 weeks. When significant outgrowths were visible, rings were then taken out and placed in fresh culture dishes. Cells were trypsinised and placed in fresh culture dishes as described above. Cells were characterised as VSMCs by positive immunofluorescent staining for α-SMA and smooth muscle myosin heavy chain (SMMHC), and also by light microscopic evaluation of their growth pattern, with 'hill-and-valley' morphology considered typical of VSMCs (Proudfoot & Shanahan 2012) (shown in Chapter 3).

2.13.4 Culture of rodent aortic rings.

Unless otherwise stated, all aortic ring culture experiments were performed using medium M199 containing Earle's buffered salt solution, 4mM L-glutamine, 6 g/L 4-(2-hydroxyethyl)-1-piperazineethanesulfonic acid (HEPES) and 2.2 g/L NaHCO3 (Lonza), supplemented with 25ug/ml gentamicin and 50ng/ml amphotericin.

Wistar rats (of similar characteristics as those described for *in vivo* work above) were sacrificed by exposure to an elevated carbon dioxide concentration. Aortas were immediately dissected out using standard sterile procedures and placed into culture medium on ice. Fine dissection of the aorta was then performed using a dissecting microscope in a Class II lamina flow cabinet. Blood, fat and connective tissue was removed but a small covering of adventitia was left *in situ* to minimise injury to the medial layer. Injury to the arterial media at time of harvest has been shown to contribute to calcification (Lomashvili *et al* 2004). Aortas were then divided into segments of approximately 3-4mm in length, taken from the thoracic to the distal abdominal section, measured using a ruler under the microscopic. Segments were placed into individual wells of a 24-well plate containing culture medium which had been left to equilibrate in an incubator at 37°C and 5% CO_2 for a number of hours beforehand. A typical aorta yielded around 20 segments of this size.

The following day rings were exposed to experimental medium. Rings from adjacent segments of aorta would be exposed to different study conditions. To make experimental medium, individual volumes (one per condition) of basal medium were placed in an incubator for at least 1 hour to equilibrate to 37°C and 5% CO_2. Individual volumes were then quickly taken out of the incubator, an appropriate volume of NaH_2PO_4 added to bring the phosphate concentration up to the required

level, and then placed back in the incubator for at least another hour. This was necessary to avoid major increases in medium pH (due to loss of CO_2 buffering) which might result in precipitation of the supplemented ions (Lomashvili *et al* 2004). Following this, the necessary volume of reagent (e.g. P2X7R antagonist) was added to generate the final experimental medium. Rings were then cultured in their respective medium for 10 days. Medium was changed every 2-3 days following this protocol.

2.14 Viability Testing Of Cultured Aortas

Viability of cultured aortas was assessed as a function of the ATP-metabolising capacity of the vessel. Rings were cultured as described above except that the medium did not contain phenol-red (Invitrogen). At desired time-points medium was removed from rings and immediately snap-frozen in liquid nitrogen and stored at -20ºC until required. Rings were immediately placed into fresh medium.

The ATP content of culture medium was determined using the Adenosine 5'-triphosphate (ATP) Bioluminescent Assay Kit (FLAA). A master mix of reaction reagents was made up in the following proportions: 300µl ATP Assay Mix (containing luciferase, luciferin, $MgSO_4$, dithiothreitol (DTT), EDTA, bovine serum albumin (BSA) and tricine buffer salts) made up initially in H_2O, 600µl Dilution Buffer (containing $MgSO_4$, DTT, EDTA, BSA and tricine buffer salts) made up initially in H_2O and 600µl H_2O.

Culture medium (50µl) was added to 100µl master mix. A standard curve was also prepared. Samples were then analysed using an Anthos Lucy 1 Luminometer (Anthos Labtech Instruments, Salzburg, Austria).

2.15 O-Cresolphthalein Complexone Method To Quantify The Calcium Content Of A Solution

2.15.1 General principle.

This method utilises the principle that in an alkaline medium, calcium ions form a violet-coloured complex with o-cresolphthalein. 8-hydroxyquinoline is included in the reaction to minimise any interference from magnesium ions (Sarkar & Chauhan

1967). The absorbance of the resultant complex can be measured spectophotometrically and compared to a standard curve.

2.15.2 Sample preparation.

Medium was removed and cells and aortic rings were washed twice in PBS (free of calcium and magnesium), and in the case of rings, as much as possible of the adventitia was removed under a dissecting microscope (usually all although this was not possible in the case of rings from mice). Rings were then placed in 150ul 0.6M HCl overnight to liberate the deposited calcium. For cells, 0.6M HCl was applied directly into the wells and plates were then left overnight. For *in vivo* samples, aortic segments were cleaned of adherent blood clot and fat, washed twice in PBS, and placed overnight in 0.6M HCl (500µl for rat aortas and 150µl for mouse tissue). Calcium content of the HCl was subsequently quantified using the o-cresolphthalein complexone method.

2.15.3 Reagents.

Colour reagent: 25mg o-cresolphthalein complexone powder was dissolved in a solution containing 15ml 11.6M HCl and 25ml H_2O. Following this 250mg 8 hydroxy-quinoline was added and the volume made up to 250ml with H_2O before dissolving completely.

Alkaline buffer: 37.8 ml of 2-amino-2-methyl-1-propanol with 150ml H_2O. The pH was adjusted to 10.7 with 11.6M HCl and the volume made up to 250ml with H_2O.

Both the colour reagent and alkaline buffer were shielded from light prior to use.

For each analysis appropriate calcium standards were prepared from a 50mg/dl stock standard which was made by dissolving 625 mg of dried and desiccated calcium carbonate with 3.5ml 11.6M HCl in a total volume of 500ml H_2O.

2.15.4 Quantification of calcium.

Test samples and appropriately diluted standards (all 100µl) were pipetted into sterile 5ml tubes. Colour reagent (2ml) was added to each, followed by 2ml of alkaline-buffer. Samples were then incubated at room temperature in the dark for 15 minutes in order for the colour to stabilize. Duplicate 100µl volumes were then

pipetted into a flat bottomed, transparent 96-well plate and read at 562nm on a microplate reader (EZ Read 400; Biochrom Ltd). A standard curve was constructed against which test sample readings were compared (Figure 2.3).

The calcium concentration was then 'corrected' for tissue dry weight, (for aortic samples), or protein content for cells. Aortic rings/segments were dried at 50ºC overnight and weighed on a semi-micro balance capable of measuring down to 10µg (ME235S, Sartorius, Epsom, UK). For cells, 2 washes in PBS were performed before lysis in 0.1% sodium docecyl sulphate (SDS) and 0.1M NaOH. The lysate protein concentrations were then measured using the bicinchoninic acid (BCA) assay (Pierce) (method described under 'Western blotting').

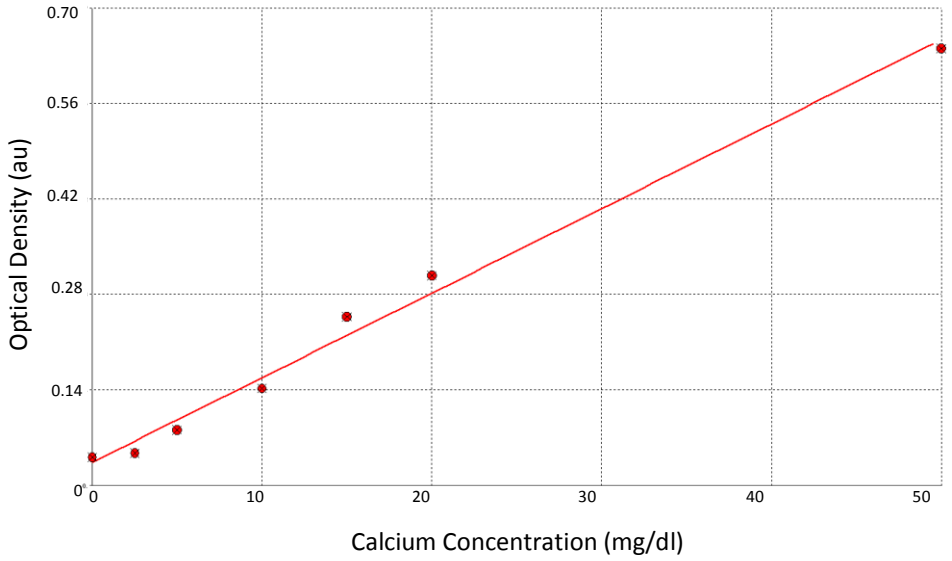

Figure 2.3. Representative Standard Curve for Quantifying Calcium Concentration. Optical density is plotted linearly against calcium concentration with an R^2 value of 0.996 in this example.

2.16 Quantitative Polymerase Chain Reaction (qPCR)

2.16.1 General principles.

The purpose of PCR is to amplify, (by making several million copies of), a gene sequence from a small starting quantity of DNA in order to permit its detection. A DNA template is entered into a reaction alongside oligonucleotide primers specific for the gene of interest, deoxynucleotides (dNTPs) and a DNA-polymerase enzyme. Following an initial exposure to 95ºC to activate the polymerase, reactants pass through 3 steps, each at optimised temperatures, to permit DNA denaturing, primer annealing and product extension respectively. These steps are repeated for a number of cycles. After each cycle the amount of product doubles, meaning that an exponential increase occurs as the reaction proceeds, and this continues until one or more of the reagents has been exhausted.

Quantitative PCR is an adaptation of this basic technique, and has been designed in order to measure the magnitude of gene expression in the starting material. Analysis is made during the exponential phase of the reaction so that reagents are not limited, and before the products are so abundant that they may hybridize and interfere with primer binding. All qPCR formats rely on the detection of a fluorescent signal which increases with rising product. The fluorescent dye SYBR green was used for all qPCR assays in this thesis.

SYBR green binds strongly to double-stranded DNA, and in the bound state the level of fluorescence increases 100-fold. It can therefore be included in a qPCR assay, where the increase in fluorescence will be directly proportional to the accumulating product (Schneeberger *et al* 1995). Fluorescence intensity at a defined threshold can be compared to that of known standards in order to determine the starting quantity of mRNA, following normalisation to a number of 'housekeeping' genes.

Due to the extreme sensitivity of qPCR, and the almost ubiquitous presence of RNAse enzymes in the environment, it is of paramount importance to adhere to strict handling and operating procedures when carrying out work with RNA. Ideally, specific work surfaces should be reserved for PCR work, and gloves and laboratory coats should be worn at all times. All reagents should be 'PCR-grade' and all equipment verified as being 'RNAse free'. It is also vital to apply a high level of

quality control to the RNA samples used for downstream applications, and this should include an assessment of purity and integrity.

2.16.2 RNA extraction from aortas.

RNA extraction was performed using the RNeasy Fibrous Tissue Mini Kit (Qiagen) according to the provided protocol. This is a column-based system whereby tissue is exposed to a number of agents, proprietary buffers and centrifugation wash steps, ultimately resulting in RNA binding to a silica membrane from which it can be eluted.

Arterial tissue was placed in RNAlater (Qiagen) following harvest, and stored at -20ºC prior to RNA extraction. Segments were taken from storage, cleaned of residual blood clot and as much adventitia as possible, then placed in individual, round bottomed, 2ml tubes, each containing 2 x 5mm stainless steel beads (all Qiagen). 'Buffer RLT' (300µl), supplemented with 10µl/ml of β-mercaptoethanol, was then added to each sample and these were then immediately shaken for 5-10 minutes at 50Hz using a TissueLyzer LT (Qiagen) to achieve full lysis and homogenisation. 'Buffer RLT' contains guanidine thiocyanate, a chaotropic agent, which aids both lysis of tissue and binding of RNA to the silica membrane. The addition of β-mercaptoethanol serves to inactivate RNAses.

Lysates were transferred to fresh tubes, and 590µl of RNAse-free H_2O followed by 10µl of proteinase K added, before heating at 55ºC for 10 minutes. Proteinase K serves to remove contractile proteins and connective tissue, usually high in abundance within fibrous tissue such as aorta, in order to aid RNA purification.

Tubes were then centrifuged for 3 minutes at 10000xg, the supernatant transferred into a fresh tube and 450µl 100% ethanol mixed with the lysate to provide favourable binding conditions to the membrane. Each sample was added to a spin column and centrifuged at 8000xg for 15 seconds, following which the membrane was washed by centrifuging through 350µl 'buffer RW1'.

To remove any potential contamination from DNA, an on-column DNAse digestion step was performed. Prior to use, 1500 Kunitz units of lyophilised DNase were reconstituted in 550µl of RNase-free water and aliquotted. Following reconstitution,

10µl was added to 70µl of 'buffer RDD', gently mixed, and applied directly to the membrane for 15 minutes.

The membrane was then washed as before with 'buffer RW1', following which 500µl 'buffer RPE' containing 4 volumes of 100% ethanol was added to remove trace salts. The column was then centrifuged for 15 seconds at 8000xg. In order to dry the membrane and avoid carryover of ethanol, this step was repeated but with centrifugation for 2 minutes.

Finally, to elute the RNA, 30µl was added to the membrane and the column centrifuged at 8000xg for 1 minute. To maximise the RNA yield, the elutant was then re-applied onto the membrane and the column was again centrifuged. RNA was aliquotted for analysis of concentration, purity and integrity, and for use in downstream applications. Samples were stored at -80ºC until required.

2.16.3 Measurement of RNA concentration and purity.

The concentration and purity of all RNA samples used for qPCR were measured, using a Nanodrop 2000 (Thermo Fisher Scientific). This instrument is a scanning spectrophotometer which uses fibre-optic technology. Nucleic acid has a peak absorption wavelength of 260nm and this property can be used to determine the concentration of RNA or DNA within a sample. Potential contaminants have different absorbance wavelengths, for example protein absorbs at 280nm, and the ratio of 260/280 can be measured. 260/280 ratios of over 1.7 are generally considered to indicate an acceptable level of RNA purity (Fleige & Pfaffl 2006). RNA (1µl) was loaded onto the instrument pedestal for readings to be taken (Figure 2.4).

2.16.4 Assessment of RNA integrity.

RNA integrity was assessed using a Bioanalyzer 2100 (Agilent, Wokingham, UK). This technology involves a 'chip' containing micro-channels, into which a sieving polymer and a fluorescent dye (combined beforehand in the form of a 'gel-matrix') are loaded. Samples are electrophoresed through the gel-matrix, and due to the presence of a constant mass-to-charge ratio RNAs are separated according to size. Each RNA molecule takes up the dye, and RNA-dye complexes are detected using a laser. The information obtained is converted into an electropherogram (Figure 2.5)

and used to generate an RNA integrity number (RIN). Values exceeding 5 are suggested to be imply sufficient integrity for qPCR assays with values above 8 said to represent highly preserved RNA integrity (Fleige & Pfaffl 2006). In some instances, usually due to a low yield of RNA following extraction from tissue, integrity was not measured. This was mainly an issue for tissue culture work and samples from human vessels. All aortas from *in vivo* animal experiments had an assessment of RNA integrity performed.

2.16.5 Synthesis of complementary DNA (cDNA).

For PCR to proceed, a starting DNA template is required. It was therefore first necessary to generate cDNA templates by subjecting each RNA sample to a reverse transcription (RT) reaction. The SuperScript VILO cDNA Synthesis kit (Invitrogen) was used for this purpose and reactions were performed using a G-Storm Thermal Cycler (G-Storm, Somerton, UK).

A mastermix containing 10X SuperScript Enzyme Mix (2µl per sample), and 5X Reaction Mix (4µl per sample,) was made first. The Enzyme Mix contains an engineered Moloney-Murine Leukemia Virus (M-MLV) reverse transcriptase, RNase H activity, recombinant ribonuclease inhibitor and a proprietary helper protein. The Reaction Mix contains random primers, $MgCl_2$ and dNTPs in an optimised buffer. Mastermix (6µl) was then added to the appropriate volume of RNA and the reaction volume made up to 20µl. 'Non-RT' control reactions were also set up for samples in an identical fashion, except RNAse-free water replaced the 10X Enzyme Mix. For samples taken from rat *in vivo* experiments, 1µg of aortic RNA was reverse transcribed. Due to less available tissue and lower RNA yields, 200ng of RNA was reverse transcribed from cultured rings, and 100ng from human arteries.

Samples were incubated at 25ºC for 10 minutes to permit primer annealing, followed by 42ºC for an hour in order for cDNA synthesis to occur. The reaction was then terminated by heating to 85ºC for 5 minutes. After cooling, products were diluted down 1.10 (*in vivo* samples) in yeast transfer RNA (tRNA) (10µg/ml) (which acts as a carrier molecule). Aliquots were made and stored at -80ºC. Tissue culture samples were diluted 1.5 and human samples were used undiluted.

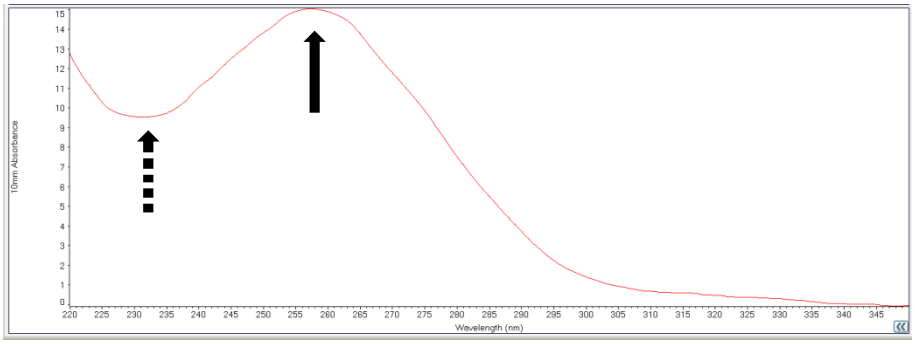

Figure 2.4. Assessment of RNA Purity. Representative spectral pattern of RNA extracted from rat aorta analysed on a Nanodrop. The trace has a peak at 260nm due to absorbance by nucleic acid (closed arrow). There is a trough at 230nm consistent with uncontaminated RNA (broken arrow). The 260/280 ratio of this sample was 1.98.

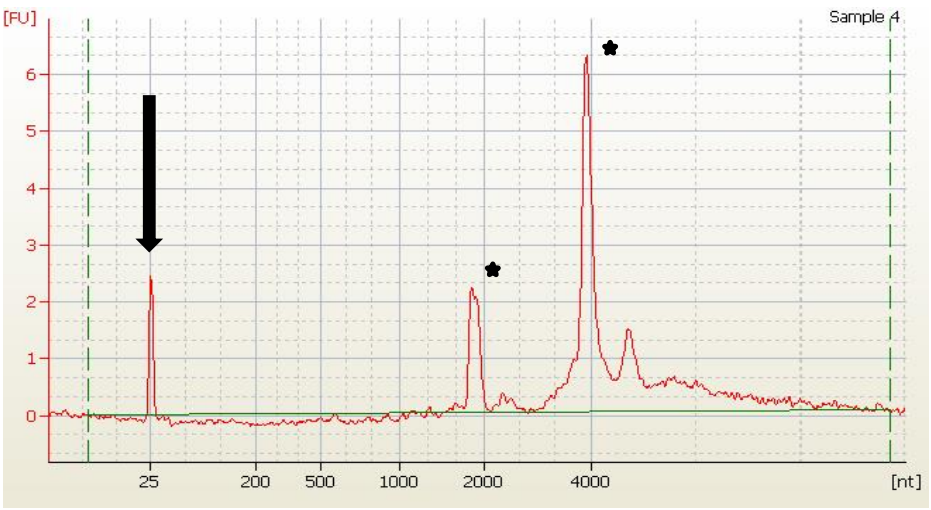

Figure 2.5. Assessment of RNA Integrity. Representative appearance of an electropherogram generated by analysing a sample of RNA extracted from a rat aorta on the Bioanalyser. The key elements suggestive of high quality RNA are a single marker peak (arrow) and 2 major ribosomal peaks corresponding to 18S and 28S (starred). The RIN of this sample was 9.4 indicating highly preserved integrity of RNA.

2.16.6 Primer design and optimisation.

Primers were designed using Primer-Blast software, freely available online from the National Centre for Biotechnology Information. Intron-spanning primers pairs were designed and selected for use if the amplicon product was less than 200 base pairs (bps) in length. Secondary structure formation was minimised by assessing primer pairs using the 'two-state melting' application, freely available through the mfold web server (hosted by the RNA Institute, College of Arts and Sciences, State University of New York at Albany). Primers which generate a positive 'delta G' value with this tool are less likely to form secondary structures.

If optimisation of assay conditions was required for primer pairs, a series of reactions were run on a G-Storm Thermal Cycler (G-Storm) set up to include a temperature gradient step (56ºC-66ºC) during the annealing phase of each cycle. A range of primer concentrations was trialled under these conditions. Products were then electrophoresed in a similar fashion to that described below, and the reaction conditions yielding the strongest, single band, selected for use in the final assay (Figure 2.6). Details of specific primers pairs for each gene studied along with the PCR conditions used for each assay are given in Table 2.3 (human) and Table 2.4 (rat).

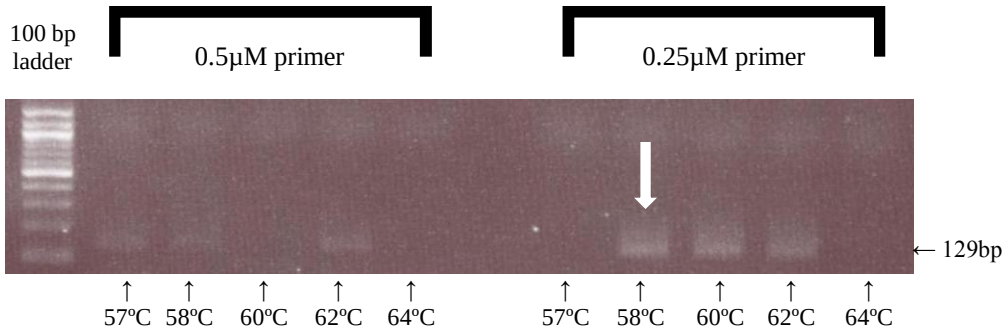

Figure 2.6. Optimisation of qPCR Assay for Runx-2. A series of reactions were run on a G-Storm Thermal Cycler set up to include a temperature gradient step (56º-66º) during the annealing phase of each cycle. A range of primer concentrations was trialled under these conditions. Products were then electrophoresed on a 2% agarose gel and the reaction conditions yielding the strongest, single band, selected for use in the final assay. In this example, 5 annealing temperatures were trialled (57º, 58º, 60º, 62º and 64º as indicated) at 2 different primer concentrations as shown. The strongest single product (at the correct size of 129bp for runx-2) was detected at a concentration of 0.25µM primer at 58º (white arrow) so these reaction conditions were used for the final assay. A 100bp reference ladder was also run as indicated.

Gene	Forward Primer	Reverse Primer	Primer Concentration (μM)	No. of cycles	Annealing Temp. (deg. C)
RPL13a	CCTGGAGGAGAAGAGGAAAGAGA	TTGAGGACCTCTGTGTATTTGTCAA	0.50	40	58
SDHA	AGAAGCCCTTTGAGGAGCA	CGATCACGGGTCTATATTCCAGA	0.50	40	58
HPRT	TGACACTGGCAAAACAATGCA	GGTCCTTTTCACCAGCAAGCT	0.50	40	58
ENPP-1	AAAGTACTCTCGCTGGTATTGTC	TCACAGCGACAGTTCCCAAA	0.50	40	60
ANK	GCAGCCCACATCAAGAAGTT	TCCAAAACATCACGAAACAGA	0.50	40	60

Table 2.3. qPCR of Human RNA. Primers used for qPCR analysis of RNA extracted from human arterial tissue and details of cycle number and annealing temperature for each assay. RPL13a: ribosomal protein L13a; SDHA: succinate dehydrogenase complex, subunit A; HPRT: hypoxanthine-guanine phosphoribosyltransferase.

Gene	Forward Primer	Reverse Primer	Primer Concentration (μM)	No. of cycles	Annealing Temp. (deg. C)
β-actin	CCCGCGAGTACAACCTTCT	CGTCATCCATGGCGAACT	0.25	30	58
YWHAZ	CTACCGCTACTTGGCTGAGG	TGTGACTGGTCCACAATTCC	0.50	40	57
28S	TGCAGATCATGCTGTTTAAGAAC	GGACCTGCTCCCCAGATT	0.50	40	57
SDHA	CCCTGAGCATTGCAGAATC	CATTTGCCTTAATCGGAGGA	0.50	40	60
HPRT	GACCGGTTCTGTCATGTCG	ACCTGGTTCATCATCACTAATCAC	0.50	40	57
P2X7R	AAGAAGTGTGAGCCCATCGT	GCTCGTCCACAAAGGACAC	0.50	40	60
α-SMA	GTGTGAAGAGGAAGACAGCACA	ATTCCAACCATCACTCCCTGGTG	0.25	30	58
SM22	CCAAGCCTTTTCTGCCTCAA	GCCATTCTTCAGCCACACCT	0.50	40	60
Smoothelin	GGCTCGTCCACTCCAATGAC	GTTTGGTCCTCTCGGTCGAA	0.50	40	60
Runx-2	AACCACAGAACCACAAGTGC	TTGCAGCCTTAAATGACTCGGT	0.25	45	58
Osterix	GCCACCCATTGCCAGTAATCT	AGCTTCTTCCTGGGGAGGCTA	0.50	40	60
BMP-2	GACTGCGGTCTCCTAAAGGTC	GGGGAAGCAGCAACACTAGA	0.50	40	60
Caspase-3	CCGACTTCCTGTATGCTTACTA	CATGACCCGTCCCTTGAA	0.50	40	60
NLRP3	CTGCAGAGCCTACAGTTGGG	GTCCTGCTTCCACACCTACC	0.50	40	60
ENPP-1	TTCCTGTCCCAGTGTCCAAT	TGATCGGCACAATCGAAG	0.50	40	60
CD73	CTTCTGAACAGCACCATTCG	CCTCCACTGGTTAATGTCTGC	0.50	40	60
CD39	GGGCCTATGGGTGGATTACT	AAGTTTAGCCAACTCTGTTCCTG	0.50	40	60
TNAP	GCACAACATCAAGGACATCG	TCAGTTCTGTTCTTGGGGTAT	0.50	40	62
ANKH	TCCACACCCTGATAGCCTAC	ATTGAGGCACATCCCACCAG	0.50	40	60

Table 2.4. qPCR of Rat RNA. Primers used for qPCR analysis of RNA extracted from rat aorta and details of cycle number and annealing temperature for each assay. YWHAZ: Tyrosine 3-Monooxygenase/Tryptophan 5-Monooxygenase Activation Protein Zeta; 28S: 28S Ribosomal RNA.

2.16.7 Preparation of cDNA standards.

To generate standards for each gene, a qPCR assay was performed using cDNA from a single control sample (non-calcified vessel for human tissue). Five replicates were run in the case of rodent samples whereas only a single assay was possible with human tissue due to the limited starting material available. Melt curves (see section 2.16.8) were inspected to ascertain whether single peaks were present.

The PCR products were then pooled and added in a ratio of 4:1 to 10X 'Bluejuice' PCR loading buffer (Invitrogen) which was pre-diluted 1 in 20 (so as not to obscure visualisation of bands under UV light). Samples were then electrophoresed at 80V for 40 minutes on a 2% agarose gel made with 1x TAE containing 0.04ul/ml ethidium bromide. A 100bp reference ladder (Thermo Fisher Scientific) was run in one lane in order to ascertain the size of DNA bands. Gels were viewed under UV light with the presence of a single band of the expected size taken as confirmation of primer specificity (Figure 2.7).

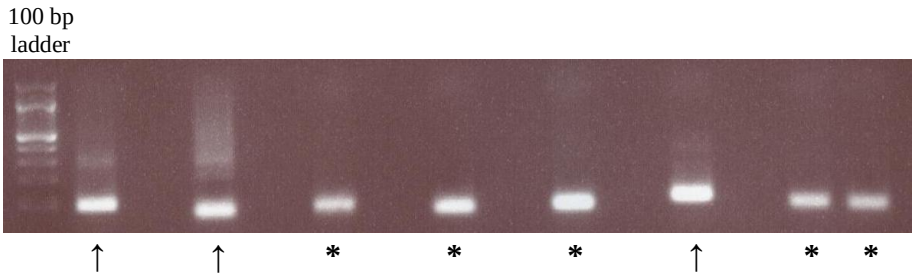

Figure 2.7. Assessing Specificity of Primers. Upon completion of a qPCR assay the products from the replicate samples were pooled, electrophoresed on a 2% agarose gel and then visualised under UV light. Primer pairs were accepted if a single band of the expected size was evident (starred). If multiple bands were detected (arrowed lanes) primers were rejected. A reference 100bp ladder is shown in the left-hand lane.

The Geneclean Spin Kit (MPBiomedicals, Solon, USA) was then used to extract and purify cDNA from gels. This kit employs the principle that DNA will bind to silica in an environment high in chaotropic salt, and will elute when the salt concentration is lowered. DNA bands were excised from agarose gels under UV light, placed into a spin column containing 400µl 'Geneclean Spin Glassmilk' and melted at 55ºC. The Glassmilk contains a suspension of proprietary silica matrix and chaotropic binding salt thereby providing the necessary conditions for DNA binding.

Following a centrifugation step with 'Geneclean Spin New Wash', a solution containing NaCl, Tris, EDTA and ethanol (added prior to use) which acts to remove any remaining salt and agarose whilst ensuring DNA remains bound, the column was centrifuged for 2 minutes at 14000xg to dry the pellet. 'Geneclean Spin Elution Solution' (15µl), (PCR-grade water provided with the kit), was added to the column and the pellet suspended within it. DNA was eluted and collected by centrifugation at 14000xg for 30 seconds.

The concentration of extracted cDNA was measured using a Nanodrop (Thermo Fisher Scientific) thereby enabling subsequent calculation of the number of DNA copies present in 1µl by applying the following equations:

1. MMW of amplicon = amplicon length (in bp) x 660

   [MMW: mean molecular weight; 660 = MMW of 1bp]

2. Amplicon copy number in 1ng = $(6.02 \times 10^{23} / \text{MW amplicon}) \times 10^{-9}$

   [6.02×10^{23} = Avogadro's constant]

3. Number of copies in 1µl = cDNA/µl x copies of amplicon/ng

By diluting the concentrated cDNA it was possible to prepare standards from 10^7 - 10^2 per 2µl (the volume used in qPCR assays). These were made up in tRNA and stored at -80ºC.

2.16.8 Quantitative PCR.

For every gene, each test sample was run in duplicate, and 6 standards (10^2 – 10^7), were run in triplicate. RT-negative and tRNA (diluent alone) samples were also run as negative controls on each occasion.

Reactions volumes of 10µl were prepared using a CAS-1200 robotic pipetting device (Qiagen). cDNA (2µl) was added to a mastermix containing 5µl SensiMix SYBR Hi-ROX (Bioline, London, UK) and an equal volume and concentration of forward and reverse primers (see Tables 2.3 and 2.4 for details), made up to 8µl with RNase-free water. The SensiMix reagent contains SYBR Green I dye, dNTPs, stabilisers and enhancers.

Reactions were run on a RotorGene 6000 (Qiagen). Reactions commenced with a 10 minute hold at 95ºC for polymerase activation, followed by repeated cycles of denaturation, annealing and extension steps, all 10 seconds in length. The number of cycles and annealing temperature varied according to the primer pairs, details of which are given in Tables 2.3 (human) and 2.4 (rat). After the final cycle, a melt curve was constructed by increasing the temperature from 72ºC to 95ºC by 1ºC every 5 seconds.

Upon completion of the run, an assessment was made of the standard curve linearity (r^2 value) and reaction efficiency (Figure 2.8A). Accepted values were >0.99 and 0.85-1.10 respectively. Melt curves were also inspected to verify that single peaks had been obtained (Figure 2.8B). Gene copy numbers from each sample were then determined by comparing the cycle number (Ct value) at which the fluorescence threshold (automatically determined by the RotorGene system) was reached, to the standard curve (Figure 2.8C). Final copy numbers were calculated from the geometric means of duplicate samples.

2.16.9 Calculation of gene copy number.

In order to compare copy numbers of a gene of interest between samples from different treatment groups, it is necessary to normalise the results to one or more stable ‘housekeeping’ genes, the expression of which should not change regardless of experimental conditions. By using a panel of stable housekeeping genes in

combination for this normalisation process, a greater level of accuracy can be achieved.

GeNorm software was used to facilitate the choosing of the most stable housekeeping genes to use for normalisation. The mathematical principles underlying this programme were originally described by Vandesompele *et al* (2002). GeNorm calculates the average pairwise variation for a gene with all other tested reference genes, to derive a stability factor 'M'. It is then possible to choose the most stable combination of housekeeping genes. From this selection, the geometric mean is calculated in order to derive a 'normalisation factor' for each test sample, by which all raw copy numbers are divided in order to obtain the final corrected copy number for each gene of interest.

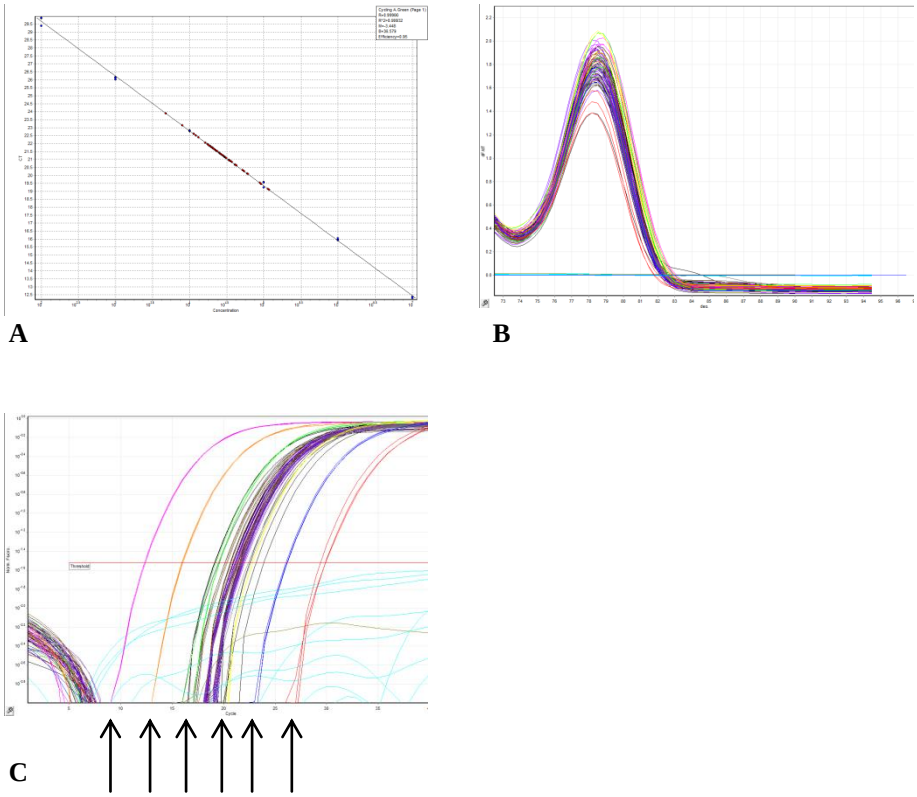

Figure 2.8. An Optimised qPCR Assay. Representative results obtained from an optimised qPCR assay analysing rat aortic RNA. A: Standard curve generated from the results in Figure C. In this example R^2 was 0.999 and the efficiency was 0.95. B: Typical melt-curve showing a single peak for all samples and standards suggestive of a single reaction product. C: Typical results of a qPCR assay. Fluorescence is plotted against cycle number with the red horizontal line representing the automatically derived threshold at which Ct readings are taken. Standards (each in triplicate) are seen as the pink, orange, green, yellow, blue and red lines (10^7 - 10^2 respectively) (arrows). Samples are indicated by purple lines. Turquoise and brown lines represent reverse transcription-negative and tRNA samples respectively and all fall below the threshold line indicating absence of RNA content.

2.17 Western Blotting

2.17.1 General principles.

The purpose of a Western blot is to detect the presence of a protein within a biological sample. The starting material (cells or tissue) is homogenised in a lysis buffer, containing protease and phosphatase inhibitors to minimise degradation, in order to liberate proteins. The denatured lysate is then electrophoresed through a SDS polyacrylamide gel, resulting in the separation of proteins according to their molecular weight. The protein bands are then transferred onto a membrane, usually nitrocellulose, by applying a voltage across the gel. Once transferred onto the membrane, an antibody specific to the protein of interest (primary antibody) can be applied, followed by a secondary antibody, commonly an HRP-conjugated. Numerous secondary antibodies can bind to one primary antibody, and by cleaving the chemiluminescent agent that is subsequently applied to the membrane, the signal generated is amplified. The final signal is detected by exposing the membrane to a photosensitive film which is then developed.

2.17.2 Solutions.

Radioimmunoprecipitation assay (RIPA) buffer: 1% Triton X100; 0.1% SDS; 150mM NaCl; 10mM Tris pH 7.2; 0.5% NP40; Protease and phosphatase inhibitor cocktail, 1 tablet in 10ml (Thermo Fisher Scientific).

Stacking gel: 3.4ml water; 630ul 1M Tris pH 6.8; 750ul 30% Protogel acrylamide (National Diagnostics, Hessle, UK); 50ul 10% SDS; 75ul 10% ammonium persulfate (APS); 10ul tetramethylethylenediamine (TEMED) (BioRad).

10% resolving gel: 4ml water; 2.5ml 1.5M Tris pH 8.8; 3.34ml 30% Protogel acrylamide (National Diagnostics); 100ul 10% SDS; 80ul 10% APS; 10ul TEMED (BioRad).

10x SDS Polyacrylamide Gel Electrophoresis (PAGE) Running buffer: 30.3g Tris base; 144.1g glycine; 10ml 10% SDS; made up to 1L with distilled water.

Transfer buffer (Bjerrum and Schafer-Nielson): 5.82g Tris; 2.93g glycine; 3.75ml 10% SDS; 200ml methanol; made up to 1L with distilled water.

10x Tris-Buffered Saline (TBS): 900 ml distilled ater; 24g Tris base; 88g NaCl; pH then adjusted to 7.6 with 12M HCl and solution made up to 1L with distilled water.

Blocking solution: Required % protein (non-fat milk powder or BSA as indicated) added to 1L 1xTBS/T (TBS/Tween) (made by adding 1ml Tween to 999ml of 1x TBS i.e. 0.1% Tween).

2.17.3 Protein extraction from aortic tissue.

Aortic rings were snap-frozen in liquid nitrogen immediately following harvest and subsequently stored at -80ºC. For protein extraction, the frozen tissue was transferred into a 2ml round-bottomed collection tube containing 2x5mm steel balls (all Qiagen) which had all been kept on dry ice for 30 minutes beforehand. RIPA buffer (150µl) was then added and the tube immediately rapidly shaken at 50Hz for approximately 4x5 minute bursts using a TissueLyzer LT (Qiagen) in order to homogenise the tissue. The resultant lysate was then transferred into a fresh tube on ice and centrifuged at 8000xg for 5 minutes. The supernatant was removed and aliquots made for long-term storage at -20ºC. A 5µl aliquot was used to determine the protein concentration as described below.

2.17.4 Measurement of sample protein content.

The protein concentration of tissue lysates was determined using the BCA protein assay (Pierce). This technique utilises the fact that in the presence of an alkaline medium, protein will reduce Cu^{2+} to Cu^{1+}. The resulting Cu^{1+} will chelate with BCA to form a purple, water soluble compound, the absorbance of which increases linearly with increasing protein concentration over a wide range of values, and can be measured spectophotometrically at 562nm. Using this method, a standard curve can be constructed using known concentrations of BSA, against which experimental samples can be compared in order to measure total protein content.

To generate protein standards, appropriate dilutions of BSA stock solution (2mg/ml) were made using H_2O to form volumes of 20µl. To each 20µl standard, 5µl of RIPA buffer was added. For test samples, 5µl of lysate was added to 20µl H_2O. A mixture was then made, in a 50:1 ratio, of ‘reagent A’ (containing sodium carbonate, sodium bicarbonate, BCA and sodium tartrate in 0.1M sodium hydroxide), and ‘reagent B’ (containing 4% cupric sulphate). The working reagent (200µl) was then added to

each standard and test sample before incubating at 37ºC for 30 minutes. After cooling to room temperature, the absorbance of duplicate 100µl aliquots, placed in a 96 well, transparent, flat-bottomed plate was read on a microplate reader (EZ Read 400; Biochrom Ltd). A standard curve was generated and test sample protein concentrations calculated.

2.17.5 Electrophoresis.

Electrophoresis was performed using a BioRad Mini-Protean II System (BioRad). To prepare samples for electrophoresis, appropriate volumes of lysis (RIPA) buffer were added to each to equalise volumes, following which a 1X loading buffer (Biorad) was added in a ratio of 1:1. Samples were heated at 95°C for 10 minutes to denature and then centrifuged at 10000xg for 30 seconds. Samples were loaded onto the gel immersed in 1x running buffer. A Spectra Multi-colour Broad Range Protein Ladder (Thermo Fisher Scientific) (10µl) was loaded into one of the lanes in order to ascertain the molecular weight of subsequently detected protein bands. Gels were initially run at 10mA. When samples had stacked at the stacking gel/resolving gel interface, the current was increased to 20mA and the gel run until the loading dye reached the bottom of the gel.

2.17.6 Transfer.

For semi-dry transfer, gels were removed from the cassette and gently rocked in transfer buffer for 30 minutes. Following this the gel was placed on top of 0.2µm nitrocellulose membrane (GE Healthcare Life Science, Amersham, UK) which was placed onto 4-5 layers of filter paper on the transfer plate (Semi-dry Transblot, BioRad). Air bubbles were removed and the gel covered in further filter paper. All filter paper and nitrocellulose had also been pre-soaked in transfer buffer. Transfer was performed at 12V for 45 minutes. Successful transfer was assessed by staining the nitrocellulose membrane with Ponceau S. This stain was removed by washing several times in water. The membrane was then blocked by gently agitating in blocking solution for at least 2 hours at room temperature.

2.17.7 Protein labelling and visualisation.

Primary antibodies were made up in blocking solution and applied at the appropriate concentration for the indicated time period (Table 2.5). Membranes were washed for

5 minutes 4 times in TBS/T following which the secondary antibody, made up in blocking solution was applied for the required time (Table 2.5). Membranes were washed for 5 minutes 3 times in TBS/T, followed by a final 5 minute wash in PBS. The chemiluminescent substrate Lumiglo (New England Biolabs, Hitchin, UK) was then applied for 1 minute. Excess substrate was dabbed off, the membrane wrapped in parafilm and placed in a developing cassette (Kodak, Rochester, New York, USA). In a darkroom, photo-sensitive film was applied to the wrapped membrane and held within the cassette for the required length of time (typically a number of seconds). Blots were then developed using a Compact X4 automatic processor (Xograph, Stonehouse, UK). Image J software was used to compare bands by densitometry.

2.18 Immunofluorescence

Cells were grown in 8 well chamber slides (BD Falcon, Oxford, UK) until 80% confluent. Culture medium was then gently tipped off, cells were washed once in PBS supplemented with 0.9mM calcium and 0.49mM magnesium and 200ul 4% PFA was then applied for 5 minutes followed by 3 washes in PBS. If permeabilisation was required, 200ul ice-cold methanol was applied to wells for 5 minutes followed by 3 PBS washes. Cells were then blocked for 30 minutes with 200µl serum from the species in which the secondary antibody was derived. The primary antibody (Table 2.6), made up in PBS, was then applied for the indicated length of time. IgG from the primary species was applied at equivalent concentrations as a control for non-specific binding. Slides were washed 3 times in PBS and the appropriate secondary antibody (Table 2.6), made up in PBS, was applied for 1 hour. Cells were then washed 3 times in PBS and finally in H_2O before being mounted with hard-set mounting medium (Vector Labs, Peterborough, UK) which included 4',6-diamidino-2-phenylindole (DAPI) for nuclear visualisation. Once set, slides were examined using an epifluorescence microscope (Zeiss, Cambridge, UK).

Target Protein	Primary Antibody	Primary Dilution (Time and incubation temperature)	Secondary Antibody	Secondary Dilution (Time and incubation temperature)
Human P2X7R	ab109246 (Abcam) Rabbit monoclonal	1:1000 (overnight at 4ºC)	HRP-conjugated Goat anti-Rabbit polyclonal (Thermo Fisher)	1:3000 (1 hour at room temperature)
Rat P2X7R	ab109246 (Abcam) Rabbit monoclonal	1:1000 (overnight at 4ºC)	HRP-conjugated Goat anti-rabbit polyclonal (Thermo Fisher)	1:3000 (1 hour at room temperature)
Rat α-actin	A2228 (Sigma) Mouse monoclonal	1:10,000 (1 hour at room temperature)	HRP-conjugated Rabbit anti-mouse polyclonal (Abcam)	1:3000 (1 hour at room temperature)
Human GAPDH	ab8245 (Abcam) Mouse monoclonal	1:10,000 (1 hour at room temperature)	HRP-conjugated Rabbit anti-mouse polyclonal (Abcam)	1:3000 (1 hour at room temperature)
Rat GAPDH	ab8245 (Abcam) Mouse monoclonal	1:10,000 (1 hour at room temperature)	HRP-conjugated Rabbit anti-mouse polyclonal (Abcam)	1:3000 (1 hour at room temperature)

Table 2.5. Antibodies used for Western Blots. GAPDH: Glyceraldehyde 3-Phosphate Dehydrogenase.

Target Protein	Primary Antibody	Primary Dilution (Time and incubation temperature)	Secondary Antibody	Secondary Dilution (Time and incubation temperature)
Human P2X7R	ab109246 (Abcam) Rabbit monoclonal	1:250 (overnight at 4ºC)	Dylight 488-conjugated goat anti-rabbit (Vector Labs)	1:100 (1hour at room temperature)
Rat α-SMA	M0851 (DAKO)	1:50 (overnight at 4ºC)	Dylight 488-conjugated horse anti-mouse (Vector Labs)	1:100 (1hour at room temperature)
Rat SMMHC	sc6956 (Santa Cruz)	1:500 (overnight at 4ºC)	Dylight 488-conjugated horse anti-mouse (Vector Labs)	1:100 (1hour at room temperature)

Table 2.6. Antibodies used for Immunofluorescence.

2.19 Histological Analysis

2.19.1 Sample preparation and deparaffinisation of sections.

Tissue samples were fixed in either 4% PFA or 10% NBF as indicated. Initial processing, embedding into paraffin and cutting of sections, along with staining for haematoxylin and eosin (H & E) and Picrosirius red was performed by Ms Mahrokh Nohadani.

Slides were deparaffinised and rehydrated by performing the following washes:

1. Xylene: 2 x 3 minutes
2. 100% ethanol: 2 x 3 minutes
3. 95% ethanol: 3 minutes
4. 70 % ethanol: 3 minutes
5. 50 % ethanol: 3 minutes
6. H_2O

2.19.2 Silver nitrate stain according to von Kossa.

The von Kossa technique for staining tissue mineralisation was first described in 1901 (von Kossa 1901). Under a strong light source, calcium ions within salt compounds, (usually calcium-phosphate), become reduced and replaced with silver. This is visualised as a deep metallic silver colour on microscopy.

All reagents were purchased from Merck Millipore (Watford, UK). Following deparaffinisation and hydration to water, slides were rinsed in several changes of distilled water and incubated with 1% silver nitrate solution under ultraviolet light for 25 minutes. Slides were rinsed in H_2O. 5% sodium thiosulfate was applied for 5 minutes to remove unreacted silver before rinsing again in H_2O. Nuclear fast red counterstain was applied for 5 minutes. Slides were rinsed in H_2O, dehydrated through graded alcohol and cleared in xylene. Coverslips were applied using permanent mounting medium (Vector Labs).

2.19.3.i Semi-quantitative scoring of calcium deposition.

Sections of von Kossa-stained human vessels were examined using light-microscopy. The positively-stained vessel circumference was scored on a semi-quantitative scale of 0, < 25, 25-50 or < 50% calcified.

2.19.3 Alizarin red staining.

Alizarin red will complex with di-cationic ions in a chelation process. As such this stain is not strictly specific for calcium, however, because other di-cations are rarely present in as high abundance as calcium in tissues of interest, it can be used as a complementary stain to the von Kossa method (Puchtler *et al* 1969).

Following deparaffinisation and hydration to water, slides were stained with 2% Alizarin red stain (pH adjusted to 4.2 using 10% ammonium hydroxide) for 2 minutes. Slides were dehydrated by dipping 20 times in acetone and then 20 times in a 1:1 solution of acetone-xylene. Slides were cleared in xylene and mounted with permanent mounting medium.

2.19.4 Quantification of renal fibrosis on Picrosirius red stained kidney sections.

Picrosirius red is a strong anionic dye which binds to basic groups present within collagen resulting in a distinct red stain (Junqueira *et al* 1979). When applied to kidney tissue it can therefore be used to assess the extent of interstitial fibrosis. Starting from the top of each histological section and moving clockwise around the cortex, 4 random digital images were taken of the interstitial compartment, ensuring that glomeruli and large vessels were excluded.

Image J software was then used to quantify the amount of fibrosis within each section. This was achieved by first opening the image and defining the 'area at risk' by adjusting the brightness and saturation sliders in such a way so as to leave the tubulointerstitium selected whilst excluding tubular lumen (Figure 2.9A). The number of pixels within this defined area was then quantified. By adjusting the sliders again it was possible to highlight just the positively-stained red areas (Figure 2.9B) in which the total number of pixels was measured. The percentage of the area at risk that was stained red was then calculated. This protocol was followed in a

blinded fashion for all samples from all rodents and the mean percentage was determined for each animal.

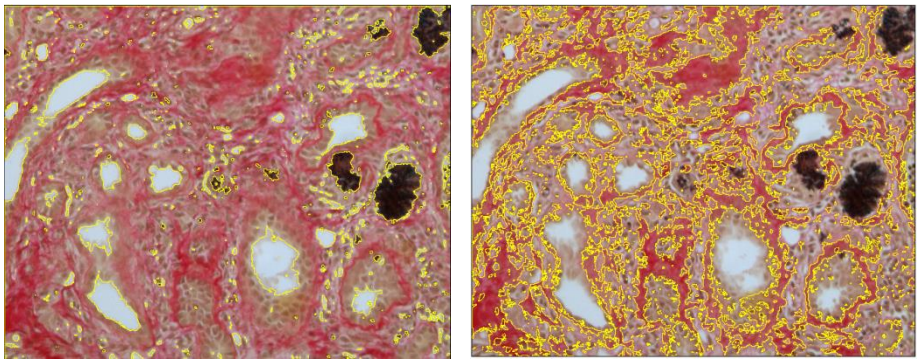

A **B**

Figure 2.9. Quantification of Picrosirius Red Staining of Kidney Sections. Analysis was performed using Image J Software. A: Defining the 'area at risk' of fibrosis (tubulointerstitium). Colour threshold sliders were adjusted to define the 'area at risk' i.e. tubulointerstitial compartment. The number of pixels was determined in the total area excluding the sections outlined in yellow i.e. tubular lumens including those containing 2,8-dihydroxyadenine crystals (seen as black intra-tubular structures). B: Defining the fibrotic tubulointerstitium. Colour slider threshold sliders were adjusted to define only the tissue stained red (fibrotic areas) and the number pixels was determined. This figure was then divided by the 'area at risk' value to determine the % fibrosis.

2.20 Statistical Analysis

Unless stated otherwise all data in this thesis have been presented as mean ± standard deviation (SD). Statistical analysis was performed using either Prism (GraphPad, San Diego, USA) or SPSS (IBM, Armonk, USA). Differences between two groups were compared using a 2-tailed t-test or Mann-Whitney U (MWU) test for normally- or non-normally-distributed data respectively. For comparisons between more than 2 groups, Analysis of Variance (ANOVA) was used for normally-distributed data and the Kruskal Wallis (KW) test if non-normally-distributed. In the case of multiple comparisons, a *post hoc* Bonferroni correction was made (Dunn's post-test following KW tests). Groups compared by *post hoc* testing are clearly indicated in the relevant figures. Correlation analyses were performed by determining Spearman's rho. P values of < 0.05 were considered statistically significant.

CHAPTER 3 – OPTIMISATION OF A TISSUE CULTURE MODEL TO ASSESS THE ROLE OF P2X7R IN ARTERIAL CALCIFICATION

3.1 Introduction

Much of the current understanding about the pathogenic pathways involved in AC has come from the results of *in vitro* studies (Shanahan *et al* 2011, Shanahan 2013). Experiments whereby primary VSMCs (Proudfoot *et al* 1998), and more recently intact arterial rings (Lomashvili *et al* 2004, Shroff *et al* 2010), have been cultured in a medium containing an elevated concentration of phosphate and/or calcium have permitted investigators to assess the cellular responses and changes occurring under these conditions. With relevance to the potential role of P2X7R, a number of groups using these experimental systems have been able to advance the concepts of osteogenic transformation and apoptosis of VSMCs as being of fundamental importance in the pathogenesis of AC in patients with CKD (see Shroff *et al* 2013).

The work in this chapter sought to optimise a tissue culture model of, and subsequently investigate the role of P2X7R in, AC. A number of P2X7R antagonists are commercially available, and BzATP, whilst not entirely specific, is a receptor agonist (Wiley *et al* 2011). These agents have been widely used in tissue culture models to investigate P2X7R in other biological contexts, and thus they were employed here to examine the role of this receptor in AC. The generation of $P2X7^{-/-}$ mice in this thesis (described in Chapters 2 and 4) permitted another way of examining the effect of P2X7R ligation under these experimental conditions.

3.2 Results

3.2.1 P2X7R is expressed in primary hVSMCs *in vitro.*

An initial aim of the *in vitro* work was to determine whether hVSMCs express P2X7R. To address this question, cells were cultured and examined by immunofluorescence, and cellular protein was extracted for Western blotting. By immunofluorescence, expression of P2X7R was clearly evident in hVSMCs (Figure 3.1). In many cells there appeared to be sparing in the peri-nuclear region. By Western blotting a distinct, single band was detected at 69kDa consistent with the molecular weight of P2X7R (Figure 3.2).

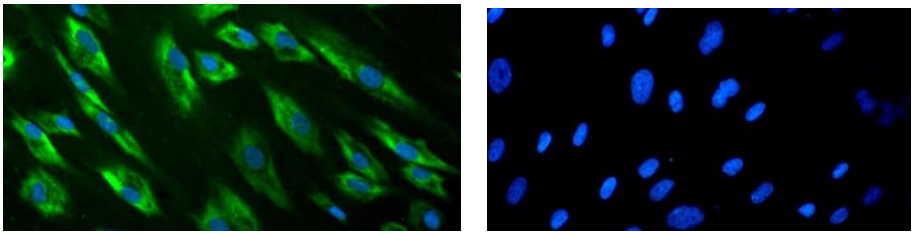

A **B**

Figure 3.1. Immunofluorescent Staining of P2X7R in hVSMCs. Cells were cultured for 3 days before fixing. A: P2X7R staining (green). Nuclei are counterstained blue with DAPI. B: Corresponding rabbit IgG control. Magnification x10.

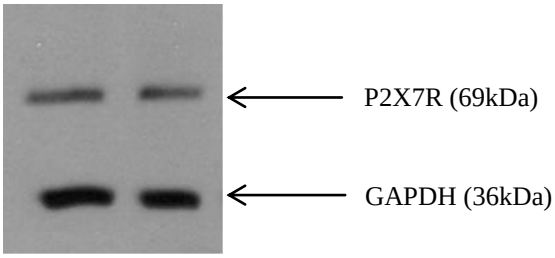

Figure 3.2. Western Blot of P2X7R Protein from Cultured hVSMCs A single band of approximately 69kDa was detected consistent with P2X7R (upper band). The lower bands represents GAPDH at a molecular weight of 36kDa. The 2 lanes shown are duplicates from the same batch of (uncalcified) hVSMCs cultured in normal Medium-199.

3.2.2 Experiments culturing VSMCs in high calcium and phosphate-containing medium yield inconsistent results.

With P2X7R expression confirmed in VSMCs, its role in VSMC-associated calcification *in vitro* was assessed. A commonly used model of AC is the *in vitro* culture of VSMCs in a medium containing an elevated concentration of phosphate and/or calcium (see Chapter 1, section 1.4.1). This *in vitro* system was therefore initially employed to assess the influence of the selective P2X7R antagonist, A438079, on hVSMC-associated calcium deposition. Several experiments were performed, using commercially-available hVSMCs from two different donors.

In hVSMCs from donor 1, the addition of 10µM A438079 to the calcification medium resulted in a trend towards decreased calcium deposition after 6 days (6.4 ± 3.4 vs 2.8 ± 1.6µg/µg without and with A438079, respectively; $p = 0.200$) (Figure 3.3). However, a second, repeat experiment using cells from this donor yielded minimal calcification in all groups, including the control cells cultured in calcification medium alone (data not shown).

The supply of cells from this first donor was limited, so a second donor's cells were obtained for use. In contrast to the results for donor 1, in hVSMCs from donor 2 a trend was seen towards *enhanced* calcium deposition in the presence of increasing concentrations of A438079 at day 6 (0.61 ± 0.11 vs 0.78 ± 0.06 vs 0.86 ± 0.16µg/µg for control, 5µM and 10µM A438079, respectively; $p = 0.067$). A similar but less marked trend was seen at day 4 ($p = 0.177$) (Figure 3.4). However, a repeat experiment with these cells yielded equivocal calcium deposition at days 4 and 6 across all groups ($p = 0.112$ and 0.733 respectively) (Figure 3.4), and two subsequent experiments with cells from this donor failed to result in calcification in any culture well (data not shown).

A striking feature of this model which became apparent after a number of experiments had been performed was the inconsistency of calcification. It was not uncommon to observe calcium deposition in association with cells in one experiment, only for it to be absent when culturing cells from the same donor under identical conditions a second or third time. In addition to the 'inter-experiment' calcification variability, in experiments where calcium deposition was observed, the cell donor appeared to be exerting a major influence on the outcome i.e. the effect of

A438079 on mineralisation. Given this latter observation, it was decided to try and standardise the genetic background of cells in an attempt to gain more reproducible results by eliminating the potential effects of human variation.

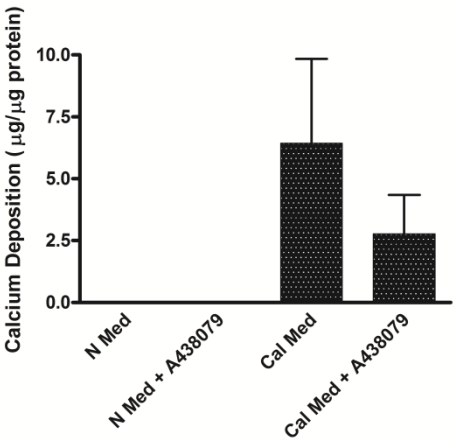

Figure 3.3. The Effect of the Specific P2X7R Antagonist A438079 on hVSMC-Associated Calcification (Donor 1). Cells from the first donor were cultured for 6 days in either normal control Medium-199 (N Med) or in 'calcification' Medium-199 (Cal Med) containing calcium and phosphate concentrations of 2.7mM and 2mM respectively. The specific P2X7R antagonist A438079 was added where indicated to a final concentration of 10μM. N=3 per group. Error bars represent mean ± SD.

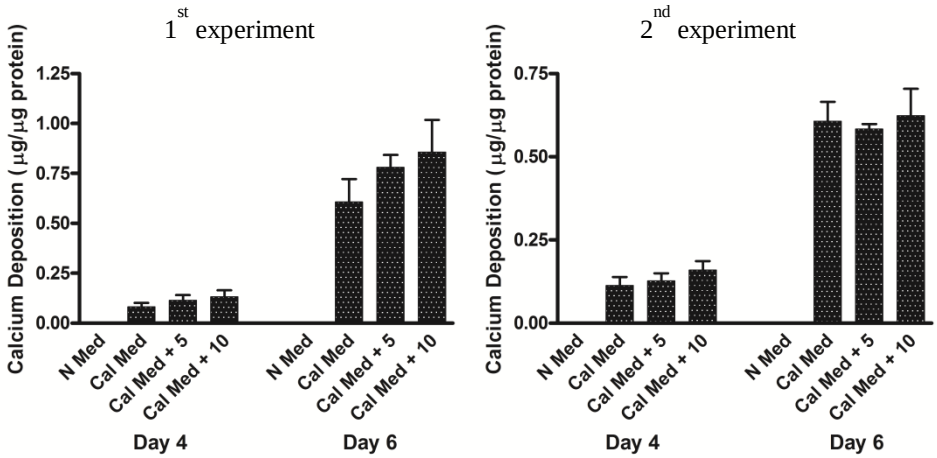

Figure 3.4. The Effect of the Specific P2X7R Antagonist A438079 on hVSMC-Associated Calcification (Donor 2). Cells from the second donor were cultured for either 4 or 6 days in normal control Medium-199 (N Med) or 'calcification' Medium-199 (Cal Med) containing calcium and phosphate concentrations of 2.7mM and 2mM respectively. The specific P2X7R antagonist A438079 was added where indicated to a final concentration of either 5 (+5) or 10 (+10) μM. N=3 per group. Error bars represent mean ± SD.

3.2.2.i Generation of, and calcification experiments using, rat VSMCs.

Rat VSMCs (rVSMCs) were obtained by isolating VSMCs from outgrowths from Sprague-Dawley rat aortas as described in Chapter 2 (section 2.13.3). Cells were characterised by demonstrating positive immunofluorescence for the VSMC-specific markers α-SMA and SMMHC, in addition to the typical 'hill-and-valley' VSMC growth pattern (Proudfoot & Shanahan 2012) (Figure 3.5).

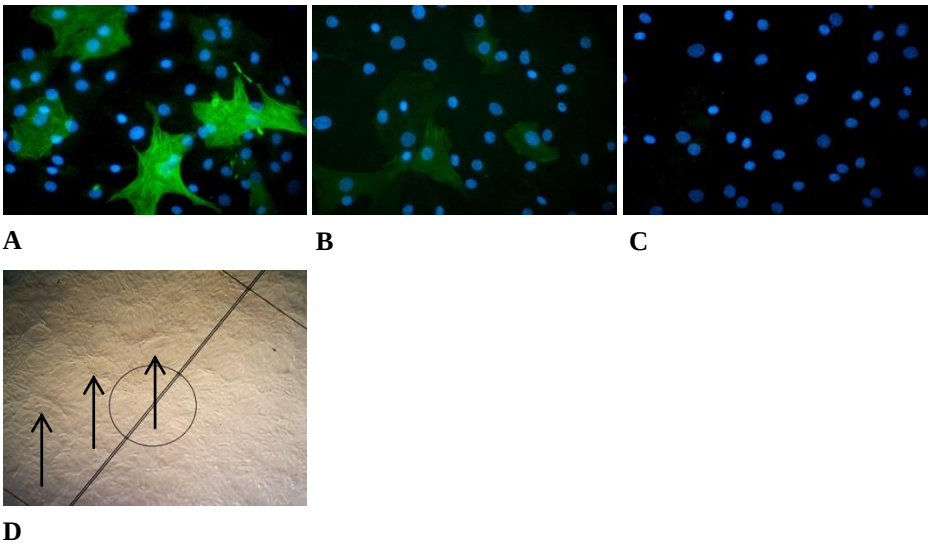

Figure 3.5. Characterisation and Culture of rVSMCs. A-C: Immunofluorescent staining of fixed, permeablised cells for VSMC specific markers. A: α-SMA (green). B: SMMHC (green). C: Corresponding anti-mouse IgG control. Nuclei are stained blue with DAPI. D: Phase-contrast appearance of cell growth pattern displaying a 'hill-and-valley' morphology typical of VSMCs (arrows represent 'hills'). A-C: magnification x40. D: magnification x4.

Several experiments were performed using rVSMCs at early passage number ($P < 3$) to assess the effect of A438079 on calcification and also to ascertain the optimal culture conditions for this cell type in this model. Despite numerous attempts, as with hVSMCs, experimental results were inconsistent. Specifically, in a number of experiments no calcification occurred at all in several culture wells, including some containing cells just cultured in calcification medium alone, whereas in other wells it did (data not shown).

At this point a review of the model was undertaken. Given both the gross inconsistency in calcium deposition and the documented concerns regarding its

biological relevance, both of which are discussed below, this *in vitro* system was abandoned as an experimental tool for work in this thesis in favour of the aortic ring *ex vivo* culture model.

3.2.3 Characterisation and optimisation of an *ex vivo* aortic ring calcification model.

3.2.3.i Calcification of rat aortic rings can be induced by culturing in a medium containing phosphate concentrations above 2.5mM.

Previous reports had suggested that normal vessels, from both humans (Shroff *et al* 2010) and rats (Lomashvili *et al* 2004), would maintain viability but not calcify if cultured in a high phosphate-containing medium alone. To test these observations, rings of rat aorta were cultured in media containing a range of increasing phosphate concentrations (1 - 3.8mM) for 10 days.

Calcification was evident in rings cultured in phosphate concentrations of ≥ 2.5mM as assessed by von Kossa staining (Figure 3.6). Mineralisation was seen as linear deposits, tracking along the elastic laminae between VSMCs (Figure 3.7). VSMCs in these vessels appeared morphologically normal on H & E staining (Figure 3.8). In rings containing heavier calcium deposition, more notable in those cultured in phosphate concentrations > 3mM, marked, circumferential mineralisation was evident, completely disrupting the normal vessel architecture, presumably as a consequence of the more brittle sections 'fracturing' during sectioning (Figure 3.6). Calcification was also frequently observed in the adventitia (Figure 3.7), highlighting the importance of removing this layer prior to calcification quantification in order to accurately ascertain the degree of medial calcium deposition.

Rings cultured in 3mM phosphate had marked calcium deposition without overt disruption of the vessel wall on histological assessment. It was therefore decided to set 3mM as the phosphate concentration for subsequent work with this model.

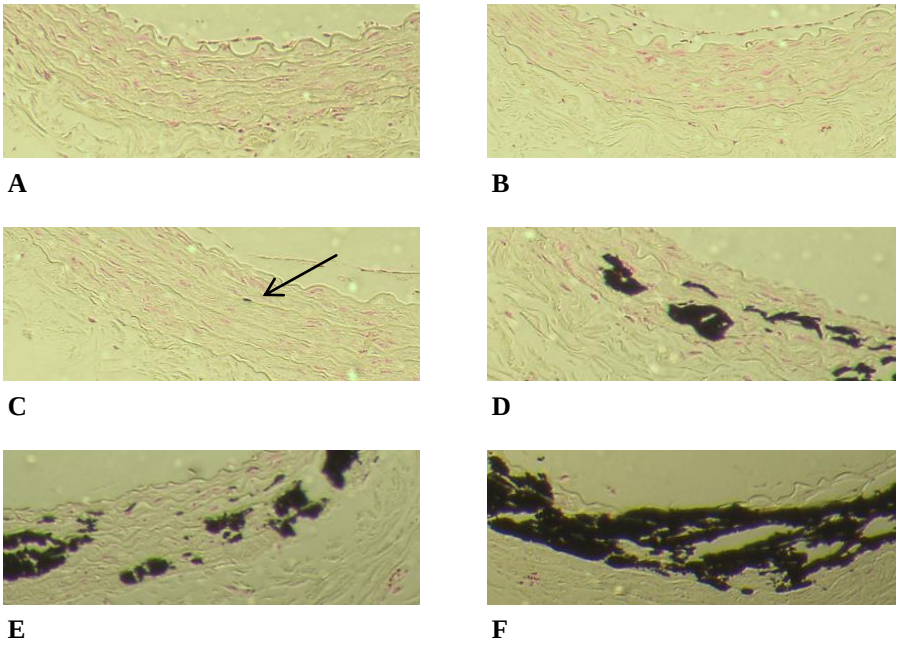

Figure 3.6. Calcification of Rat Aortic Rings in vitro with Increasing Phosphate Concentrations. Rat aortic rings were cultured in Medium-199 containing increasing concentrations of phosphate (A-F: 0.9 (basal), 2.0, 2.5, 3.0, 3.3 and 3.8mM, respectively). Silver nitrate stained (von Kossa stain) calcium deposits appear black (arrow in C) and cell nuclei are counterstained with aluminium red stain. Calcium deposition was evident at phosphate concentrations ≥ 2.5mM. Tissue cultured in phosphate concentrations above 3mM (E and F) was profoundly calcified which led to sections 'fracturing' upon processing limiting histochemical assessment of VSMCs. Magnification x10.

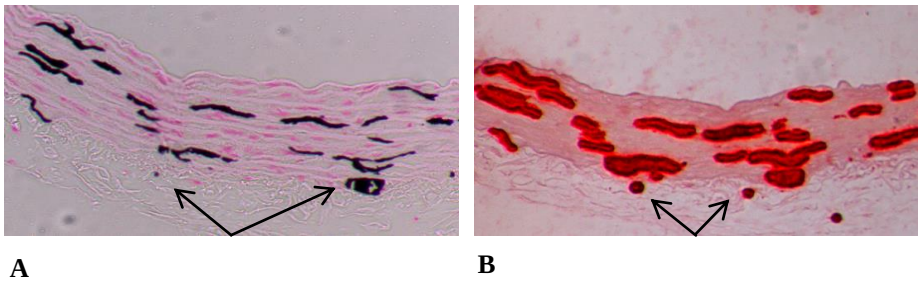

Figure 3.7. Digitally Magnified Images of Calcified Rat Aorta. A: Von Kossa stain with aluminium-red counterstain. B: Alizarin Red stain. With both stains, mineral deposits are seen 'tracking' along elastin fibres between VSMCs. Areas of positive staining are also seen within the adventitia (arrows). Original magnification x10, image cropped using Microsoft Office 2010.

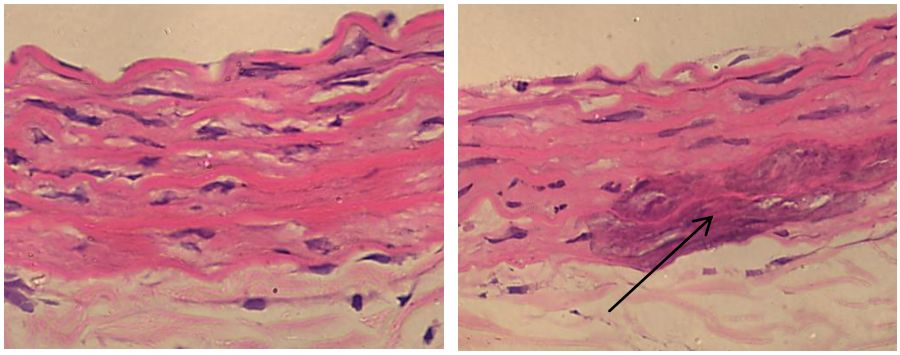

A **B**

Figure 3.8. H & E Stain of Normal and Calcified Aortic Rings. Rat aortic rings were cultured in A: basal or B: 3mM phosphate-containing Medium-199 for 10 days. H & E stained calcified regions appear purple (arrow). VSMCs in areas adjacent to calcification appear similar compared with normal tissue. Magnification x63.

3.2.3.ii Viability of rings is maintained following culture in 3mM phosphate for 10 days.

Whilst it was noted that VSMCs appeared normal on H & E staining in rings cultured under these conditions, a more robust assessment of tissue viability was desirable. One indicator of viability was the change in colour of culture medium. Consistent with the generation of acidic products from metabolic activity, in wells containing arterial rings the phenol red pH indicator in the culture medium changed colour from red to orange-yellow in the 2-3 days between media changes.

Quantitative measurement of tissue metabolic activity (and hence viability) was undertaken by determining the ATP content of culture medium from wells containing rings as compared with 'ring-free' medium at day 10. Culture medium containing phosphate concentrations of 1, 2 and 3mM was studied. The ATP content of 'tissue-naïve' culture medium (all phosphate concentrations combined) at day 10 was 445 ± 59nM. In contrast, ATP was barely detectable (0.03 ± 0.03nM) in culture medium in which rings had been present, consistent with active consumption and tissue viability. No differences were detected between media of different phosphate concentrations (Figure 3.9).

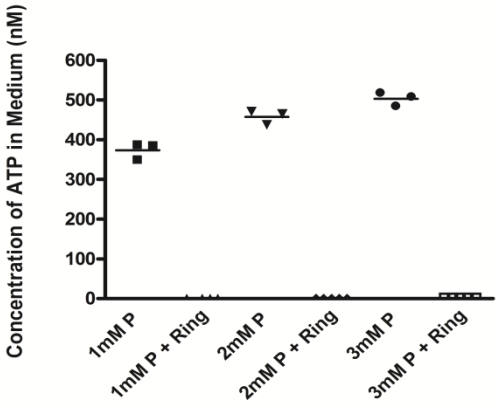

Figure 3.9. Measurement of ATP in Culture Medium to Assess Tissue Viability. Rat aortic rings were cultured for 10 days in Medium-199 containing 1, 2 or 3mM phosphate (P) as indicated. Wells containing Medium-199 at the same phosphate concentrations were maintained under identical conditions but without aortic rings. The ATP concentration in the medium from each well was measured. Each symbol represents a single culture well. Horizontal bars represent group means.

3.2.3.iii Time-course of cultured aortic ring calcification.

To ascertain the temporal relationship between time in culture and calcium deposition, rings were cultured in 3mM phosphate medium and examined by von Kossa staining at baseline and 3, 7 and 10 days. No calcification was observed in rings at baseline. At day 3 rings were essentially free of mineralisation, however occasionally a tiny speck of calcium was detected on an elastin fibre suggesting that calcium deposition is initiated at approximately this time-point in this model. Calcification was established although not florid on day 7 and widespread by day 10 (Figure 3.10).

A

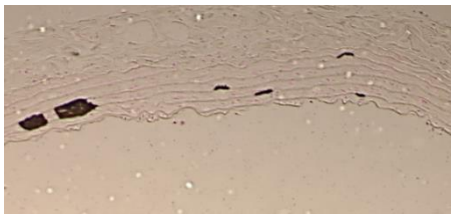

B

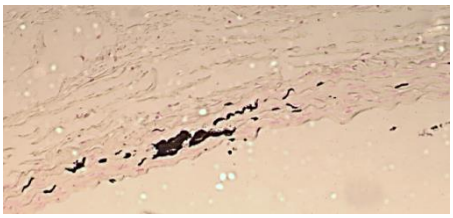

C

Figure 3.10. Calcification of Rat Aortic Rings Over Time. Rat aortic rings were cultured in Medium-199 containing 3mM phosphate. Rings were removed from culture after A: 3, B: 7 and C: 10 days and stained with von Kossa reagent. Calcification was barely detectable at day 3 (arrow shows one tiny speck of staining). By day 7 calcification was more established and widespread by day 10. Magnification x10.

3.2.3.iv Attempts to improve the consistency of aortic ring calcification.

In contrast to the VSMC culture model, it was extremely rare for aortic rings not to calcify. However, the degree of calcification between rings within experiments did vary widely, and it was observed that rings which originated from the abdominal section of the aorta tended to calcify more than those from the thoracic region. There are a number of reports describing modifications to this model which are suggested to improve its consistency and so further optimisation was attempted.

One group suggested that pre-incubating rings in porcine pancreatic elastase (0.01 units/ml) for 24 hours leads to more reliable calcification, presumably as a result of initiating elastin breakdown and facilitating adherence of mineral deposits (Scialla *et al* 2013). However, in the current model, after 10 days of culture in 3mM phosphate medium, *less* calcium was detected in rings that had been pre-incubated with elastase compared with those which had not (39.4 ± 20.2 vs 3.8 ± 6.6µg/mg without and with elastase treatment respectively; n = 3 for each group; p = 0.100) (Figure 3.11A, B and C). Rings that had been exposed to elastase weighed significantly less than controls (0.61 ± 0.28 vs 0.27 ± 0.07mg for controls vs elastase treated; p = 0.016) (Figure 3.11D) and on H & E staining the structure appeared much less organised (Figure 3.11E and F), both factors presumably reflecting elastin degradation and integral tissue 'scaffolding' loss.

In the original description of the aortic ring model, alkaline phosphatase was added to the culture medium to induce calcification (Lomashvili *et al* 2004). This effect was assumed to occur as a result of the enzyme hydrolysing the calcification inhibitor, PPi, generated by the cultured tissue. It was therefore assessed, in a single experiment, whether following this method would produce more uniform calcification in the present model. Unexpectedly, not only was a similar, wide range of mineralisation observed between rings, there was a *reduction* in calcification, albeit non-significant, in rings treated with alkaline phosphatase (data not shown).

It is well documented that calcium deposition is favoured by a more alkaline environment (Lomashvili *et al* 2006, Villa-Bellosta *et al* 2011b). Therefore in a final attempt to obtain a more consistent level of calcification within experiments, the culture medium pH was adjusted to 7.4 with the addition of NaOH. This resulted in

crystals, (presumably calcium-phosphate in composition), precipitating in the culture medium, usually within 48 hours. This limited the available soluble mineral and resulted in decreased in calcification.

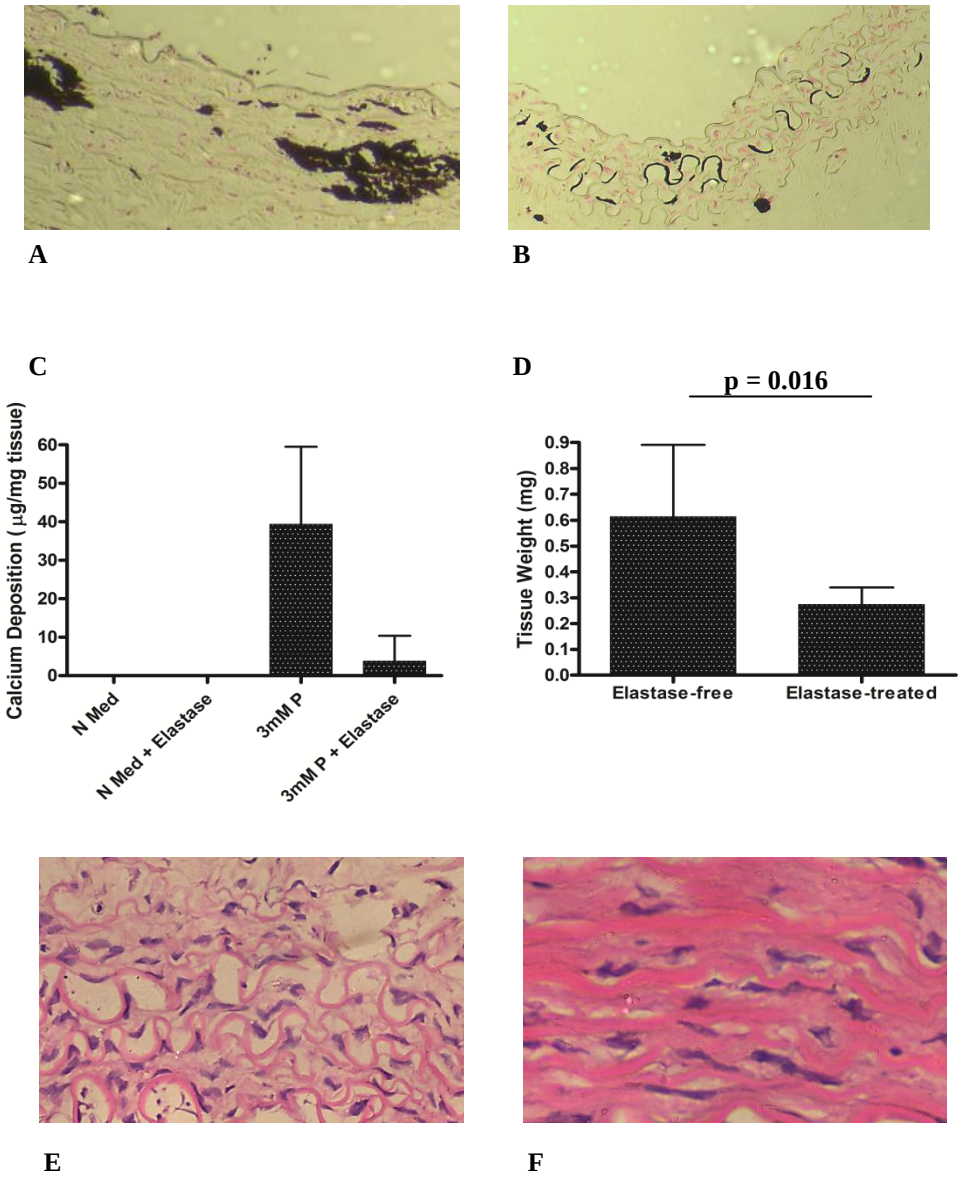

Figure 3.11. The Effect of Elastase on Cultured Aortic Rings. Rat aortic rings were cultured in either basal (N Med) or 3mM phosphate-containing (3mM P) Medium-199 for 10 days (n=6 per group). Prior to high phosphate exposure, 3 rings from each group were incubated in 0.01 units/ml porcine pancreatic elastase for 24 hours. A and B: Representative von Kossa stain of rings cultured in 3mM P without or with elastase treatment respectively. C: Quantification of calcium deposition in all groups. D: Weights of rings treated with elastase compared with controls. E and F: H & E staining of rings with and without elastase treatment respectively. Those exposed to elastase exhibited deranged architecture (E) compared with controls (F). Error bars represent mean ± SD. A & B: original magnification x10 (digitally cropped with Microsoft Office 2010). E & F: magnification x63.

As none of these steps lead to any improvement in the consistency of calcification it was accepted that this would be a feature of the model. Therefore, to aid interpretation and increase the precision of results, it was decided to aim for an arbitrary minimum of 5 replicates per group for each subsequent experiment.

3.2.4 The role of P2X7R in AC using an *ex vivo* model.

3.2.4.i The effect of pharmacological manipulation of P2X7R on rat aortic ring calcification.

To investigate the role of P2X7R in AC, rat aortic rings were first cultured in 3mM phosphate for 10 days with or without the presence of either the selective receptor antagonist A438079 (20μM), or agonist BzATP (100μM). Three consecutive experiments were initially performed, each using an aorta from a different rat.

Experiment 1: 6 rings were used per group with half taken for quantification of calcium and half for histological analysis. Calcification was similar in all three groups (3.6 ± 3.4 vs 4.8 ± 7.1 vs 4.6 ± 4.1μg/mg for control vs antagonist vs BzATP-treated rings, respectively; p = 0.733) (Figure 3.12A). The pattern of calcium deposition was identical for all groups as assessed by von Kossa staining. In addition, H & E staining demonstrated that VSMCs in vessels treated with both A438079 and BzATP appeared identical to those from control tissue (not shown).

Experiment 2: A non-statistically significant reduction in calcification was detected in rings treated with both A438079 and BzATP. The mean calcium deposition in rings cultured in 3mM phosphate alone was 79.2 ± 48.8 compared with 52.9 ± 51.1 and 54.4 ± 28.6μg/mg for the A438079 and BzATP treated rings, respectively (n = 8 per group; p = 0.357) (Figure 3.12B).

Experiment 3: A similar reduction in calcification was apparent in rings cultured in the presence of both pharmacological agents (45.6 ± 35.9, 15.8 ± 13.5 and 24.7 ± 15.1μg/mg for control, A438079 and BzATP-treated rings, respectively) (n = 6 per group; p = 0.113) (Figure 3.12C).

As wide standard deviations were seen within groups, a fourth study was conducted comparing just A438079 treatment to control, but increasing the number of rings per group to 10. In this experiment calcium deposition was more equivalent between

groups, in keeping with the results from the first experiment. Control ring calcification was 5.5 ± 5.9 vs 4.2 ± 7.1µg/mg for those treated with the antagonist (p = 0.248) (Figure 3.12D).

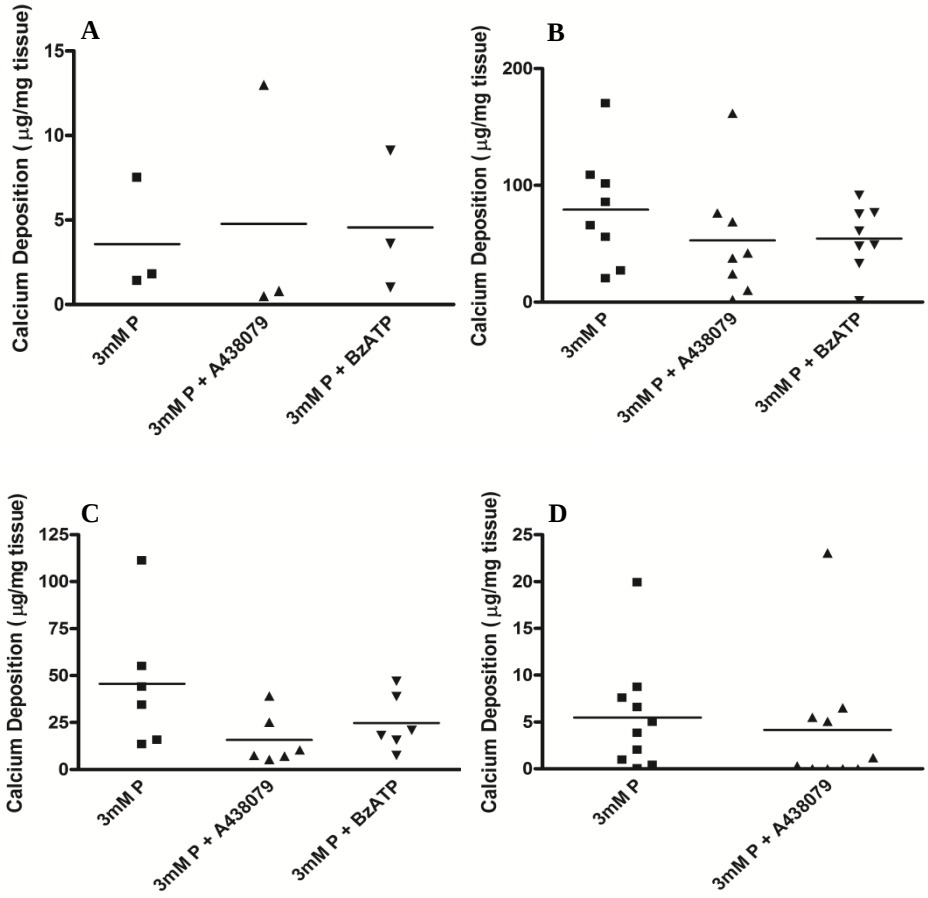

Figure 3.12. The Effect of the Specific P2X7R Antagonist A438079 and Agonist BzATP on Aortic Ring Calcification. Rings were cultured for 10 days in Medium-199 containing a phosphate concentration of 3mM (3mM P) with or without the presence of either the specific P2X7R antagonist A438079 (20µM) or agonist BzATP (100µM) (only A438079 in D). A-D represent consecutive experiments. Each symbol represents an individual ring and horizontal bars represent group means.

With no significant impact observed after 4 experiments using A438079, a single experiment was performed with a second P2X7R antagonist, A839977, tested over a range of concentrations (50nM, 500nM and 5µM). Again the wide standard deviations limited interpretation of the data, however, no significant differences in calcification were detected across the 4 groups (p = 0.411) (Figure 3.13).

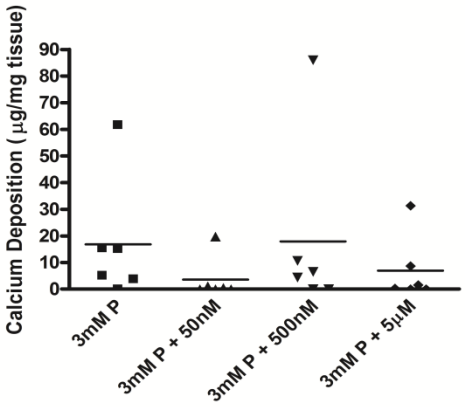

Figure 3.13. The Effect of the Specific P2X7R Antagonist A839977 on Aortic Ring Calcification. Rings were cultured for 10 days in Medium-199 containing 3mM phosphate (3mM P) alone or the specific P2X7R antagonist A839977 at the concentrations indicated. Each symbol represents an individual ring and horizontal bars represent group means.

3.2.4.ii Cultured aortic rings from WT and P2X7$^{-/-}$ mice exhibit a similar degree of calcification.

To complement the studies using pharmacological agents active at P2X7R, 2 experiments were performed using a similar *ex vivo* model, but culturing aortic rings from WT and P2X7$^{-/-}$ female mice. These mice had been backcrossed through 5 generations onto the calcification-prone DBA/2 background (Eaton *et al* 1978) (see Chapter 2, section 2.5). Due to the extremely small size of the murine aortic segments, when rings were harvested after 10 days in culture it was essentially impossible to remove the adventitial layer without damaging the rings and losing some calcified deposits. Therefore it was decided to quantify the calcium deposition for each ring with the adventitia intact. To ensure that medial calcification had occurred, von Kossa staining of a selection of rings was undertaken. This demonstrated mineral deposits along medial elastin fibres. Staining was, as expected, also present in the adventitia (Figure 3.14A).

In the first of these experiments, there was a non-significant increase in calcification in the KO rings (27.7 ± 40.3 vs 105.8 ± 87.6μg/mg for WT vs KO; n = 6 per group; p = 0.093) (Figure 3.14B). In the second, calcium deposition was similar for both genotypes (356.8 ± 182.0 vs 409.8 ± 209.2μg/mg for WT vs KO; n = 5 per group; p = 0.548) (Figure 3.14C). The magnitude of calcification was several-fold higher in

the second experiment, possibly owing to a greater amount of residual adventitia being left on these rings following the initial dissection.

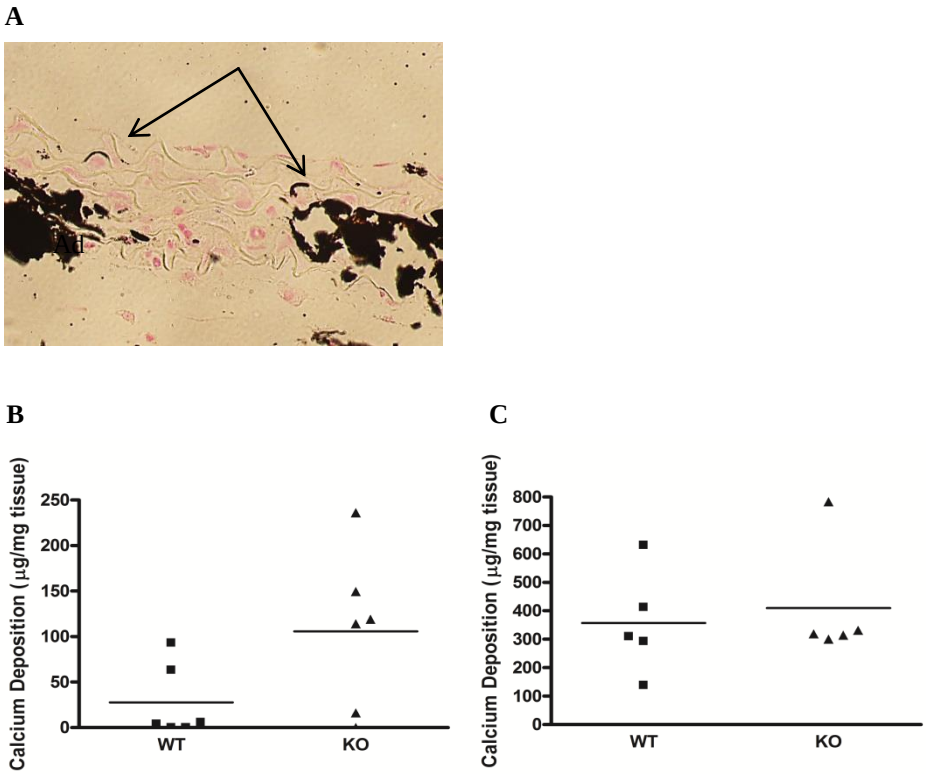

Figure 3.14. The Influence of P2X7R Gene Deletion on Aortic Ring Calcification. Aortic rings from WT and P2X7$^{-/-}$ (KO) female mice were cultured for 10 days in Medium-199 containing 3mM phosphate. A: Von Kossa staining of a calcified ring from a WT mouse after 10 days in culture. Arrows indicate calcium deposition along elastin fibres. 'Ad' indicates the adventitia. This could not be removed during these experiments due to technical difficulty (described in the text) and did stain for mineral deposits. B and C: Calcium quantification results from 2 consecutive experiments. Each symbol represents one ring and horizontal bars represent group means. A: magnification x63.

3.2.5 Expression of mRNA for P2X7R, markers of VSMC phenotype and caspase-3.

The expression of P2X7R mRNA was assessed in cultured rodent aortic rings at baseline and at 3 time-points (days 3, 7 and 10) under control and calcification-promoting (3mM phosphate) conditions (i.e. 7 groups). Aortas from 3 rats were cut into rings and distributed between the 7 groups, ($n \geq 5$ per group). In addition, to ascertain whether osteogenic transformation and apoptosis occur in this model, mRNA expression of the VSMC-specific marker SM-22, the osteogenic

transcription factors runx-2 and osterix and caspase-3 (as an indicator of apoptosis) was examined (Table 3.1, Figures 3.15 and 3.16).

It was notable that time in culture alone seemed to exert an effect on mRNA expression i.e. results from the baseline samples differed from those rings cultured in normal medium, and that at the later time-points – especially by day 10, the standard deviation became extremely wide (Table 3.1). The A260/280 ratios of samples varied although all groups contained a spread of values and the expression of mRNA for the housekeeping genes examined (HPRT, 28S and SDHA) did not significantly differ between groups (not shown). The mean absolute copy numbers of mRNA for these three housekeeping genes were 9,088 ± 3,745, 35,371 ± 15,521 and 50,702 ± 20,404 respectively.

Overall there was no significant difference in the expression of P2X7R mRNA between groups (Figure 3.15A, Table 3.1). Notably, the absolute copy numbers of mRNA were extremely low being in the order of just a few hundred. Protein extraction from these small samples was difficult however a Western blot was performed to confirm that P2X7R protein was expressed in cultured aortic rings (Figure 3.15B). The regulation of arterial protein expression by calcification was assessed *in vivo* and is described in Chapter 5.

Expression of mRNA for the VSMC-specific marker SM-22 was examined. A striking contrast was seen between the expression in baseline tissue and control samples at later time-points with a statistically significant decrease observed on days 3 and 7. No significant difference was detected for samples cultured in high phosphate medium compared with the time-point controls (Figure 3.16A, Table 3.1). An attempt was made to quantify the expression of mRNA for the osteogenic transcription factors runx-2 and osterix, however, these were barely detectable (< 100 copies) in all groups (control and calcified) (not shown). Expression of mRNA for the apoptosis marker caspase-3 increased from baseline in control samples at subsequent time-points. This reached statistical significance by day 7 and remained significant at day 10. Again, culture in high phosphate medium did not significantly influence mRNA expression (Figure 3.16B, Table 3.1).

Gene	Baseline n=7	Day 3 – Control n=5	Day 3 - HP n=5	Day 7 – Control n=5	Day 7 - HP n=5	Day 10 – Control n=5	Day 10 – HP n=6	p value (KW test)
P2X7R	238 ± 32	126 ± 54	111 ± 45	162 ± 54	151 ± 106	280 ± 111	126 ± 62	0.007
SM-22	2,833,000 ± 454,601	77,586 ± 87,614**	39,795 ± 35,792	90,013 ± 56,516*	128,843 ± 177,288	689,904 ± 749,773	156,555 ± 205,496	0.001
Caspase-3	5,121 ± 1,373	13,532 ± 2,466	10,804 ± 2,195	18,216 ± 4,283***	15,962 ± 5,282	20,394 ± 2,801***	12,608 ± 3,579	<0.001

Table 3.1. mRNA Copy Numbers for P2X7R, SM-22 and Caspase-3 in Cultured Rat Aortic Rings Over Time. Quantification of mRNA copy numbers for indicated genes in rat aortic rings cultured in either control or 3mM (high) phosphate-containing (HP) Medium-199 over time. As initial KW test indicated $p<0.05$ for all genes, *post hoc* tests compared all control groups with baseline and control with HP at each time-point. *$p<0.05$; **$p<0.01$;***$p<0.001$ (all compared to baseline). Data are presented as mean ± SD.

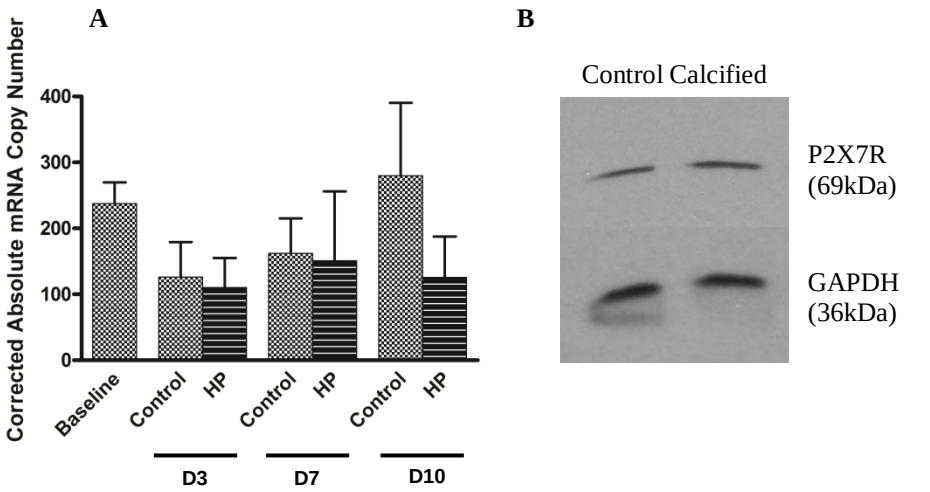

Figure 3.15. Expression of P2X7R in Control and Calcified Rat Aortic Rings. A: Quantification of P2X7R mRNA copy numbers in rat aortic rings cultured in either control or 3mM (high) phosphate-containing (HP) Medium-199 over time. *Post hoc* tests compared all control groups with baseline and control with HP at each time-point. 'D' designates number of days in culture. Error bars represent mean ± SD. Number of rings per group from left to right = 7,5,5,5,5,5,6. B: Western blot of protein extracted from a single control and a single calcified aortic ring after 10 days in culture demonstrating the presence of P2X7R protein.

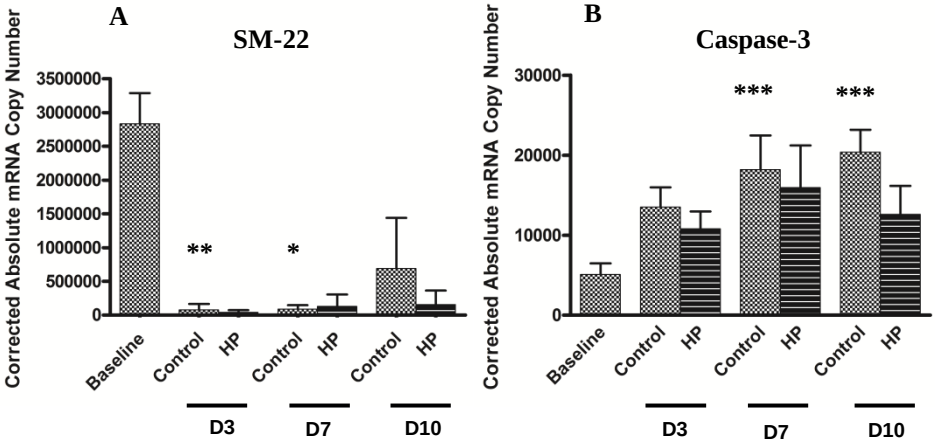

Figure 3.16. mRNA Copy Numbers for SM-22 and Caspase-3 in Cultured Rat Aortic Rings Over Time. Quantification of A: SM-22 and B: Caspase-3 mRNA copy numbers in rat aortic rings cultured in either control or 3mM (high) phosphate-containing (HP) Medium-199 over time. Initial KW test indicated $p<0.05$ for both genes. *Post hoc* tests compared all control groups with baseline and control with HP at each time-point. *$p<0.05$; **$p<0.1$; ***$p<0.001$ all compared to baseline. 'D' designates number of days in culture. Error bars represent mean ± SD. Number of rings per group from left to right = 7,5,5,5,5,5,6.

3.3 Discussion

Previous reports investigating the expression profiles of P2 receptors in the vasculature (Wang *et al* 2002, Schuchardt *et al* 2011) have indicated that P2X7R is expressed at the mRNA level in VSMCs although its presence at the protein level has not been described. In the current work, P2X7R mRNA appeared to be expressed at a very low level in normal rat aorta and *in vitro* was not modified by a 'pro-calcification' environment. Despite the low level of mRNA, P2X7R protein is expressed in hVSMCs and in rat aorta.

The primary objective of the work described in this chapter was to ascertain whether P2X7R influences calcium deposition in an *in vitro* model of AC. A number of experiments, using a variety of culture systems, give the overriding impression that it does not, at least not to any major extent. Some experiments showed trends towards an attenuating effect of P2X7R, whilst others suggested that it might enhance calcification. There were also a number of experiments which suggested no effect and overall there was no convincing evidence to indicate a significant role either way for P2X7R in this setting. However, this conclusion does need to be taken within the context of the experimental systems used and with consideration of their limitations.

The lack of effect of P2X7R is unlikely to be explained by suboptimal dosing of the pharmacological agents employed. A438079 is a P2X7R antagonist with an IC_{50} value of 0.1 and 0.3μM for BzATP induced Ca^{2+} influx through human and rat P2X7Rs respectively (Donnelly-Robert *et al* 2007). The compound has been shown to not be active at other purine receptors (P2X3, P2X4 and P2Y2) at concentrations up to approximately 10μM (Nelson *et al* 2006) and this limit of specificity is probably higher (McGaraughty *et al* 2007). Subtle effects at other purine receptors cannot be excluded but would be expected to be minor at most, given the lack of effect at the selected P2 receptors examined in the study by Nelson *et al* (2006). A438079 has also been shown to have little activity at a wide array of other cell surface receptors (Donnelly-Robert *et al* 2007). Thus whilst only a single dose of 20μM was used for experiments with rat aortic rings, this concentration should have achieved essentially total blockade of P2X7R. The second antagonist employed, A839977, has not been so widely used, 3 concentrations (50nM, 500nM and 5μM) were trialled in the single experiment examining its effect. Nonetheless, the IC_{50} of

this agent at rat P2X7R is 42nM (Honore *et al* 2009) and hence adequate antagonism should have been achieved. BzATP, whilst frequently cited as such, is not a specific agonist at P2X7R having partial activity a number of other P2 receptors (Bianchi *et al* 1999, Michel *et al* 2001). However, 100μM (the concentration used in this chapter), is generally considered to be appropriate to obtain relatively specific activation of P2X7R (Orriss *et al* 2012), and in practical terms provides the best means of achieving this. Taken together these data suggest that the pharmacological manipulation of P2X7R in this chapter should have been successful.

Of the number of theoretical ways in which P2X7R might influence AC (outlined in Chapter 1, summarised in Figure 1.3), only some are relevant and potentially able to be evaluated in these *in vitro* models. In essence, the systems described in this chapter are modelling 'phosphate-induced calcification'. This is clearly very different from calcification induced by a uraemic milieu where phosphate is only one of several factors likely to be involved. It therefore follows that only the influence of P2X7R on phosphate-driven VSMC osteogenic transformation and/or apoptosis can be assessed in these models, whereas its effect on a pathway such as uraemia-induced disruption of normal bone physiology and related vascular effects cannot be.

That osteogenic transformation is necessary to induce calcification is a frequently stated conclusion from experiments using cultured VSMCs (Shanahan *et al* 2011, Shanahan 2013, Shroff *et al* 2013). However, this has been refuted by some groups. For example, a study which exposed both formalin-fixed and viable control VSMCs to high phosphate medium *in vitro* found greater calcium deposition associated with the fixed cells (Villa-Bellosta *et al* 2011b). The authors therefore concluded that VSMC-associated calcification was actively inhibited by viable cells rather than induced following an active switch in phenotype. Another report, from a different group, demonstrated that a change in phenotype of VSMCs towards an osteoblast-like cell only occurred *after* mineralisation was present, thereby suggesting that it was the calcium-phosphate crystals themselves causing the switch, not vice-versa (Sage *et al* 2011). Reports of osteogenic transformation occurring in the ring culture model are also variable. Some authors have shown positive immunohistochemical staining for osteogenic markers in calcified cultured arteries (Shroff *et al* 2010). However, other groups that have published widely using this system have suggested

that the switch in cell phenotype does not occur (Lomshvili *et al* 2008, Lomshvili *et al* 2011). The same can be said for apoptosis (Lomashvili *et al* 2004).

The aim of the work in this chapter was not specifically to confirm or refute these previous findings, however the analysis of mRNA expression for the genes of interest described here raises some points of note. No significant differences were found at any time-point for control versus calcified aortas in any marker of VSMC phenotype or the apoptosis marker caspase-3. No markers of osteogenic transformation were detected. These findings would seem to support the view that VSMC osteogenic transformation and apoptosis are not involved in the calcification process in this experimental system and therefore raise questions about their involvement in the process of AC in general. If in fact these 2 mechanisms do not occur in this context, then it is unsurprising that P2X7R did not exert any significant impact on calcium deposition in the experiments described in this chapter.

The results from experiments using cultured VSMCs are difficult to interpret due to the profound experimental variability. In a number of experiments, some cells, and on occasion all cells, cultured in 'calcification' medium alone, i.e. those intended to serve as control calcified cells, failed to exhibit any calcium deposition. This was not an infrequent finding, essentially meaning that any differences in calcium deposition occurring in groups treated with A438079 could not, with any confidence, be assigned to the effect of treatment.

The reliability and consistency of this model have been challenged previously, with a number of authors commenting that the range of phosphate added to the culture medium in order to observe calcification varies tremendously between laboratories (Villa-Bellosta *et al* 2011b). Indeed, some groups have reported calcification with as little as 2mM P in the culture medium (Villa-Bellosta *et al* 2011b), whereas others have not been able to induce any calcium deposition with concentrations below 5mM (Ciceri *et al* 2012a). Furthermore, groups have reported that in some circumstances they were unable to induce any calcification in certain batches of cells which were therefore not used for experiments (Shalhoub *et al* 2010). There are also instances of groups having to alter the length of time cells were left in culture to yield calcification when experiments were performed on different occasions (Ciceri *et al* 2012a, Ciceri *et al* 2012b). Personal communications to a number of researchers in

the field have also added weight to the conclusion that this model suffers from marked variability and inconsistency.

Whilst these inconsistencies make results difficult to interpret, potentially a more fundamental limitation of this model might be its lack of biological relevance. This was ultimately the reason for abandoning it as an experimental tool for work in this thesis. VSMCs in culture lack their normal ECM. In particular, the elastic lamina is absent, which is the initial site of calcification within the arterial wall as shown by work in this thesis (Figure 3.6 and also see Chapters 5 & 6) and other investigators (Lanzer *et al* 2014). In addition, the use of serum and associated growth factors, along with variations in cell passage number, can grossly influence VSMC phenotype and may promote proliferation (Zeidan *et al* 2000, Lomashvili *et al* 2004, Nakano-Kurimoto *et al* 2009). Therefore this system simulates a very different environment from that seen *in vivo*. Furthermore, exactly what is 'calcifying' in this setting is not altogether clear. Cultured VSMCs are reported to secrete matrix-vesicles upon which calcium is deposited (Reynolds *et al* 2004). However, there are reports demonstrating that much of the 'calcification' that is seen results from passive deposition of calcium-phosphate crystals onto the culture plate (Sage *et al* 2011). Additionally, calcium deposition has been shown to occur in this context with other, non-vascular cells, such as those from the renal proximal tubule (Villa-Bellosta *et al* 2011b, Sage *et al* 2011).

Some, but by no means all, of these issues are overcome with the aortic ring *ex vivo* model. Here, tissue is essentially 'intact' and, as demonstrated, calcification occurs along elastin fibres thereby bearing a closer resemblance to findings in patients with CKD (see Chapter 6). Aortic rings cultured in 3mM phosphate consistently calcified without the need for any additional supplements to the medium or pre-treatment. This is in contrast to previous reports using this model. Rat rings cultured in 3.8mM phosphate were shown to be free of calcification after 10 days in culture unless alkaline phosphatase was added to the culture medium (Lomashvili *et al* 2004), and human vessels from healthy control patients did not calcify in a medium containing 2mM phosphate plus 2.7mM calcium whereas those from patients on dialysis did (Shroff *et al* 2010). The latter of these reports can conceivably be explained by the differences in species and/or the concentrations of phosphate and calcium used

(although the calcium x phosphate product is identical to that used in the current work, the individual ion concentrations differ). It is more difficult to reconcile the lack of calcification described in the former study with the observations made in this chapter, especially as a lower phosphate concentration was used here. Indeed, when rings were cultured in 3.8mM phosphate in the present work, calcification of almost the entire vessel was seen. In addition, when rings were cultured with alkaline phosphatase, *less* calcification was observed. Apart from the basic culture medium and strain of rat (Dulbecco's Modified Eagle Medium (DMEM) and Sprague-Dawley, respectively, in the original report by Lomashvili *et al* (2004)), an identical protocol to that described was used so it is unclear why the opposite effect occurred. It is possible that there were subtle differences in the composition of reagents and/or culture environment not specified in the initial paper. As the primary goal of using alkaline phosphatase in the current work was to improve the consistency of calcification, and after one attempt a reduction in calcium deposition was seen, this approach was not pursued further. It is therefore possible that the findings in this single experiment were spurious, however, the use of 3mM phosphate to induce calcification without additional reagents was consistent throughout the work described in this chapter and is clearly in contrast to this original report.

Another advantage of the ring culture system is that serum and growth factor supplementation are unnecessary to maintain cell viability, thereby minimising the effect these additives can have on cell activity and phenotype. However, the analysis of mRNA for SM-22 suggests that expression of this VSMC marker, and therefore possibly VSMC phenotype, are modified by simply maintaining rings in normal culture medium. In addition, the results for caspase-3 indicate that even these 'control' conditions may induce some degree of apoptosis. That changes in gene expression profiles can be induced by culture conditions alone was shown in a previous report which described a change from baseline in runx-2 mRNA expression in control rings cultured for 3 days without the addition of any 'extra' reagent (Lomashvili *et al* 2011). Although the ring culture model has a number of advantages over primary cell culture, maintenance of cell phenotype and absence of apoptosis, previously cited to be additional benefits (Lomashvili *et al* 2004, Shroff *et al* 2010) were not observed in the studies presented herein.

The magnitude of calcification differed between experiments performed in this chapter and wide standard deviations in calcification were frequently seen within groups of cultured rings. Attempts to improve the consistency of calcification were unsuccessful. Unexpectedly, the 'pre-treatment' of rings with elastase for 24 hours led to a reduction in calcification. The report originally detailing this method suggested that *in vitro*, elastase initiates elastin breakdown, mimicking the *in vivo* histological findings from calcified mouse aortas described by the same group, leading to more consistent calcification (Scialla *et al* 2013). As this group cultured mouse aortic rings, (in contrast to the rat vessels used in the present work), it is possible that species differences account for the disparate findings. The fact that in the current study elastase-treated rings weighed much less than the corresponding controls suggests that the enzyme was in effect causing overt elastin dissolution rather than just initiating its breakdown. This might also explain the reduced calcification.

A number of potential reasons exist to account for the variability in calcification between rings within individual experiments. The importance of removing the adventitia from vessels prior to quantifying medial calcium deposition was demonstrated histologically, with deposits frequently seen within the adventitial layer. However, in removing the adventitia there is the potential to damage the vessel and dislodge adherent calcium. This may occur to different, random extents between rings. Removing the adventitia prior to commencing the experiment is not a solution to this problem as this can damage the medial layer resulting in more calcification and thus cause greater variability overall (Lomashvili *et al* 2004). It is also possible that rings from different sections of the aorta calcify differently. A notable feature of the rat *in vivo* work in this thesis (Chapter 5) is that the abdominal aorta seems to calcify before the thoracic segment and the aortic arch, as has been described previously in animal experiments (Shobeiri *et al* 2013). Whatever the explanation(s), none of these factors should have biased the outcome in either direction since all rings were handled in the same way. Additionally, adjacent rings were exposed to different treatments thereby eliminating the potential effects conferred by where on the aorta the ring originated from.

3.4 Summary

The results from this chapter suggest that P2X7R does not influence AC in the tissue culture models employed. How relevant these experimental systems are to 'real life' biology remains unclear. In particular, it is uncertain whether some mechanisms widely reported to be important in the pathogenesis of AC occur in these settings. The role(s) of P2X7R in AC pathways which are dependent upon a uraemic milieu cannot easily be tested under these conditions. *In vivo* studies are necessary to investigate these processes and were the focus of the work described in Chapters 4 and 5.

CHAPTER 4 – DEVELOPMENT OF A NOVEL MOUSE MODEL TO STUDY THE EFFECT OF P2X7R DEFICIENCY ON CHRONIC KIDNEY DISEASE-ASSOCIATED ARTERIAL CALCIFICATION

4.1 Introduction

VSMC or ring culture models can be used to study calcium deposition and cellular changes that occur in response to agents thought to be important in the process of CKD-associated AC. However, as alluded to in Chapter 3 it is extremely difficult to simulate a 'uraemic milieu' per se *in vitro,* and these models have a number of other limitations. *In vivo* systems provide a complementary approach to *in vitro* studies and permit investigation under more biologically and physiologically relevant conditions.

A number of pathways thought to contribute to the pathogenesis CKD-associated AC have been described which are dependent upon systemic changes induced by renal impairment, and therefore can only really be assessed *in vivo*. Two examples of these are disturbances in bone homeostasis (Persy & D'Haese 2009) and arterial ECM degradation (Pai & Giachelli 2010). P2X7R is potentially relevant to both, having been linked to these processes in other contexts (Grol *et al* 2009, Gu & Wiley 2006). In addition, P2X7R has been shown to attenuate progression of CKD itself in some animal models (Goncalves *et al* 2006) and therefore in so doing might concurrently retard progression of AC. Finally, the work in Chapter 3 cast some doubt as to whether osteogenic transformation and apoptosis of VSMCs, pathways that hypothetically might be influenced by P2X7R, are involved in the development of AC. Assessing these pathways *in vivo* and specifically in the setting of CKD along with any impact of P2X7R is therefore relevant and desirable.

The aim of the work described in this chapter was to assess whether P2X7R deficiency influences the development and progression of CKD-associated AC *in vivo* by comparing $P2X7^{-/-}$ mice with WT controls in an appropriate disease model. As reviewed in Chapter 1 (section 1.4.3), just one murine model of CKD-associated AC is described in the literature (El Abadi *et al* 2009). The original report detailing the development of this model indicated that CKD alone was not sufficient for AC to develop and that it had to be combined with a high phosphate diet. The model itself involves extensive surgical manipulation ($5/6^{th}$ nephrectomy) thereby limiting its

availability to those with specialist expertise and is inevitably associated with a high rate of animal loss. Furthermore, it appears the effect is limited to female mice and requires a number of months for established arterial disease to develop. An initial objective of the current work was therefore to develop a non-surgical and more convenient mouse model of CKD-associated AC to use as an experimental tool.

Importantly, DBA/2 mice, a strain prone to arterial calcification, were used in this original study as the C57Bl/6 genetic background is thought to confer resistance to this disease (Eaton *et al* 1978). $P2X7^{-/-}$ mice were created in the C57Bl/6 strain (Solle *et al* 2001). It was therefore necessary to backcross these mice through 5 generations onto the DBA/2 background prior to performing the experiments examining the role of genetic deletion on AC (as described in Chapter 2). While the backcrossing was in progress, attempts to develop the experimental model were carried out with WT DBA/2 mice.

The propensity of 2 agents, folic acid and adenine, to induce CKD was investigated in this chapter. Folic acid has been widely used to induce renal fibrosis in mice (Fink *et al* 1987, Long *et al* 2008, Bechtel *et al* 2010), although no reports are available detailing its use in female DBA/2 animals. This work therefore first sought to determine whether this agent, in combination with high phosphate feeding, would lead to AC. Dietary adenine is widely used to induce CKD and AC in rats (Shobeiri *et al* 2010, Neven & D'Haese 2011) and was the basic model employed for the work detailed in Chapter 5. However, adenine has only recently been administered to mice and AC has not previously been described (Tamura *et al* 2009, Tanaka *et al* 2009, Oyama *et al* 2010, Schiavi *et al* 2012, Jia *et al* 2013, Santana *et al* 2013). Of relevance, these studies all administered adenine to mice on calcification-resistant backgrounds. In addition, studies in rats have highlighted the importance of using a low dietary protein content in order to reliably induce AC (Price *et al* 2006). This work therefore also investigated whether an adenine-containing diet with adjustments in protein content could induce CKD and AC in calcification-prone mice.

4.2 Results

4.2.1 Administration of folic acid to WT DBA/2 mice.

Folic acid has successfully been used to induce CKD in other (non-DBA/2) strains of mice, with an ip dose of generally 240µg/g or less reported to result in renal fibrosis (Long *et al* 2008). This concentration was therefore initially administered to 6 WT female DBA/2 mice with a further 4 receiving vehicle control. High phosphate feeding (Diet A, Table 2.1) commenced the day after the ip injection for all animals and continued for 20 weeks.

The appearance, movement and social interaction of all 6 mice injected with 240µg/g folic acid was indistinguishable from the 4 controls at all times following treatment. Mean weight change after 7 days in controls was +2.5 ± 7.6% compared with -1.0 ± 5.7% in folic acid-treated animals (p = 0.430). The corresponding values at 20 weeks were +0.1 ± 3.4 vs +2.4 ± 5.8% (p = 0.493) (Figure 4.1).

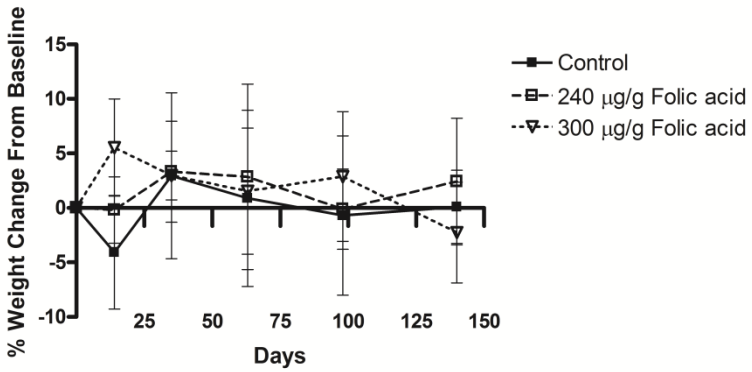

Figure 4.1. Weight Loss in Mice Treated with Folic Acid. Percent weight loss at selected time-points compared with baseline in control mice (n=4, filled squares) and those treated with 240 (n=6, unfilled squares) and 300µg/g folic acid (n=3, unfilled triangles). Data are presented as mean ± SD.

Serum concentrations of urea, creatinine, phosphate, calcium (uncorrected due to insufficient serum for additional measurement of albumin) and alkaline phosphatase were measured at baseline, 2, 5, 9, 15 and 20 weeks. In addition, serum was collected from 2 mice after 3 days in order to assess for acute kidney injury. With the exception of phosphate, which showed an approximate 2-fold increase at 20 weeks compared to baseline in both groups, all biochemical parameters remained relatively

stable throughout the study period. There were no significant differences between groups in the absolute change of any analyte at week 20 compared to baseline (Figure 4.2).

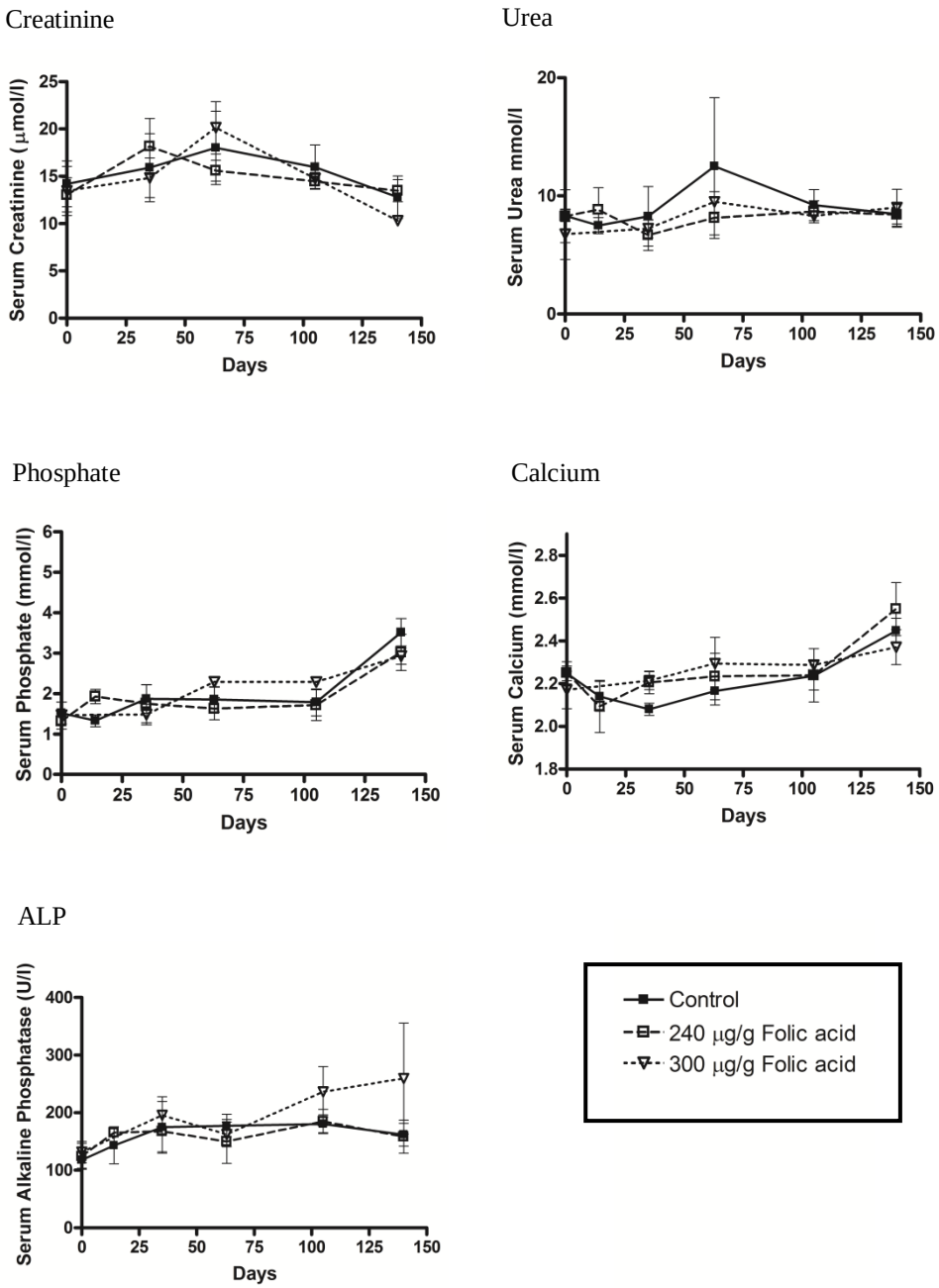

Figure 4.2. Serum Biochemistry in Mice Treated with Folic Acid. Concentrations of indicated serum parameters over time in control mice (n=4, filled squares) and those treated with 240 (n=6, unfilled squares) and 300µg/g folic acid (n=3, unfilled triangles). Data are presented as mean ± SD.

Histologically, kidneys taken from animals in both groups were indistinguishable, exhibiting essentially a normal appearance (Figure 4.3). No calcification was

detected in any aorta from these mice either biochemically or histologically (Figure 4.3).

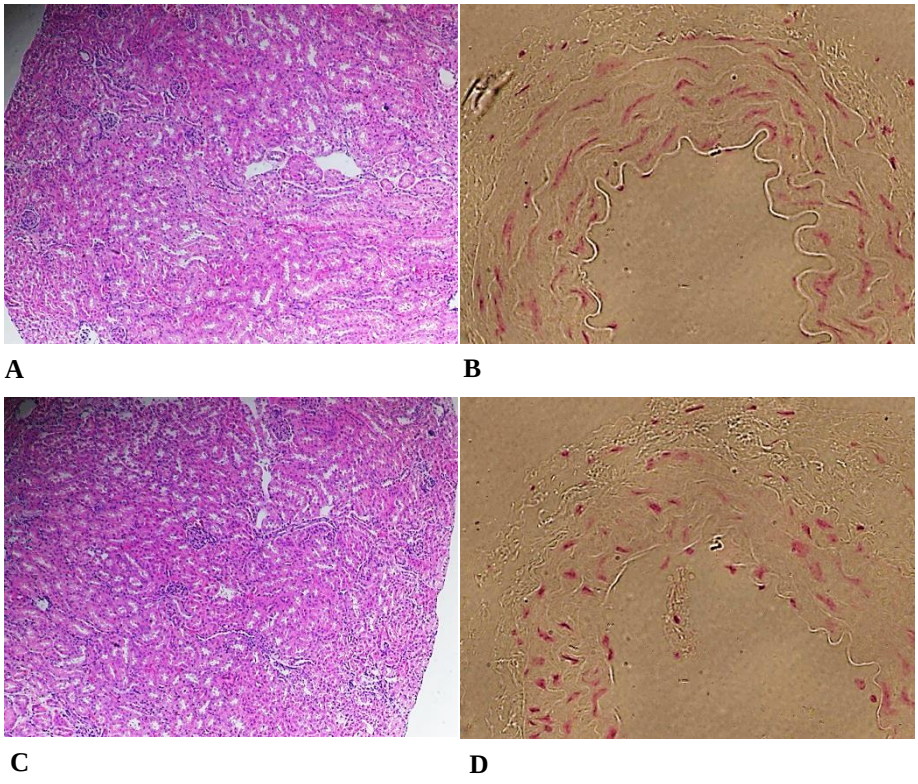

Figure 4.3. Absence of Kidney and Aortic Disease in Mice Treated with 240µg/g Folic Acid. Representative H & E staining of kidney sections with corresponding von Kossa staining of aortas taken from female mice. A & B: Control mice. C & D: 240µg/g folic acid-treated. A & C magnification x10. B & D magnification x63.

As no disease was induced by this protocol, a further 4 mice were given an ip dose of 300µg/g (an increase of 25%). One of these mice died in the first week following injection, however this was deemed to have occurred due to peritonitis, as cloudy peritoneal fluid was observed during post-mortem examination, rather than any folic acid-induced acute kidney injury. The other 3 mice remained well for the 20 week study period. Serum urea taken at day 3 from these mice showed a mean fold increase of 2.0 ± 0.7 possibly suggesting some degree of kidney injury but there were no clinical manifestations of this and in particular all 3 animals *gained* a small amount of weight during the first 14 days of study. After this point all serum parameters remained relatively stable compared to baseline and of similar magnitudes to the results obtained for the control and 240µg/g groups described

above (Figure 4.2). There was no aortic calcification and no histological abnormality in aortas or kidneys after 20 weeks.

Given that the concentrations of folic acid administered to this point had no effect, it seemed likely that much higher doses would be required to induce renal injury. It was therefore decided to double the original starting dose to 480µg/g and examine the effect in a further 6 female DBA/2 mice. All but one of these animals died in the first week. Histological examination of kidneys from deceased mice revealed dilated tubules with flattened epithelium, a number containing casts and other debris - all findings consistent with a folic acid-induced acute kidney injury (Figure 4.4).

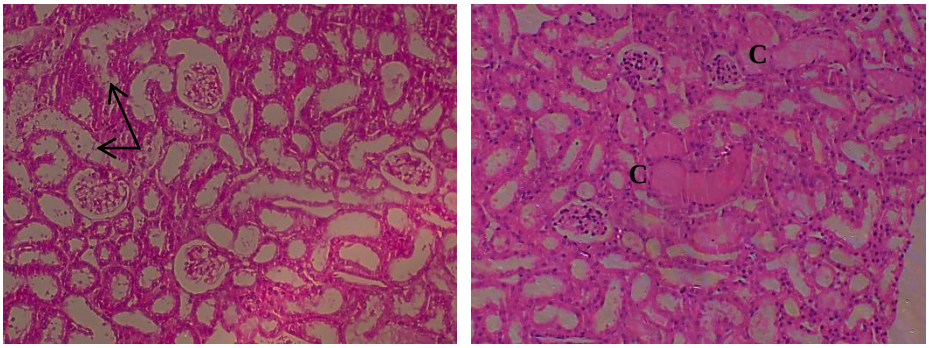

Figure 4.4. Acute Tubular Injury in Mice Treated with 480µg/g Folic Acid.
H & E stained kidney sections from a mouse which died within 3 days following treatment with 480µg/g folic acid. Features of acute tubular injury are present including epithelial flattening and intra-luminal debris (arrows) and tubular casts ('C'). Magnification x20.

Of particular note, the one mouse that did not die in the first week initially lost weight without appearing overtly unwell and had a serum urea rise from 4.4mmol/l at baseline to 71.0mmol/l at day 3. However, it gained weight over subsequent days to survive the 20 week study period. Following sacrifice, the histological appearance of the kidney from this mouse was not noticeably different from the control kidneys previously examined (Figure 4.5A). However, von Kossa staining demonstrated calcium deposits within the aorta which were clearly seen to be associated with elastin fibres in the medial layer of the vessel (Figure 4.5B and C).

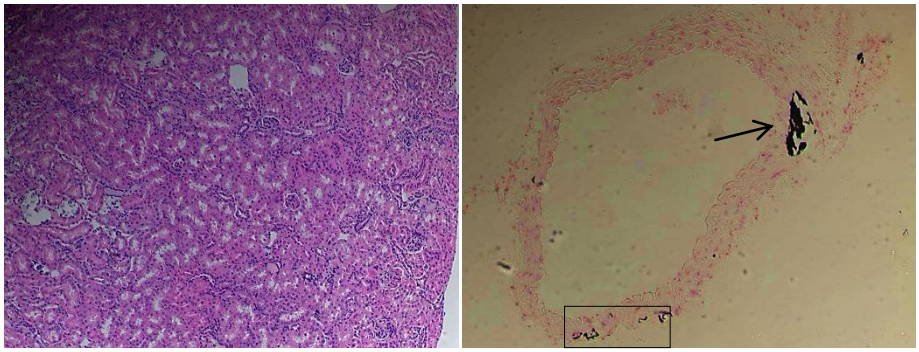

A B

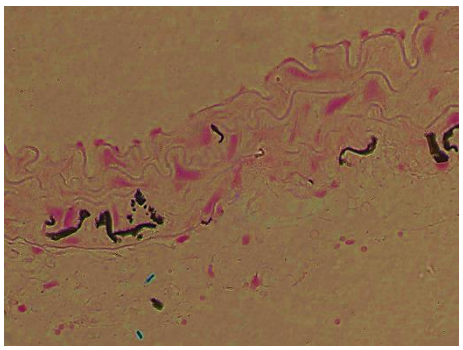

C

Figure 4.5. Kidney and Aortic Disease in One Mouse Treated with 480µg/g Folic Acid. A: H & E stain of kidney tissue demonstrating essentially normal features. B: von Kossa stain of aorta. Calcium deposits are stained black (arrows and inside box). Counterstained with aluminium red. C: Close up of boxed section in 'B' demonstrating calcium deposition along elastic fibres. A & B magnification x10; C magnification x63.

Although AC was evident in this one animal, the mortality rate of 83% associated with this higher dose of folic acid was clearly unacceptably high. A further dose adjustment was therefore made and 360µg/g was administered to 2 mice. Both animals died during the first week following injection of folic acid with similar histological renal findings to those described for 480µg/g (not shown). Following these attempts it became clear that the use of folic acid was unlikely to prove successful for inducing the required clinical characteristics. An alternative chemical agent for induction of renal disease with AC was therefore sought.

4.2.2 Optimisation of an adenine-based regime.

4.2.2.i A diet containing high phosphate, low protein and adenine induces CKD and AC in male DBA/2 mice.

Initially 16 WT DBA/2 mice, (8 male and 8 female), were assigned to receive a high phosphate diet containing 0.25% adenine and either 7.5% or 2.5% protein (split evenly between genders) for 6 weeks (Diet B, Table 2.1). Of the 4 male mice on the 7.5% protein diet, 2 had to be caged individually as they did not have any littermates. One of these mice was noted to display atypical behaviour from the outset of the experiment and died during the first week. Post-mortem examination revealed a massively distended bladder probably caused by 2,8-dihydroxyadenine crystals causing obstructive nephropathy (Santana *et al* 2013). The other mouse died at day 13 and of note, von Kossa staining of the abdominal aorta revealed calcium deposition within the arterial media. It became clear that mice fed this diet could not be caged individually. Therefore to assess whether aortic calcification would occur consistently with the 7.5% protein diet it was decided to administer it to a further 8 males and 4 females (not needing to be caged individually). One further male receiving this diet died but all other mice (including those in other arms of this pilot study) survived through to 6 weeks.

Changes in weight varied significantly between groups (Figure 4.6). The male mice on 2.5% protein had the greatest weight loss, exceeding that of the females on 2.5% protein although not reaching statistical significance. Male mice on 7.5% protein also lost weight but significantly less than males on 2.5% protein. Females on 7.5% protein gained a little weight overall. Although the weight loss was quite extensive in some cases, no surviving mice displayed any manifestations of distress and exhibited normal behaviour throughout the experiment.

Calcium was detected in the aortic arch and abdominal aorta from 3 of the 4 male mice fed 2.5% protein and 2 of the 9 surviving males fed 7.5% protein. Aortic calcification was only detectable in one female mouse fed 2.5% protein and was absent in all 8 females fed 7.5% protein (Figure 4.7). Histologically, kidneys from animals with demonstrable aortic calcification exhibited increased tubulointerstitial changes (tubular dilatation and epithelial flattening) and fibrosis when compared with those from animals without arterial mineral deposition. Green-brown crystals

were frequently observed in tubular lumen consistent with precipitation of 2,8-dihydroxyadnine (Figure 4.7).

A summary of the serum biochemical changes from baseline for all surviving mice is given in Table 4.1 and Figure 4.8. Creatinine and phosphate both increased significantly more in males fed 2.5% protein compared with females fed 2.5% and males fed 7.5%. Males on the 2.5% protein diet also had a significantly greater increase in corrected calcium compared with males on 7.5% and a significantly smaller drop in albumin compared with females fed 2.5%. Females fed 7.5% protein had a significantly greater increase in corrected calcium and albumin compared with males fed 7.5% and females fed 2.5% respectively. No statistically significant differences were detected between any group for either urea or ALP. It was notable that serum urea concentrations were usually not elevated compared with baseline and actually decreased in 3 groups.

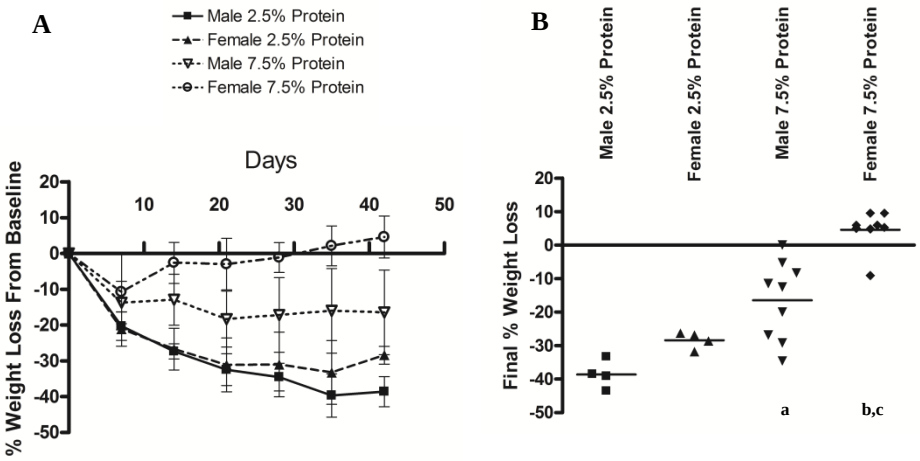

Figure 4.6. Weight Loss in Adenine-Fed Mice. Graphs depicting the weight loss during the pilot study of feeding male and female mice a 0.25% adenine-containing diet with varying protein contents as indicated. A: Percent weight loss compared with baseline at various time-points. Data is presented as mean ± SD. B: Final percent weight loss compared with baseline. *Post hoc* tests were performed when ANOVA indicated $p<0.05$ and compared groups matched for gender and protein. [a] $p<0.001$ compared with male 2.5% protein. [b] $p<0.001$ compared with female 2.5% protein. [c] $p<0.001$ compared with male 7.5% protein. Each points represents an individual animal. Horizontal bars represent group means.

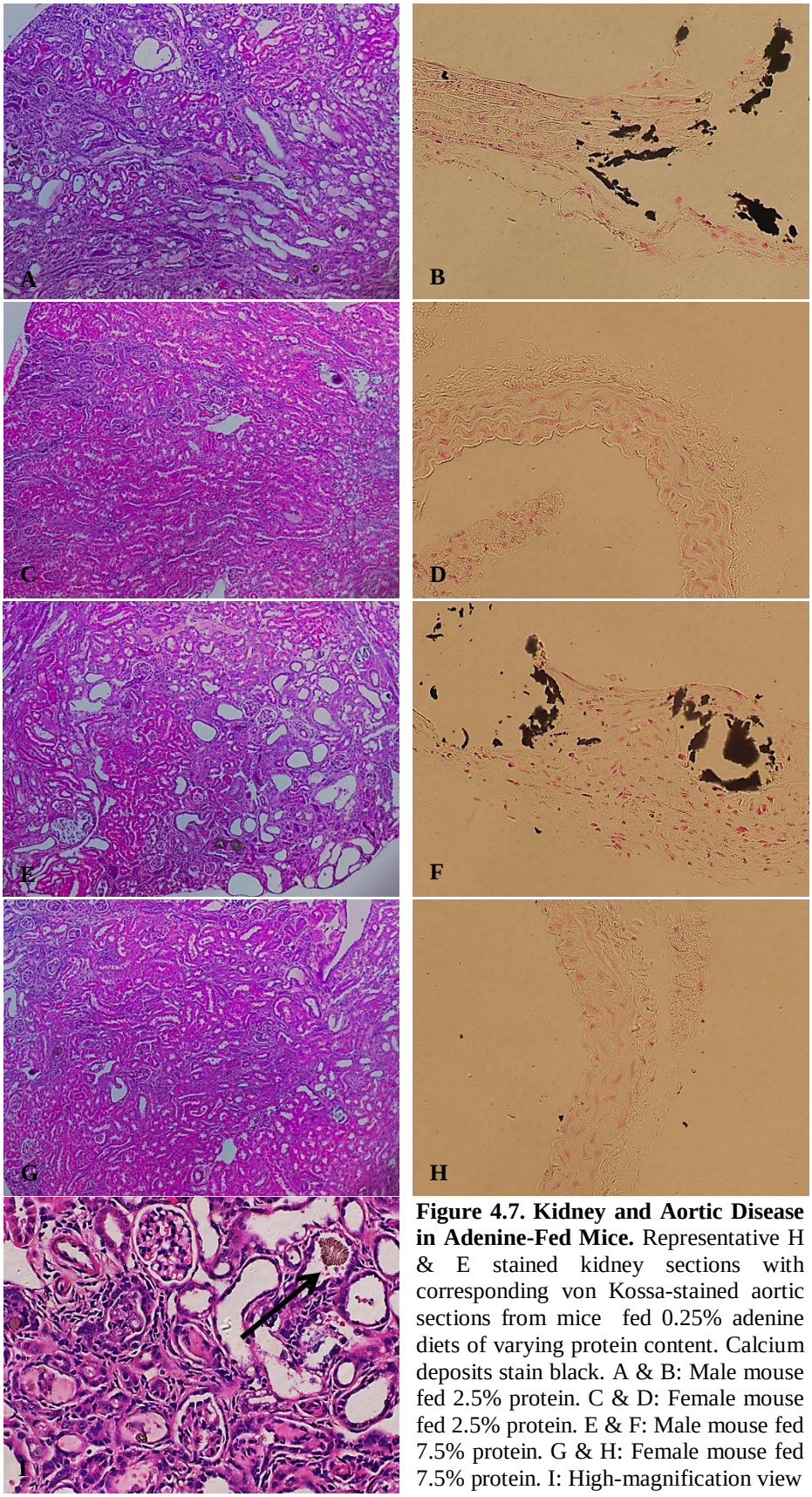

Figure 4.7. Kidney and Aortic Disease in Adenine-Fed Mice. Representative H & E stained kidney sections with corresponding von Kossa-stained aortic sections from mice fed 0.25% adenine diets of varying protein content. Calcium deposits stain black. A & B: Male mouse fed 2.5% protein. C & D: Female mouse fed 2.5% protein. E & F: Male mouse fed 7.5% protein. G & H: Female mouse fed 7.5% protein. I: High-magnification view showing an intra-luminal 2,8-dihydroxyadenine crystal (arrow). A, C, E and G magnification x10. B, D, F, H and I magnification x40.

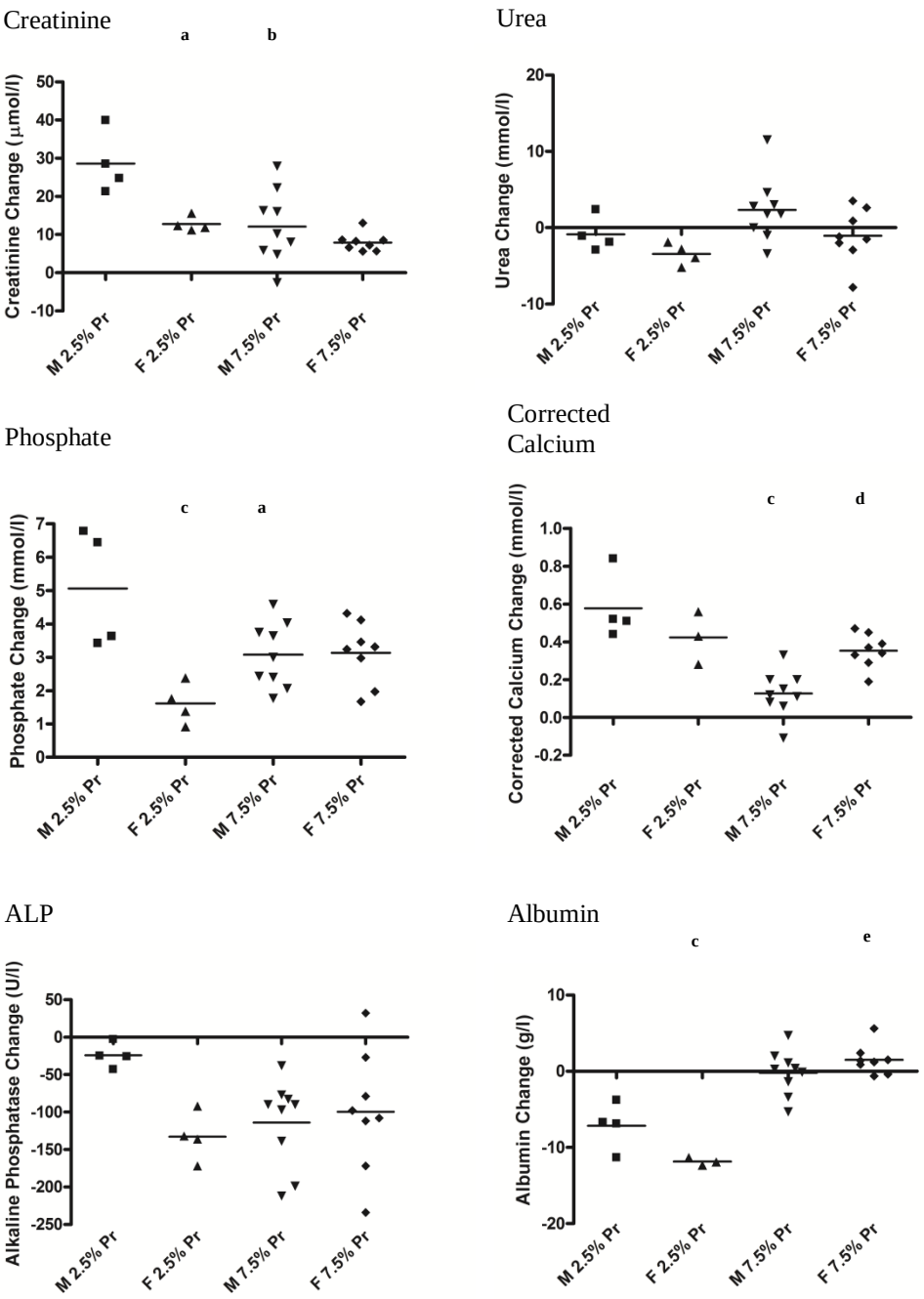

Figure 4.8. Changes in Serum Biochemistry in Adenine-Fed Mice. Changes in serum biochemistry from baseline in male (M) and female (F) mice fed a 0.25% adenine-containing diet with varying protein (Pr) contents as indicated for 6 weeks. *Post hoc* tests were performed if ANOVA indicated $p<0.05$ and compared groups matched for gender and protein. These conditions were met for all parameters except urea and ALP. [a] $p<0.05$; [b] $p<0.01$; [c] $p<0.001$ compared with male 2.5% protein. [d] $p<0.001$ compared with male 7.5% protein. [e] $p<0.001$ compared with female 2.5% protein. Each point represents an individual animal. Horizontal bars represent group means.

Parameter (Change From Baseline)	Male 2.5% Protein	Female 2.5% Protein	Male 7.5% Protein	Female 7.5% Protein	P value (ANOVA)
Creatinine (µmol/l)	28.6 ± 8.1	12.8 ± 1.9[a]	12.1 ± 9.5[b]	7.9 ± 2.4	<0.001
Urea (mmol/l)	-0.9 ± 2.3	-3.5 ± 1.4	2.3 ± 4.2	-1.1 ± 3.5	>0.5
Phosphate (mmol/l)	5.1 ± 1.8	1.6 ± 0.6[c]	3.1 ± 1.0[a]	3.1 ± 0.9	0.002
Corrected Calcium (mmol/l)	0.58 ± 0.18	0.42 ± 0.14	0.13 ± 0.12[c]	0.35 ± 0.09[d]	<0.001
Albumin (g/l)	-7.2 ± 3.1	-11.8 ± 0.5[c]	-0.2 ± 2.9	1.5 ± 1.9[e]	<0.001
ALP (U/l)	-24.3 ± 16.4	-133.0 ± 32.7	-113.9 ± 58.1	-99.8 ± 81.5	>0.05

Table 4.1. Changes in Serum Biochemistry in Adenine-Fed Mice. Changes in serum biochemistry from baseline in male and female mice fed a 0.25% adenine-containing diet with varying protein contents as indicated for 6 weeks. *Post hoc* tests were performed if ANOVA indicated $p<0.05$ and compared groups matched for gender and protein. These conditions were met for all parameters except urea and ALP. [a] $p<0.05$; [b] $p<0.01$; [c] $p<0.001$ compared with male 2.5% protein. [d] $p<0.001$ compared with male 7.5% protein. [e] $p<0.001$ compared with female 2.5% protein. Data are presented as mean ± SD.

4.2.2.ii A modified adenine-containing diet is poorly tolerated by C57Bl/6 mice.

Previous reports had suggested that mice on the C57Bl/6 background are resistant to AC (Eaton *et al* 1978, El Abbadi *et al* 2009). To confirm whether this was also the case using an adenine-containing diet to induce disease, the most efficacious regime from the previous experiment (Diet B with 2.5% protein, Table 2.1) was fed to 5 male C57Bl/6 mice. This proved to be tolerated extremely poorly. One mouse had to be sacrificed after 3 weeks and the other 4 by the end of the 4th week. By this time-point all mice had lost 40-50% body weight and exhibited a range of signs indicating poor health. A post-mortem examination was performed on all 5 animals and of note the mouse removed in the 3rd week did have evidence of aortic calcification, however no arterial disease was observed in the other 4 mice. Baseline biochemistry was not measured in these animals, however the final serum creatinine and phosphate concentrations were 93.8 ± 14.1µmol/l and 6.7 ± 0.8mmol/l respectively, indicating advanced renal impairment.

4.2.2.iii Male offspring of 5th generation backcrossed mice exhibit AC on a modified adenine-diet.

The unsuccessful use of the adenine-containing diet in C57Bl/6 mice confirmed the necessity of moving the P2X7R gene deletion onto the DBA/2 background. Therefore when offspring were produced from mice backcrossed through 5 generations, 4 WT males were fed Diet B (2.5% protein) (Table 2.1) to assess whether disease could be induced. These 4 mice were first fed a high phosphate diet (Diet A, Table 2.1) for one week in an attempt to aid acclimatisation to the adenine-diet (being of similar consistency and texture). Diet A (Table 2.1) had previously been shown (having been used as the control diet in the experiments using folic acid described above) to have minimal effects on biochemistry or weight change and was again well tolerated here by these 4 mice. The trajectory of weight loss over the next 6 weeks was similar to that seen with the original 4 WT DBA/2 males fed this diet (not shown). One mouse died one day before the 6 week time-point and post-mortem examination revealed calcification within the aortic arch. At the end of 6 weeks the other 3 mice were switched back to the high phosphate ‘acclimatisation’ diet (Diet A, Table 2.1) in order to see whether they would gain weight whilst potentially permitting any AC to continually develop in the context of established CKD.

Unexpectedly this intervention was not tolerated and all 3 animals died during the subsequent 7 days. However, post-mortem examination and subsequent analysis demonstrated calcium deposition in the aortic arches of all 3 animals confirming the propensity of this new strain (5^{th} generation back-crossed mice) to develop AC when fed Diet B (containing 2.5% protein, Table 2.1).

4.2.2.iv Diets containing a higher adenine content or flavour enhancers are poorly tolerated.

A number of further dietary modifications were evaluated in an attempt to produce a regime that was more palatable, in the hope of inducing CKD and AC that was not associated with such a degree of weight loss. To assess whether a 0.75% adenine-containing diet could be given for a brief (3 day) period with subsequent high phosphate feeding alone, 3 male 5^{th} generation mice were fed this regime. All animals became extremely sick within 3 days, 2 died and the other was returned to a high phosphate diet alone. After 6 weeks this mouse showed no evidence of disease.

Chocolate-flavoured diets are commercially available which mice are reported to find very palatable (personal communications with scientists at SSNIFF). To investigate whether this would improve the intake of adenine-containing diets, 2 chocolate-flavoured formulations were trialled, one containing 0.25% and the other 0.20% adenine. Both contained 2.5% protein (Diet C, Table 2.1). Each diet was fed to 4 male 5^{th} generation mice and overall they were tolerated extremely poorly. All mice had to be sacrificed by 4 weeks. No AC was detected in these animals.

4.2.3 The effect of P2X7R gene deletion on CKD-associated AC.

4.2.3.i Selection of dietary regime.

Given the results from all of the pilot studies detailed above it was clear that the optimal experimental conditions were met when male mice (5^{th} generation backcross) were fed a high phosphate, 0.25% adenine, 2.5% protein-containing diet (Diet B, Table 2.1) for 6 weeks without any initial 'acclimatisation' feeding. This regime was therefore administered to 11 WT (WTA) and 10 $P2X7^{-/-}$ (KOA) mice. A control (C) diet (Diet B without adenine, Table 2.1) was fed to 8 mice of each genotype (WTC and KOC respectively).

4.2.3.ii Survival and qualitative outcomes.

Generally animals tolerated their respective diets very well and remained well throughout the study period. Only one animal (a KOA mouse) died. All mice lost weight with both genotypes losing more weight on the adenine-diet compared with their respective controls. Genotype did not significantly influence the degree of weight loss with either diet (Figure 4.9).

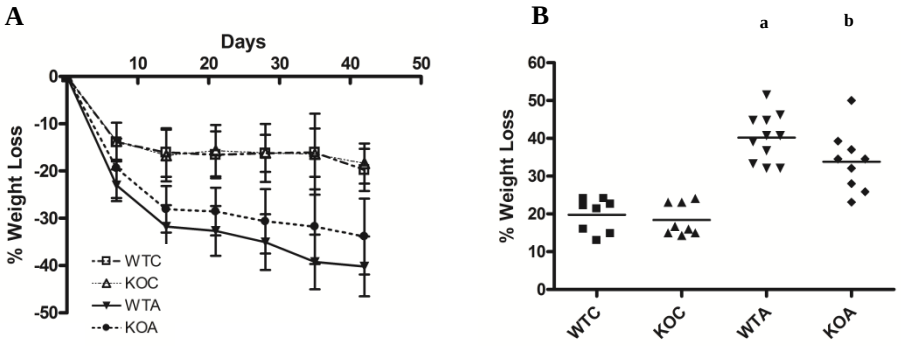

Figure 4.9. Weight Loss in WT and KO Mice. Graphs depicting the weight loss seen during the final experiment feeding a 0.25% adenine-containing diet with a 2.5% protein content to WT and KO mice. A: Percent weight loss compared with baseline over time. Data is presented as mean ± SD. B: Final percent weight loss compared with baseline. *Post hoc* tests were performed when ANOVA indicated $p<0.05$ and compared groups matched for diet and genotype. [a] $p<0.001$ compared with WTC. [b] $p<0.001$ compared with KOC. Each points represents an individual animal. Horizontal bars represent group means.

4.2.3.iv Analysis of aortic calcification

The number of animals exhibiting aortic calcification at the end of 6 weeks was very low. No animals on the control diet had disease. A single WTA mouse and 2 KOA mice had detectable aortic calcium deposition. The magnitude of calcification was higher in the WTA mouse than in the 2 KO animals (255 vs 62 and 31µg/mg tissue, respectively).

4.2.3.v Analysis of biochemistry.

There were no significant differences in the change of any serum parameter between KO mice and their corresponding WT controls on either diet (Table 4.2 and Figure 4.10). Serum creatinine remained largely unchanged in control mice with a significant increase occurring in both genotypes fed the adenine diet. Urea

concentrations dropped in all groups. The degree of this drop was less in adenine-fed mice but only reached significance in the KO cohort. In contrast, phosphate concentrations increased in all groups with a greater elevation seen in adenine-fed animals but only reaching significance in WT mice. Due to limited serum, baseline phosphate could not be measured in one KOA mouse and it is possible that the change in phosphate would have reached significance in KO mice had this measurement been available. No significant differences were detected for either corrected calcium or albumin which increased and decreased, respectively, in all 4 groups. The change in ALP did not reach statistical significance, although it only increased in the KOA group (having decreased in the other 3).

4.2.3.vi Relationship of aortic calcification to biological parameters.

The 2 KOA mice with detectable aortic calcification were also the 2 with the greatest weight loss in that group. In contrast, in the WTA group 6 mice (55%) lost more weight than the animal exhibiting arterial disease.

Taking all mice into account, the 3 with aortic calcification had the 3 highest end-point creatinine values. Due to limited serum a baseline reading could not be measured for one of these mice, however the other 2 also had the greatest creatinine increase. Similar findings were apparent for serum urea concentrations, with these 3 mice having the first, second and fourth highest final readings.

The final serum phosphate in the calcified WTA mouse exceeded the upper limit of the assay and one of the KOA mice with AC had the second highest phosphate overall. However, there were 3 mice with final phosphates exceeding that of the other KOA mouse with AC (however a baseline value was again absent for this mouse and the change in phosphate may well have exceeded that of these other 3 mice).

Parameter (Change From Baseline)	WTC	KOC	WTA	KOA	P value (ANOVA)
Creatinine (µmol/l)	-3.2 ± 3.0	0.6 ± 6.7	22.0 ± 12.3[b]	18.7 ± 13.5[d]	<0.001
Urea (mmol/l)	-4.2 ± 1.3	-6.3 ± 2.8	-0.8 ± 4.4	-1.2 ± 3.0[c]	0.005
Phosphate (mmol/l)	2.4 ± 0.5	2.8 ± 0.5	3.8 ± 1.3[a]	3.9 ± 1.3	0.016
Corrected Calcium (mmol/l)	0.41 ± 0.05	0.29 ± 0.24	0.42 ± 0.17	0.40 ± 0.18	0.449
Albumin (g/l)	-2.9 ± 1.7	-2.2 ± 5.4	-3.7 ± 2.3	-3.3 ± 3.2	0.847
ALP (U/l)	-14.5 ± 26.1	-24.0 ± 44.6	-35.4 ± 53.3	16.4 ± 22.3	0.066

Table 4.2. Serum Biochemistry Changes in WT and KO Mice. Absolute changes from baseline in serum biochemistry for each group. *Post hoc* tests were performed if the initial ANOVA indicated $p<0.05$ and compared groups matched for diet and genotype. These conditions were not met for corrected calcium, albumin and ALP. [a] $p<0.05$; [b] $p<0.001$ (both compared with WTC). [c] $p<0.05$; [d] $p<0.01$ (both compared with KOC). Data are presented as mean ± SD.

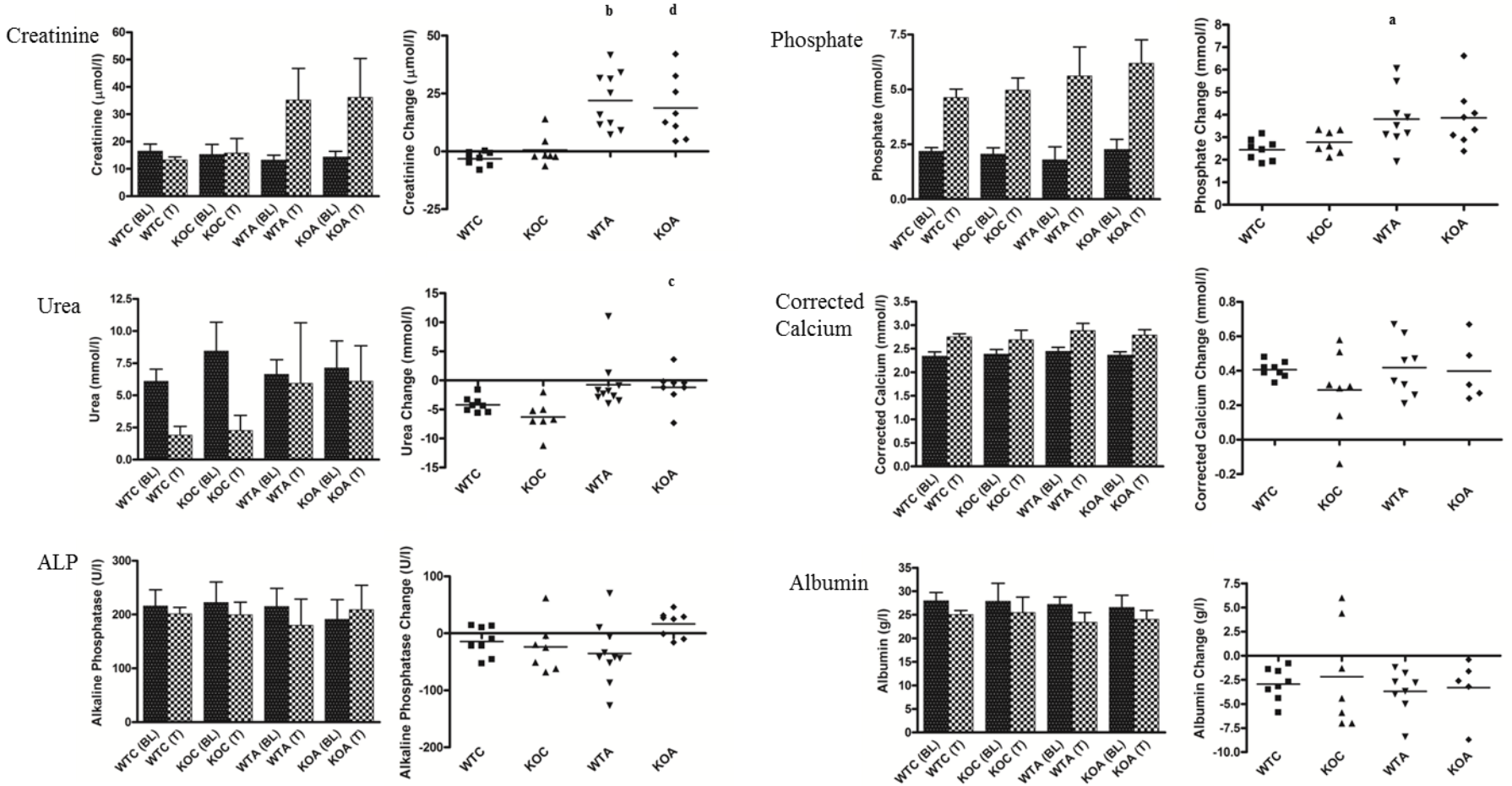

Figure 4.10. Serum Biochemistry in WT and KO Mice. Bar charts depicting baseline (BL) and terminal (T) serum concentrations of indicated parameters for each group are shown adjacent to dot plots depicting the absolute change from baseline for each animal. Post hoc tests were performed if the initial ANOVA (comparing absolute changes between groups) indicated $p<0.05$ and compared groups matched for diet and genotype. These conditions were not met for corrected calcium, albumin and ALP. [a] $p<0.05$; [b] $p<0.001$ (both compared with WTC). [c] $p<0.05$; [d] $p<0.01$ (both compared with KOC). Error bars (bar charts) represent mean ± SD and horizontal bars (dot plots) represent group means with each point representing an individual mouse.

4.3 Discussion

The number of mice with detectable aortic calcification in the final experiment was unexpectedly and disappointingly low, making it difficult to draw any conclusions about the effect of P2X7R-deficiency on CKD-associated AC. The fact that 2/10 KOA mice developed AC and a further one died, compared with just 1/11 in the WTA group manifesting arterial disease coupled with zero mortality might suggest that P2X7R-deficiency is detrimental in this context. Realistically the 'event rate' was too low to definitively make any judgement, however the results perhaps hint that lack of P2X7R is not beneficial.

$P2X7^{-/-}$ mice are described to be viable, fertile and undistinguishable from WTs by simple observation (Solle *et al* 2001). This was found to be the case here even after moving onto the new genetic background. Furthermore there were no differences in serum biochemistry between WT and KO mice at baseline or after 6 weeks feeding on either diet (adenine-containing or control). Previous reports that have implicated a protective effect of P2X7R deletion on renal fibrosis have used histological parameters as primary outcomes (Goncalves *et al* 2006). An in-depth histopathological analysis of kidney tissue was beyond the scope of the work in this chapter and so it is therefore possible, despite the lack of difference in biochemistry between genotypes, that there were changes in inflammatory infiltrates (which have been described by other groups that have fed adenine to mice) (Oyama *et al* 2010, Jia *et al* 2013).

The immediate and most fundamental question arising from the work described in this chapter is why there was so much disparity between the pilot and final studies in the success of inducing AC. There appears to be no obvious answer to this. In terms of other measureable parameters, disease progression seems to have been similar between male mice fed 2.5% protein in the adenine pilot studies and those in the final experiment. Weight loss in WT mice during the final experiment was essentially identical to that seen in the pilot study. The change in serum creatinine was a little higher in pilot mice overall, however there were a number of WTA and KOA animals that did not display AC but had creatinine changes in excess of all pilot study mice. It therefore seems that other factors must have been present to explain the contrasting findings.

One possibility is that there were subtle genetic differences between the 5th generation mice used in the pilot study, all of which developed AC, and those in the main experiment. However, the 3 mice with aortic disease in the final study were all of different parentage and housed with littermates which did not display AC thus arguing against a genetic-related factor.

Another potential explanation is the one week 'acclimatisation' period employed in the pilot study during which mice were fed a high phosphate diet (Diet A, Table 2.1). This was not done in the main experiment as in the pilot study it had not obviously influenced subsequent dietary intake of the adenine-containing feed, or weight loss, and one animal had died before 6 weeks on the adenine diet. Diet A (Table 2.1) did not influence any biochemical parameter during the first 2 weeks of feeding as shown by the studies with folic acid during which it was fed to all mice. Therefore whilst not impossible, it is difficult to see how an initial one week period on this diet would greatly enhance rates of aortic calcification. Mice in the pilot study were converted back to Diet A (Table 2.1) after 6 weeks of adenine feeding but all died within a few days of the switch. This brief period of time after the dietary change seems too short for extensive disease to develop and AC was almost certainly present before this point. A further possible reason for the contrasting findings could relate to subtle differences in the make-up of the diets however this also seems unlikely given that although different batches, they were made by the same manufacturer to the same formulation and specification and stored in identical fashion.

All *in vivo* models of AC are reported to result in variable rates of calcification which may ultimately have been the reason for the present findings. Only one murine model of CKD-associated AC has previously been described (El-Abbadi *et al* 2009) and in this original report all mice (n=7) exhibited some degree of aortic calcification but a wide range of values was seen. Of note however, all control animals were found to have mild degrees of aortic calcification and some CKD mice only had AC to a similar degree as this 'healthy' cohort. A number of subsequent studies (all by the Giachelli laboratory) have employed this model (Pai *et al* 2011, Lau *et al* 2012a, Lau *et al* 2012b, Scialla *et al* 2013) and confirm variability in calcification. The study by Scialla *et al* (2013) reported only a 50% success of AC induction. No

definitive explanation for this variability has been put forward by any group - it is almost certainly multi-factorial and likely that many of these unidentified determinants were at play in the current work.

When considering the potential utility of the model developed in this chapter as a future experimental tool, it is worth making comparisons (in respect of factors other than calcification consistency) with that established by Giachelli's group (El-Abbadi *et al* 2009). Advantages of adenine feeding include the no requirement for surgery, and hence no peri-operative mortality, a relatively short length of time necessary for AC to develop (mice are usually followed for at least 3 months with the surgical model) and the no gender dependence (male mice are not used in the surgical model due to an increased resistance to AC). In terms of biochemistry, only selected parameters have been reported in the surgical model. Urea rather than creatinine has been used as a marker of renal impairment and shows an approximate 3-fold elevation compared with controls. This is in contrast to the present work in which serum urea was, if anything, slightly decreased - almost certainly a reflection of both decreased body weight and protein intake. This is definitely a limitation of the adenine-based model. Weight loss also occurs in the surgical model but has not been reported in terms of 'percentage loss' so it is difficult to make an accurate comparison with the results here. Creatinine appears to be a better marker of renal function in the adenine-model as it consistently increased. Elevations in serum phosphate are comparable between the two models, however an increase in ALP is seen in the Giachelli model (in contrast to a general decrease with adenine) along with an elevated PTH (which was not measured in the present work due to the limited volume of serum). In keeping with these serum results, high-turnover bone disease has been demonstrated with the surgical model (Lau *et al* 2012a). Analysis of bone was not performed in the current work so it is unclear whether the two systems are equivalent in this respect.

The work by Giachelli's group and the results from the adenine experiments here do indicate that for AC to occur, an advanced state of renal impairment needs to be reached. Folic acid was essentially unsuccessful for inducing renal disease in the present work. In retrospect, successful studies that have employed folic acid to induce CKD report obtaining less than 30% fibrosis after 20 weeks associated with

serum creatinine values of around half those detected in adenine-fed mice with AC in this work (Bechtel *et al* 2010). Folic acid is therefore unlikely to achieve the necessary degree of renal impairment required for AC to develop.

When considering the conditions necessary for AC to develop *in vivo*, the fates of 3 mice involved in the pilot studies, all of which displayed calcified aortas, are particularly intriguing. The animals in question are the one female DBA/2 administered 480µg/g folic acid, the one male C57Bl/6 (which died in week 3) and the male DBA/2 (which died at day 13). These mice are biologically diverse differing in gender, strain and method used to induce disease. Furthermore, disease in the latter 2 animals developed relatively rapidly (in less than 3 weeks). The uniting factor seems to be that all 3 had pronounced weight loss over a few days and whilst one remained fairly well and recovered, the other 2 quickly declined. A number of systemic changes are likely to be present in this clinical setting. Renal impairment is inevitable with a consequential elevation in serum phosphate. Additionally, these animals were almost certainly profoundly volume-contracted. The fact that AC appears to be able to develop very quickly (within days) under these circumstances raises the possibility that in this context ectopic calcification occurs due to mechanisms other than those requiring 'active' and 'cell-mediated' changes. C57Bl/6 mice are resistant to AC and this is thought to be due in part to a greater expression of the Abcc6 gene (Meng *et al* 2007). The fact that one of these mice developed AC demonstrates that this resistance can be overcome in certain situations. One possibility is that under these conditions of advanced dehydration and mineral imbalance the systemic environment simply favours passive precipitation of mineral.

Male mice were more prone to disease with adenine feeding whereas only females are reported to develop AC with the surgical model (El-Abbadi *et al* 2009). In many mouse models of renal disease males appear to be affected to a greater degree than females (Si *et al* 2009). This disparity has often been attributed to hormonal influences and may well be the explanation here. Clearly with surgical induction disease will be induced irrespective of hormonal effects, although why males should be resistant to AC in this context is unknown. The greater success of AC induction with lower dietary protein is consistent with the findings in rats and is thought to

possibly result due to a higher bioavailability of phosphate (Neven & D'Haese 2011).

4.4 Summary

A novel mouse model of CKD-associated AC has been developed based on a modified adenine-containing diet. Unfortunately at present this model suffers from a high level of inconsistency and proved to be unhelpful in addressing the primary question of whether P2X7R deficiency attenuates disease. To try and provide an answer to this an alternative *in vivo* system was sought and is the focus of the work described in Chapter 5.

CHAPTER 5 – EXPERIMENT TO ASSESS THE INFLUENCE OF A SELECTIVE P2X7R ANTAGONIST ON CHRONIC KIDNEY DISEASE-ASSOCIATED ARTERIAL CALCIFICATION IN RATS

5.1 Introduction

The experiments described in Chapter 4 were ultimately unhelpful for assessing the effect of P2X7R deficiency on AC due to the low number of mice exhibiting arterial calcium deposition. It was therefore necessary to find an alternative method of examining the influence of *in vivo* receptor ligation on disease progression.

Although adenine diet-based models are infrequently used in mice, they have successfully been employed to induce the combination of CKD and aortic calcification in rats for several years (Katsumata *et al* 2003). The P2X7R antagonist, AZ11657312, has previously been administered to rats in other disease models (AstraZeneca unpublished data) and was available for use in this work. Thus, this agent along with the rat adenine model provided the necessary experimental tools to test the hypothesis that P2X7R blockade could ameliorate CKD-associated AC *in vivo*.

5.2 Results

5.2.1 Optimisation of the rat adenine model.

It was first necessary to confirm that feeding an adenine-containing diet to rats would lead to AC and CKD, as is described in the literature (Shobeiri *et al* 2010, Neven & D'Haese 2011). In addition, it was important to ascertain what degree of consistency of AC would be achieved using this model and whether it would therefore be a suitable model with which to assess the impact of a pharmacological agent.

5.2.1.i The addition of 0.75% adenine to a high phosphate diet leads to AC and marked renal impairment in rats by 4 weeks.

A high phosphate diet (Diet D, Table 2.1) was administered to 8 male Wistar rats for 4 weeks. In the case of 4 of these 8 rats, the diet was supplemented with 0.75% adenine. Rats fed the high phosphate control diet gained 1.2 ± 4.5% body weight, whereas those on the adenine diet lost 25.9 ± 3.4% by the end of 4 weeks. Despite

the weight loss, those in the adenine group continued to display normal activity and social interaction. No animals died during this experiment.

Quantitative and qualitative assessment (von Kossa staining) of aortas from control rats revealed complete absence of calcification (Figure 5.1A). In contrast, all aortas from rats fed the adenine-containing diet had at least some calcium deposition. The degree of calcification within vessels was extremely variable, ranging from circumferential calcium deposition of the entire vessel, essentially dividing the medial layer in half (Figure 5.1B), to smaller, scattered, linear deposits along sections of elastin within the media (Figure 5.1C-E). No staining was detected along the internal elastic lamina (IEL). Calcification was detected in the abdominal aortas from all adenine-fed rats with a mean of 13.6 ± 11.0µg/mg. However, calcium was only detected in the thoracic aorta and aortic arch in one (the same) animal.

Kidneys from control rats looked normal both macroscopically and histologically (Figure 5.2A and B). In contrast, kidneys from adenine-fed rats appeared grossly enlarged and 'sandy' coloured (Figure 5.2A). The mean kidney weight from control rats was 2.77 ± 0.21g compared with 9.57 ± 1.40g in the adenine fed cohort ($p < 0.001$). The respective kidney to body weight ratios were 0.006 ± 0.000 vs 0.030 ± 0.004 ($p < 0.001$). H & E staining of kidneys from adenine-fed rats showed morphologically normal glomeruli but marked abnormalities in the tubulointerstitial compartment (Figure 5.2C). Many tubules appeared dilated with epithelial flattening, and many contained green-brown crystals, consistent with 2,8-dihydroxyadenine deposition (Monico & Milliner 2012). Interstitial fibrosis was apparent as evidenced by expansion of the tubulointerstitium and ECM accumulation (Norman & Fine 1999).

Serum biochemical results were in keeping with these histological findings, with the adenine-fed rats having significantly higher levels of urea, creatinine and phosphate compared with controls (Table 5.1).

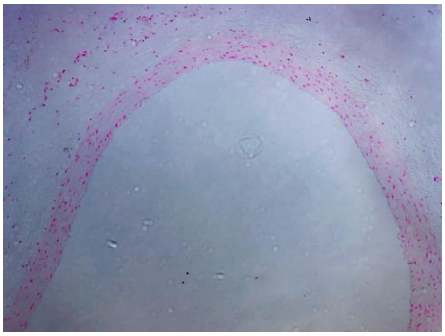

A

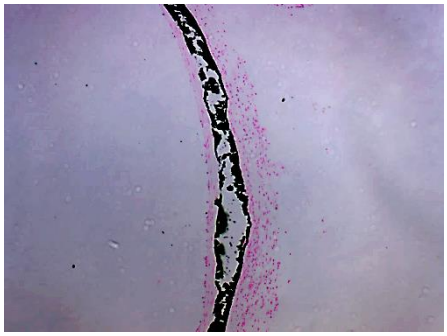

B

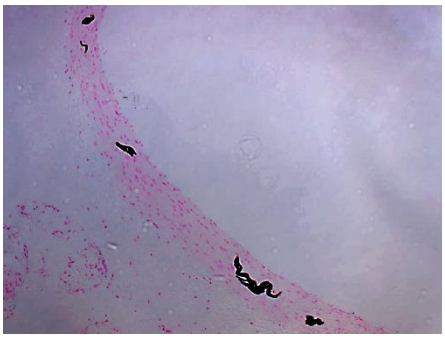

C

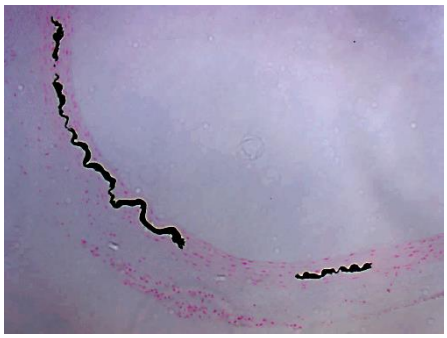

D

E

Figure 5.1. Aortic Calcium Deposition in Rats. Aortic sections were stained with silver nitrate (von Kossa stain) for calcification (stained black). A: Negative calcium staining in an aorta from a control rat. B-D: Positive staining in aortas from 3 different adenine-fed rats showing varying extents of mineral deposition. E: Higher magnification (x63) image showing calcification along elastin fibres running between intact VSMCs. All sections counterstained with aluminium red. A-D magnification x10.

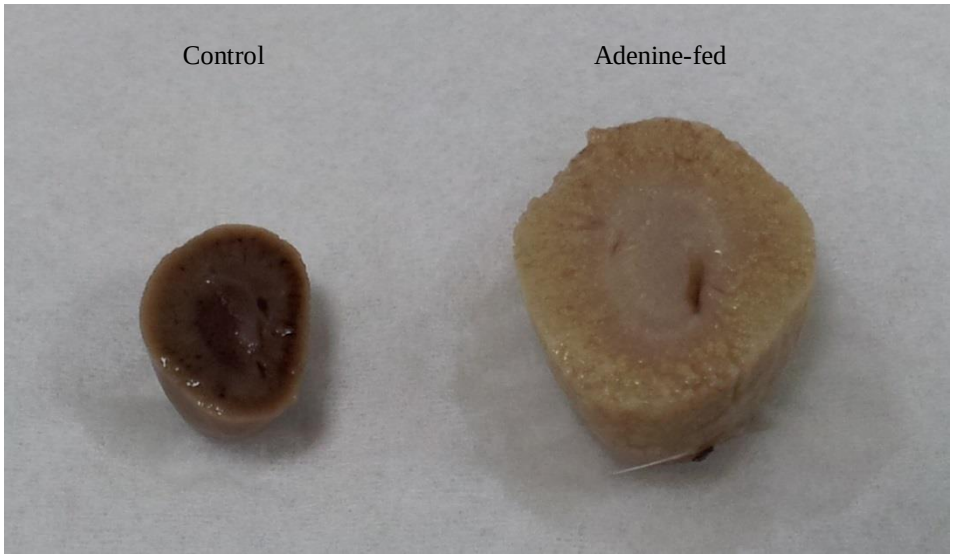

A

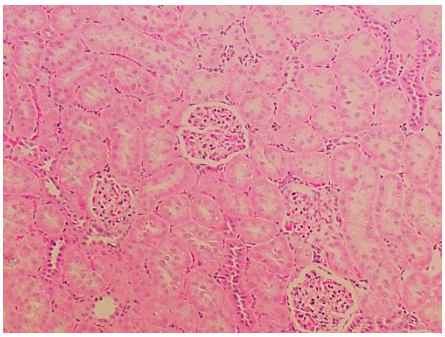

B

C

Figure 5.2. Macro- and Microscopic Appearance of Kidneys from Rats. A: Macroscopic appearance of kidneys from control and adenine-fed rats. Control kidneys appeared normal whereas those from adenine-fed animals were grossly dilated and 'sandy' coloured. H & E stain of B: control kidney with essentially normal morphology; C: a kidney from an adenine-fed rat exhibiting tubular dilation with epithelial flattening. Interstitial inflammation and fibrosis is evident. Some tubules contain green-brown material (arrows) consistent with 2,8-dihyroxyadenine crystals. B and C magnification x20.

Group	Urea mmol/l	Creatinine µmol/l	Phosphate mmol/l
Control (n=4)	1.32 ± 0.35	31.7 ± 5.7	1.72 ± 0.14
Adenine (n=4)	33.8 ± 13.1	441.6 ± 79.8	6.68 ± 0.7

Table 5.1. Serum Biochemistry from Rats in First Pilot Experiment. Data are presented as mean ± SD.

5.2.1.ii Reduction of the dietary adenine content to 0.25% does not increase the consistency of AC when administered for 6 weeks.

Given that the extent of calcification was not uniform in the aortas of the 0.75% adenine-fed rats in the initial pilot experiment, a second diet was trialled, containing 0.25% adenine (Diet E, Table 2.1). This was administered to 4 rats for a longer period (6 weeks). The rationale behind this was a report suggesting that more consistent aortic calcification could be achieved by lowering the adenine content of the diet to this level and administering for an extended time-course (Shobeiri *et al* 2013). A 6 week feeding period was selected for this experiment, representing the greatest length of time that it would have been practically possible to conduct twice daily oral gavages of P2X7R antagonist to rats.

Despite being housed in the same cage, after 6 weeks on Diet E (Table 2.1), 2 rats had extensive calcification of their entire aorta whereas the other 2 had no detectable calcification whatsoever. Those with calcified aortas lost more weight, had larger kidneys and worse renal impairment than the 2 without (Table 5.2).

AC present?	%Weight loss	Kidney to body wt ratio	Urea mmol/l	Creatinine µmol/l	Phosphate mmol/l
YES	-25.6	0.020	35.9	482.0	5.84
YES	-20.9	0.019	15.0	395.7	5.80
NO	-14.3	0.013	7.2	80.3	3.52
NO	-11.1	0.016	6.3	81.3	3.53

Table 5.2. Kidney Parameters and Serum Biochemistry from Rats (n=4) in Second Pilot Experiment.

5.2.2 Experiment to assess the influence of a selective P2X7R antagonist on AC.

5.2.2.i Selection of diets.

In the pilot studies, although the first trial diet (Diet D, Table 2.1) did not induce a uniform degree of calcification between animals, all rats that received it did exhibit some aortic calcium deposition. In contrast, AC was much more variable with the second diet (Diet E, Table 2.1) as no calcification was detected in some animals. Therefore, the 0.75% adenine-containing high phosphate diet (Diet D, Table 2.1) was selected to be administered to the vehicle (V), low-dose P2X7R antagonist-treated (20mg/kg, LD) and high-dose P2X7R antagonist-treated (60mg/kg, HD)

groups. Control groups ‘N’ and ‘A’ were fed a diet containing normal phosphate without or with 0.75% adenine (Diets F and G, respectively, Table 2.1) (see Chapter 2, section 2.7).

5.2.2.ii Survival and tolerability of oral gavage.

There was no mortality in the N, A or V groups. In contrast, 4/7 rats in the LD and 2/8 in the HD groups died. Three of these deaths were due to immediate complications of the gavage procedure itself. The other 3 rats had a more insidious onset of morbidity. One lost an excessive amount of weight, one exhibited a sub-acute onset of respiratory distress, and the other displayed an unacceptably high degree of agitation.

The extent to which each individual animal tolerated the oral gavage procedure was variable, with some remaining calm and un-fazed, and others showing varying degrees of agitation. Whilst difficult to objectively measure, it was noted throughout the experiment that rats receiving vehicle alone seemed to be more tolerant of the procedure than those receiving the study drug. On isolated occasions, due to either encountering severe resistance at the level of the proximal oesophagus when attempting to pass the gavage cannula, or the rat displaying severe agitation, the dose could not be administered. Of the surviving animals, the V group received 89.5% of scheduled doses, the LD group received 79.2% and the HD group 88.4% ($p = 0.39$ for V vs HD). Only 4 rats (all in the V group) received all of the scheduled doses. The rats in the N group all gained weight, whereas all those in the other 4 groups lost weight to a similar degree (Table 5.3).

Group	% Weight change
N (n = 10)	+11.2 ± 5.9
A (n = 6)	-29.2 ± 2.8
V (n = 9)	-28.5 ± 2.6
LD (n = 3)	-33.4 ± 3.8
HD (n = 6)	-28.9 ± 2.8

Table 5.3. Weight Changes. Percent weight changes from baseline after 4 weeks. Data are presented as mean ± SD.

Due to the low final numbers of LD rats, this group was excluded from subsequent statistical analysis of biological parameters.

5.2.2.iii Serum levels of P2X7R antagonist.

The mean serum concentration of AZ11657312, taken 2 hours after the first dose (peak level) in 4 HD rats was 4039 ± 2486 ng/ml. The corresponding concentration immediately before the second dose (trough level) was 1926 ± 1297 ng/ml. After 2 weeks of study, another trough level was taken which was 1785 ± 662 ng/ml. Only 2/4 of these rats survived to the end of the study. A final serum sample was taken at sacrifice with drug levels of 29 and 200 ng/ml detected in these 2 animals. The other 4 rats in the HD group had a peak drug level taken at 2 weeks to confirm absorption of the compound. This was measured at 3005 ± 1432 ng/ml.

5.2.2.iv P2X7R expression in normal and calcified aorta.

The absolute mRNA copy numbers for P2X7R for each group are given in Table 5.4 ($p = 0.046$). The mean copy number in the 3 adenine-treated groups was higher than controls without reaching statistical significance following *post hoc* testing. There was no significant difference between the A, V and HD groups.

N (n=10)	**A (n = 6)**	**V (n = 9)**	**HD (n = 6)**
607 ± 379	1,114 ± 308	989 ± 292	1,191 ± 747

Table 5.4. Corrected Absolute mRNA Copy Numbers for P2X7R. *Post hoc* testing compared all groups to N and V as initial KW test indicated $p<0.05$. Following this, no significant differences were detected. Data are presented as mean ± SD.

P2X7R protein expression in normal and calcified aorta was assessed by Western blotting. Protein lysates from the A group were excessively haemorrhagic, so to avoid potential contamination from blood proteins, the N group was compared to the V and HD groups only. A blot was run using the 3 samples in each group with calcification closest to the respective group mean (Figure 5.3). By densitometry the mean band intensity between the 3 groups was very similar suggesting equivalent protein expression ($p = 0.19$).

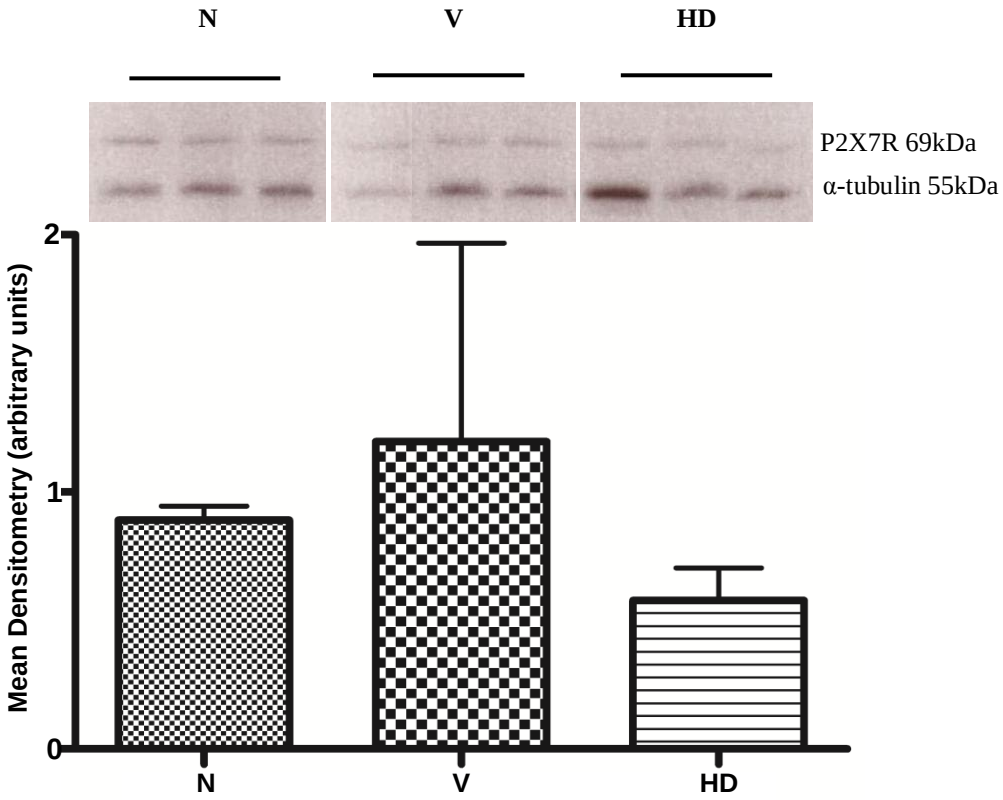

Figure 5.3. P2X7R Protein Expression in Control and Calcified Rat Aorta. Western blot of protein lysates from aorta taken from 3 rats in each of the N, V and HD groups shown with the corresponding band densitometry below. Error bars represent mean ± SD.

5.2.2.v P2X7R antagonism does not influence the development of AC in adenine-fed rats.

The differences in arterial calcium deposition between the V and HD groups, and the V and A groups were not statistically significant (Table 5.5 and Figures 5.4 and 5.5). As expected, no calcification was detected in the aortas from control rats. In the other 4 groups, calcium was present in all but 2 aortas (both from HD rats) when analysed colourimetrically. Of note, these 2 rats missed the most doses of those in the HD group (8 and 13 doses missed). In addition, the rat with the lowest aortic calcium content in the V group was the one with the greatest number of missed doses (24 doses missed). For the V and HD groups together, there was a strong negative correlation between doses missed and aortic calcification (Spearman rho = -0.62; p = 0.013) (Figure 5.6).

Group	Aortic calcium content (µg/mg tissue)
N (n = 10)	0 ± 0
A (n = 6)	46.2 ± 31.0**
V (n = 9)	35.7 ± 34.2 **
LD (n = 3)	41.8 ± 30.4
HD (n = 6)	35.0 ± 28.5 *

Table 5.5. Aortic Calcification. Quantification of total aortic calcium content in each group. *Post hoc* testing compared all groups (except LD) to N and V as initial KW test indicated $p<0.05$. *$p<0.05$; **$p<0.01$ all compared to N. Data are presented as mean ± SD.

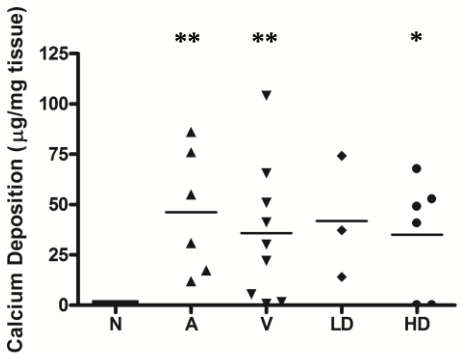

Figure 5.4. Quantification of Aortic Calcium Deposition. Quantification of total aortic calcium content in each rat in the indicated groups. *Post hoc* testing compared all groups (except LD) to N and V as initial KW test indicated $p<0.05$. *$p<0.05$; **$p<0.01$ all compared to N. Each symbol represents one animal. Horizontal bars represent group means.

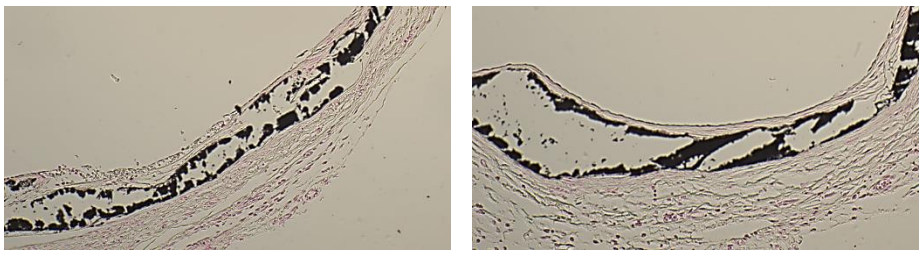

A **B**

Figure 5.5. Calcium Deposition in Adenine-Fed Rat Aortas. Representative images of von Kossa stained rat aortas. Extensive, heavy calcification (stained black) is seen throughout the arterial media in both vessels shown. A: Vehicle-treated. B: High-dose P2X7R antagonist-treated. Counterstained with aluminium red. Magnification x10.

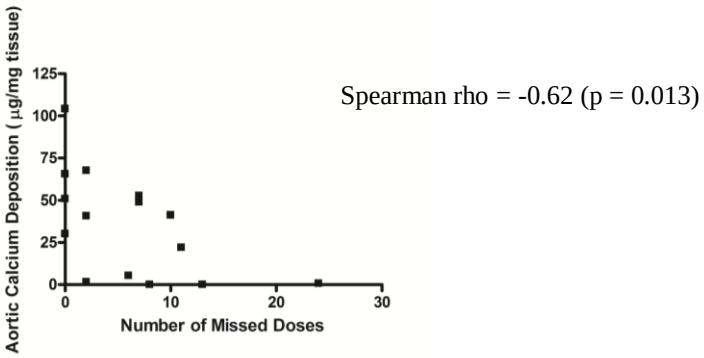

Figure 5.6. Correlation of Aortic Calcium Content and Number of Missed Gavages. Spearman's rank correlation of aortic calcification and number of missed gavages from rats in the V and HD groups combined.

As was seen in the first pilot experiment, the extent of calcification between aortas was extremely variable. Once again the most consistently calcified segment was the abdominal aorta. Calcification of the aortic arch and thoracic aorta was not seen unless abdominal aortic calcium deposition was present. Three aortas, all from the V group, had calcification of the abdominal portion in isolation, and a further aorta, taken from an LD rat, had calcification in all but the thoracic segment. It was notable that pan-aortic calcification was seen in all rats in the A group.

The majority of aortas had such extensive calcification that when histological sections were cut, the tissue 'fractured' making assessment of both calcification localisation and morphology of surrounding tissue and cells extremely difficult (Figure 5.5). However, in samples where calcification was not so severe, early calcium deposition could clearly be seen 'tracking' along the elastin layers between VSMCs within the arterial media in an identical fashion to the observations made in the pilot study.

5.2.2.vi Analysis of mRNA expression of molecules implicated in AC pathways.

Although the overall extent of aortic calcification was not modified by treatment with AZ11657312, it was conceivable that P2X7R blockade might confer subtle influences on one or more pathogenic pathways thought to be involved in AC. To investigate this possibility aortic mRNA expression was assessed for a number of

molecules implicated in disease progression (Table 5.6 and Figure 5.7). The A260/280 ratios of all RNA samples were above 1.7 and all RIN values exceeded 8, indicating high levels of purity and integrity, respectively.

The stability of five housekeeping genes was assessed (β-actin, HPRT, 28S, SDHA and YWHAZ) with β-actin found to be the least stable. Final absolute mRNA copy numbers were calculated by correcting for the combination of HPRT, 28S, SDHA and YWHAZ, as determined by the GeNorm programme (see Chapter 2, section 2.16.9). These 4 housekeeping genes had mean absolute copy numbers of 16,040 ± 3,678, 43,565 ± 14,847, 31,914 ± 22,249 and 188,593 ± 151,961, respectively.

A significant reduction in mRNA expression of the VSMC-specific markers α-SMA, SM-22 and smoothelin (Proudfoot & Shanahan 2012) was seen in the A, V and HD groups compared with controls. However, no difference was seen in expression between these 3 groups. The absolute mRNA copy numbers for these 3 genes were in the order of several tens of thousands, and several million in the case of α-SMA, indicating abundant expression relative to the housekeeping genes (Figure 5.7A-C, Table 5.6).

To assess for osteogenic transformation of VSMCs, mRNA expression of the osteogenic transcription factors runx-2 (Komori *et al* 1997, Ducy *et al* 1997) and osterix (Nakashima *et al* 2002), along with a key regulator of their induction, BMP-2 (Celil *et al* 2005, Hruska *et al* 2005), was measured (Figure 5.7D-F). A significant increase was seen in runx-2 expression in the A, V and HD groups compared with the controls, but there was no difference between these 3 groups. No differences were detected between any groups for osterix or BMP-2 mRNA expression. Absolute copy numbers for BMP-2 were of the order of a few thousand in all groups, however, the copy numbers for runx-2, even in the calcified groups, were very low, and in the case of osterix, mRNA expression was barely detectable (Table 5.6).

Copy numbers of mRNA for the apoptotic marker caspase-3, and the NLRP3 inflammasome, both showed a significant up-regulation in calcified vessels compared with controls but no difference in the HD group compared with V. Absolute copy numbers for both were in the order of several thousand (Figure 5.7G and H, Table 5.6).

Gene	N (n=10)	A (n=6)	V (n=9)	HD (n=6)	p value (KW)
α-SMA	10,068,417 ± 3,888,662	2,473,818 ± 1,142,494*	2,805,836 ± 2,116,936**	2,909,573 ± 2,572,880**	<0.001
SM-22	3,727,314 ± 1,599,672	696,480 ± 452,396**	904,225 ± 668,699**	947,389 ± 819,106**	<0.001
Smoothelin	231,679 ± 84,502	68,785 ± 28,359**	80,379 ± 35,659**	95,306 ± 58,678*	<0.001
Runx-2	35 ± 21	294 ± 156 *	446 ± 518 *	744 ± 718 *	0.003
Osterix	9 ± 5	6 ± 4	9 ± 9	10 ± 6	0.582
BMP-2	2,073 ± 889	1,985 ± 845	2,726 ± 1,229	2,038 ± 398	0.277
Caspase-3	5,318 ± 4,120	19,293 ± 5,362*	22,794 ± 5,378**	19,514 ± 9,762*	<0.001
NLRP3	2,313 ± 1,348	9,786 ± 1,598	13,813 ± 2,408***	10,089 ± 3,478*	<0.001

Table 5.6. Corrected Absolute mRNA Copy Numbers. RNA was extracted from rat aortas and qPCR assays performed for the genes indicated. *Post hoc* testing compared all groups to N and V if initial KW test indicated $p<0.05$. This condition was met for all genes except osterix and BMP-2. *$p<0.05$; **$p<0.01$; ***$p<0.001$ all compared to N. Data are presented as mean ± SD.

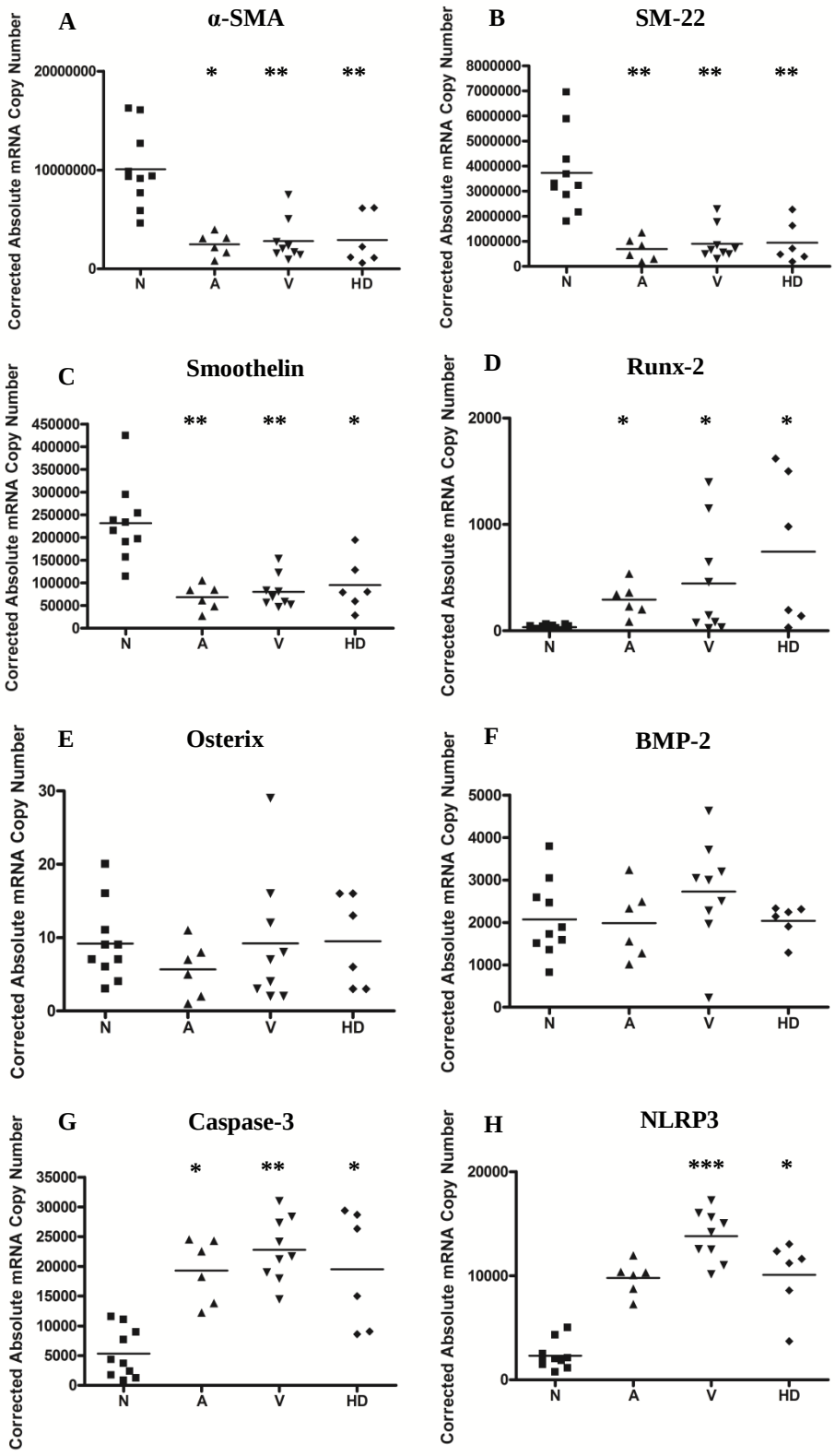

Figure 5.7. Expression of Molecules Implicated in AC. RNA was extracted from rat aortas and qPCR assays performed for the genes indicated. *Post hoc* testing compared all groups to N and V if initial KW test indicated $p<0.05$. This condition was met for all genes except osterix and BMP-2. *$p<0.05$; **$p<0.01$; ***$p<0.001$ all compared to N. Each symbol represents one animal. Horizontal bars represent group means.

5.2.2.vii P2X7R antagonism does not impact on the degree of renal impairment observed in the adenine nephropathy model.

Histologically, kidneys from adenine-fed rats were grossly different from controls, with similar changes seen to those observed in the pilot experiments. The amount of interstitial fibrosis in V and HD kidney sections was assessed using Picrosirius red staining (Figure 5.8). The mean fibrosis score in kidneys from V rats was 21.6 ± 6.7% compared with 21.8 ± 8.1% in HD rats (p = 0.936).

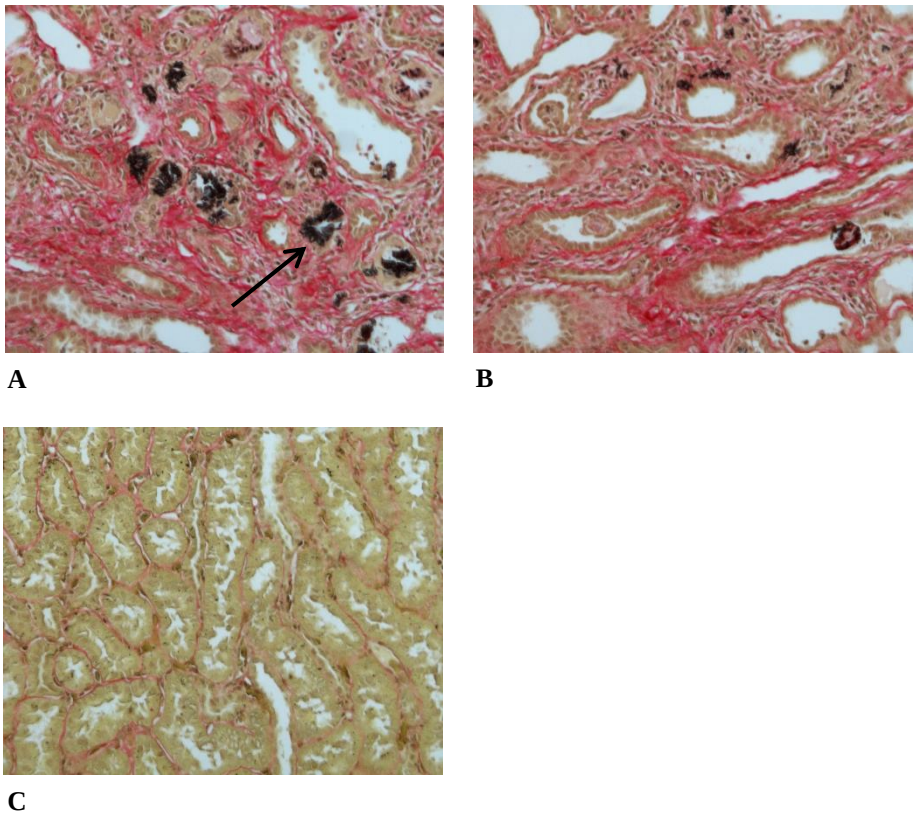

Figure 5.8. Picrosirius Red Staining of Rat Kidney Tissue. Representative Picrosirius red stained kidney sections. A: Vehicle-treated (V) group. B: High-dose antagonist-treated (HD) group. C: Control (N) group. 2,8-dihydroxyadenine crystals stain as black (arrow in A). Quantitative analysis of collagen staining (see text) showed no significant difference between the V and HD groups. Magnification x40.

Adenine-fed rats had a significantly greater kidney-to-body weight ratio, 24 hour urine output and daily water intake compared with controls. No differences for these 3 parameters were noted between the A, V and HD groups (Table 5.7 and Figure 5.9).

	N (n=6)	**A (n=5)**	**V (n=9)**	**HD (n=6)**	**p value (ANOVA)**
Kidney:Body weight ratio	0.006 ± 0.000	0.033 *** ± 0.004	0.031*** ± 0.004	0.031 *** ± 0.010	<0.001
24 hr urine output (ml/kg/hr)	2.0 ± 0.8	4.4 *** ± 1.3	3.8 ** ± 1.1	4.6 *** ± 0.9	<0.001
24 hr water intake (ml)	26.8 ± 10.8	39.3 ± 11.6	42.6 * ± 13.3	43.2 ± 11.1	0.022

Table 5.7. Kidney:Body Weight Ratio and Fluid Balance. *Post hoc* testing compared all groups to N and V as initial ANOVA indicated p<0.05. *p<0.05; **p<0.01; ***p<0.001 all compared to N. Data are presented as mean ± SD.

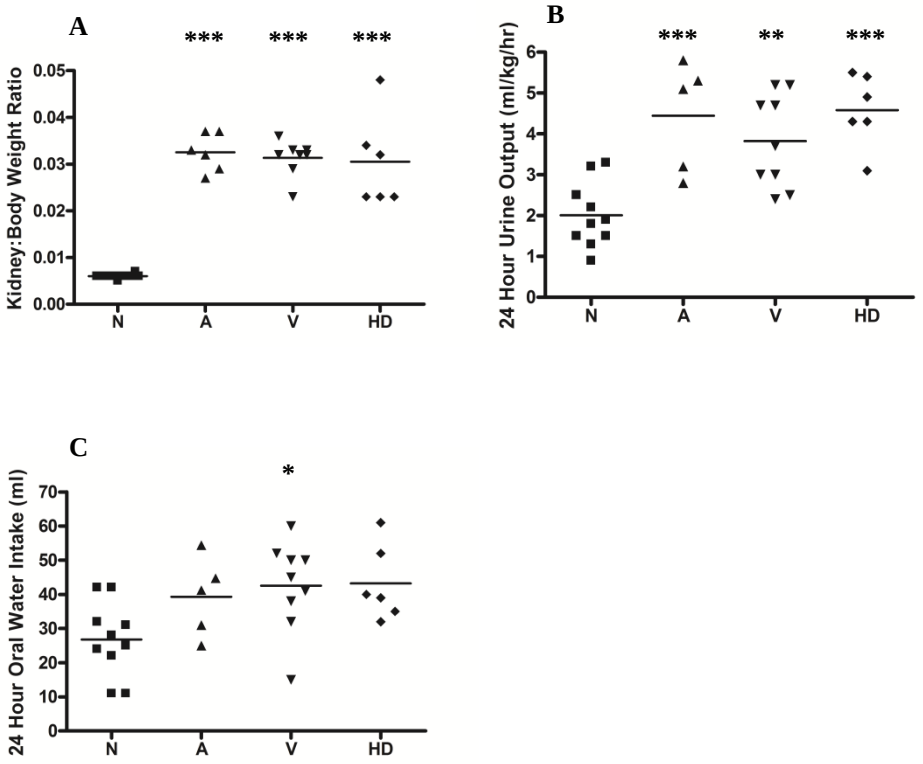

Figure 5.9. Kidney:Body Weight Ratio and Fluid Balance. A: Kidney:Body weight ratios. B: 24 hour urinary output (ml/kg/hr). C: 24 hour oral water intake (ml). *Post hoc* testing compared all groups to N and V as initial ANOVA indicated p<0.05. *p<0.05; **p<0.01; ***p<0.001 all compared to N. Each symbol represents one animal. Horizontal bars represent group means.

Serum biochemistry was assessed at 2 weeks in V and HD rats (Table 5.8 and Figure 5.10) and in all animals following sacrifice (Tables 5.9 and Figures 5.11). Additionally, Table 5.10 and Figure 5.12 summarise the results from analysis of urine (samples collected during the 24 hours prior to tissue harvest).

At 2 weeks there was no significant difference in any serum analyte between the V and HD groups except for ALP which was increased in V rats (Table 5.8, Figure 5.10). However, the ALP concentration measured at the end of the experiment did not differ. There was no significant difference in any other serum parameter measured at the end of the experiment between these 2 groups (Table 5.9, Figure 5.11), although HD rats had a significantly higher 24 hour protein excretion (Table 5.10, Figure 5.12).

Compared with N rats, those in groups A, V and HD had increased serum concentrations of creatinine, urea, phosphate and PTH and decreased levels of corrected calcium, albumin, ALP and ALT. All differences were statistically significant except those for urea, corrected calcium and PTH for HD animals (Table 5.9, Figure 5.11).

A, V and HD rats had significantly lower creatinine clearances and significantly higher 24 hour urinary protein excretion compared with the N group. The 24 hour urinary phosphate excretion was also lower in these 3 groups compared with N rats and this was statistically significant except for in HD animals. No differences were seen in urinary calcium excretion across all 4 groups (Table 5.10, Figure 5.12).

Comparisons between the V and A groups were also non-significant in most cases. Of note, the serum concentrations of both creatinine and urea were significantly greater in the A group Table 5.9, Figure 5.11), however the creatinine clearance was similar in both cohorts (Table 5.10, Figure 5.12). Urinary protein excretion was significantly increased in the A group (Table 5.10, Figure 5.12).

	V (n=9)	HD (n=8)	P value (t-test)
Creatinine (µmol/l)	126.6 ± 29.3	119.1 ± 22.5	0.566
Urea (mmol/l)	7.9 ± 2.8	8.0 ± 2.2	0.914
Phosphate (mmol/l)	3.4 ± 0.5	3.0 ± 0.6	0.139
Corrected Calcium (mmol/l)	2.6 ± 0.1	2.6 ± 0.2	0.920
Albumin (g/l)	29.2 ± 1.6	30.0 ± 1.7	0.302
Alkaline Phosphatase (U/l)	174.6 ± 25.3	138.6 ± 29.7	0.017
ALT (U/l)	58.3 ± 37.7	43.3 ± 15.3	0.308

Table 5.8. Serum Biochemistry Measured at 2 Weeks in V and HD Groups. Measurement of indicated serum parameters at 2 weeks from V and HD rats. Data are presented as mean ± SD.

	N (n=10)	A (n=6)	V (n=9)	HD (n=6)	P value (ANOVA)
Creatinine (µmol/l)	32.7 ± 4.3	633.9 ± 153.8^{c,e}	404.8 ± 103.6^{c}	318.4 ± 106.8^{c}	<0.001
Urea (mmol/l)	1.7 ± 0.8	54.4 ± 24.1^{c,d}	28.2 ± 12.5^{c}	18.8 ± 8.4	<0.001
Phosphate (mmol/l)	4.4 ± 0.6	8.0 ± 0.9^{c}	7.0 ± 0.9^{c}	6.8 ± 1.5^{c}	<0.001
Corrected Calcium (mmol/l)	3.3 ± 0.1	3.0 ± 0.2^{b}	3.1 ± 0.2^{a}	3.2 ± 0.2	0.005
PTH (pg/ml)	1013 ± 379	2203 ± 1047^{b}	2003 ± 362^{b}	1736 ± 493	0.001
Albumin (g/l)	33.2 ± 1.8	28.7 ± 2.2^{c}	28.9 ± 1.5^{c}	28.1 ± 1.1^{c}	<0.001
Alkaline Phosphatase (U/l)	288.2 ± 81.8	108.5 ± 31.7^{c}	147.4 ± 47.0^{c}	166.7 ± 33.5^{c}	<0.001
ALT (U/l)	56.3 ± 25.4	30.0 ± 7.9^{a}	30.0 ± 8.7^{b}	28.3 ± 9.5^{a}	0.003

Table 5.9. End-Point Serum Biochemistry. Measurements of indicated serum parameters at the time of sacrifice. *Post hoc* testing compared all groups to N and V as initial ANOVA indicated $p<0.05$. ^{a} $p<0.05$; ^{b} $p<0.01$; ^{c} $p<0.001$ (all compared to N). ^{d} $p<0.05$, ^{e} $p<0.01$ (all compared to V).

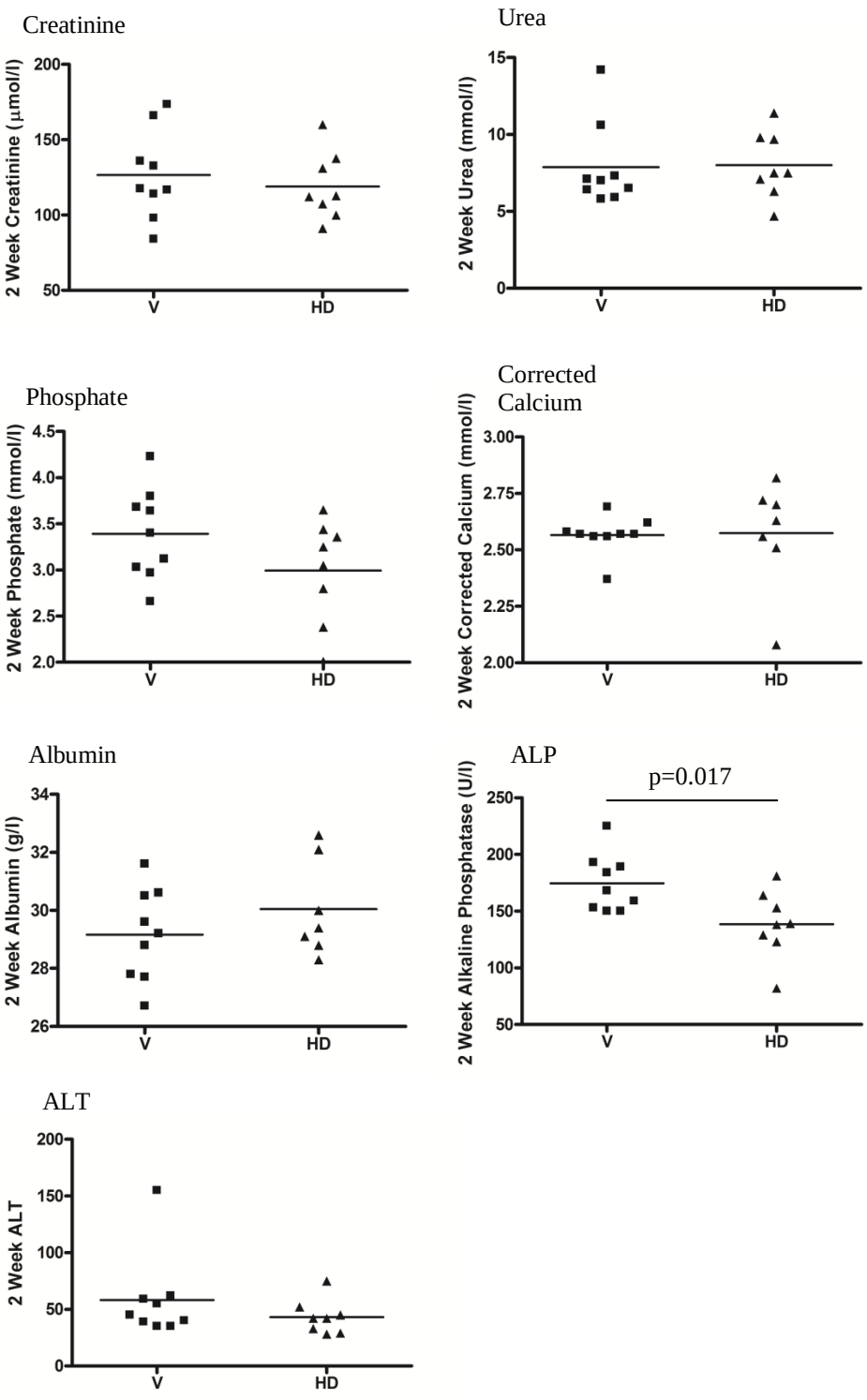

Figure 5.10. Serum Biochemistry Measured at 2 Weeks in V and HD groups. Measurements of indicated serum parameters taken at 2 weeks from V and HD rats. Each symbol represents one animal. Horizontal bars represent group means. Significant results are indicated (evaluated by unpaired t-test).

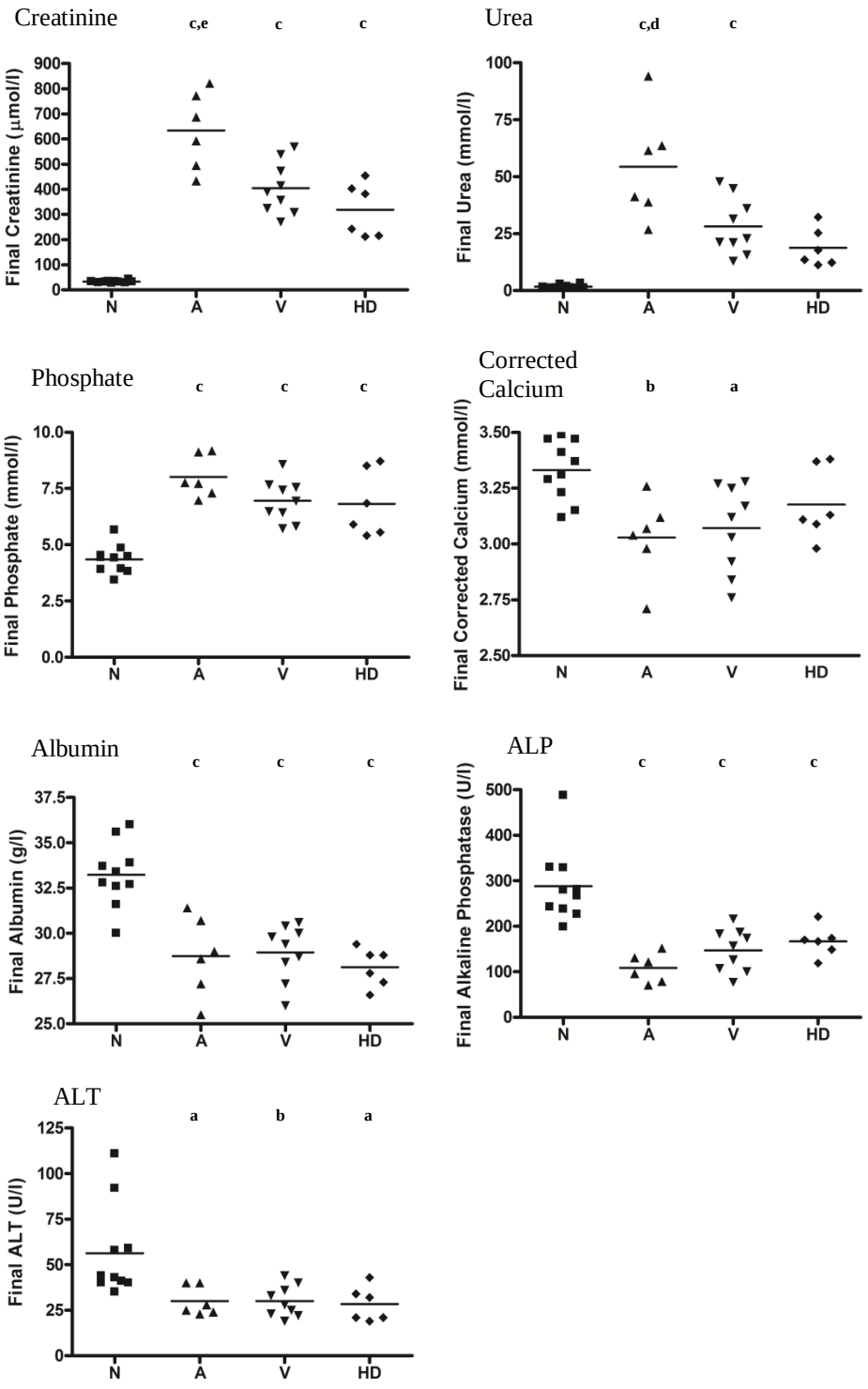

Figure 5.11. End-Point Serum Biochemistry. Measurements of indicated serum parameters taken at the time of sacrifice. *Post hoc* testing compared all groups to N and V as initial ANOVA indicated $p<0.05$. [a] $p<0.05$; [b] $p<0.01$; [c] $p<0.001$ (all compared to N). [d] $p<0.05$, [e] $p<0.01$ (all compared to V). Each symbol represents one animal. Horizontal bars represent group means.

	N (n=10)	A (n=5)	V (n=9)	HD (n=6)	P value (ANOVA)
Creatinine Clearance (ml/min)	2.07 ± 0.37	0.08 ± 0.03[c]	0.13 ± 0.04[c]	0.20 ± 0.08[c]	<0.001
Phosphate Excretion (mmol/day)	0.85 ± 0.27	0.28 ± 0.11[c]	0.53 ± 0.11[b]	0.63 ± 0.10	<0.001
Calcium Excretion (mmol/day)	0.04 ± 0.01	0.03 ± 0.02	0.03 ± 0.01	0.04 ± 0.02	>0.05
Total Protein Excretion (mg/day)	6.1 ± 2.2	15.7 ± 3.8[c,d]	10.2 ± 1.6[a]	16.2 ± 4.6[c,e]	<0.001

Table 5.10. End-Point Creatinine Clearance and Urine Biochemistry. Measurements of indicated parameters quantified in urine taken during the final 24 hours of the experiment. *Post hoc* testing compared all groups to N and V if initial ANOVA indicated p<0.05. This condition was met for all parameters except urinary calcium. [a] p<0.05; [b] p<0.01; [c] p<0.001 (all compared to N). [d] p<0.05, [e] p<0.01 (all compared to V).

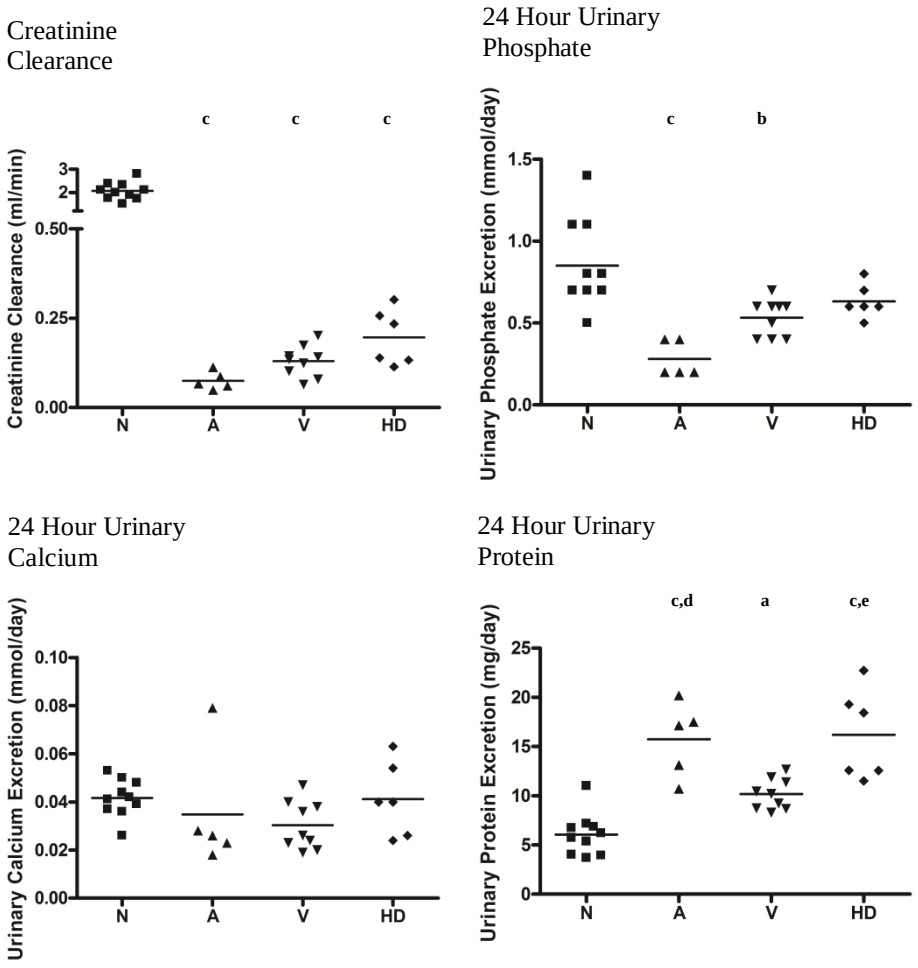

Figure 5.12. End-Point Creatinine Clearance and Urine Biochemistry. Measurements of indicated parameters quantified in urine collected during the final 24 hours of the experiment. *Post hoc* testing compared all groups to N and V if initial ANOVA indicated p<0.05. This condition was met for all parameters except urinary calcium. [a] p<0.05; [b] p<0.01; [c] p<0.001 (all compared to N). [d] p<0.05, [e] p<0.01 (all compared to V). Each symbol represents one animal. Horizontal bars represent group means.

5.2.2.viii P2X7R antagonism does not influence changes in bone induced by adenine feeding.

Given the proposed inverse relationship between bone health and AC (Persey & D'Haese 2009), and reports linking P2X7R to bone homeostasis (Grol *et al* 2009), the femurs of animals from this study were analysed using micro-CT. During the harvesting process 4 femurs from the N group were damaged but all those intact were included in the subsequent analyses. Representative images from the 4 groups are shown in Figure 5.13. The results are summarised in Figure 5.14 and Table 5.11.

There was no statistically significant difference in any parameter for the HD group compared with V animals. However, there appeared to be a trend towards decreased trabecular separation in HD rats. There was a statistically significant difference in percentage trabecular bone volume by KW test, with *post hoc* testing indicating a significant difference between the N and V groups. Similar results were obtained for trabecular separation but no differences between groups were detected for either trabecular number or thickness. The A group had significantly less cortical bone volume compared with controls (Figure 5.14).

For each parameter, the overall spread of data was wide. In order to try and gain a clearer insight into the influence of renal impairment in this context, given the lack of difference between A, V and HD rats, these 3 groups were combined to form a 'CKD' group and compared with the controls (Figure 5.15). This CKD group showed a significant decrease in both percentage trabecular bone (17.1 ± 6.6 v 11.0 ± 3.2%; $p = 0.039$) and cortical bone volume (6.7 ± 0.4 v 6.2 ± 0.5 mm^3; $p = 0.033$).

Another question was whether there was any correlation between trabecular and/or cortical bone volume and aortic calcification. Assessing aortic calcification against percentage trabecular bone yielded Spearman's rho -0.217 ($p = 0.277$). However, for cortical bone volume Spearman's rho was -0.383 ($p = 0.049$). Trabecular thickness was also significantly correlated (negatively) with aortic calcification (Spearman's rho = -0.424; $p = 0.028$), although there was no relationship between AC and either trabecular number or separation (not shown).

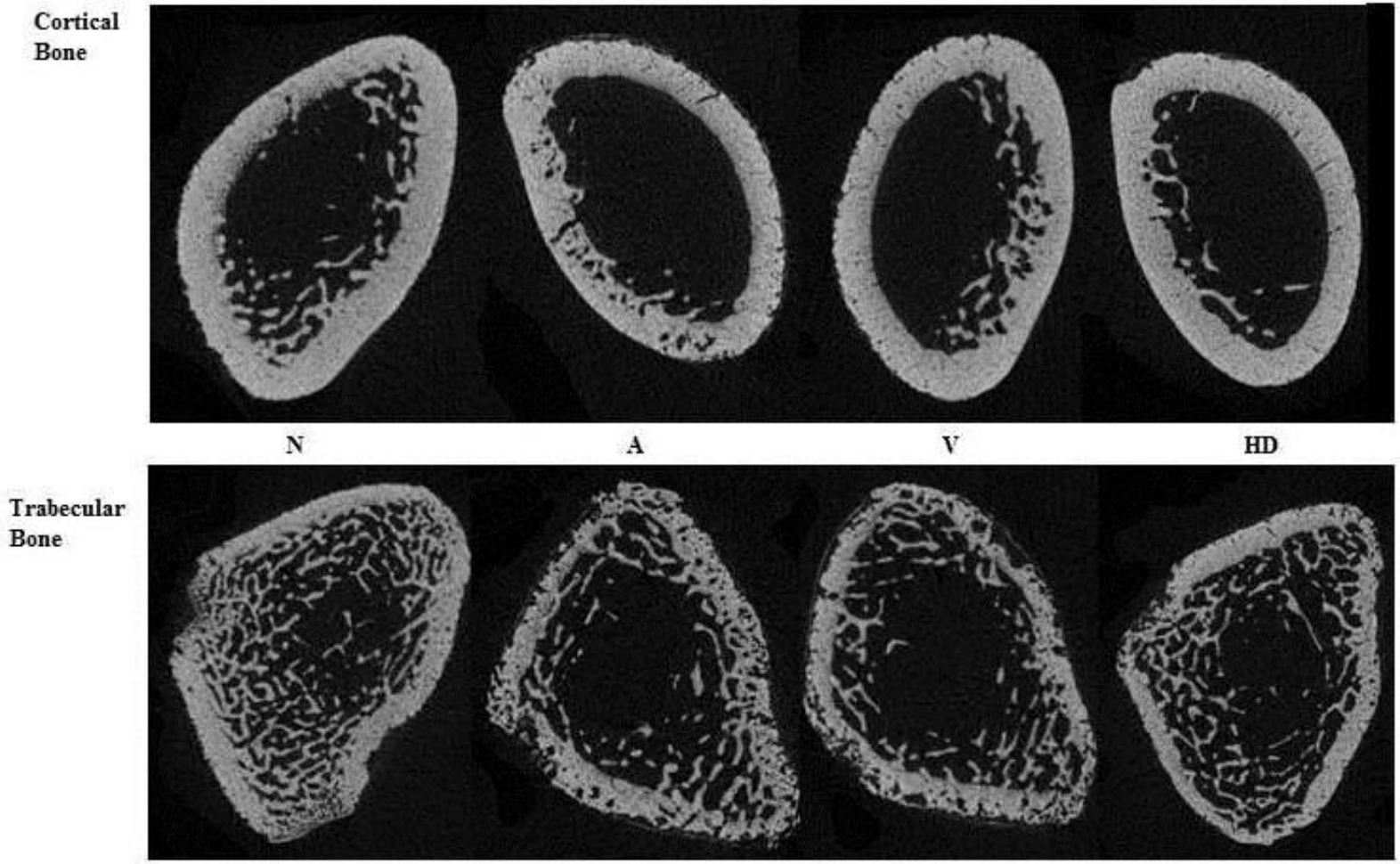

Figure 5.13. Micro-CT Imaging of Cortical and Trabecular Bone. Representative micro-CT images of cortical and trabecular bone from rats in the indicated groups. Rats with CKD (A, V and HD) had lower bone volumes (cortical and trabecular) compared with control animals (N).

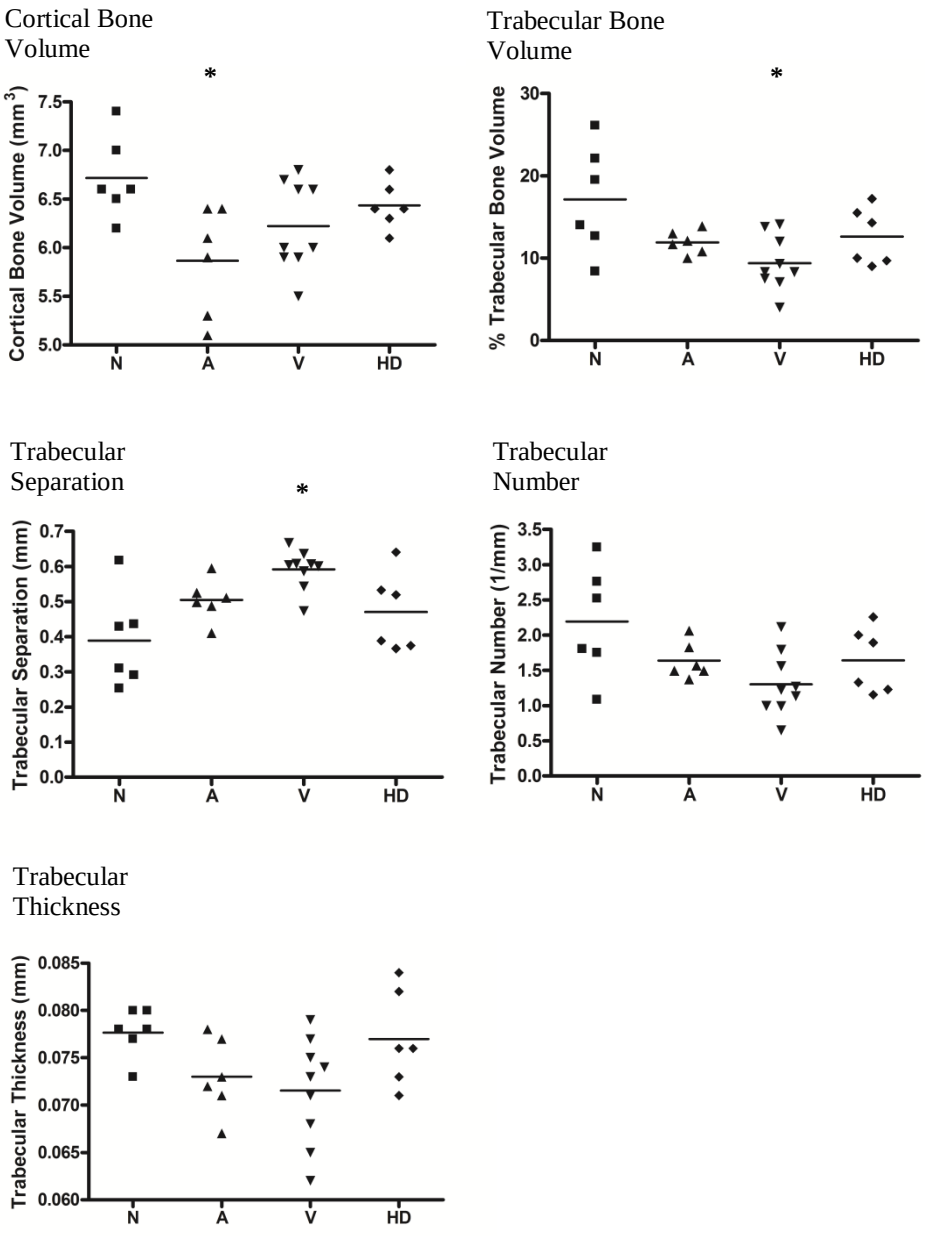

Figure 5.14. Micro-CT Analysis of Bone. Measurement of indicated bone parameters by micro CT-scanning. *Post hoc* testing compared all groups to N and V if initial KW test indicated $p<0.05$. This condition was met for all parameters except trabecular number and thickness. Each symbol represents an individual rat and horizontal lines represent group means. *$p<0.05$ compared with N.

	N (n=6)	A (n=6)	V (n=9)	HD (n=6)	p value (KW)
Trabecular bone volume (%)	17.1 ± 6.6	11.9 ± 1.4	9.4 * ± 3.3	12.6 ± 3.5	0.042
Trabecular separation (mm)	0.39 ± 0.13	0.50 ± 0.06	0.59 * ± 0.06	0.47 ± 0.11	0.019
Trabecular number (1/mm)	2.19 ± 0.79	1.64 ± 0.26	1.30 ± 0.45	1.64 ± 0.47	0.089
Trabecular thickness (mm)	0.078 ± 0.003	0.073 ± 0.004	0.072 ± 0.006	0.077 ± 0.005	0.071
Cortical bone volume (mm^3)	6.7 ± 0.4	5.9 * ± 0.6	6.2 ± 0.5	6.4 ± 0.2	0.047

Table 5.11. Micro-CT Analysis of Bone. Measurement of indicated bone parameters by micro CT. *Post hoc* testing compared all groups to N and V if initial KW test indicated $p<0.05$. This condition was met for all parameters except trabecular number and thickness. Data are presented as mean ± SD. *$p<0.05$ compared with N.

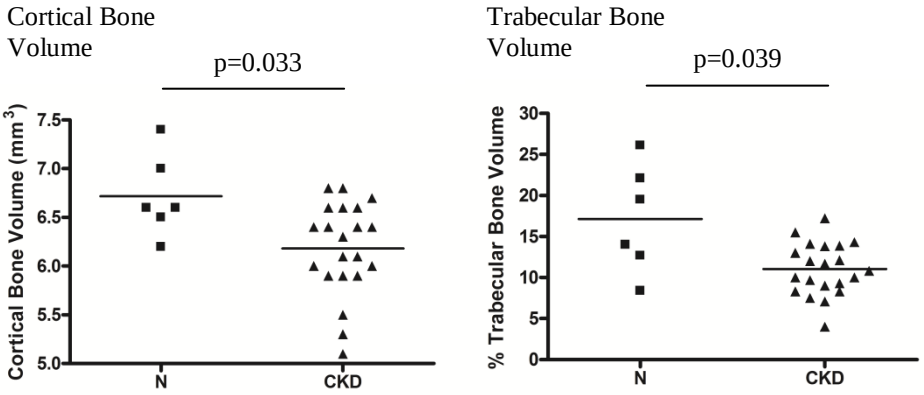

Figure 5.15. Comparison of Bone Volume Between Control and CKD Rats. Rats in groups A, V and HD were combined to form a 'CKD' cohort. This group was compared with controls (N) to evaluate the influence of renal impairment on cortical and trabecular bone volumes (as indicated). Each symbol represents one animal and horizontal bars represent group means. Groups compared using MWU test.

5.3 Discussion

Pharmacological blockade of P2X7R had no effect on the degree of AC seen in this experiment. The high dose of 60mg/kg antagonist employed here was selected based on unpublished data (held by AstraZeneca) showing it to be effective in rat models including the streptococcal cell wall model of rheumatoid arthritis in which it significantly reduced ankle swelling. Pharmacokinetic studies (AstraZeneca, unpublished observations) had demonstrated that this dose, administered twice daily, maintains serum levels above 10 x pA_2 (reported to be 225 ng/ml). The pA_2 value is the concentration of antagonist required to necessitate a doubling of the agonist concentration to elicit the original response (Schild 1947) and ten times this value are frequently targeted in pre-clinical studies. Serum levels measured in HD rats demonstrated that adequate trough concentrations were obtained during this study and although on average animals received approximately 90% of the originally intended doses it can be reasoned that sufficient receptor antagonism was achieved for the majority of the experimental period and that sub-therapeutic dosing is therefore unlikely to account for the lack of effect on AC. However, tissue levels of antagonist were not quantified and therefore inadequate cellular uptake of drug cannot be excluded although there is no obvious reason to suggest that this should have occurred.

The qPCR experiments described in this chapter were primarily performed because although overall calcification was not affected by P2X7R blockade, it was possible that cellular pathways thought to be involved in AC, such as VSMC osteogenic transformation and/or apoptosis (Shanahan *et al* 2011, Shanahan 2013, Shroff *et al* 2013), were still being influenced. The qPCR experiments described in Chapter 3 suggested that in the ring culture model of AC these mechanisms may not even occur, thereby going some way to explain the lack of effect of P2X7R ligation on arterial calcium deposition *in vitro*. It was therefore also clearly relevant to assess whether they could be demonstrated at all *in vivo* and specifically under uraemic conditions.

Expression of mRNA for all 3 VSMC-specific markers studied, α-SMA, SM-22 and smoothelin, significantly decreased in calcified tissue, suggesting that in calcification-promoting conditions *in vivo,* VSMCs do undergo a change of

phenotype. These changes were not, however, influenced by P2X7R blockade. Most reports in the literature assign this change in phenotype to cells taking on characteristics of 'bone-like' cells and show a concurrent up-regulation in osteogenic markers (Shroff *et al* 2010). In the current work, mRNA for the osteogenic transcription factor osterix (Nakashima *et al* 2002) was essentially absent in all samples. Furthermore, expression of mRNA for BMP-2, a key regulator of osterix (Celil *et al* 2005, Hruska *et al* 2005) was unchanged in calcified vessels compared to controls. Although the osteogenic transcription factor runx-2 (Komori *et al* 1997, Ducy *et al* 1997) was up-regulated in calcified vessels, the mRNA copy numbers were extremely low, even in the arteries containing mineral deposition. Its functional significance is therefore doubtful. These findings, like those in Chapter 3, challenge the relevance of osteogenic transformation in the development of CKD-associated AC and are in agreement with some previous work.

Of particular note is a recent study which employed a well-controlled immunohistochemistry protocol to stain normal and calcified arteries of varying sizes from humans with and without CKD (O'Neill & Adams 2014). Staining for both osterix and osteocalcin (bone gla protein) was absent. A number of reports using the rat adenine model have also failed to detect any significant increase in mRNA for osteogenic markers in calcified tissue (O'Neill *et al* 2008, Lomashvili *et al* 2011). One group have suggested that VSMCs undergo chondrocytic rather than osteogenic transformation in the adenine model (Neven *et al* 2010) associated with an up-regulation of sox9. There is minimal evidence linking P2X7R with cartilage formation and hence this possibility was not examined in this thesis.

In contrast to the *in vitro* findings in Chapter 3, an increase in mRNA expression of the apoptosis marker, caspase-3, was seen in calcified vessels compared with controls. This suggests that a factor present in the uraemic environment is required to induce VSMC apoptosis in this model. In keeping with this theory, increased apoptosis has been demonstrated in arterial tissue from dialysis patients as compared with healthy controls (Shroff *et al* 2008). It is unclear from the current work whether apoptosis is a causative phenomenon, occurring prior to the onset of calcification as suggested by some groups (Shroff *et al* 2010), or a late, consequence of tissue damage as suggested by others (O'Neill & Adams 2014). It is also possible that the

increased apoptosis is unrelated to calcification and is the effect of another toxin. In this regard, and as discussed below, it is unknown whether adenine exerts any direct effects on vascular cells. P2X7R inhibition did not influence the expression of caspase-3 mRNA suggesting that the receptor does not mediate apoptosis in this context.

The ability of P2X7R to activate the NLRP3 inflammasome is well described (Di Virgilio 2007) and one recent report suggested that NLRP3 is involved in AC (Wen *et al* 2013). In keeping with this study, calcified aorta had significantly greater levels of inflammasome mRNA in the present work, however this was not altered by P2X7R blockade. One possible explanation for these apparently paradoxical findings is that inflammasome activation in calcified arteries might be P2X7R-independent, as has been described in adipose tissue (Sun *et al* 2012).

The expression of P2X7R at both the mRNA and protein level was unchanged in calcified vessels compared with controls. This is consistent with the results from Chapter 3 and the data taken together indicate that expression of P2X7R in rat aorta is not affected by the presence of calcium deposition either alone or in the presence of a uraemic environment. At present it is unclear what functional role the receptor plays in arterial tissue.

As emphasised in the KDIGO guidelines for CKD-MBD (Kidney Disease: Improving Global Outcomes (KDIGO) CKD–MBD Work Group 2009) (see Chapter 1, section 1.5.2), a spectrum of bone disturbances can occur in CKD. These include abnormalities in turnover, mineralisation and volume. Compared with traditional 2-dimensional (2D) histomorphometric-based procedures and with relevance to CKD-MBD, because micro-CT gives a 3D view, it is superior for measuring bone volume (Bouxsein *et al* 2010). Indeed, micro-CT is now considered the 'gold-standard' method of assessing small rodent bone morphology and microstructure under experimental conditions and the results generated by this technique have been shown to correlate very well with those obtained from histomorphometry (Bouxsein *et al* 2010).

As outlined in Chapter 1 (section 1.9.4.i), the exact role of P2X7R in bone biology is a point of controversy with 2 strains of $P2X7^{-/-}$ mice reported to show opposing

changes in bone volume compared with WT controls (Ke *et al* 2002, Gartland *et al* 2003a) and different groups using cultured bone cells reporting either positive (Panupinthu *et al* 2008) or negative effects (Orriss *et al* 2012) of the receptor on bone formation. This study is the first to examine the effect of pharmacological P2X7R blockade on CKD-related bone disease and overall, receptor antagonism failed to exert a significant impact on any parameter measured by micro-CT. Assuming that adequate uptake of antagonist into bone was achieved, the implication is that any effect of P2X7R blockade on bone remodelling was outweighed by the influences of other factors, which probably include increased PTH (which was shown to occur in the present study), and suppressed vitamin D, which is also known to occur in this model (Neven *et al* 2010).

Investigators that have used histomorphometry to assess bone from adenine-fed rats have consistently demonstrated features consistent with a high-turnover state such as increased osteoid and osteoblast parameters (Henley *et al* 2009, De Schutter *et al* 2011, O'Neill *et al* 2011). Micro-CT cannot be used to directly assess bone turnover, as histological assessment of cell-types is required. However, previous studies have demonstrated that on micro-CT imaging, high-turnover disease associates with loss of trabecular bone volume and increased trabecular separation (De Schutter *et al* 2011, Hopper *et al* 2007). These findings are consistent with those presented here. A decrease in cortical bone volume was also seen in adenine-fed animals in the present study which is consistent with a previous report (De Schutter *et al* 2011).

No correlation was found between final trabecular bone volume and AC in this work, although a negative correlation was found with final cortical bone volume and trabecular thickness. One previous study (De Schutter *et al* 2011), correlated changes in cortical bone volume, as measured on micro-CT, with the magnitude of aortic calcification. For practical reasons scanning could only be performed post-mortem in this study. Change in bone volume is likely to better represent uraemia-induced bone disease compared with just a final reading, however, the findings in the present work are in keeping with this study by De Schutter *et al* (2011) and suggest that cortical bone volume is related to AC.

Serum biochemistry cannot definitively predict the degree of bone turnover (Kidney Disease: Improving Global Outcomes (KDIGO) CKD–MBD Work Group 2009),

however, elevated PTH, ALP and phosphate are usually observed in high-turnover disease whilst PTH and ALP are often normal or decreased in low-turnover states. The serum biochemistry from the adenine-fed rats in the current work is mainly consistent with high bone turnover with the exception of ALP, which was, surprisingly, suppressed compared with controls. Most studies that have employed the rat adenine model have not specifically measured serum ALP. A recent study (Sun *et al* 2013) found no difference in ALP in adenine-fed rats compared with controls and an older report (Okada *et al* 1999) compared results after 2 and 6 weeks of adenine feeding, (there was no control group) and again found no difference. Of note an increase in ALP with this model has not been reported. Serum albumin levels were found to decline in adenine-fed animals in this work and this is often reported (Yokozawa *et al* 1986, Price *et al* 2006). It is therefore possible that synthetic liver function is suppressed with this model and the ALP is a reflection of this, rather than indicating bone disturbances. In keeping with this is the fact that ALT was also decreased in the adenine groups in the current study.

In both the initial pilot experiment and the main study, the abdominal aortic segment was the most consistently calcified region. Most other studies examining AC *in vivo* have not specifically looked at each aortic segment individually however this observation is in keeping with one previous report (Shobeiri *et al* 2013). It is also consistent with the *in vitro* work described in Chapter 3 in which abdominal aortic segments calcified to a greater extent than those from more proximal regions. Differences in AC between vascular beds has rarely been studied in man, although one report found a greater incidence of AC in the abdominal aorta compared to the thoracic region in obese patients (Jensky *et al* 2011). Although not widely studied, potential reasons to account for the regional differences include maladaptive responses to haemodynamic changes in the abdominal aorta compared with the thoracic region (Ameer *et al* 2014) and differences in embryological origin of cells from each anatomical site which has been shown to influence the propensity to calcify (Leroux-Berger *et al* 2011).

The magnitude of renal impairment, AC and other associated clinical features seen with the adenine model is unquestionably related to dietary intake and therefore any factor that suppresses the ability or willingness of an animal to eat will potentially

attenuate development and progression of disease. This issue is perhaps the greatest limitation of this experiment. Although not statistically significant, for some outcome measures, particularly biochemical markers of renal function, there were arguably trends towards a more favourable outcome for the HD group compared with the V controls. Despite these results, the overall subjective impression throughout the experiment was that HD rats, whilst not sick, were not faring as well. These apparent paradoxical observations are probably best explained by considering the negative correlation between the number of missed gavages and aortic calcification. Rats did not receive a dose of antagonist on a particular occasion if either the gavage cannula could not be passed due to resistance at the level of the oesophagus, or there were other concerns over an animal's condition. Thus the number of missed doses is in effect a surrogate marker of poorer animal health and likely to reflect a suppressed dietary intake of adenine. The implication of this is that the likelihood of any one animal developing AC is intimately linked to how well it tolerates the oral gavage procedure, with those less tolerant more likely to sustain oesophageal trauma during dosing with the knock-on effect of decreasing oral intake, thereby confounding any real pharmacological effect of the substance being administered. Rats in the HD group (and in fact the LD group too) subjectively seemed to tolerate the gavage procedure less well than V controls and a subtle influence conferred by the smell or taste of the antagonist cannot be excluded as a contributing factor to this. The fact that these two groups were less tolerant of the procedure probably also explains, to a large extent, why they both suffered from a higher mortality rate compared with the V group as the procedure itself was made more difficult in these situations.

The adenine rat model is commonly used for investigating AC *in vivo*. The rates of calcification reported with this model vary widely and can be enhanced by reducing the protein content of the diet to 2.5% (Price *et al* 2006). The protein content of all diets administered in this chapter was set to this level and of those rats fed 0.75% adenine, aortic calcification occurred in all but 2. It was notable that calcification occurred in all rats fed the diet containing 0.75% adenine and normal phosphate (Diet G, Table 2.1). The original rationale for including this group was to try and obtain a control cohort that had uraemia without AC. The adenine diet is almost always used in combination with high (usually 0.9%) phosphate (Shobeiri *et al* 2010,

Neven *et al* 2011), however one previous study (Lomashvili *et al* 2008) had employed a 0.75% adenine diet combined with normal (0.4%) phosphate to successfully induce renal impairment alone. This report was the basis for employing Diet G (Table 2.1) in the current work. In retrospect, the disparity in calcification described in the study by Lomashvili *et al* (2008) and this chapter is almost certainly down to the protein content of the respective diets. This was not specifically stated in the work by Lomashvili *et al* and it is likely that normal dietary protein was given rather than the 2.5% utilised here.

The fact that calcification occurred in all rats in the A group meant it was not possible to determine whether any particular biological effect observed in adenine-fed rats, (when compared with controls), was specifically due to calcification, or secondary to uraemia per se. There are also other factors, unrelated to the degree of CKD, which could have contributed to the differences observed between control rats and those fed adenine. It is unknown whether the AC seen in adenine-fed animals is only attributable to the uraemic state invoked, or whether adenine itself is a direct vascular toxin. A large proportion of adenine within the intestinal lumen has been shown to be taken up into the circulation un-metabolised (Salati *et al* 1984) and the free base has been shown to be directly toxic to some cell types including human lymphoblasts (Snyder *et al* 1978). Work performed over 50 years ago, when the effects of adenine-feeding to rodents were just beginning to be described, suggested that the clinical manifestations are purely attributable to renal impairment (Philips *et al* 1951), however, until proven otherwise a direct effect on the vasculature cannot be excluded particularly considering the increased expression of the apoptosis marker caspase-3 in calcified vessels seen here.

Adenine-fed animals also lost a considerable amount of weight compared with controls (in which there was mild weight gain) and this is another potentially confounding factor. The weight loss of approximately 30% seen in this study is in keeping with most other reports using this model (Price *et al* 2006) and is likely due to both the adenine diet being less palatable and also the increased catabolism known to occur in advanced renal disease (Slee 2012). Some groups have tried to control for the weight loss by adopting a paired-feeding strategy (Lomashvili *et al* 2009) however a lot of wastage of dietary pellets was seen in this study, which makes

accurate monitoring of oral intake very difficult. In addition, because much of the weight loss seen is almost certainly a consequence of uraemia, rather than suppressed intake (although this unquestionably does occur), it can be argued that limiting the availability of diet for non-CKD animals in effect adds another variable into the experiment rather than acting as a control procedure.

Given the number of limitations with this experiment it is worthwhile considering whether either an alternative experimental model and/or method of drug delivery could have been employed. As discussed in Chapter 1, there are 2 other rat models of CKD-associated AC described – the 5/6th nephrectomy model (Chauntin & Ferris 1932) and the Cy/+ rat model (Kaspareit-Rittinghausen *et al* 1990). AC in the 5/6th model is much less consistent than with adenine, often reported to be less than 50% (Shobeiri *et al* 2010, Neven & D'Haese 2011). In addition, both of these alternative models require a number of months for AC to develop which make them impractical from the point of view of drug delivery by oral gavage. The potential options for administration of the antagonist were extensively discussed prior to commencing the experiment. More convenient methods such as integration of the compound into feed or drinking water, or the use of an implantable drug delivery system were not viable due to issues surrounding drug stability (AstraZeneca personal communications). Twice daily ip administration has been used by some, including others in our group (Booth *et al* unpublished observations), however not without adverse effects. In addition, the strongest pharmacokinetic data was obtained using oral dosing (AstraZeneca personal communications). It was therefore felt that overall, this model and method of dosing were the best available options.

5.4 Summary

Pharmacological P2X7R blockade failed to influence the extent of CKD-associated AC in the rat adenine model and did not appear to modulate any of the biological pathways to which it might be linked that are thought to mediate this disease. The work in this chapter further challenges the relevance of osteogenic transformation to the aetiology of AC but suggests that apoptosis may occur, although the timing of this is unclear. This work has also demonstrated that both trabecular and cortical bone loss occur in this *in vivo* model although again, this was not influenced by ligation of P2X7R.

CHAPTER 6 – ATP METABOLIC PATHWAYS IN ARTERIES FROM RODENTS AND HUMANS WITH CHRONIC KIDNEY DISEASE

6.1 Introduction

The results of the work described in Chapters 3-5 did not provide any significant indication that P2X7R is implicated in the pathogenesis of CKD-associated AC. Therefore for the latter part of this thesis the focus switched from investigating P2X7R in isolation to considering more broadly the potential involvement of ATP in the calcification process.

As discussed in detail in Chapter 1 (section 1.10), there is increasing interest in the importance of ATP metabolism in the evolution of AC. In particular, the role of ATP as a substrate for the enzyme ENPP-1, which catalyses the conversion of ATP to AMP and (more relevantly) the calcification inhibitor, PPi, (Figure 1.2, re-printed as an aide memoire on the following page), has received attention (Persy & McKee 2011, O'Neill *et al* 2011, Villa-Bellosta & Sorribas 2013, Lomashvili *et al* 2014). PPi can directly inhibit hydroxyapatite formation (Fleisch *et al* 1965), however conversely, it can be metabolised by TNAP to generate phosphate, thereby promoting calcification (Murshed *et al* 2005). Genetic deficiency of ENPP-1 causes extensive AC in both mice (Sakamoto *et al* 1994) and humans (Rutsch *et al* 2003) leading to premature death. Increased arterial TNAP expression and activity have been demonstrated in uraemic rats (Lomashvili *et al* 2008) and in patients with CKD (Shroff *et al* 2008), possibly contributing to AC, however it is unknown whether there are also changes in ENPP-1 in this clinical setting. Other components of the ATP-metabolising system present in the vasculature might also play a role in the calcification process but have not been studied in the context of renal impairment. These include the enzymes CD39 and CD73 and the putative PPi transporter, ANK (Figure 1.2).

The primary objective of the work described in this chapter was to determine, with an emphasis on ENPP-1, whether the expression of enzymes involved in ATP metabolism is altered in calcified arteries from subjects with CKD. The rodent tissue collected during the work performed in previous chapters provided the necessary resources to address this question in an *in vivo* model. In addition, segments of inferior epigastric artery from patients undergoing renal transplantation were

available for study. This provided the opportunity to not only assess some facets of vascular ATP metabolism but also the histological appearance of CKD-associated AC in man which has only rarely been previously described (Shroff *et al* 2008, Shlieper *et al* 2010, O'Neill & Adams 2014).

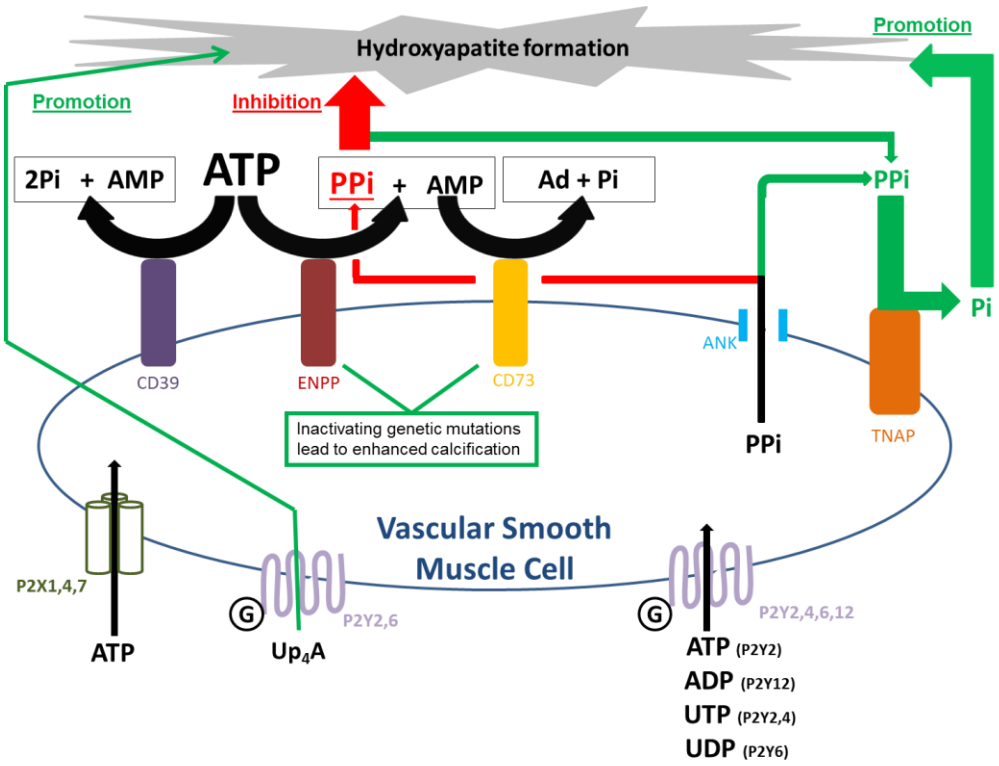

Figure 1.2 (re-printed with abbreviated legend). The Purinergic System and its Regulation of AC in VSMCs.

ATP and other ligands for P2X and P2Y receptors gain access to the extracellular space in a number of ways (see text). ATP is hydrolysed by either CD39 (ecto-nucleoside triphosphate diphosphohydrolases (NTPDases)) into AMP plus 2 phosphates (Pi), or by ecto-nucleotide pyrophosphatase/phosphodiesterases (ENPPs) into AMP plus inorganic pyrophosphate (PPi). AMP is hydrolysed into adenosine (Ad) and Pi by CD73 (ecto-5'-nucleotidase). PPi can also reach the extracellular space from within the cell through the putative membrane transporter ANK (ankylosis) protein. PPi is subsequently hydrolysed into Pi by tissue non-specific alkaline phosphatase (TNAP).

PPi is a potent inhibitor of calcification, however it is also the substrate for generation of Pi by TNAP and subsequent hydroxyapatite formation. The balance between ENPP1 and TNAP activity is therefore critical in determining whether calcification pursues. Autosomal recessive mutations in ENPP1 cause arterial calcifications in infancy and autosomal recessive mutations in CD73 cause arterial calcifications in adulthood.

6.2 Results

6.2.1 Studies in rodent arteries.

6.2.1.i ENPP-1 mRNA expression and enzyme activity are increased in calcified rodent arteries.

The expression of mRNA for ENPP-1 was quantified in abdominal aortic tissue collected from rats fed the control (N), adenine/normal-phosphate (A) and adenine/high phosphate (V) diets (Chapter 5). AC of the abdominal aorta and advanced renal impairment were present in all animals in the latter 2 groups.

Compared with control rats, ENPP-1 mRNA expression was significantly increased in both the A and V groups with no significant difference in expression seen between these 2 cohorts (Table 6.1 and Figure 6.1). Absolute copy numbers were relatively low in the N group but rose to the order of several thousand in both A and V animals. The data for the 9 V animals seemed to divide into 2 distinct clusters, one well above (n=4) and the other well below (n=5) the overall group mean (Figure 6.1). Of note, the 4 V rats with the highest mRNA expression were also the 4 with the greatest amount of abdominal aortic calcium deposition. The magnitude of calcification was significantly higher in these 4 rats compared with the other 5 in this group (66.3 ± 27.6 vs 14.2 ± 12.8 respectively; p = 0.016).

Gene	N (n=10)	A (n=6)	V (n=9)	p value (KW test)
ENPP-1	571 ± 716	4,765 ± 1,614**	6,284 ± 3,767***	<0.001
CD39	157,304 ± 70,884	66,718 ± 23,572**	90,041 ± 27,617	0.006
TNAP	12,072 ± 4,553	4,027 ± 3,663*	7,321 ± 4,957	0.018
CD73	4.495 ± 4,787	19,674 ± 4,227**	20,833 ± 7,488***	<0.001
ANK	68,245 ± 28,845	143,392 ± 37,120**	146,468 ± 49,990**	0.001

Table 6.1. mRNA Copy Numbers for ATP-Metabolism Related Molecules in Rat Aorta. RNA was extracted from rat aortas and qPCR assays performed for the genes indicated. As initial KW test indicated p<0.05 *post hoc* testing compared all groups with N and A with V. *p<0.05; **p<0.01; ***p<0.001 all compared to N. Data are presented as mean ± SD.

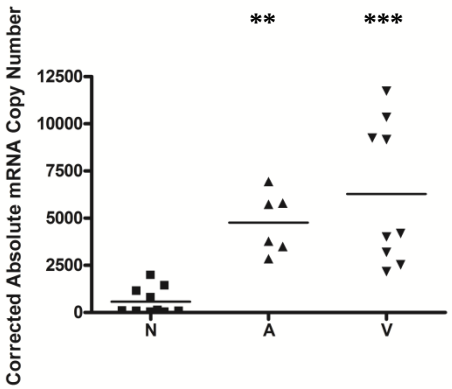

Figure 6.1. ENPP-1 mRNA Expression in Rat Aorta. RNA was extracted from rat aortas (abdominal aorta) and a qPCR assay performed for ENPP-1. *Post hoc* testing compared all groups with N and compared A with V. **p<0.01; ***p<0.001 all compared to N. Each symbol represents one animal. Horizontal bars represent group means.

To assess whether ENPP-1 was also increased at the protein level in arteries from A and V rats several efforts were made to perform Western blots of aortic protein lysates. Unfortunately despite trialling several commercially-available primary antibodies these attempts proved unsuccessful with no bands of appropriate molecular weights ever being detected.

Although ENPP-1 protein expression could not be evaluated, it was possible to quantify actual enzyme activity by measuring the metabolism of the synthetic substrate pNP-TMP (Nam *et al* 2011, Lomashvili *et al* 2011). Using this method, ENPP-1 activity was assessed in segments of aortic arch obtained from 7, 6 and 7 rats in the N, A and V groups, respectively. In keeping with the mRNA results, a significant increase in activity was detected in arteries from A and V rats compared with controls, with both groups exhibiting an approximate doubling in enzyme function (Figure 6.2A). Three aortic arch segments from the V group had no detectable calcification when analysed colourimetrically. Therefore in order to ascertain the effect of uraemia alone, the enzyme activity in these 3 samples was compared with the N group. A significant increase was detected in these non-calcified, uraemic vessels which had a mean change in optical density (enzyme activity) of 0.74 ± 0.16 arbitrary units/mg tissue compared with 0.47 ± 0.10 in controls ($p = 0.012$) (Figure 6.2B).

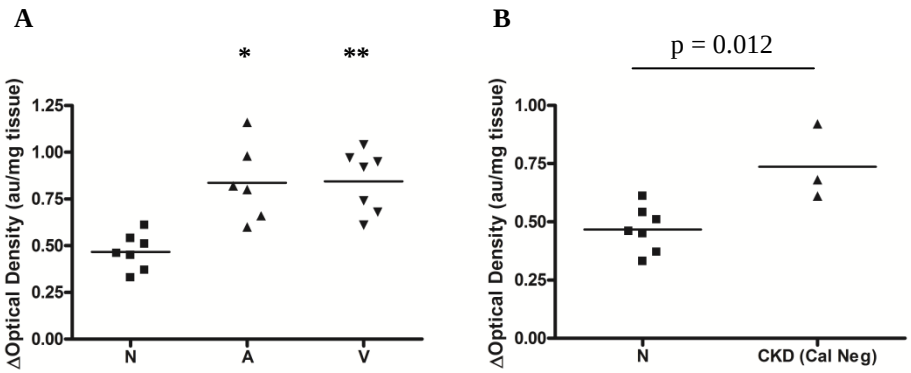

Figure 6.2. ENPP-1 Activity in Rat Aorta. Activity was measured in segments of aortic arch as the change in optical density following a 1 hour incubation of each vessel with the synthetic enzyme substrate pNP-TMP. A: Comparison of enzyme activity between all groups. *Post hoc* tests were performed as initial KW test showed $p<0.05$ and compared all groups with N and compared A with V. *$p<0.05$; **$p<0.01$ all compared to N. B: Comparison of enzyme activity in non-calcified vessels from rats with CKD (CKD (Cal Neg)) with controls (MWU test). Each symbol represents one vessel segment. Horizontal bars represent group means.

6.2.1.ii Serum PPi measurements in rodents with and without CKD.

To assess whether greater aortic ENPP-1 activity resulted in an increase in circulating PPi, the relative serum concentrations of this molecule were compared between groups (Figure 6.3A). Overall there were no significant differences detected. Given the comparable results for A and V rats the data from these 2 groups were combined. The mean change in optical density (relative PPi concentration) was less in this 'CKD group' compared with controls but it did not reach statistical significance (Figure 6.3B).

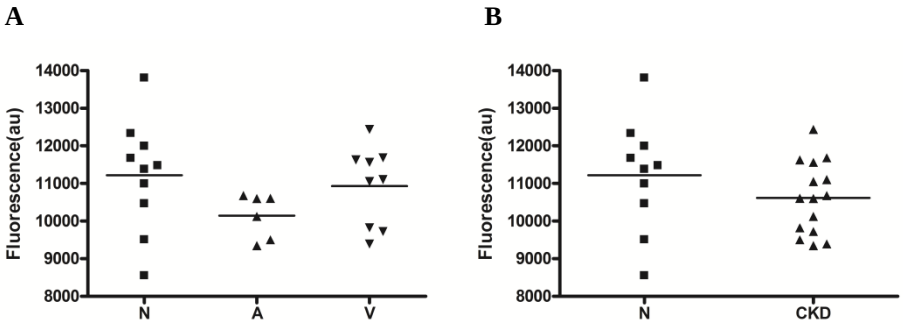

Figure 6.3. PPi Content of Rat Serum. The fluorescence of serum from each rat was measured following the addition of a proprietary PPi sensor and compared between groups to assess for relative differences. A: Comparison of all groups. B: Comparison of control animals with all rats with CKD (A and V groups combined). Each symbol represents one animal. Horizontal bars represent group means.

6.2.1.iii Analysis of mRNA expression for other ATP metabolism-related molecules.

Following the findings for ENPP-1 expression and activity, other components of the ATP-metabolising system were assessed in rodent vessels. Quantification of mRNA expression for the enzymes CD39, TNAP and CD73, along with the ANK protein, was performed (Table 6.1 and Figure 6.4).

In the case of CD39, mRNA expression was reduced in calcified arteries compared with controls. This only reached statistical significance for the A group following *post hoc* testing although there was also a marked decrease in the V group. It was notable that the magnitude of CD39 mRNA expression was in the order of several tens of thousands.

A decrease in mRNA expression for TNAP was also seen in calcified vessels, although once again only reaching statistical significance in the A group after *post hoc* analysis. The level of TNAP mRNA expression was much lower than CD39 being present in the order of only a few thousand copies.

In contrast to the findings for these 2 enzymes, a statistically significant increase in mRNA expression for both CD73 and ANK were seen in both the A and V groups compared with controls. Orders of magnitude of expression were several thousands and tens of thousands respectively.

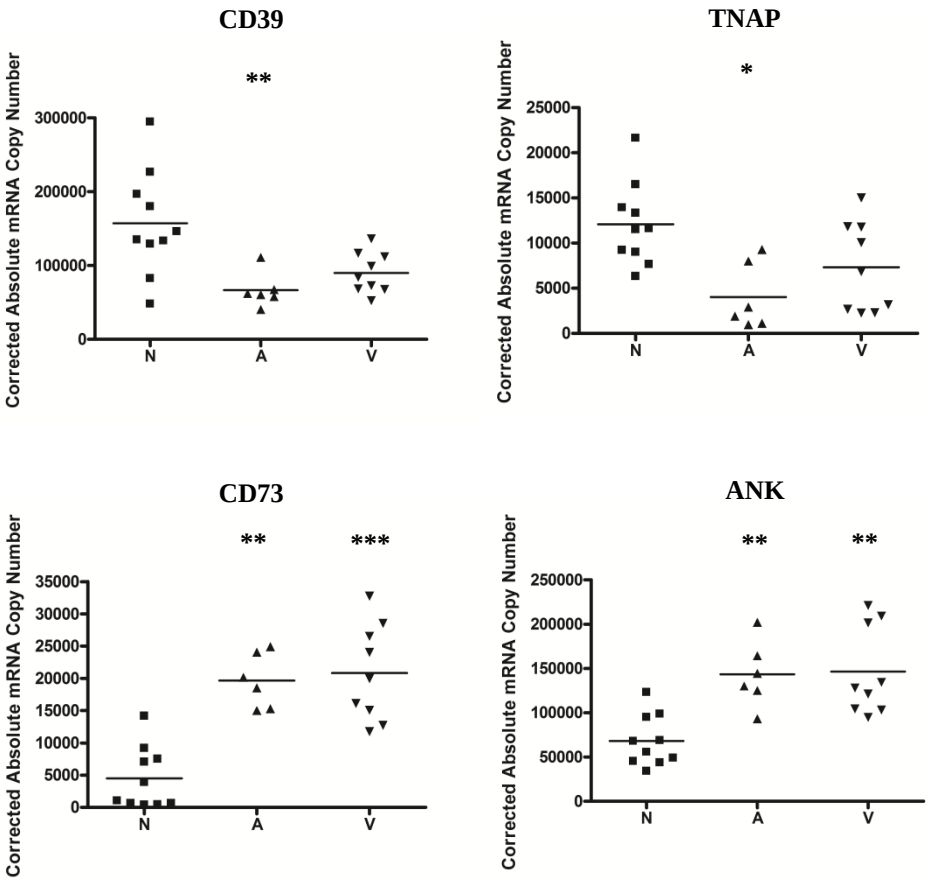

Figure 6.4. Expression of ATP-Metabolism Related Molecules in Rat Aorta. RNA was extracted from rat aortas and qPCR assays performed for the genes indicated. *Post hoc* testing compared all groups with N and A with V as initial KW test indicated $p<0.05$. *$p<0.05$; **$p<0.01$; ***$p<0.001$ all compared to N. Each symbol represents one animal. Horizontal bars represent group means.

6.2.1.iv Analysis of ATP metabolism-related molecules over time using an ex vivo model of AC.

To try and begin to understand the factors governing these altered expression profiles, the *ex vivo* ring culture model (described in Chapter 3) was used to investigate the changes over time in vessels exposed to an elevated phosphate concentration. Analysis was conducted using the samples obtained from the time-course experiment detailed in Chapter 3, section 3.2.5 – 'Expression of mRNA for P2X7R, markers of VSMC phenotype and caspase-3', in which cultured rings, obtained from 3 rats, were distributed evenly between control and high phosphate groups for each time-point (baseline and 3, 7 and 10 days). The results are summarised in Table 6.2 and Figure 6.5.

For ENPP-1 there was a general trend towards an increase in mRNA expression in the control samples compared with baseline with increasing time in culture - this was statistically significant at days 7 and 10. At each time-point there was no significant difference between ENPP-1 expression in control rings and those exposed to high phosphate. In the case of CD39, mRNA expression was suppressed in control rings compared with baseline and this was statistically significant at days 3 and 7. Again no differences were detected between control and corresponding high phosphate samples at any time-point. TNAP mRNA expression was markedly suppressed in all control ring groups compared with baseline, reaching statistical significance at day 3 and day 10 (a clear trend was also evident at day 7). No differences were detected in phosphate-treated rings compared with their time-point controls. Expression of mRNA for CD73 was elevated in all control rings compared with baseline vessels with statistically significant differences detected at all time-points. High phosphate conditions again did not exert any significant impact. Results for ANK mRNA expression were much more equivalent between groups and although the initial KW test indicated significant differences overall, none were detected with *post hoc* tests comparing control samples to baseline and groups matched for time-point (control vs high phosphate).

Gene	Baseline n=7	Day 3 – Control n=5	Day 3 - HP n=5	Day 7 – Control n=5	Day 7 - HP n=5	Day 10 – Control n=5	Day 10 – HP n=6	p value (KW test)
ENPP-1	770 ± 175	1,277 ± 176	1,059 ± 154	1,731 ± 906*	1,906 ± 649	2,426 ± 539***	1,353 ± 424	<0.001
CD39	88,995 ± 7,878	26,021 ± 4,558**	22,336 ± 6,148	33,457 ± 9,162*	38,060 ± 10,050	57,598 ± 24,905	31,409 ± 14,754	<0.001
TNAP	11,589 ± 5,541	971 ± 1,164*	857 ± 864	493 ± 356	352 ± 335	221 ± 119**	346 ± 285	0.007
CD73	3,367 ± 814	14,713 ± 1,720**	9,651 ± 1,287	13,914 ± 2,928*	15,251 ± 5,666	12,575 ± 3,344*	15,377 ± 4,013	0.001
ANKH	41,071 ± 4,814	33,145 ± 1,324	31,072 ± 5,512	45,486 ± 23,615	48,745 ± 20,102	92,199 ± 29,848	45,132 ± 14,610	0.008

Table 6.2. mRNA Copy Numbers for ATP Metabolism-Related Molecules in Cultured Rat Aortic Rings Over Time. Quantification of mRNA copy numbers for indicated genes in rat aortic rings cultured in either control or 3mM (high) phosphate-containing (HP) Medium-199 over time. As initial KW test indicated $p<0.05$ for all genes *post hoc* tests compared all control groups with baseline and control with HP at each time-point. *$p<0.05$; **$p<0.1$; ***$p<0.001$ (all compared with baseline). Data are presented as mean ± SD.

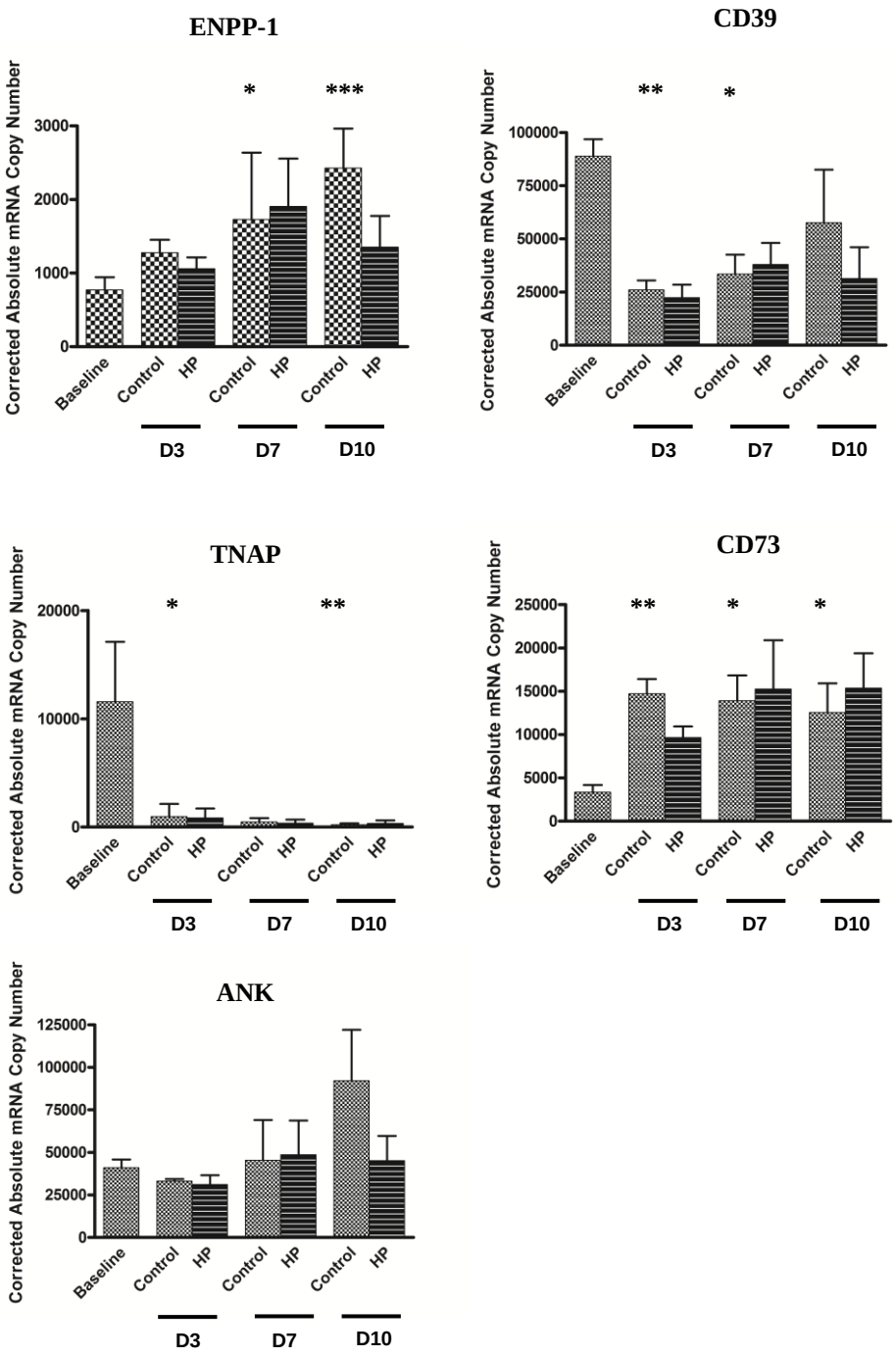

Figure 6.5. mRNA Copy Numbers for ATP Metabolism-Related Molecules in Cultured Rat Aortic Rings Over Time. Quantification of mRNA copy numbers for indicated genes of interest in rat aortic rings cultured in either control or 3mM (high) phosphate-containing (HP) Medium-199 over time. Initial KW test indicated $p<0.05$ for all genes. *Post hoc* tests compared all control groups with baseline and control with HP at each time-point. *$p<0.05$; **$p<0.1$; ***$p<0.001$ all compared with baseline. 'D' designates number of days in culture. Error bars represent mean ± SD. Number of rings per group from left to right = 7,5,5,5,5,5,6.

6.2.2 Studies in human arteries.

6.2.2.i Clinical characteristics.

A total of 15 inferior epigastric artery segments were available for study. Table 6.3 summarises the clinical characteristics for these 15 patients. The average patient age was 47 ± 15 years (range 19-71) and the cohort contained 8 males. All except one patient (patient 2) received a live-donor TP. No patients were diabetic and 3 had a known history of ischaemic heart disease (IHD). In terms of renal replacement therapy, 4 patients were transplanted pre-emptively (including one with a failing graft which had originally been placed before the requirement for dialysis). One further patient was transplanted with their first, failing graft in situ having originally received peritoneal dialysis (PD) for a year. Four patients were on HmD and 6 were receiving PD. At the time of transplantation 6 patients were taking phosphate binders, 2 of which were calcium-based compounds. No patients were taking warfarin.

6.2.2.ii Calcification in arteries from patients with ESRD.

Calcium deposition was detectable with von Kossa staining in 12 out of the 15 samples (80%). Calcification, when present, was most frequently seen as speckled deposits, scattered throughout the medial layer of the vessel wall. Calcification predominantly localised to the outer region of the media with relative sparing of the medial tissue proximal to the arterial lumen. The specks of calcification were associated with ECM fibres rather than with cells (Figure 6.6). In the 12 vessels with positive von Kossa staining, calcification was detectable in at least 50% of the section circumference in 4 samples, 5 arteries had 25-50% of the circumference affected, with the other 3 exhibiting small clusters of speckled calcification in a few discrete areas (Figure 6.6 and Table 6.3). Calcification of the IEL was mainly seen in vessels exhibiting the greatest degree (>50% circumference effected) of medial deposition (Figure 6.6). One sample (patient 8) was an exception to this with only IEL staining detectable. Of note, the cause of ESRD in this patient was enteric hyperoxaluria and nephrocalcinosis necessitating the use of calcium carbonate as treatment.

Patient no.	Gender	Age	Cause of ESRD	RRT modality	Time on RRT	IHD	Phosphate binder	Circumference Calcified	IEL calcification
1	M	46	IgA nephropathy	HmD	1 month	N	N	>50%	Y
2	M	45	IgA nephropathy	TP	14 yr	N	N	>50%	N
3	F	57	unknown	PD	4 yr	N	Sevelamer	25-50%	N
4	F	19	Bilateral nephrectomy for NS	PD/TP	1yr/15yr	N	N	25-50%	N
5	F	60	ADPKD	PD	2yr	N	Lanthanum	0	N
6	M	31	ANCA vasculitis	HmD	1yr	N	N	25-50%	N
7	F	67	Renovascular disease	PD	6 months	N	Lanthanum	>50%	Y
8	F	49	Enteric hyperoxaluria/nephrocalcinosis	HmD	2 yr	N	Calcium	25-50%	Y
9	M	54	IgA nephropathy	PD	2 yr	Y	N	25-50%	N
10	F	33	IgA nephropathy	PD	6 months	N	N	0	N
11	M	61	Membranous nephropathy	N/A	N/A	Y	N	>50%	Y
12	F	45	IgA nephropathy	PD	6 months	N	N	0	N
13	M	35	Renal dysplasia	N/A	N/A	N	Sevelamer	<25%	N
14	M	27	Fabrys disease	N/A	N/A	N	N	<25%	N
15	M	71	Renal tuberculosis	HmD	1 yr	Y	Calcium	<25%	N

Table 6.3. Summary of Patient Characteristics. NS: nephrotic syndrome; ANCA: anti-neutrophil cytoplasmic antibody.

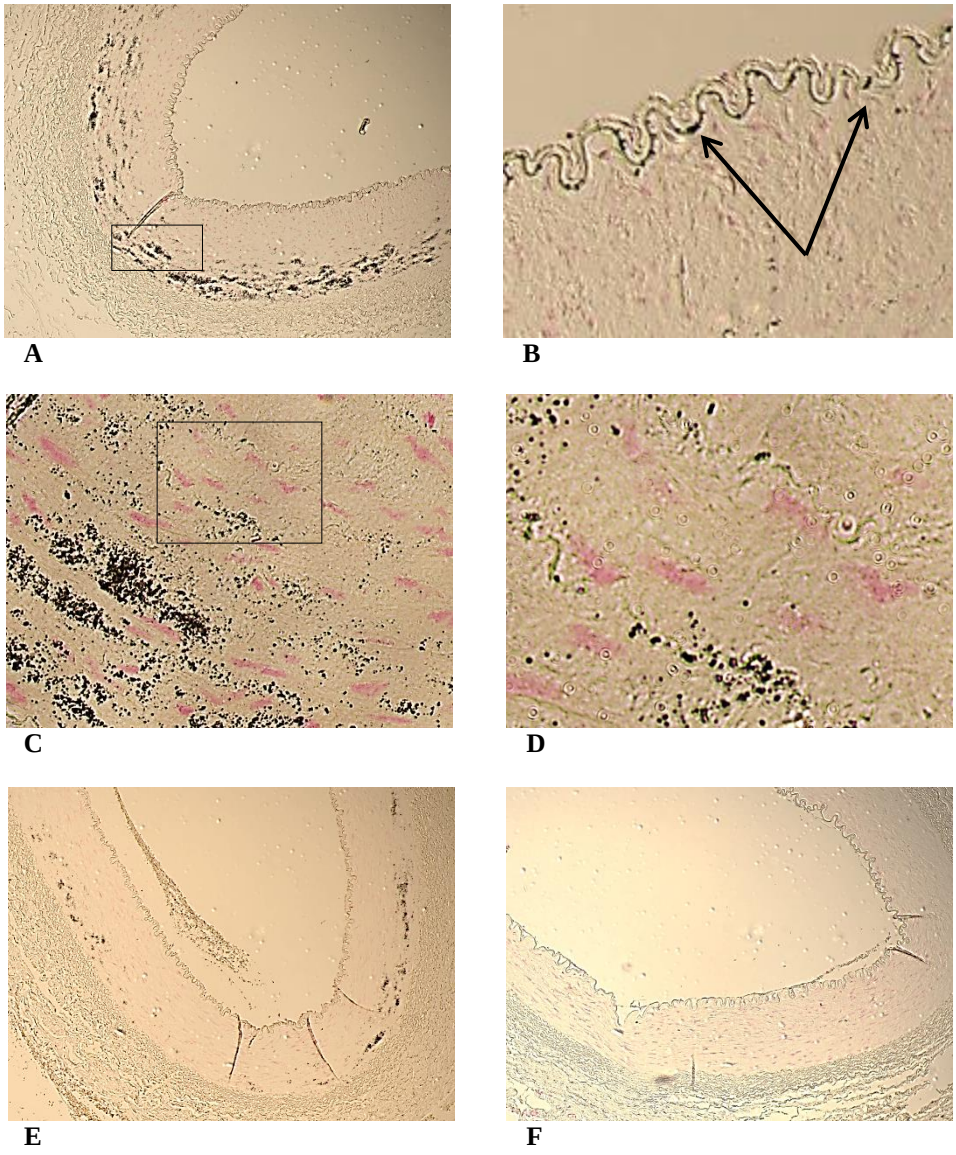

Figure 6.6. Calcium Deposition in Arteries from Patients with ESRD. Sections of human inferior epigastric artery taken at time of kidney transplantation stained with von Kossa reagent to visualise calcium deposits (stained black). A: Extensive calcification involving >50% vessel circumference. B: Digitally magnified image of the luminal surface of the vessel in A showing calcium deposits on the IEL (arrows). C: Higher magnification of the boxed region in A demonstrating the speckled pattern of calcification. D: Digitally magnified image of the boxed region in C demonstrating the association of calcium deposits with ECM. E: A vessel containing less extensive calcification. F: A vessel without calcification. A, E and F: magnification x10. C: magnification x63 (boxed region cropped using Microsoft Office 2010 for image D). All sections counterstained with aluminium red.

The patients without AC were all female. Neither renal replacement therapy vintage or patient age were related to AC in this small cohort - all 4 patients receiving pre-emptive TPs had detectable AC whereas the 3 patients without any vascular calcium deposition had all been on dialysis for at least 6 months. The mean age of the patients without AC was almost identical to those with disease (46 ± 14 vs 47 ± 16 years respectively; p = 0.936). The 3 patients with known IHD all had detectable calcification.

6.2.2.iii Analysis of arterial mRNA expression for ENPP-1 and ANK.

Owing to limited tissue availability, the yield of RNA extracted from human arteries was low. It was therefore only possible to reverse transcribe 100ng for each sample and to evaluate ENPP-1 and ANK mRNA expression. The expression of three housekeeping genes, SDHA, HPRT and RPL13a was quantified and mean copy numbers were 22,280 ± 8161, 18,143 ± 9346 and 871,779 ± 463,771 respectively. RPL13a was the least stable and was therefore not used to generate final corrected copy numbers. In the case of HPRT, 3 technical replicates displayed a standard deviation exceeding 2 cycles, raising concern about the validity of using it as a calibrator gene for this work. It was therefore decided to correct the copy numbers for all genes of interest in 2 ways: using the combination of SDHA/HPRT and SDHA in isolation. One sample (a calcified vessel) showed copy numbers very much lower than the overall mean for all 3 housekeeping genes (e.g. a factor of 10 lower for HPRT) and was excluded from the analyses. Comparisons were made between the 3 un-calcified vessels and all those with calcium deposition.

For quantification of ENPP-1 mRNA expression, one sample from a calcified vessel failed to amplify leaving n=10 in this group. Using the HPRT/SDHA combination to correct copy numbers, mRNA expression in calcified vessels showed a non-significant increase compared with un-calcified tissue (1579 ± 401 vs 3306 ± 3013 for un-calcified vs calcified respectively; p = 0.077). When corrected for SDHA alone, the increase in expression in the calcified samples became statistically significant (1594 ± 513 vs 3526 ± 3025 for un-calcified vs calcified respectively; p = 0.049) (Figure 6.7). There appeared to be 2 outliers in the calcified group – one well above and one well below the group mean (Figure 6.7). Both results were included in

the analysis described above however their exclusion only strengthened the significance of the result (p = 0.012 following removal of these 2 data points).

In contrast to the findings for ENPP-1, expression for ANK mRNA was similar between groups (Figure 6.7). When corrected for HPRT/SDHA mean copy numbers were 86,832 ± 43,301 vs 77,323 ± 19,437 for un-calcified compared with calcified vessels respectively (p = 0.350). Using SDHA alone as the calibrator gene, the corresponding corrected copy numbers were 85,548 ± 41,233 vs 83,000 ± 21,693 (p = 0.436).

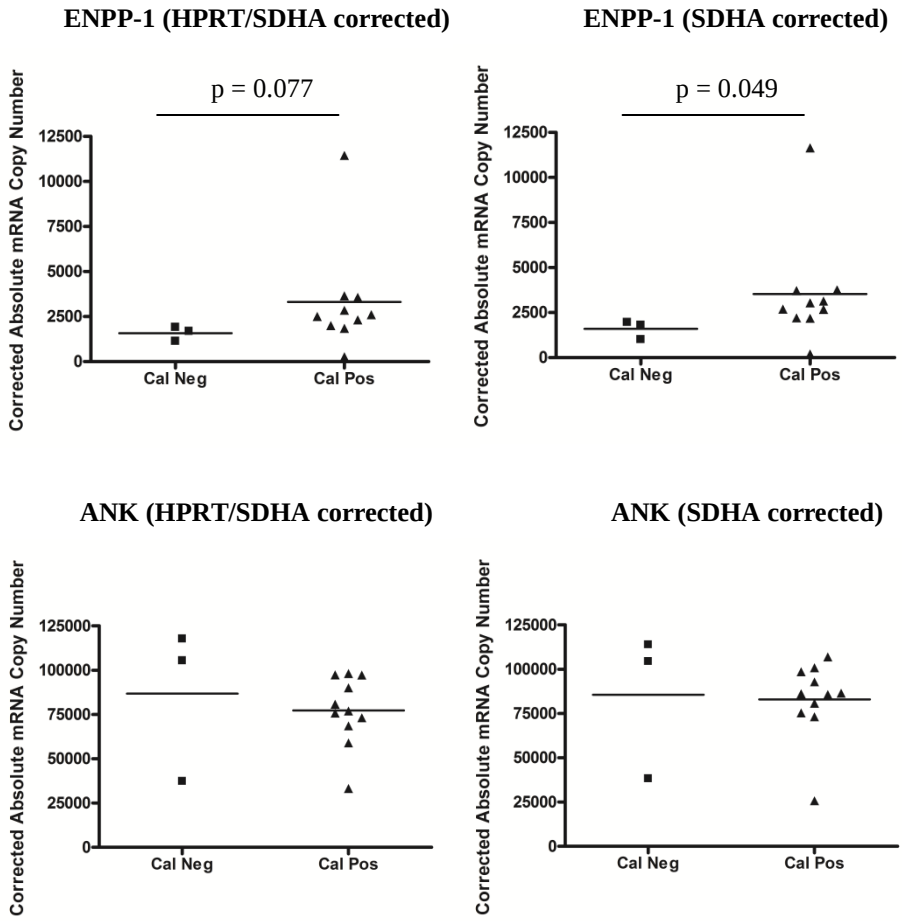

Figure 6.7. Expression of ENPP-1 and ANK mRNA in Arteries from Patients with ESRD. RNA was extracted from segments of inferior epigastric artery obtained at the time of kidney transplantation from patients with ESRD. qPCR assays were performed for the genes indicated Copy numbers of mRNA for each gene were corrected for both the combination of HPRT/SDHA and SDHA alone (see text). Groups compared with MWU test. Each symbol represents one vessel. Horizontal bars represent group means.

6.3 Discussion

The most notable findings from the rat *in vivo* work described in this chapter were that ENPP-1 mRNA expression increased in calcified arteries taken from rodents with CKD and that functional enzyme activity was also elevated in aortas from these animals. As discussed in Chapter 5, because all adenine-fed animals developed calcification of the abdominal aorta, (the section harvested for qPCR experiments), it was impossible to determine whether this increase in mRNA expression was related to the presence of uraemia or the calcium deposition itself. However, the fact that the aortic arch did not calcify in all rats made it possible to evaluate the effect of uraemia in isolation. The results suggest that arterial ENPP-1 activity increases in the setting of CKD even in the absence (or presumably prior to the onset of) calcification.

No up-regulation of ENPP-1 mRNA was seen in calcified rings *in vitro* indicating that under these conditions calcification per se does not induce expression and neither does the presence of an elevated phosphate concentration. However, ENPP-1 mRNA expression did increase in calcified human vessels which were all taken from patients with ESRD suggesting that in the presence of uraemia, calcification is associated with an increase in ENPP-1. A link between ENPP-1 mRNA expression and arterial calcium deposition in the setting of CKD was also suggested by the rat *in vivo* data which implied that the magnitudes of each were directly related. The results from the human tissue analysis are consistent with the rat *in vivo* findings and therefore confirm that the results from the animal experiment are related to calcification rather than a 'model-specific' factor such as adenine.

As ENPP-1 is heavily expressed in bone cells (Johnson *et al* 2000) the increase in expression and activity seen in calcified vessels could be a reflection of VSMC osteogenic transformation. However, given the findings in Chapters 3 and 5, which suggested that this process may not occur to any major extent during the development of AC, it seems an unlikely explanation for the increased ENPP-1 expression. Based on current understanding (Mackenzie *et al* 2012), the main role of ENPP-1 appears to be the generation of PPi and it therefore seems likely that the changes in expression seen in the current work are related to this biological function.

Serum PPi concentrations were not elevated in rodents with AC despite the increase in arterial ENPP-1 activity. In fact, although not statistically significant, if anything a *reduction* was apparent in CKD animals. This is consistent with the suppressed serum PPi that has been detected in patients with renal impairment (Lomashvili *et al* 2005, O'Neill *et al* 2010). At present the tissue source of systemic PPi is unclear but some authors have suggested that bone is likely to be the major contributor (Lomashvili *et al* 2014). The vasculature undoubtedly produces PPi as shown by its presence in medium following aortic ring culture (Lomashvili *et al* 2004). However, whether *in vivo* it is released to a sufficient degree to contribute to systemic levels or only utilised locally is unknown. The results from the current study would suggest that arterial production does not influence serum levels. Whilst impossible to measure, presumably the increase in arterial ENPP-1 activity did result in a greater amount of local PPi production and a fundamental question is therefore what was the fate of this PPi? Potentially it may have been metabolised by TNAP, which would favour the development of calcification, or alternatively perhaps it was generated in an attempt to directly inhibit hydroxyapatite growth, as part of a protective response by the vasculature against ensuing AC.

Which of these 2 apparently opposing hypotheses is more likely has been unwittingly evaluated, albeit under non-uraemic conditions, in a recent report (Lomashvili *et al* 2014). In this study, aortas from WT (calcification-resistant) mice were transplanted into *ENPP-1* KO recipients, (which have minimal circulating PPi and therefore develop spontaneous AC) thereby modelling increased arterial ENPP-1 expression in a 'pro-calcification' systemic environment. Whilst the grafted (WT) aortic segments did calcify, the surrounding vessel (ENPP-1-deficient aorta) calcified to a much greater extent. TNAP activity was equal in both genotypes so could not explain these findings. The data imply that an increase in arterial ENPP-1 (PPi generation) will attenuate local calcium deposition rather than promote it and therefore suggest that the greater enzyme activity detected in calcified vessels in the current study arises as part of a protective response by the vasculature against the calcification-inducing factors present in the uraemic circulation.

CD39 activity results in the formation of 2 phosphate ions (along with AMP) (Figure 1.2) and therefore seemingly provides conditions to favour calcification. Expression

was significantly decreased in adenine-fed rats theoretically limiting the availability of phosphate whilst increasing PPi, both of which also seem to be in keeping with an 'anti-calcification' response. Clearly this increased PPi could be hydrolysed by TNAP and therefore enhance calcification, however if this does represent a pathogenic mechanism it would appear to be a rather redundant and complex way of generating, in effect, the same end-product i.e. phosphate from PPi.

Mutations of the NT5E gene, which encodes the CD73 enzyme, have been shown to be associated with calcification of distal arteries in humans (St Hilaire *et al* 2011) although, as discussed in Chapter 1 (section 1.10.2.ii), the mechanism underlying this finding is not completely understood. CD73 catalyses the conversion of AMP into phosphate and adenosine (Figure 1.2) and it is most plausible that the latter product is the key regulator of calcification in this context (St Hilaire *et al* 2011). Vascular CD73 expression in the setting of CKD-associated AC has not been previously described. However, the increase in CD73 mRNA seen in the current work coupled with the known deleterious effect of genetic deficiency would also be consistent with an adaptive, protective response by arterial cells.

Previous studies have demonstrated an increase in TNAP activity in arteries from both rats (Lomashvili *et al* 2008) and patients (Shroff *et al* 2008) with CKD and so it seems surprising that expression of TNAP mRNA was decreased in calcified rodent vessels in the present work. The study by Lomashvili *et al* (2008) used 2 rodent models of CKD (adenine and 5/6th nephrectomy) and notably AC was not present in any animal. TNAP protein expression and activity were increased in aortas from these rats however mRNA levels were no different from controls indicating that regulation of TNAP is probably mainly post-transcriptional. In the study by Shroff *et al* (2008) examining human tissue, only TNAP activity (not mRNA expression) was measured and notably, in patients with CKD not yet on dialysis, no increase in arterial TNAP activity was apparent despite the presence of early calcium deposition. Activity was increased in patients that were on dialysis. The findings from these 2 studies seem to differ somewhat and the exact role for this protein in the pathogenesis of AC therefore remains to be fully elucidated. Limited tissue availability meant that TNAP activity could not be measured in the present work and because mRNA expression may not reflect functional enzyme activity it is difficult

to interpret the data obtained here. If in fact arterial TNAP activity does reduce in this setting it should result in an elevated local PPi concentration (Figure 1.2) and protect against calcification.

The expression of mRNA for ANK was increased in calcified rodent, but not human vessels. Differences in species and/or the small number of non-calcified human samples are 2 immediately obvious potential reasons for this. However, the changes in expression of the other proteins examined in calcified arteries all seem to favour an elevation in extracellular PPi and so an increase in ANK expression would be consistent with this. Just one previous study (Zhao *et al* 2012) has assessed ANK specifically in the setting of CKD and the authors of this paper concluded that expression of the protein was decreased in rodents and patients with renal impairment. However, it is unclear in this report how many human samples were assessed and the rodent model differed significantly from that used in the current study, involving extensive surgical manipulation of the aorta in order to deliberately induce inflammation.

The results from the ring culture experiment, like those described in Chapter 3, indicated that time in culture alone can significantly influence the mRNA expression profiles for a number of genes in arterial tissue. Again wide standard deviations were seen in most groups, especially for the samples cultured for 10 days, further limiting interpretation. However, it was notable that the presence of an elevated phosphate concentration did not influence the expression of any molecule either before (day 3) or after (days 7 and 10) the appearance of overt calcification. This implies that the alterations in expression seen in calcified vessels *in vivo* are mediated by 'uraemic-specific' factors.

The histological appearance of AC in humans with CKD has only been examined in a small number of previous reports (Shroff *et al* 2008, Shlieper *et al* 2010, O'Neill & Adams 2014). These studies, in keeping with the findings in this chapter, have all reported a speckled, punctate pattern of calcium deposition within the arterial media. Calcification has consistently been shown to be associated with ECM, as was observed in the current work, with variable involvement of the IEL. A notable difference in the present work however was the apparent relative sparing of the inner media from mineral deposition. There is no immediately obvious explanation for this

and in fact some previous studies have specifically commented that, in complete contrast to the findings here, the sub-intimal region of the media was predominantly effected (O'Neill & Adams 2014). This is the first study to analyse inferior epigastric artery specimens in patients with CKD with previous work examining vessels of larger or smaller calibre. It is possible, as suggested by some authors (Schliper 2014), that the mechanisms contributing to AC along with how the disease manifests differ depending on the anatomical site of the vascular bed.

There are a number of limitations to the work reported in this chapter. Owing to limited tissue, with the exception of ENPP-1, protein expression and/or enzyme activity could not be assessed for any of the other molecules examined. In the case of CD39, mRNA expression has been shown to correlate well with enzyme activity in other contexts (Liao *et al* 2010), although whether this holds true for CD73 and ANK is less clear. As discussed above, this does not seem to be the case for TNAP. The number of human samples available for study was low, making it difficult to draw comparisons between calcified and non-calcified vessels. Furthermore, the calcification 'status' of each patient was assessed in a single histological section and it is possible that the staining pattern seen was not representative of the whole vessel. The lack of a non-CKD control group is a further limitation. The low yield of RNA from human tissue made qPCR experiments technically challenging. In particular it was not possible to obtain an RNA integrity number (RIN) for many samples.

6.4 Summary

The work in this chapter has shown for the first time that ENPP-1 expression and activity are increased in calcified arteries from rodents and humans with CKD. This increase appears to begin prior to the onset of calcification but seems to continue as disease progresses and may well be part of a vascular defence mechanism against, as yet unidentified, uraemic-specific factors which induce mineral deposition. Other vascular proteins involved in ATP metabolism also appear to be regulated in this context, possibly in order to protect against increasing calcification. Manipulating certain components of this pathway may potentially offer therapeutic benefit. This concept is expanded upon as part of the general discussion in Chapter 7.

CHAPTER 7 – GENERAL DISCUSSION

7.1 Summary Of Key Findings

The main aim of the work described in this thesis was to answer a fundamental research question: 'Is P2X7R involved in the pathogenesis of CKD-associated AC?'. With respect to addressing this aim the following key findings have emerged:

1. P2X7R is expressed in human and rodent vascular smooth muscle with expression remaining unaltered in the presence of calcification (Chapters 3 & 5).

2. Neither pharmacological blockade nor genetic deletion of P2X7R influence AC *in vitro* (Chapter 3).

3. Pharmacological blockade of P2X7R does not influence AC *in vivo* using the adenine nephropathy model (Chapter 5).

The hypothesis that P2X7R might participate in the pathogenesis of AC was based upon studies linking it, in non-vascular-related contexts, to mechanisms thought to be important in the aetiology of disease (Figure 1.3, re-printed on the following page as an aide memoire). Whilst not a primary aim of this thesis, the work conducted here has made some intriguing observations in regard to some of these previously described 'disease-mediating' pathways:

1. The VSMC-specific markers α-SMA, SM-22 and smoothelin are down-regulated at the mRNA level in calcified arteries *in vivo* (Chapter 5).

2. Arterial expression of mRNA for some classic markers of osteogenic transformation is absent in both *in vitro* and *in vivo* models of AC (Chapters 3 & 5).

3. Expression of mRNA for the apoptosis marker caspase-3 is up-regulated in calcified arteries *in vivo* but not *in vitro* (Chapters 3 & 5).

4. None of these changes in mRNA expression are influenced by P2X7R blockade *in vivo*.

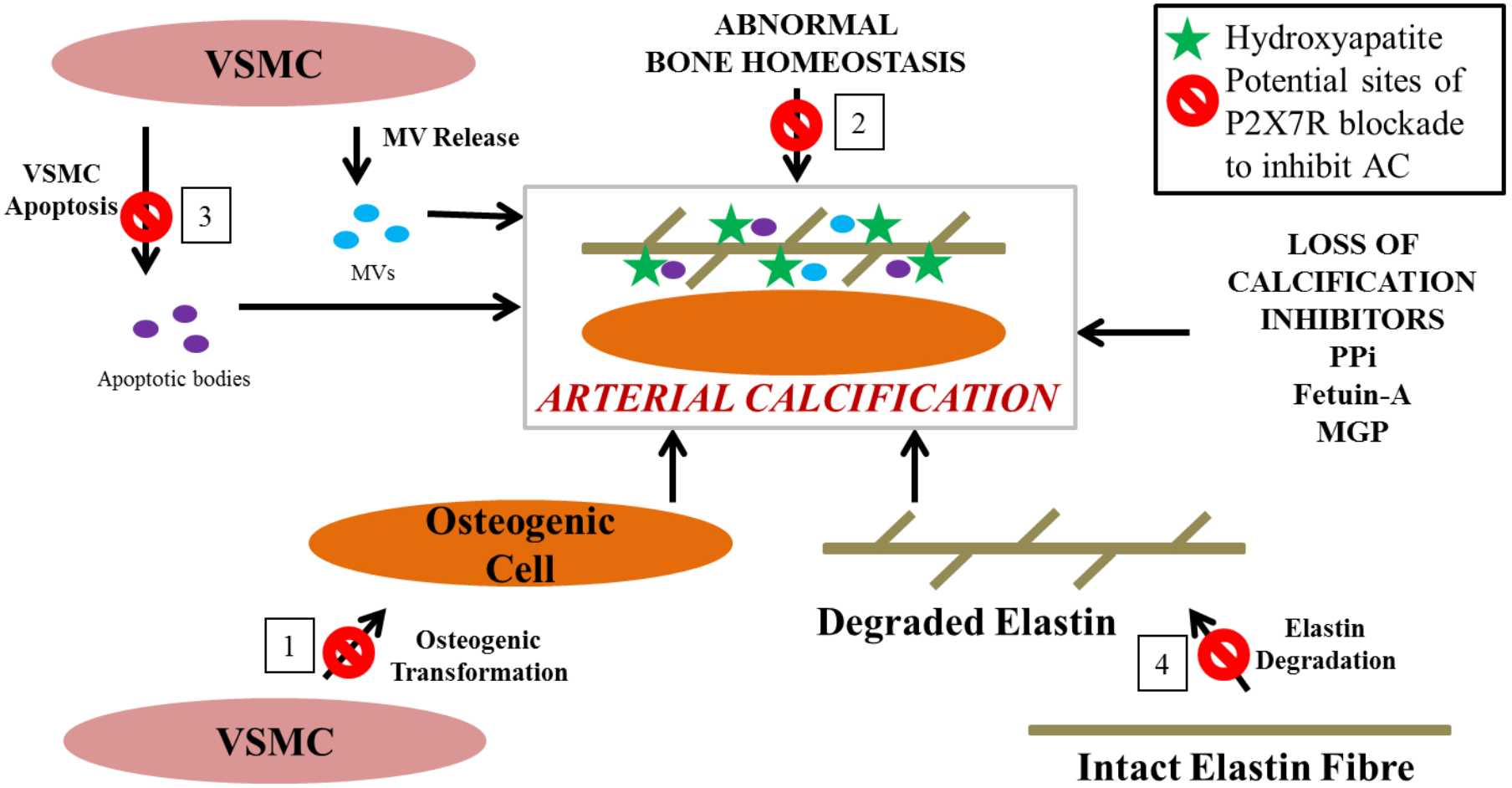

Figure 1.3. Pathogenic Pathways of AC Potentially Modifiable by P2X7R Blockade. Blockade of P2X7R might potentially attenuate AC by: 1. Inhibiting VSMC osteogenic transformation. 2. Maintaining systemic bone health. 3. Preventing VSMC apoptosis. 4. Limiting elastin degradation. In addition P2X7R blockade might prevent the progression of CKD in general (not shown, see text). PPi: inorganic pyrophosphate; MGP: matrix gla protein

Studies in the latter parts of this thesis (Chapter 6) moved away from P2X7R directly to focus on arterial ATP-metabolic pathways. Time constraints permitted some preliminary studies to be conducted to assess whether there are changes in expression profiles of components of this system associated with AC. The following novel findings emerged:

1. ENPP-1 mRNA expression and activity are increased *in vivo* in calcified rodent arteries.

2. ENPP-1 mRNA expression is increased in calcified arteries from patients with ESRD.

3. Calcified rodent arteries *in vivo* have increased expression of CD73 and ANK mRNA while expression of mRNA for CD39 and TNAP decreases.

4. Phosphate and/or the presence of calcification *per se* do not appear to mediate the changes in gene expression profiles observed *in vitro*.

7.2 P2X7R And Arterial Calcification

The overarching impression from the work conducted in this thesis is that P2X7R is not involved in the pathogenesis of AC. A number of diverse experimental systems were used to evaluate the receptor in this context but none of the data obtained suggested that it participates in mediating disease. However, to our knowledge, this work represents the first set of experiments specifically designed to assess the role of P2X7R in AC and therefore before concluding that the receptor is not involved in the evolution of disease, whether or not the original hypothesis has been adequately tested needs to be considered.

The potential relationship between P2X7R and AC was investigated robustly *in vitro*. *Ex vivo* studies in which rodent vessels were treated with high-dose, receptor-specific pharmacological agents (antagonists and agonists) in the presence/absence of calcification-promoting medium, culture of arteries from receptor-deficient mice and *in vitro* studies with primary VSMCs were performed, representing a comprehensive array of experimental strategies. Cellular deficiency of P2X7R could also have been assessed using interfering RNA methodology but as discussed in detail in Chapter 3, experiments using primary VSMCs in culture were abandoned

early on in favour of the ring culture model and the studies on cultured tissue from $P2X7^{-/-}$ mice should have achieved the same objective.

Although the majority of available *in vitro* methods were used in this thesis to try and address the primary research question, whether these models are actually suitable for examining the pathogenesis of CKD-associated AC is debatable. Failing to mimic a uraemic milieu and, as demonstrated here with the *ex vivo* model and previously with cultured VSMCs (Nakano-Kurimoto *et al* 2009), the induction of changes in gene expression with or without the addition of 'calcification-enhancing' reagents, are major disadvantages common to both primary cell- and arterial ring-based systems. The absence of intact elastin fibres, the initial sites of calcium deposition (Lanzer *et al* 2014, O'Neill & Adams 2014), is another major limitation of studies using cultured VSMCs. How translatable any findings from experiments using these models are to human disease therefore remains uncertain.

From these perspectives it might be seen that *in vivo* experiments are preferable. As discussed in Chapter 5, to investigate AC *in vivo*, especially when assessing a potential therapeutic intervention, the adenine nephropathy model is superior to the alternative options of using either the Cy/+ rat or $5/6^{th}$ nephrectomy as calcification is much more consistent and develops over weeks rather than months (Shobeiri *et al* 2010, Neven & D'Haese 2011). However, the question remains, how closely does this adenine-based system really resemble the human disease it is trying to mimic?

In general, the main benefits of animal work in this context are that calcified arteries will have been exposed to circulating 'uraemic toxins' and vessels are surrounded by their usual biological environment. Other relevant biochemical disturbances such as elevated PTH and FGF-23 and decreased vitamin D will also be present (Neven *et al* 2010). In terms of the renal lesion, adenine overload in rats results in a similar histological appearance to that seen in patients with APRT deficiency, the enzyme responsible for adenine metabolism (Hori & Henderson 1966). This rare condition is associated with renal calculi, interstitial fibrosis and progression to ESRD if untreated (Bollee *et al* 2010, Monico *et al* 2012). However, whether mineral-bone disorder is particularly severe in these patients is unknown.

One notable feature of the rat experiment described in Chapter 5 was the extremely high serum concentration of phosphate in most animals. The normal serum concentration of phosphate in Wistar rats is reported to be around 2mmol/l (Baxter *et al* 2000, Tripathi *et al* 2013). In rats treated with adenine in this thesis, serum phosphate concentrations were often in the order of 7-8mmol/l and occasionally as high as 9mmol/l i.e. over 4 times the normal value. Serum phosphate levels of this relative order are never seen in man. In clinical practice the highest serum phosphates generally occur in acute settings, typically within the contexts of tumour lysis syndrome (McBride & Westervelt 2012) or rhabdomyolysis (Efstratiadis *et al* 2007). For illustrative purposes, possibly the highest serum phosphate on record was documented by Bywaters & Beall (1941) when describing the clinical progression of traumatic crush injuries during the Blitz. The serum phosphate at the time of death in one patient is recorded at just over 4mmol/l (about 3 times the upper limit of normal).

As continually referred to throughout this work, the current conceptualisation of AC (and indeed the fundamental principle on which this thesis is centred), is that it does not occur simply due to the passive deposition of mineral in the arterial wall. In further support of this theory, calcium and phosphate, when added simultaneously to human plasma even at the upper limit of concentrations seen in acute disease states, do not precipitate out (O'Neill 2007). This study by O'Neill suggested that a calcium x phosphate product of above 16mmol/l^2 would be required for mineral to become insoluble in human serum - this is still around double the level of what might possibly be seen in patients with profoundly disturbed calcium and phosphate homeostasis i.e. this situation is unlikely to ever occur in man and therefore other mechanisms must be in play for AC to develop. Whether the findings in this study are translatable back to rodents is uncertain, however it seems plausible that elevations in calcium and in particular phosphate, to the extent seen in rat models of CKD, could result in extensive 'passive' arterial mineral deposition. Clearly 'non-passive' mechanisms (e.g. changes in VSMC gene expression profiles and levels of calcification inhibitors) will be present concurrently, as shown by the current work and numerous previous studies (Price *et al* 2006, Lomashvili *et al* 2009, Neven *et al* 2010), thereby still permitting inferences to be made about mechanistic pathways involved in the development of disease. However, a substantial calcification burden

resulting from passive mineral precipitation could well overwhelm and mask the effect of any intervention targeting 'cell-mediated' pathological pathways.

When considering how well the role of P2X7R was assessed in this work, it also needs to be evaluated how well receptor ligation was achieved in the studies performed. No firm conclusions could be drawn from the experiments with $P2X7^{-/-}$ mice due to a surprisingly low number of animals developing AC. This meant that the only available way to practically examine the effect of suppressed receptor activity *in vivo* was to pharmacologically block it, in the rat adenine model. Although the result of this study strongly suggested that P2X7R blockade does not impact on the pathogenesis of AC there were, as discussed extensively in Chapter 5, a number of limitations to the experiment. It could therefore be argued that there remains an element of uncertainty relating to the involvement of the receptor in this disease process and it is worth considering how the negative findings relating to P2X7R and AC described in this thesis might be confirmed.

P2X7R KO rats are not currently available but would be a useful tool in the future should they be developed. In the meantime, if using a rat model, receptor ligation would need to be achieved by pharmacological blockade. Probably the most obvious refinement to the experiment conducted in this thesis (Chapter 5) would be to administer the drug by a different route e.g. an implantable delivery system. This method of dosing would also open up the option of employing the 2 alternative ($5/6^{th}$ nephrectomy and Cy/+) rat CKD-AC models, as long term administration of the drug would be possible (AC takes months to develop in these two models (Neven *et al* 2011)). However, as alluded to in Chapter 5, this would require extensive optimisation of the drug for it to become feasible.

The mouse $5/6^{th}$ nephrectomy model (El-Abbadi *et* al 2009) could be employed to examine WT and KO mice but is likely to need an extended operator training period and result in a high loss of animals. An alternative would be to attempt further refinement of the adenine mouse model developed in this thesis (Chapter 4) in order to obtain more consistent disease and less animal morbidity. Potential modifications might include titration of the adenine, protein, phosphate and calcium contents of the diet and/or changing the mode of adenine administration – both ip injection and delivery in an oral suspension have been described in rat studies (Forbes 1971, Terai

et al 2009). In addition, this thesis focussed mainly on DBA/2 mice as this strain was employed by the Giachelli lab in their description of the 5/6th nephrectomy model (El-Abbadi *et al* 2009). However, the C3H strain is also described to be prone to ectopic calcification (Eaton *et al* 1978) and it would be interesting to assess the effect of these interventions in animals on this background. Finally, the work in this thesis examined the propensity of 2 agents, folic acid and adenine, to induce CKD and AC but there are numerous other 'chemical' agents available which can cause marked renal fibrosis in mice. Examples include cyclosporine (Bing *et al* 2006) and aristolochic acid (Huang *et al* 2013) and it would therefore be informative to combine these agents with high phosphate feeding to assess whether AC develops.

Given the limitations of the animal models, it might be preferable to directly assess P2X7R within the context of human CKD-associated AC. Unfortunately the number of human vessels available for study in this thesis was low (n=15), thereby limiting the number of experiments that could be undertaken with them. With a larger sample size and tissue yield it would become possible to perform a range of complementary laboratory techniques, to examine receptor expression in calcified and non-calcified vessels. It would clearly also be advantageous to obtain control tissue from healthy donors for comparison. However, whilst studies of this nature can be useful, they cannot provide information concerning causality of a particular disease or the chronology of contributing biological processes.

One method of investigating a potential link between P2X7R and AC in humans with CKD might be to assess whether SNPs that alter receptor function associate with disease severity. Whilst possible, major barriers would need to be overcome before performing such an analysis. Firstly, whilst a number of P2X7R SNPs are described, many have minor allele frequencies of less than 5% (Wiley *et al* 2011, Gartland *et al* 2012). Therefore a large patient cohort would be required to detect any association with disease. Secondly, one would need to consider how to detect arterial calcium deposition within the vessel media in these subjects. In practical terms this would probably need to be achieved using radiological methods, however plain X-rays and CT scanning cannot reliably discriminate between intimal and medial calcification (Sigrist *et al* 2007, Marinelli *et al* 2013). Newer generation ultrasound machines can distinguish between the two locations in superficial vessels such as

femoral, carotid and brachial arteries (Coll *et al* 2011) but evaluating calcification in more central sites such as the abdominal aorta or coronary arteries may be less straightforward. Finally, coronary artery calcification is now usually measured in terms of an Agatston score (Agatston *et al* 1990). This is a well-validated clinical tool permitting a quantifiable assessment of disease progression. However at present, and as commented on by some authors (Vezzoli *et al* 2014), no such method exists for gauging the extent of ultrasonically detected calcification in peripheral arteries. Defining 'progression of AC' in this setting therefore becomes problematic.

In summary, the results in this thesis do not support a role for P2X7R in the pathogenesis of CKD-associated AC. The role of the receptor in mediating disease has been evaluated rigorously within the limitations of the available experimental models. Optimisation and/or development of superior experimental systems to study this disease process will be required in order to definitively confirm redundancy of P2X7R in this clinical context. Studies in man are feasible but may first require resolution of some logistical, practical and technical issues.

7.3 Vascular ATP Metabolic Pathways And Arterial Calcification

Whilst the work described in Chapters 3-5 was aimed at testing a central hypothesis (i.e. that P2X7R mediates AC), the work in Chapter 6 was more 'hypothesis generating', as it was conducted as a preliminary exercise to assess the expression of enzymes involved in ATP-metabolism in normal and uraemic, calcified arteries. The findings from these experiments are both novel and intriguing, possibly in keeping with an adaptive, defensive response by the vasculature against persistent uraemia and subsequent calcium deposition. It should therefore now be considered what steps are required to prove or refute this hypothesis and, in addition, what the future implications may be.

The most relevant function of the ATP-metabolising system in relation to AC is the regulation of extracellular PPi. All components of this pathway can seemingly influence the level of this molecule either directly or indirectly – ENPP-1 and TNAP by direct generation and hydrolysis respectively (Terkeltaub 2001, Murshed *et al* 2005), ANK by transmembrane transport (Terkeltaub 2001) and CD39 by regulating the amount of ATP available for ENPP-1 (Kaczmarek *et al* 1996) (Figure 1.2). The

relationship between ENPP-1, TNAP and ANK in determining local PPi concentration has been shown to be critically important in relation to skeletal bone formation (Harmey *et al* 2004) and a similar situation may well occur in the vasculature regarding AC. Given these observations, a key piece of information required is how the function of each of these proteins changes in CKD and moreover, how these changes relate to each other in terms of time and function. In the current work, the activity of only one enzyme, ENPP-1, was examined. Therefore the effect of both uraemia alone and subsequent calcification needs to be confirmed for all components of this pathway in a larger sample size. To this end it might be preferable to employ the $5/6^{th}$ nephrectomy model of disease as it is likely to result in a greater number of animals with renal impairment that do not develop AC as compared with the adenine model (Neven & D'Haese 2011) thereby permitting a better evaluation of the effect of uraemia in isolation. This would also serve to exclude any change in these enzymes specifically induced by adenine. Studies on human vessels will also be valuable in terms of establishing the net changes in expression but in practical terms are unlikely to be helpful in assessing the time-course of events. When this information is obtained, future research aiming to examine any individual component of this system in the context of CKD will need to ensure that appropriate expression profiles of all other proteins in this pathway are present in order to draw translatable conclusions.

ENPP-1 deficiency is unquestionably associated with arterial calcium deposition. Rare human conditions such as GACI (Rutsch *et al* 2003), Pseudoxanthoma elasticum (Nitschke *et al* 2012) and Cole disease (Eytan *et al* 2013), all of which have ectopic calcification as part of the disease phenotype, can arise due to mutations in the *ENPP-1* gene. It might therefore intuitively seem that an increase in enzyme activity, as observed in this work in uraemic subjects, would be protective. However, mutations in this gene can also cause ARHR (Levy-Litan *et al* 2010), a disease of *deficient* skeletal mineralisation, so the situation is far from straightforward. Very few studies have examined the expression of ENPP-1 in relation to AC, but those that have been published differ somewhat in their findings. Nitschke *et al* (2011) found decreased expression in human carotid artery calcified atherosclerotic plaques, whereas Cote *et al* (2012a) reported an increased expression in human calcified aortic valves. These studies examined pathologies slightly removed from medial AC

and were performed in non-uraemic patients. However, taken together all these observations illustrate the complexity of ENPP-1 in this clinical context and emphasise the need for further work to better understand its exact role, especially in relation to CKD.

How might the functional effect of increased ENPP-1 activity be investigated experimentally? One approach might be to compare arterial ENPP-1 overexpression with WT tissue in uraemic, pro-calcifying conditions. ENPP-1 has been successfully overexpressed in a number of sites in mice including liver, muscle, brain and adipose tissue (Maddux *et al* 2006, Pan *et al* 2011). Arterial expression was not commented on in these reports. The obvious barrier to overcome in employing this methodology *in vivo* is finding a suitable CKD-AC model, the potential options for which have been discussed above. As an alternative, it would be interesting to assess whether in the *ex vivo* model, the addition of uraemic serum to the culture medium might better simulate *in vivo* conditions compared with just the addition of supplementary phosphate as used in this thesis. Supplementing culture medium with uraemic serum has been previously employed to examine other factors thought to influence AC in the context of uraemia (Lomashvili *et al* 2008, Kramann *et al* 2011).

There are currently limited alternative options for directly examining the effect of increased ENPP-1 activity. In man, SNPs of the *ENPP-1* gene are generally 'loss-of function' and although putative 'gain-of-function' mutations are described these are thought not to interfere with the catalytic site of the protein (Terkeltaub 2006). Pharmacological activators of the enzyme are not yet available as the molecular structure has only recently been determined (Kato *et al* 2012). Primary cells could be directly genetically manipulated to overexpress the protein but subsequent experiments will be limited and their translational relevance questionable, as alluded to throughout this thesis. As an indirect strategy, the response of increasing the substrate (i.e. ATP) for the enzyme could be examined, although it would need to be confirmed that subsequent metabolism of the nucleotide was occurring via ENPP-1 and not via alternative pathways (such as CD39). Possibly the easiest way to ensure these criteria are met would be to conduct experiments using CD39-deficient vessels, in parallel with suitable control tissue.

If ENPP-1 is up-regulated as a protective response against uraemic toxins and ensuing arterial calcium deposition it might point towards CKD being a state of 'relative PPi deficiency'. This concept is supported by *in vivo* studies which have prevented the development of AC in uraemic animals by direct administration of PPi (O'Neill *et al* 2011, Riser *et al* 2011). However, there is a question as to whether this relative deficiency is because PPi is all hydrolysed by TNAP or because it is all incorporated into the expanding hydroxyapatite. Alternatively, do uraemic conditions perhaps render ENPP-1 less efficient at producing PPi or even cause PPi to be less efficient at preventing calcification? It is also unclear what exactly is regulating the altered expression and activity of ENPP-1 (and other enzymes). Answering these questions may provide insight into the regulation of the calcification process overall and indicate some potential therapeutic targets.

If the aim of future therapy does prove to be attenuating a relative deficiency of PPi, it is worth speculating on the potential options. Bisphosphonates, which are analogues of PPi, prevent AC in uraemic rodents (Price *et al* 2006) and improve the prognosis in GACI (Rutsch *et al* 2008). However, these agents are likely to result in disrupted bone homeostasis in the setting of CKD (Lomashvili *et al* 2009) and are also directly nephrotoxic (Perazella & Markowitz 2008) thus limiting their use in this setting. PPi itself reduces AC in rodents, but has a very short half-life if given orally (Schibler *et al* 1968) and this would seem to restrict its use clinically. However, it is unknown how much PPi is deposited within the vessel wall (the actual target site) and, in addition, the bioavailability of PPi can be increased by ip administration (O'Neill *et al* 2011). Further research into the pharmacology of this agent is therefore needed but there is reason to be optimistic about its potential therapeutic use in the future. Some work has been conducted *in vitro* to determine whether TNAP inhibitors might be a useful treatment strategy by minimising PPi breakdown (Narisawa *et al* 2007). These drugs were effective at attenuating calcification in these models but *in vivo* analysis is clearly required as there may well be undesired side-effects of these agents, particularly relating to bone homeostasis.

Might increasing PPi production be an option? An inhibitor of CD39 would theoretically increase the available ATP for ENPP-1 production of PPi. Of interest, the ecto-ATPase inhibitor ARL67156, which has been shown to suppress the activity

of both CD39 and ENPP-1 (Levisque *et al* 2007), attenuated aortic calcification in warfarin-treated rats (Cote *et al* 2012b). However, this study by Cote *et al* is intriguing in that it failed to detect expression of CD39 mRNA in the vasculature (in complete contrast to the present study and others (Behdad *et al* 2009, Villa-Bellosta *et al* 2011a) where this enzyme was found to be extremely abundant). These findings therefore clearly need to be confirmed with a detailed assessment of the mechanisms involved. Finally, as a speculative and theoretical concept, enzyme replacement therapy is used in conditions such as Fabry's disease to correct deficiencies of proteins vital to maintain normal physiology (Rozenfeld & Neumann 2011). Perhaps in the future, if supported by research, it might be possible to develop and administer recombinant ENPP-1 in the hope of preventing, or slowing the progression of, AC in patients with CKD.

7.4 Conclusion

Arterial calcium deposition occurring in the setting of CKD is a complex, likely multifactorial process. Current experimental models to study the pathophysiology of this condition have a number of limitations and may not closely simulate human disease, making it difficult to draw consistent conclusions. P2X7R does not appear to be a mediator of CKD-associated AC however improved models are required to confirm this. The arterial expression of enzymes involved in the metabolism of ATP does seem to change in AC and future work should focus on gauging the clinical relevance of this in order to better understand the mechanisms underlying the disease and potentially develop new therapeutic interventions.

PUBLICATIONS AND PRESENTATIONS

Peer reviewed publications:

1. **Fish, R.S.**, Klootwijk, E., Tam, F.W., Kleta, R., Wheeler, D.C., Unwin, R.J. and Norman, J. (2013). ATP and Arterial Calcification. *European Journal of Clinical Investigation*, 43(4), pp.405-412.

Presentations:

1. **Richard S. Fish**, Peter Gilmour, Frederick W.K. Tam, David C. Wheeler, Jill T. Norman, Robert J. Unwin. Pharmacological blockade of the ATP-sensitive P2X7 receptor does not influence the progression of experimental arterial calcification.

   Poster presentation at 2014 UK Renal Association Conference, Glasgow.

   Awarded 'Best Poster In Group'.

2. **Richard S. Fish.** Development and Evaluation of Novel Mouse Models of Chronic Kidney Disease Associated Arterial Calcification.

   Oral presentation at 2013 Royal Society of Medicine President's Prize Meeting (Nephrology Section).

3. **Richard S. Fish**, Frederick W.K. Tam, David C. Wheeler, Jill T. Norman, Robert J. Unwin. Female DBA/2 mice have relative resistance to folic acid induced acute kidney injury.

   Poster presentation at 2013 UK Renal Association Conference, Bournmouth.

REFERENCES

Adinolfi, E., Cirillo, M., Woltersdorf, R., Falzoni, S., Chiozzi, P., Pellegatti, P., Callegari, M.G., Sandona, D., Markwardt, F., Schmalzing, G. and Di Virgilio, F. (2010). Trophic activity of a naturally occurring truncated isoform of the P2X7 receptor. *The FASEB Journal*, 24(9), pp.3393-3404.

Adirekkiat, S., Sumethkul, V., Ingsathit, A., Domrongkitchaiporn, S., Phakdeekitcharoen, B., Kantachuvesiri, S., Kitiyakara, C., Klyprayong, P. and Disthabanchong, S. (2010). Sodium thiosulfate delays the progression of coronary artery calcification in haemodialysis patients. *Nephrology Dialysis Transplantation*, 25(6), pp.1923-1929.

Adragao, T., Herberth, J., Monier-Faugere, M.C., Branscum, A., Ferreira, A., Frazao, J.M., Dias Curto, J. and Malluche, H.H. (2009). Low bone volume-a risk factor for coronary calcifications in hemodialysis patients. *Clinical Journal of the American Society of Nephrology*, 4(2), pp.450-455.

Adrogue, H.J., Frazier, M.R., Zeluff, B. and Suki, W.N. (1981). Systemic calciphylaxis revisited. *American Journal of Nephrology*, 1(3-4), pp.177-183.

Agatston, A.S., Janowitz, W.R., Hildner, F.J., Zusmer, N.R., Viamonte, M.Jr. and Detrano, R. (1990). Quantification of coronary artery calcium using ultrafast computed tomography. *Journal of the American College of Cardiology*, 15(4), pp.827-832.

Agrawal, A., Buckley, K.A., Bowers, K., Furber, M., Gallagher, J.A. and Gartland, A. (2010). The effects of P2X7 receptor antagonists on the formation and function of human osteoclasts in vitro. *Purinergic Signalling*, 6(3), pp.307-315.

Aikawa, E., Aikawa, M., Libby, P., Figueiredo, J.L., Rusanescu, G., Iwamoto, Y., Fukuda, D., Kohler, R., Shi, G.P., Jaffer, F.A. and Weissleder, R. (2009). Arterial and aortic valve calcification abolished by elastolytic cathepsin S deficiency in chronic renal disease. *Circulation*, 119(13), pp.1785-1794.

Allison, M.A., Criqui, M.H. and Wright, C.M. (2004). Patterns and risk factors for

systemic calcified atherosclerosis. *Arteriosclerosis, Thrombosis, and Vascular Biology*, 24(2), pp.331-336.

Amann, K. (2008). Media calcification and intima calcification are distinct entities in chronic kidney disease. *Clinical Journal of the American Society of Nephrology*, 3(6), pp.1599-1605.

Ameer, O.Z., Salman, I.M., Avolio, A.P., Phillips, J.K. and Butlin, M. (2014). Opposing changes in thoracic and abdominal aortic biomechanical properties in rodent models of vascular calcification and hypertension. *American Journal of Physiology-Heart and Circulatory Physiology*, 307(2), pp.H143-151.

Anderson, H.C., Harmey, D., Camacho, N.P., Garimella, R., Sipe, J.B., Tague, S., Bi, X., Johnson, K., Terkeltaub, R. and Millan, J.L. (2005). Sustained osteomalacia of long bones despite major improvement in other hypophosphatasia-related mineral deficits in tissue nonspecific alkaline phosphatase/nucleotide pyrophosphatase phosphodiesterase 1 double-deficient mice. *The American Journal of Pathology*, 166(6), pp.1711-1720.

Arch, J.R. and Newsholme, E.A. (1978). Activities and some properties of 5'-nucleotidase, adenosine kinase and adenosine deaminase in tissues from vertebrates and invertebrates in relation to the control of the concentration and the physiological role of adenosine. *The Biochemical Journal*, 174(3), pp.965-977.

Asci, G., Ok, E., Savas, R., Ozkahya, M., Duman, S., Toz, H., Kayikcioglu, M., Branscum, A.J., Monier-Faugere, M.C., Herberth, J. and Malluche, H.H. (2011). The link between bone and coronary calcifications in CKD-5 patients on haemodialysis. *Nephrology Dialysis Transplantation*, 26(3), pp.1010-1015.

Baigent, C., Burbury, K. and Wheeler, D. (2000). Premature cardiovascular disease in chronic renal failure. *The Lancet*, 356(9224), pp.147-152.

Baigent, C., Landray, M.J., Reith, C., Emberson, J., Wheeler, D.C., Tomson, C., Wanner, C., Krane, V., Cass, A., Craig, J., Neal, B., Jiang, L., Hooi, L.S., Agodoa, L., Gaziano, M., Kasiske, B.b Walker, R., Massy, Z.A., Feldt-Rasmussen, B., Krairittichai, U., Ophascharoensuk, V., Fellstrom, B., Holdaas,

H., Tesar, V., Wiecek, A., Grobbee, D., de Zeeuw, D., Gronhagen-Riska, C., Dasqupta, T., Lewis, D., Herrington, W., Mafham, M., Majoni, W., Wallendszus, K., Grimm, R., Pedersen, T., Tobert, J., Armitage, J., Baxter, A., Bray, C., Chen, Y., Chen, Z., Hill, M., Knott, C., Parish, S., Simpson, D., Sleight, P., Young, A. and Collins, R. (2011). The effects of lowering LDL cholesterol with simvastatin plus ezetimibe in patients with chronic kidney disease (Study of Heart and Renal Protection): a randomised placebo-controlled trial. *The Lancet*, 377(9784), pp.2181-2192.

Baigent, C., Keech, A., Kearney, P.M., Blackwell, L., Buck, G., Pollicino, C., Kirby, A., Sourjina, T., Peto, R., Collins, R. and Simes, R. (2005). Efficacy and safety of cholesterol-lowering treatment: prospective meta-analysis of data from 90 056 participants in 14 randomised trials of statins. *The Lancet*, 366, pp.1267-78.

Barreto, D.V., Barreto, F.de C., Carvalho, A.B., Cuppari, L., Draibe, S.A., Dalboni, M.A., Moyses, R.M., Neves, K.R., Jorgetti, V., Miname, M., Santos, R.D. and Canziani, M.E. (2008). Association of changes in bone remodeling and coronary calcification in hemodialysis patients: a prospective study. *American Journal of Kidney Diseases*, 52(6), pp.1139-1150.

Basalyga, D.M., Simionescu, D.T., Xiong, W., Baxter, B.T., Starcher, B.C. and Vyavahare, N.R. (2004). Elastin Degradation and Calcification in an Abdominal Aorta Injury Model Role of Matrix Metalloproteinases. *Circulation*, 110(22), pp.3480-3487.

Baxter, J., Shimizu, F., Takiguchi, Y., Wada, M. and Yamaguchi, T. (2000). Effect of iron (III) chitosan intake on the reduction of serum phosphorus in rats. *Journal of Pharmacy and Pharmacology*, 52(7), pp.863-874.

Bechtel, W., McGoohan, S., Zeisberg, E.M., Muller, G.A., Kalbacher, H., Salant, D.J., Muller, C.A., Kalluri, R. and Zeisberg, M. (2010). Methylation determines fibroblast activation and fibrogenesis in the kidney. *Nature Medicine*, 16(5), pp.544-550.

Behdad, A., Sun, X., Khalpey, Z., Enjyoji, K., Wink, M., Wu, Y., Usheva, A. and Robson, S.C. (2009). Vascular smooth muscle cell expression of ectonucleotidase

CD39 (ENTPD1) is required for neointimal formation in mice. *Purinergic Signalling*, 5(3), pp.335-342.

Bergfeld, G.R. and Forrester, T. (1992). Release of ATP from human erythrocytes in response to a brief period of hypoxia and hypercapnia. *Cardiovascular Research*, 26(1), pp.40-47.

Bianchi, B.R., Lynch, K.J., Touma, E., Niforatos, W., Burgard, E.C., Alexander, K.M., Park, H.S., Yu, H., Metzger, R., Kowaluk, E., Jarvis, M.F. and van Biesen, T. (1999). Pharmacological characterisation of recombinant human and rat P2X receptor subtypes. *European Journal of Pharmacology*, 376(1-2), pp.127-138.

Bing, P., Maode, L., Li, F. and Sheng, H. (2006). Expression of renal transforming growth factor-beta and its receptors in a rat model of chronic cyclosporine-induced nephropathy. *Transplantation Proceedings*, 38(7), pp.2176-2179.

Block, G.A., Martin, K.J., de Francisco, A.L., Turner, S.A., Avram, M.M., Suranyi, M.G., Hercz, G., Cunningham, J., Abu-Alfa, A.K., Messa, P., Coyne, D.W., Locatelli, F., Cohen, R.M., Evenepoel, P., Moe, S.M., Fournier, A., Braun, J., McCary, L.C., Zani, V.J., Olson, K.A., Drueke, T.B. and Goodman, W.G. (2004). Cinacalcet for secondary hyperparathyroidism in patients receiving hemodialysis. *New England Journal of Medicine*, 350(15), pp.1516-1525.

Block, G.A., Spiegel, D.M., Ehrlich, J., Mehta, R., Lindbergh, J., Dreisbach, A. and Raggi, P. (2005). Effects of sevelamer and calcium on coronary artery calcification in patients new to hemodialysis. *Kidney International*, 68(4), pp.1815-1824.

Block, G.A., Wheeler, D.C., Persky, M.S., Kestenbaum, B., Ketteler, M., Spiegel, D.M., Allison, M.A., Asplin, J., Smits, G., Hoofnagle, A.N., Kooienga, L., Thadhani, R., Mannstadt, M., Wolf, M. and Chertow, G.M. (2012). Effects of phosphate binders in moderate CKD. *Journal of the American Society of Nephrology*, 23(8), pp.1407-1415.

Bodin, P. and Burnstock, G. (1996). ATP-stimulated release of ATP by human endothelial cells. *Journal of Cardiovascular Pharmacology*, 27(6), pp.872-875.

Bohle, A., Wehrmann, M., Bogenschutz, O., Batz, C., Muller, C.A. and Muller, G.A. (1991). The pathogenesis of chronic renal failure in diabetic nephropathy: investigation of 488 cases of diabetic glomerulosclerosis. *Pathology, Research and Practice*, 187(2-3), pp.251-259.

Bollee, G., Dollinger, C., Boutaud, L., Guillemot, D., Bensman, A., Harambat, J., Deteix, P., Daudon, M., Knebelmann, B. and Ceballos-Picot, I. (2010). Phenotype and genotype characterisation of adenine phosphoribosyltransferase deficiency. *Journal of the American Society of Nephrology*, 21(4), pp.679-688.

Booth, J.W., Tam, F.W. and Unwin, R.J. (2012). P2 purinoceptors: Renal pathophysiology and therapeutic potential. *Clinical Nephrology*, 78(2), pp.154-163.

Bouxsein, M.L., Boyd, S.K., Christiansen, B.A., Guldberg, R.E., Jepsen, K.J. and Muller, R. (2010). Guidelines for assessment of bone microstructure in rodents using micro-computed tomography. *Journal of Bone and Mineral Research*, 25(7), pp.1468-1486.

Bulanova, E., Budagian, V., Orinska, Z., Hein, M., Petersen, F., Thon, L., Adam, D. and Bulfone-Paus, S. (2005). Extracellular ATP induces cytokine expression and apoptosis through P2X7 receptor in murine mast cells. *The Journal of Immunology*, 174(7), pp.3880-3890.

Burnstock, G. (2002). Purinergic signaling and vascular cell proliferation and death. *Arteriosclerosis, Thrombosis, and Vascular Biology*, 22(3), pp.364-373.

Burnstock, G. (2006). Purinergic Signalling. *British Journal of Pharmacology*, 147(S1), pp.172-181.

Burnstock, G. (2009). Purinergic regulation of vascular tone and remodelling. *Autonomic and Autacoid Pharmacology*, 29(3), pp.63-72.

Burnstock, G. (2012). Purinergic Signalling: its unpopular beginning, its acceptance and its exciting future. *Bioessays*, 34(3), pp.218-225.

Burnstock, G. and Knight, G.E. (2004). Cellular distribution and functions of P2

receptor subtypes in different systems. *International Review of Cytology*, 240, pp.31-304.

Bywaters, E.G. and Beall, D. (1941). Crush injuries with impairment of renal function. *British Medical Journal*, 1(4185), pp.427-432.

Cario-Toumaniantz, C., Loirand, G., Ladoux, A. and Pacaud, P. (1998). P2X7 receptor activation-induced contraction and lysis in human saphenous vein smooth muscle. *Circulation Research*, 83(2), pp.196-203.

Celil, A.B. and Campbell, P.G. (2005). BMP-2 and insulin-like growth factor-I mediate Osterix (Osx) expression in human mesenchymal stem cells via the MAPK and protein kinase D signaling pathways. *Journal of Biological Chemistry*, 280(36), pp.31353-31359.

Chang, M.Y., Lu, J.K., Tian, Y.C., Chen, Y.C., Hung, C.C., Huang, Y.H., Chen, Y.H., Wu, M.S., Yang, C.W. and Cheng, Y.C. (2011). Inhibition of the P2X7 receptor reduces cystogenesis in PKD. *Journal of the American Society of Nephrology*, 22(9), pp.1696-1706.

Chanutin, A. and Ferris, E.B. Jr. (1932). Experimental renal insufficiency produced by partial nephrectomy: I. Control diet. *Archives of Internal Medicine*, 49(5), pp.767-787.

Chen, N.X., O'Neill, K.D., Chen, X., Kiattisunthorn, K., Gattone, V.H. and Moe, S.M. (2011). Activation of arterial matrix metalloproteinases leads to vascular calcification in chronic kidney disease. *American Journal of Nephrology*, 34(3), pp.211-219.

Chertow, G.M., Block, G.A., Correa-Rotter, R., Drueke, T.B., Floege, J., Goodman, W.G., Herzog, C.A., Kubo, Y., London, G.M., Mahaffey, K.W., Mix, T.C., Moe, S.M., Trotman, M.L., Wheeler, D.C. and Parfrey, P.S. (2012). Effect of cinacalcet on cardiovascular disease in patients undergoing dialysis. *The New England Journal of Medicine*, 367(26), pp.2482-2494.

Chertow, G.M., Burke, S.K. and Raggi, P. (2002). Sevelamer attenuates the progression of coronary and aortic calcification in hemodialysis patients. *Kidney*

International, 62(1), pp.245-252.

Chessell, I.P., Hatcher, J.P., Bountra, C., Michel, A.D., Hughes, J.P., Green, P., Egerton, J., Murfin, M., Richardson, J., Peck, W.L., Grahames, C.B., Casula, M.A., Yiangou, Y., Birch, R., Anand, P. and Buell, G.N. (2005). Disruption of the P2X7 purinoceptor gene abolishes chronic inflammatory and neuropathic pain. *Pain*, 114(3), pp.386-396.

Chiu, Y.W., Adler, S.G., Budoff, M.J., Takasu, J., Ashai, J. and Mehrotra, R. (2010). Coronary artery calcification and mortality in diabetic patients with proteinuria. *Kidney International*, 77(12), pp.1107-1114.

Chow, A.K., Cena, J. and Schulz, R. (2007). Acute actions and novel targets of matrix metalloproteinases in the heart and vasculature. *British Journal of Pharmacology*, 152(2), pp.189-205.

Chung, A.W., Yang, H.H., Sigrist, M.K., Brin, G., Chum, E., Gourlay, W.A. and Levin, A. (2009). Matrix metalloproteinase-2 and -9 exacerbate arterial stiffening and angiogenesis in diabetes and chronic kidney disease. *Cardiovascular Research*, 84(3), pp.494-504.

Ciceri, P., Volpi, E., Brenna, I., Arnaboldi, L., Neri, L., Brancaccio, D. and Cozzolino, M. (2012a). Combined effects of ascorbic acid and phosphate on rat VSMC osteoblastic differentiation. *Nephrology Dialysis Transplantation*, 27(1), pp.122-127.

Ciceri, P., Volpi, E., Brenna, I., Elli, F., Borghi, E., Brancaccio, D. and Cozzolino, M. (2012b). The combination of lanthanum chloride and the calcimimetic calindol delays the progression of vascular smooth muscle cells calcification. *Biochemical and Biophysical Research Communications*, 418(4), pp.770-773.

Coll, B., Betriu, A., Mart'inez-Alonso, M., Amoedo, M.L., Arcidiacono, M.V., Borras, M., Valdivielso, J.M. and Fernandez, E. (2011). Large artery calcification on dialysis patients is located in the intima and related to atherosclerosis. *Clinical Journal of the American Society of Nephrology*, 6(2), pp.303-310.

Costa-Junior, H.M., Sarmento Vieira, F. and Coutinho-Silva, R. (2011). C terminus

of the P2X7 receptor: treasure hunting. *Purinergic Signalling*, 7(1), pp.7-19.

Cote, N., El Husseini, D., Pepin, A., Guauque-Olarte, S., Ducharme, V., Bouchard-Cannon, P., Audet, A., Fournier, D., Gaudreault, N., Derbali, H., McKee, M.D., Simard, C., Despres, J.P., Pibarot, P., Bosse, Y. and Mathieu, P. (2012a). ATP acts as a survival signal and prevents the mineralisation of aortic valve. *Journal of Molecular and Cellular Cardiology*, 52(5), pp.1191-1202.

Cote, N., El Husseini, D., Pepin, A., Bouvet, C., Gilbert, L.A., Audet, A., Fournier, D., Pibarot, P., Moreau, P. and Mathieu, P. (2012b). Inhibition of ectonucleotidase with ARL67156 prevents the development of calcific aortic valve disease in warfarin-treated rats. *European Journal of Pharmacology*, 689(1-3), pp.139-146.

Coutinho-Silva, R., Persechini, P.M., Bisaggio, R.D., Perfettini, J.L., Neto, A.C., Kanellopoulos, J.M., Motta-Ly, I., Dautry-Varsat, A. and Ojcius, D.M. (1999). P2Z/P2X7 receptor-dependent apoptosis of dendritic cells. *American Journal of Physiology*, 276(5 Pt 1):C1139-47.

Crouthamel, M.H., Lau, W.L., Leaf, E.M., Chavkin, N.W., Wallingford, M.C., Peterson, D.F., Li, X., Liu, Y., Chin, M.T., Levi, M. and Giachelli, C.M. (2013). Sodium-Dependent Phosphate Cotransporters and Phosphate-Induced Calcification of Vascular Smooth Muscle Cells: Redundant Roles for PiT-1 and PiT-2. *Arteriosclerosis, Thrombosis, and Vascular Biology*, 33(11), pp.2625-2632.

Davies, M.R., Lund, R.J., Mathew, S. and Hruska, K.A. (2005). Low turnover osteodystrophy and vascular calcification are amenable to skeletal anabolism in an animal model of chronic kidney disease and the metabolic syndrome. *Journal of the American Society of Nephrology*, 16(4), pp.917-928.

Dawber, T.R., Kannel, W.B., Revotskie, N., Stokes III, J., Kagan, A. and Gordon, T. (1959). Some Factors Associated with the Development of Coronary Heart Disease—Six Years' Follow-Up Experience in the Framingham Study. *American Journal of Public Health and the Nations Health*, 49(10), pp.1349-1356.

Dawber, T.R., Moore, F.E. and Mann, G.V. (1957). Coronary heart disease in the Framingham study. *American Journal of Public Health and the Nations Health*, 47(4 Pt 2), pp.4-24.

De Schutter, T.M., Neven, E., Persy, V.P., Behets, G.J., Postnov, A.A., De Clerck, N.M. and D'Haese, P.C. (2011). Vascular calcification is associated with cortical bone loss in chronic renal failure rats with and without ovariectomy: the calcification paradox. *American Journal of Nephrology*, 34(4), pp.356-366.

Desjardins, L., Liabeuf, S., Renard, C., Lenglet, A., Lemke, H.D., Choukroun, G., Drueke, T.B. and Massy, Z.A. (2012). FGF23 is independently associated with vascular calcification but not bone mineral density in patients at various CKD stages. *Osteoporosis International*, 23(7), pp.2017-2025.

Di Angelantonio, E., Chowdhury, R., Sarwar, N., Aspelund, T., Danesh, J. and Gudnason, V. (2010). Chronic kidney disease and risk of major cardiovascular disease and non-vascular mortality: prospective population based cohort study. *British Medical Journal*, 341, c4986.

Di Virgilio, F. (2007). Liaisons dangereuses: P2X7 and the inflammasome. *Trends in Pharmacological Sciences*, 28(9), pp.465-472.

Donnelly-Roberts, D.L. and Jarvis, M.F. (2007). Discovery of P2X7 receptor-selective antagonists offers new insights into P2X7 receptor function and indicates a role in chronic pain states. *British Journal of Pharmacology*, 151(5), pp.571-579.

Donnelly-Roberts, D.L., Namovic, M.T., Han, P. and Jarvis, M.F. (2009). Mammalian P2X7 receptor Pharmacology: comparison of recombinant mouse, rat and human P2X7 receptors. *British Journal of Pharmacology*, 157(7), pp.1203-1214.

Drury, A.N. and Szent-Gyorgyi, A. (1929). The physiological activity of adenine compounds with especial reference to their action upon the mammalian heart. *The Journal of Physiology*, 68(3), pp.213-237.

Ducy, P., Zhang, R., Geoffroy, V., Ridall, A.L. and Karsenty, G. (1997).

Osf2/Cbfa1: a transcriptional activator of osteoblast differentiation. *Cell*, 89(5), pp.747-754.

Duer, M.J., Friscic, T., Proudfoot, D., Reid, D.G., Schoppet, M., Shanahan, C.M, Skepper, J.N. and Wise, E.R. (2008). Mineral surface in calcified plaque is like that of bone further evidence for regulated mineralisation. *Arteriosclerosis, Thrombosis, and Vascular Biology*, 28(11), pp.2030-2034.

Eaton, G.J., Custer, R.P., Johnson, F.N. and Stabenow, K.T. (1978). Dystrophic cardiac calcinosis in mice: genetic, hormonal, and dietary influences. *The American Journal of Pathology*, 90(1), pp.173-186.

Efstratiadis, G., Voulgaridou, A., Nikiforou, D., Kyventidis, A., Kourkouni, E. and Vergoulas, G. (2007). Rhabdomyolysis updated. *Hippokratia*, 11(3), pp.129-137.

El-Abbadi, M.M., Pai, A.S., Leaf, E.M., Yang, H.Y., Bartley, B.A., Quan, K.K., Ingalls, C.M., Liao, H.W. and Giachelli, C.M. (2009). Phosphate feeding induces arterial medial calcification in uremic mice: role of serum phosphorus, fibroblast growth factor-23, and osteopontin. *Kidney International*, 75(12), pp.1297-1307.

Eller, P., Hochegger, K., Feuchtner, G.M., Zitt, E., Tancevski, I., Ritsch, A., Kronenberg, F., Rosenkranz, A.R., Patsch, J.R. and Mayer, G. (2008). Impact of ENPP1 genotype on arterial calcification in patients with end-stage renal failure. *Nephrology Dialysis Transplantation*, 23(1), pp.321-327.

Erlinge, D. and Burnstock, G. (2008). P2 receptors in cardiovascular regulation and disease. *Purinergic Signalling*, 4(1), pp.1-20.

Erlinge, D., Hou, M., Webb, T.E., Barnard, E.A. and Moller, S. (1998). Phenotype changes of the vascular smooth muscle cell regulate P2 receptor expression as measured by quantitative RT-PCR. *Biochemical and Biophysical Research Communications*, 248(3), pp.864-870.

Eytan, O., Morice-Picard, F., Sarig, O., Ezzedine, K., Isakov, O., Li, Q., Ishida-Yamamoto, A., Shomron, N., Goldsmith, T., Fuchs-Telem, D., Adir, N., Uitto, J., orlow, S.J., Taieb, A. and Sprecher, E. (2013). Cole Disease Results from Mutations in ENPP1. *The American Journal of Human Genetics*, 93(4), pp.752-

757.

Fedde, K.N., Blair, L., Silverstein, J., Coburn, S.P., Ryan, L.M., Weinstein, R.S., Waymire, K., Narisawa, S., Millan, J.L., Macgregor, G.R. and Whyte, M.P. (1999). Alkaline phosphatase knock-out mice recapitulate the metabolic and skeletal defects of infantile hypophosphatasia. *Journal of Bone and Mineral Research*, 14(12), pp.2015-2026.

Feldkamp, L.A., Davis, L.C. and Kress, J.W. (1984). Practical cone-beam algorithm. *Journal of the Optical Society of America*, 1(6), pp.612-619.

Fellstrom, B.C., Jardine, A.G., Schmieder, R.E., Holdaas, H., Bannister, K., Beutler, J., Chae, D.W., Chevaile, A., Cobbe, S.M., Gronhagen-Riska, C., De Lima, J.J., Lins, R., Mayer, G., McMahon, A.W., Parving, H.H., Remuzzi, G., Sameulsson, O., Sonkodi, S., Sci, D., Suleymanlar, G., Tsakiris, D., Tesar, V., Todorov, V., Wiecek, A., Wuthrich, R.P., Gottlow, M., Johnsson, E. and Zannad, F. (2009). Rosuvastatin and cardiovascular events in patients undergoing hemodialysis. *New England Journal of Medicine*, 360(14), pp.1395-1407.

Fink, M., Henry, M. and Tange, J.D. (1987). Experimental folic acid nephropathy. *Pathology*, 19(2), pp.143-149.

Fleige, S. and Pfaffl, M.W. (2006). RNA integrity and the effect on the real-time qRT-PCR performance. *Molecular Aspects of Medicine*, 27(2-3), pp.126-139.

Fleisch, H., Schibler, D., Maerki, J. and Frossard, I. (1965). Inhibition of aortic calcification by means of pyrophosphate and polyphosphates. *Nature*, 207(5003), pp.1300-1301.

Forbes, R.M. (1971). Attempts to Alter Kidney Calcification in the Magnesium-Deficient Rat. *The Journal of Nutrition*, 101(1), pp.35-44.

Franceschi, C., Abbracchio, M.P., Barbieri, D., Ceruti, S., Ferrari, D., Iliou, J.P., Rounds, S., Schubert, P., Schulze-Lohoff, E., Rassendren, F.A., Staub, M., Volonte, C., Wakade, A.R. and Burnstock, G. (1996). Purines and cell death. *Drug Development Research*, 39(3-4), pp.442-449.

Francis, M.D. (1969). The inhibition of calcium hydroxyapatite crystal growth by polyphosphonates and polyphosphates. *Calcified Tissue Research*, 3(1), pp.151-162.

Gartland, A., Buckley, K.A., Hipskind, R.A., Bowler, W.B. and Gallagher, J.A. (2003a). P2 Receptors in Bone-Modulation of Osteoclast Formation and Activity via P2X7 Activation. *Critical Reviews in Eukaryotic Gene Expression*, 13(2-4), pp.237-242.

Gartland, A., Buckley, K.A., Hipskind, R.A., Perry, M.J., Tobias, J.H., Buell, G., Chessell, I., Bowler, W.B. and Gallagher, J.A. (2003b). Multinucleated Osteoclast Formation In Vivo and In Vitro by P2X7 Receptor-Deficient Mice. *Critical Reviews in Eukaryotic Gene Expression*, 13(2-4), pp.243-253.

Gartland, A., Hipskind, R.A., Gallagher, J.A. and Bowler, W.B, (2001). Expression of a P2X7 receptor by a subpopulation of human osteoblasts. *Journal of Bone and Mineral Research*, 16(5), pp.846-856.

Gartland, A., Skarratt, K.K., Hocking, L.J., Parsons, C., Stokes, L., Jorgensen, N.R., Fraser, W.D., Reid, D.M., Gallagher, J.A. and Wiley, J.S. (2012). Polymorphisms in the P2X7 receptor gene are associated with low lumbar spine bone mineral density and accelerated bone loss in post-menopausal women. *European Journal of Human Genetics*, 20(5), pp.559-564.

Go, A.S., Chertow, G.M., Fan, D., McCulloch, C.E. and Hsu, C.Y. (2004). Chronic kidney disease and the risks of death, cardiovascular events, and hospitalisation. *New England Journal of Medicine*, 351(13), pp.1296-1305.

Goncalves, R.G., Gabrich, L., Rosario, A. Jr., Takiya, C.M., Ferreira, M.L., Chiarini, L.B., Persechini, P.M., Coutinho-Silva, R. and Leite, M. Jr. (2006). The role of purinergic P2X7 receptors in the inflammation and fibrosis of unilateral ureteral obstruction in mice. *Kidney International*, 70(9), pp.1599-1606.

Grol, M.W., Panupinthu, N., Korcok, J., Sims, S.M. and Dixon, S.J. (2009). Expression, signaling, and function of P2X7 receptors in bone. *Purinergic Signalling*, 5(2), pp.205-221.

Groschel-Stewart, U., Bardini, M., Robson, T. and Burnstock, G. (1999). Localisation of P2X5 and P2X7 receptors by immunohistochemistry in rat stratified squamous epithelia. *Cell and Tissue Research*, 296(3), pp.599-605.

Gu, B.J. and Wiley, J.S. (2006). Rapid ATP-induced release of matrix metalloproteinase 9 is mediated by the P2X7 receptor. *Blood*, 107(12), pp.4946-4953.

Gu, B.J., Zhang, W.Y., Bendall, L.J., Chessell, I.P., Buell, G.N. and Wiley, J.S. (2000). Expression of P2X7 purinoceptors on human lymphocytes and monocytes: evidence for nonfunctional P2X7 receptors. *American Journal of Physiology-Cell Physiology*, 279(4), C1189-1197.

Haffner, D., Hocher, B., Muller, D., Simon, K., K"onig, K., Richter, C.M., Eggert, B., Schwarz, J., Godes, M., Nissel, R. and Querfeld, U. (2005). Systemic cardiovascular disease in uremic rats induced by 1,25(OH)2D3. *Journal of Hypertension*, 23(5), pp.1067-1075.

Hao, H., Hirota, S., Tsukamoto, Y., Imakita, M., Ishibashi-Ueda, H. and Yutani, C. (1995). Alterations of bone matrix protein mRNA expression in rat aorta in vitro. *Arteriosclerosis, Thrombosis, and Vascular Biology*, 15(9), pp.1474-1480.

Harmey, D., Hessle, L., Narisawa, S., Johnson, K.A., Terkeltaub, R. and Millan, J.L. (2004). Concerted Regulation of Inorganic Pyrophosphate and Osteopontin by akp2, enpp1, and ank: An Integrated Model of the Pathogenesis of Mineralisation Disorders. *The American Journal of Pathology*, 164(4), pp.1199-1209.

Haut, L.L., Alfrey, A.C., Guggenheim, S., Buddington, B. and Schrier, N. (1980). Renal toxicity of phosphate in rats. *Kidney International*, 17(6), pp.722-731.

Henley, C., Davis, J., Miller, G., Shatzen, E., Cattley, R., Li, X., Martin, D., Yao, W., Lane, N. and Shalhoub, V. (2009). The calcimimetic AMG 641 abrogates parathyroid hyperplasia, bone and vascular calcification abnormalities in uremic rats. *European Journal of Pharmacology*, 616(1-3), pp.306-313.

Ho, A.M., Johnson, M.D. and Kingsley, D.M. (2000). Role of the mouse ank gene in control of tissue calcification and arthritis. *Science*, 289(5477), pp.265-270.

Holden, R.M., Morton, A.R., Garland, J.S., Pavlov, A., Day, A.G. and Booth, S.L. (2010). Vitamins K and D status in stages 3-5 chronic kidney disease. *Clinical Journal of the American Society of Nephrology*, 5(4), pp.590-597.

Honore, P., Donnelly-Roberts, D., Namovic, M., Zhong, C., Wade, C., Chandran, P., Zhu, C., Carroll, W., Perez-Medrano, A., Iwakura, Y. and Jarvis, M.F. (2009). The antihyperalgesic activity of a selective P2X7 receptor antagonist, A-839977, is lost in IL-1alphabeta knockout mice. *Behavioural Brain Research*, 204(1), pp.77-81.

Hopper, T.A., Wehrli, F.W., Saha, P.K., Andre, J.B., Wright, A.C., Sanchez, C.P. and Leonard, M.B. (2007). Quantitative microcomputed tomography assessment of intratrabecular, intertrabecular, and cortical bone architecture in a rat model of severe renal osteodystrophy. *Journal of Computer Assisted Tomography*, 31(2), pp.320-328.

Hori, M. and Henderson, J.F. (1966). Kinetic studies of adenine phosphoribosyltransferase. *Journal of Biological Chemistry*, 241(14), pp.3404-3408.

Hosaka, N., Mizobuchi, M., Ogata, H., Kumata, C., Kondo, F., Koiwa, F., Kinugasa, E. and Akizawa, T. (2009). Elastin degradation accelerates phosphate-induced mineralisation of vascular smooth muscle cells. *Calcified Tissue International*, 85(6), pp.523-529.

Hosoda, Y., Yoshimura, Y. and Hiqaki, S. (1981). A new breed of mouse showing multiple osteochondral lesions – twy mouse. *Ryumachi*, 21 Suppl, pp.157-164.

Hough, T.A., Nolan, P.M., Tsipouri, V., Toye, A.A., Gray, I.C., Goldsworthy, M., Moir, L., Cox, R.D., Clements, S., Glenister, P.H., Wood, J., Selley, R.L., Strivens, M.A., Vizor, L., McCormack, S.L., Peters, J., Fisher, E.M., Spurr, N,. Rastan, S., Martin, J.E., Brown, S.D. and Hunter, A.J. (2002). Novel phenotypes identified by plasma biochemical screening in the mouse. *Mammalian Genome*, 13(10), pp.595-602.

Hruska, K.A., Mathew, S. and Saab, G. (2005). Bone morphogenetic proteins in

vascular calcification. *Circulation Research*, 97(2), pp.105-114.

Huang, L., Scarpellini, A., Funck, M., Verderio, E.A. and Johnson, T.S. (2013). Development of a chronic kidney disease model in C57BL/6 mice with relevance to human pathology. *Nephron Extra*, 3(1), pp.12-29.

Huang, M.S., Sage, A.P., Lu, J., Demer, L.L. and Tintut, Y. (2008). Phosphate and pyrophosphate mediate PKA-induced vascular cell calcification. *Biochemical and Biophysical Research Communications*, 374(3), pp.553-558.

Ishibashi, S., Goldstein, J.L., Brown, M.S., Herz, J. and Burns, D.K. (1994). Massive xanthomatosis and atherosclerosis in cholesterol-fed low density lipoprotein receptor-negative mice. *Journal of Clinical Investigation*, 93(5), pp.1885-1893.

Ivandic, B.T., Utz, H.F., Kaczmarek, P.M., Aherrahrou, Z., Axtner, S.B., Klepsch, C., Lusis, A.J. and Katus, H.A. (2001). New Dyscalc loci for myocardial cell necrosis and calcification (dystrophic cardiac calcinosis) in mice. *Physiological Genomics*, 6(3), pp.137-144.

Ix, J.H., Shlipak, M.G., Brandenburg, V.M., Ali, S., Ketteler, M. and Whooley, M.A. (2006). Association between human fetuin-A and the metabolic syndrome data from the heart and soul study. *Circulation*, 113(14), pp.1760-1767.

Jahnen-Dechent, W., Heiss, A., Schafer, C. and Ketteler, M. (2011). Fetuin-A regulation of calcified matrix metabolism. *Circulation Research*, 108(12), pp.1494-1509.

Jamal, S.A., Vandermeer, B., Raggi, P., Mendelssohn, D.C., Chatterley, T., Dorgan, M., Lok, C.E., Fitchett, D. and Tsuyuki, R.T. (2013). Effect of calcium-based versus non-calcium-based phosphate binders on mortality in patients with chronic kidney disease: an updated systematic review and meta-analysis. *The Lancet*, 382(9900), pp.1268-1277.

Jawien, J., Nastalek, P. and Korbut, R. (2004). Mouse models of experimental atherosclerosis. *Journal of Physiology and Pharmacology*, 55(3), pp.503-517.

Jensky, N.E., Criqui, M.H., Wright, C.M., Wassel, C.L., Alcaraz, J.E. and Allison,

M.A. (2011). The association between abdominal body composition and vascular calcification. *Obesity (Silver Spring)*, 19(12), pp.2418-2424.

Jia, T., Olauson, H., Lindberg, K., Amin, R., Edvardsson, K., Lindholm, B., Andersson, G., Wernerson, A., Sabbagh, Y., Schiavi, S. and Larsson, T.E. (2013). A novel model of adenine-induced tubulointerstitial nephropathy in mice. *BMC Nephrology*, 14(1), pp.116.

Johnson, K.A., Hessle, L., Vaingankar, S., Wennberg, C., Mauro, S., Narisawa, S., Goding, J.W., Sano, K., Millan, J.L. and Terkeltaub, R. (2000). Osteoblast tissue-nonspecific alkaline phosphatase antagonizes and regulates PC-1. *American Journal of Physiology-Regulatory, Integrative and Comparative Physiology*, 279(4), R1365-1377.

Jono, S., McKee, M.D., Murry, C.E., Shioi, A., Nishizawa, Y., Mori, K., Morii, H. and Giachelli, C.M. (2000). Phosphate regulation of vascular smooth muscle cell calcification. *Circulation Research*, 87(7), E10-17.

Jorgensen, N.R., Henriksen, Z., Sorensen, O.H., Eriksen, E.F., Civitelli, R. and Steinberg, T.H. (2002). Intercellular calcium signaling occurs between human osteoblasts and osteoclasts and requires activation of osteoclast P2X7 receptors. *Journal of Biological Chemistry*, 277(9), pp.7574-7580.

Junqueira, L.C., Bignolas, G. and Brentani, R.R. (1979). Picrosirius staining plus polarisation microscopy, a specific method for collagen detection in tissue sections. *The Histochemical Journal*, 11(4), pp.447-455.

Kaczmarek, E., Koziak, K., Sevigny, J., Siegel, J.B., Anrather, J., Beaudoin, A.R., Bach, F.H. and Robson, S.C. (1996). Identification and characterisation of CD39/vascular ATP diphosphohydrolase. *Journal of Biological Chemistry*, 271(51), pp.33116-33122.

Kapustin, A.N., Davies, J.D., Reynolds, J.L., McNair, R., Jones, G.T., Sidibe, A., Schurgers, L.J., Skepper, J.N., Proudfoot, D., Mayr, M. and Shanahan, C.M. (2011). Calcium regulates key components of vascular smooth muscle cell-derived matrix vesicles to enhance mineralisation. *Circulation Research*, 109(1),

e1-12.

Kaspareit-Rittinghausen, J., Deerberg, F., Rapp, K.G. and Wcislo, A. (1990). A new rat model for polycystic kidney disease of humans. *Transplantation Proceedings*, 22(6), pp.2582–2583.

Kato, K., Nishimasu, H., Okudaira, S., Mihara, E., Ishitani, R., Takagi, J., Aoki, J. and Nureki, O. (2012). Crystal structure of Enpp1, an extracellular glycoprotein involved in bone mineralisation and insulin signaling. *Proceedings of the National Academy of Sciences of the United States of America*, 109(42), pp.16876-16881.

Katsumata, K., Kusano, K., Hirata, M., Tsunemi, K., Nagano, N., Burke, S.K. and Fukushima, N. (2003). Sevelamer hydrochloride prevents ectopic calcification and renal osteodystrophy in chronic renal failure rats. *Kidney International*, 64(2), pp.441-450.

Katsuragi, T., Tokunaga, T., Ogawa, S., Soejima, O., Sato, C. and Furukawa, T. (1991). Existence of ATP-evoked ATP release system in smooth muscles. *Journal of Pharmacology and Experimental Therapeutics*, 259(2), pp.513-518.

Kauffenstein, G., Drouin, A., Thorin-Trescases, N., Bachelard, H., Robaye, B., D'Orleans-Juste, P., Marceau, F., Thorin, E. and Sevigny, J. (2010a). NTPDase1 (CD39) controls nucleotide-dependent vasoconstriction in mouse. *Cardiovascular Research*, 85(1), pp.204-213.

Kauffenstein, G., Furstenau, C.R., D'Orleans-Juste, P. and Sevigny, J. (2010b). The ecto-nucleotidase NTPDase1 differentially regulates P2Y1 and P2Y2 receptor-dependent vasorelaxation. *British Journal of Pharmacology*, 159(3), pp.576-585.

Kawata, T., Nagano, N., Obi, M., Miyata, S., Koyama, C., Kobayashi, N., Wakita, S. and Wada, M. (2008). Cinacalcet suppresses calcification of the aorta and heart in uremic rats. *Kidney International*, 74(10), pp.1270-1277.

Ke, H.Z., Qi, H., Weidema, A.F., Zhang, Q., Panupinthu, N., Crawford, D.T., Grasser, W.A., Paralkar, V.M., Li, M., Audoly, L.P., Gabel, C.A., Lee, W.S., Dixon, S.J., Sims, S.M. and Thompson, D.D. (2003). Deletion of the P2X7

nucleotide receptor reveals its regulatory roles in bone formation and resorption. *Molecular Endocrinology*, 17(7), pp.1356-1367.

Ketteler, M., Bongartz, P., Westenfeld, R., Wildberger, J.E., Mahnken, A.H., Bohm, R., Metzger, T., Wanner, C., Jahnen-Dechent, W. and Floege, J. (2003). Association of low fetuin-A (AHSG) concentrations in serum with cardiovascular mortality in patients on dialysis: a cross-sectional study. *The Lancet*, 361(9360), pp.827-833.

Keystone, E.C., Wang, M.M., Layton, M., Hollis, S. and McInnes, I.B. (2011). Clinical evaluation of the efficacy of the P2X7 purinergic receptor antagonist AZD9056 on the signs and symptoms of rheumatoid arthritis in patients with active disease despite treatment with methotrexate or sulphasalazine. *Annals of the Rheumatic Diseases*, 71(10), pp.1630-1635.

Kidney Disease: Improving Global Outcomes (KDIGO) CKD Work Group. (2013). KDIGO 2012 clinical practice guideline for the evaluation and management of chronic kidney disease. *Kidney International Supplements*, 3(1), pp.1-150.

Kidney Disease: Improving Global Outcomes (KDIGO) CKD–MBD Work Group. (2009). KDIGO clinical practice guideline for the diagnosis, evaluation, prevention, and treatment of Chronic Kidney Disease-Mineral and Bone Disorder (CKD-MBD). *Kidney International Supplement*, 76 (Suppl 113), S1-S130.

Komori, T., Yagi, H., Nomura, S., Yamaguchi, A., Sasaki, K., Deguchi, K., Shimizu, Y., Bronson, R.T., Gao, Y.H., Inada, M., Sato, M., Okamoto, R., Kitamura, Y., Yoshiki, S. and Kishimoto, T. (1997). Targeted Disruption of Cbfa1 Results in a Complete Lack of Bone Formation owing to Maturational Arrest of Osteoblasts. *Cell*, 89(5), pp.755-764.

Koos, R., Brandenburg, V., Mahnken, A.H., Muhlenbruch, G., Stanzel, S., Gunther, R.W., Floege, J., Jahnen-Dechent, W., Kelm, M. and Kuhl, H.P. (2009). Association of fetuin-A levels with the progression of aortic valve calcification in non-dialyzed patients. *European Heart Journal*, 30(16), pp.2054-2061.

Kramann, R., Couson, S.K., Neuss, S., Kunter, U., Bovi, M., Bornemann, J.,

Knuchel, R., Jahnen-Dechent, W., Floege, J. and Schneider, R.K. (2011). Exposure to uremic serum induces a procalcific phenotype in human mesenchymal stem cells. *Arteriosclerosis, Thrombosis, and Vascular Biology*, 31(9), e45-54.

Krueger, T., Schlieper, G., Schurgers, L., Cornelis, T., Cozzolino, M., Jacobi, J., Jadoul, M., Ketteler, M., Rump, L.C., Stenvinkel, P., Westenfeld, R., Wiecek, A., Reinartz, S., Hilgers, R.D. and Floege, J. (2013). Vitamin K1 to slow vascular calcification in haemodialysis patients (VitaVasK trial): a rationale and study protocol. *Nephrology Dialysis Transplantation*, [Epub ahead of print].

Lanzer, P., Boehm, M., Sorribas, V., Thiriet, M., Janzen, J., Zeller, T., St Hilaire, C. and Shanahan, C. (2014). Medial vascular calcification revisited: review and perspectives. *European Heart Journal*, 35(23), pp.1515-1525.

Laroche, M. and Delmotte, A. (2005). Increased arterial calcification in Paget's disease of bone. *Calcified Tissue International*, 77(3), pp.129-133.

Lau, W.L., Leaf, E.M., Hu, M.C., Takeno, M.M., Kuro-o, M., Moe, O.W. and Giachelli, C.M. (2012b). Vitamin D receptor agonists increase klotho and osteopontin while decreasing aortic calcification in mice with chronic kidney disease fed a high phosphate diet. *Kidney International*, 82(12), pp.1261-1270.

Lau, W.L., Linnes, M., Chu, E.Y., Foster, B.L., Bartley, B.A., Somerman, M.J. and Giachelli, C.M. (2012a). High phosphate feeding promotes mineral and bone abnormalities in mice with chronic kidney disease. *Nephrology Dialysis Transplantation*, 28(1), pp.62-69.

Leroux-Berger, M., Queguiner, I., Maciel, T.T., Ho, A., Relaix, F. and Kempf, H. (2011). Pathologic calcification of adult vascular smooth muscle cells differs on their crest or mesodermal embryonic origin. *Journal of Bone and Mineral Research*, 26(7), pp.1543-1553.

Levesque, S.A., Lavoie, E.G., Lecka, J., Bigonnesse, F. and Sevigny, J. (2007). Specificity of the ecto-ATPase inhibitor ARL 67156 on human and mouse ectonucleotidases. *British Journal of Pharmacology*, 152(1), pp.141-150.

Levey, A.S. and Coresh, J. (2012). Chronic kidney disease. *The Lancet*, 379(9811), pp.165-180.

Levey, A.S., de Jong, P.E., Coresh, J., El Nahas, M., Astor, B.C., Matsushita, K., Gansevoort, R.T., Kasiske, B.L. and Eckardt, K.U. (2010). The definition, classification, and prognosis of chronic kidney disease: a KDIGO Controversies Conference report. *Kidney International*, 80(1), pp.17-28.

Levy-Litan, V., Hershkovitz, E., Avizov, L., Leventhal, N., Bercovich, D., Chalifa-Caspi, V., Manor, E., Buriakovsky, S., Hadad, Y., Goding, J. and Parvari, R. (2010). Autosomal-Recessive Hypophosphatemic Rickets Is Associated with an Inactivation Mutation in the ENPP1 Gene. *The American Journal of Human Genetics*, 86(2), pp.273-278.

Lew, M.J. and White, T.D. (1987). Release of endogenous ATP during sympathetic nerve stimulation. *British Journal of Pharmacology*, 92(2), pp.349-355.

Lewis, C.J. and Evans, R.J. (2001). P2X receptor immunoreactivity in different arteries from the femoral, pulmonary, cerebral, coronary and renal circulations. *Journal of Vascular Research*, 38(4), pp.332-340.

Li, X., Yang, H.Y. and Giachelli, C.M. (2006). Role of the sodium-dependent phosphate cotransporter, Pit-1, in vascular smooth muscle cell calcification. *Circulation Research*, 98(7), pp.905-912.

Liao, H., Hyman, M.C., Baek, A.E., Fukase, K. and Pinsky, D.J. (2010). cAMP/CREB-mediated transcriptional regulation of ectonucleoside triphosphate diphosphohydrolase 1 (CD39) expression. *Journal of Biological Chemistry*, 285(19), pp.14791-14805.

Lohman, A.W., Billaud, M. and Isakson, B.E. (2012). Mechanisms of ATP release and signalling in the blood vessel wall. *Cardiovascular Research*, 95(3), pp.269-280.

Lomashvili, K., Garg, P. and O'Neill, W.C. (2006). Chemical and hormonal determinants of vascular calcification in vitro. *Kidney International*, 69(8), pp.1464-1470.

Lomashvili, K.A., Cobbs, S., Hennigar, R.A., Hardcastle, K.I. and O'Neill, W.C. (2004). Phosphate-induced vascular calcification: role of pyrophosphate and osteopontin. *Journal of the American Society of Nephrology*, 15(6), pp.1392-1401.

Lomashvili, K.A., Garg, P., Narisawa, S., Millan, J.L. and O'Neill, W.C. (2008). Upregulation of alkaline phosphatase and pyrophosphate hydrolysis: potential mechanism for uremic vascular calcification. *Kidney International*, 73(9), pp.1024-1030.

Lomashvili, K.A., Khawandi, W. and O'Neill, W.C. (2005). Reduced plasma pyrophosphate levels in hemodialysis patients. *Journal of the American Society of Nephrology*, 16(8), pp.2495-2500.

Lomashvili, K.A., Monier-Faugere, M.C., Wang, X., Malluche, H.H. and O'Neill, W.C. (2009). Effect of bisphosphonates on vascular calcification and bone metabolism in experimental renal failure. *Kidney International*, 75(6), pp.617-625.

Lomashvili, K.A., Narisawa, S., Millan, J.L. and O'Neill, W.C. (2014). Vascular calcification is dependent on plasma levels of pyrophosphate. *Kidney International*, 85(6), pp.1351-1356.

Lomashvili, K.A., Wang, X., Wallin, R. and O'Neill, W.C. (2011). Matrix Gla protein metabolism in vascular smooth muscle and role in uremic vascular calcification. *Journal of Biological Chemistry*, 286(33), pp.28715-28722.

London, G.M., Guerin, A.P., Marchais, S.J, Metivier, F., Pannier, B. and Adda, H. (2003). Arterial media calcification in end-stage renal disease: impact on all-cause and cardiovascular mortality. *Nephrology Dialysis Transplantation*, 18(9), pp.1731-1740.

London, G.M., Marty, C., Marchais, S.J., Guerin, A.P., Metivier, F. and de Vernejoul, M.C. (2004). Arterial calcifications and bone histomorphometry in end-stage renal disease. *Journal of the American Society of Nephrology*, 15(7), pp.1943-1951.

Long, D.A., Price, K.L., Ioffe, E., Gannon, C.M., Gnudi, L., White, K.E., Yancopoulos, G.D., Rudge, J.S. and Woolf, A.S. (2008). Angiopoietin-1 therapy enhances fibrosis and inflammation following folic acid-induced acute renal injury. *Kidney International*, 74(3), pp.300-309.

Lopez-Castejon, G., Theaker, J., Pelegrin, P., Clifton, A.D., Braddock, M. and Surprenant, A. (2010). P2X7 receptor-mediated release of cathepsins from macrophages is a cytokine-independent mechanism potentially involved in joint diseases. *The Journal of Immunology*, 185(4), pp.2611-2619.

Lorenz-Depiereux, B., Schnabel, D., Tiosano, D., Hausler, G. and Strom, T.M. (2010). Loss-of-Function ENPP1 Mutations Cause Both Generalized Arterial Calcification of Infancy and Autosomal-Recessive Hypophosphatemic Rickets. *The American Journal of Human Genetics*, 86(2), pp.267-272.

Luo, G., Ducy, P., McKee, M.D., Pinero, G.J., Loyer, E., Behringer, R.R. and Karsenty, G. (1997). Spontaneous calcification of arteries and cartilage in mice lacking matrix GLA protein. *Nature*, 386(6620), pp.78-81.

Mackenzie, N.C., Huesa, C., Rutsch, F. and MacRae, V.E. (2012). New insights into NPP1 function: lessons from clinical and animal studies. *Bone*, 51(5), pp.961-968.

Mackenzie, N.C., Zhu, D., Milne, E.M., van't Hof, R., Martin, A., Darryl Quarles, L., Millan, J.L., Farquharson, C. and MacRae, V.E. (2012). Altered bone development and an increase in FGF-23 expression in Enpp1(-/-) mice. *PloS One*, 7(2), e32177.

Maddux, B.A., Chang, Y.N., Accili, D., McGuinness, O.P., Youngren, J.F. and Goldfine, I.D. (2006). Overexpression of the insulin receptor inhibitor PC-1/ENPP1 induces insulin resistance and hyperglycemia. *American Journal of Physiology-Endocrinology and Metabolism*, 290(4), E746-749.

Maeda, N., Doi, K. and Mitsuoka, T. (1986). Development of heart and aortic lesions in DBA/2NCrj mice. *Laboratory Animals*, 20(1), pp.5-8.

Marinelli, A., Pistolesi, V., Pasquale, L., Di Lullo, L., Ferrazzano, M., Baudena, G., Della Grotta, F. and Di Napolie, A. (2013). Diagnosis of Arterial Media

Calcification in Chronic Kidney Disease. *Cardiorenal Medicine*, 3(2), pp.89-95.

Massy, Z.A., Ivanovski, O., Nguyen-Khoa, T., Angulo, J., Szumilak, D., Mothu, N., Phan, O., Daudon, M., Lacour, B., Drueke, T.B. and Muntzel, M.S. (2005). Uremia accelerates both atherosclerosis and arterial calcification in apolipoprotein E knockout mice. *Journal of the American Society of Nephrology*, 16(1), pp.109-116.

Matsumoto, T., Tostes, R.C. and Webb, R.C. (2011). The role of uridine adenosine tetraphosphate in the vascular system. *Advances in Pharmacological Sciences*, 2011, pp.435132.

McBride, A. and Westervelt, P. (2012). Recognizing and managing the expanded risk of tumor lysis syndrome in hematologic and solid malignancies. *Journal of Hematology & Oncology*, 5, pp.75.

McCabe, K.M., Booth, S.L., Fu, X., Shobeiri, N., Pang, J.J., Adams, M.A. and Holden, R.M. (2013). Dietary vitamin K and therapeutic warfarin alter the susceptibility to vascular calcification in experimental chronic kidney disease. *Kidney International*, 83(5), pp.835-844.

McGaraughty, S., Chu, K.L., Namovic, M.T., Donnelly-Roberts, D.L., Harris, R.R., Zhang, X.F., Shieh, C.C., Wismer, C.T., Zhu, C.Z., Gauvin, D.M., Fabiyi, A.C., Honore, P., Gregg, R.J., Kort, M.E., Nelson, D.W., Carroll, W.A., Marsh, K., Faltynek, C.R. and Jarvis, M.F. (2007). P2X7-related modulation of pathological nociception in rats. *Neuroscience*, 146(4), pp.1817-1828.

Meier, M., Weng, L.P., Alexandrakis, E., Ruschoff, J. and Goeckenjan, G. (2001). Tracheobronchial stenosis in Keutel syndrome. *European Respiratory Journal*, 17(3), pp.566-569.

Meng, H., Vera, I., Che, N., Wang, X., Wang, S.S., Ingram-Drake, L., Schadt, E.E., Drake, T.A. and Lusis, A.J. (2007). Identification of Abcc6 as the major causal gene for dystrophic cardiac calcification in mice through integrative genomics. *Proceedings of the National Academy of Sciences of the United States of America*, 104(11), pp.4530-4535.

Michel, A.D., Xing, M. and Humphrey, P.P. (2001). Serum constituents can affect 2'-& 3'-O-(4-benzoylbenzoyl)-ATP potency at P2X(7) receptors. *British Journal of Pharmacology*, 132(7), pp.1501-1508.

Moe, S., Drueke, T., Cunningham, J., Goodman, W., Martin, K., Olgaard, K., Ott, S., Sprague, S., Lameire, N. and Eknoyan, G. (2006). Definition, evaluation, and classification of renal osteodystrophy: a position statement from Kidney Disease: Improving Global Outcomes (KDIGO). *Kidney International*, 69(11), pp.1945-1953.

Moe, S.M., O'Neill, K.D., Duan, D., Ahmed, S., Chen, N.X., Leapman, S.B., Fineberg, N. and Kopecky, K. (2002). Medial artery calcification in ESRD patients is associated with deposition of bone matrix proteins. *Kidney International*, 61(2), pp.638-647.

Moe, S.M., Reslerova, M., Ketteler, M., O'Neill, K., Duan, D., Koczman, J., Westenfeld, R., Jahnen-Dechent, W. and Chen, N.X. (2005). Role of calcification inhibitors in the pathogenesis of vascular calcification in chronic kidney disease (CKD). *Kidney International*, 67(6), pp.2295-2304.

Moe, S.M., Seifert, M.F., Chen, N.X., Sinders, R.M., Chen, X., Duan, D., Henley, C., Martin, D. and Gattone, V.H. 2nd. (2009). R-568 reduces ectopic calcification in a rat model of chronic kidney disease-mineral bone disorder (CKD-MBD). *Nephrology Dialysis Transplantation*, 24(8), pp.2371-2377.

Monico, C.G. and Milliner, D.S. (2011). Genetic determinants of urolithiasis. *Nature Reviews Nephrology*, 8(3), pp.151-162.

Montes de Oca, A., Madueno, J.A., Martinez-Moreno, J.M., Guerrero, F., Munoz-Castaneda, J., Rodriguez-Ortiz, M.E., Mendoza, F.J., Almaden, Y., Lopez, I., Rodriguez, M. and Aquilera-Tejero, E. (2010). High phosphate-induced calcification is related to SM22-alpha promoter methylation in vascular smooth muscle cells. *Journal of Bone and Mineral Research*, 25(9), pp.1996-2005.

Mornet, E. (2007). Hypophosphatasia. *Orphanet Journal of Rare Diseases*, 2, pp.40.

Munroe, P.B., Olgunturk, R.O., Fryns, J.P., Van Maldergem, L., Ziereisen, F.,

Yuksel, B., Gardiner, R.M. and Chung, E. (1999). Mutations in the gene encoding the human matrix Gla protein cause Keutel syndrome. *Nature Genetics*, 21(1), pp.142-144.

Murshed, M., Harmey, D., Millan, J.L., McKee, M.D. and Karsenty, G. (2005). Unique coexpression in osteoblasts of broadly expressed genes accounts for the spatial restriction of ECM mineralisation to bone. *Genes & Development*, 19(9), pp.1093-1104.

Nakano-Kurimoto, R., Ikeda, K., Uraoka, M., Nakagawa, Y., Yutaka, K., Koide, M., Takahashi, T., Matoba, S., Yamada, H., Okigaki, M. and Matsubara, H. (2009). Replicative senescence of vascular smooth muscle cells enhances the calcification through initiating the osteoblastic transition. *American Journal of Physiology-Heart and Circulatory Physiology*, 297(5), H1673-1684.

Nakashima, K., Zhou, X., Kunkel, G., Zhang, Z., Deng, J.M., Behringer, R.R. and de Crombrugghe, B. (2002). The novel zinc finger-containing transcription factor osterix is required for osteoblast differentiation and bone formation. *Cell*, 108(1), pp.17-29.

Nam, H.K., Liu, J., Li, Y., Kragor, A. and Hatch, N.E. (2011). Ectonucleotide pyrophosphatase/phosphodiesterase-1 (ENPP1) protein regulates osteoblast differentiation. *Journal of Biological Chemistry*, 286(45), pp.39059-39071.

Nangaku, M. (2004). Mechanisms of Tubulointerstitial Injury in the Kidney: Final Common Pathways to End-stage Renal Failure. *Internal Medicine*, 43(1), pp.9-17.

Narisawa, S., Harmey, D., Yadav, M.C., O'Neill, W.C., Hoylaerts, M.F. and Millan, J.L. (2007). Novel inhibitors of alkaline phosphatase suppress vascular smooth muscle cell calcification. *Journal of Bone and Mineral Research*, 22(11), pp.1700-1710.

Nelson, D.W., Gregg, R.J., Kort, M.E., Perez-Medrano, A., Voight, E.A., Wang, Y., Grayson, G., Namovic, M.T., Donnelly-Roberts, D.L., Niforatos, W., Honore, P., Jarvis, M.F., Faltynek, C.R. and Carroll, W.A. (2006). Structure-activity relationship studies on a series of novel, substituted 1-benzyl-5-phenyltetrazole

P2X7 antagonists. *Journal of Medicinal Chemistry*, 49(12), pp.3659-3666.

Neven, E. and D'Haese, P.C. (2011). Vascular Calcification in Chronic Renal Failure What Have We Learned From Animal Studies? *Circulation Research*, 108(2), pp.249-264.

Neven, E., Dams, G., Postnov, A., Chen, B., De Clerck, N., De Broe, M.E., D'Haese, P.C. and Persy, V. (2009). Adequate phosphate binding with lanthanum carbonate attenuates arterial calcification in chronic renal failure rats. *Nephrology Dialysis Transplantation*, 24(6), pp.1790-1799.

Neven, E., Persy, V., Dauwe, S., De Schutter, T., De Broe, M.E. and D'Haese, P.C. (2010). Chondrocyte rather than osteoblast conversion of vascular cells underlies medial calcification in uremic rats. *Arteriosclerosis, Thrombosis, and Vascular Biology*, 30(9), pp.1741-1750.

Nicke, A., Kuan, Y.H., Masin, M., Rettinger, J., Marquez-Klaka, B., Bender, O., Gorecki, D.C., Murrell-Lagnado, R.D. and Soto, F. (2009). A functional P2X7 splice variant with an alternative transmembrane domain 1 escapes gene inactivation in P2X7 knock-out mice. *Journal of Biological Chemistry*, 284(38), pp.25813-25822.

Nitschke, Y., Baujat, G., Botschen, U., Wittkampf, T., du Moulin, M., Stella, J., Le Merrer, M., Guest, G., Lambot, K., Tazarourte-Pinturier, M.F., Chassaing, N., Roche, O., Feenstra, I., Loechner, K., Deshpande, C., Garber, S.J., Chikarmane, R., Steinmann, B., Shahinvan, T., Martorell, L., Davies, J., Smith, W.E., Kahler, S.G., McCulloch, M., Wraige, E., Loidi, L., Hohne, W., Martin, L., Hadj-Rabia, S., Terkeltaub, R. and Rutsch, F. (2012). Generalized Arterial Calcification of Infancy and Pseudoxanthoma Elasticum Can Be Caused by Mutations in Either ENPP1 or ABCC6. *The American Journal of Human Genetics*, 90(1), pp.25-39.

Nitschke, Y., Hartmann, S., Torsello, G., Horstmann, R., Seifarth, H., Weissen-Plenz, G. and Rutsch, F. (2011). Expression of NPP1 is regulated during atheromatous plaque calcification. *Journal of Cellular and Molecular Medicine*, 15(2), pp.220-231.

Norman, J.T. and Fine, L.G. (1999). Progressive renal disease: fibroblasts, extracellular matrix, and integrins. *Experimental Nephrology*, 7(2), pp.167-177.

North, R.A. (2002). Molecular physiology of P2X receptors. *Physiological Reviews*, 82(4), pp.1013-1067.

Nurnberg, P., Thiele, H., Chandler, D., Hohne, W., Cunningham, M.L., Ritter, H., Leschik, G., Uhlmann, K., Mischung, C., Harrop, K., Goldblatt, J., Borochowitz, Z.U., Kotzot, D., Westermann, F., Mundlos, S., Braun, H.S., Laing, N. and Tinschert, S. (2001). Heterozygous mutations in ANKH, the human ortholog of the mouse progressive ankylosis gene, result in craniometaphyseal dysplasia. *Nature Genetics*, 28(1), pp.37-41.

Ohlendorff, S.D., Tofteng, C.L., Jensen, J.E., Petersen, S., Civitelli, R., Fenger, M., Abrahamsen, B., Hermann, A.P., Eiken, P. and Jorgensen, N.R. (2007). Single nucleotide polymorphisms in the P2X7 gene are associated to fracture risk and to effect of estrogen treatment. *Pharmacogenetics and Genomics*, 17(7), pp.555-567.

Okada, H., Kaneko, Y., Yawata, T., Uyama, H., Ozono, S., Motomiya, Y. and Hirao, Y. (1999). Reversibility of adenine-induced renal failure in rats. *Clinical and Experimental Nephrology*, 3(2), pp.82-88.

Okawa, A., Nakamura, I., Goto, S., Moriya, H., Nakamura, Y. and Ikegawa, S. (1998). Mutation in Npps in a mouse model of ossification of the posterior longitudinal ligament of the spine. *Nature Genetics*, 19(3), pp.271-273.

O'Neill, W.C. (2007). The fallacy of the calcium-phosphorus product. *Kidney International*, 72(7), pp.792-796.

O'Neill, W.C. and Adams, A.L. (2014). Breast arterial calcification in chronic kidney disease: absence of smooth muscle apoptosis and osteogenic transdifferentiation. *Kidney International*, 85(3), pp.668-676.

O'Neill, W.C., Lomashvili, K.A., Malluche, H.H., Faugere, M.C. and Riser, B.L. (2011). Treatment with pyrophosphate inhibits uremic vascular calcification. *Kidney International*, 79(5), pp.512-517.

O'Neill, W.C., Sigrist, M.K. and McIntyre, C.W. (2010). Plasma pyrophosphate and vascular calcification in chronic kidney disease. *Nephrology Dialysis Transplantation*, 25(1), pp.187-191.

Orriss, I.R., Burnstock, G. and Arnett, T.R. (2010). Purinergic signalling and bone remodelling. *Current Opinion in Pharmacology*, 10(3), pp.322-330.

Orriss, I.R., Key, M.L., Brandao-Burch, A., Patel, J.J., Burnstock, G. and Arnett, T.R. (2012). The regulation of osteoblast function and bone mineralisation by extracellular nucleotides: The role of p2x receptors. *Bone*, 51(3), pp.389-400.

Orriss, I.R., Utting, J.C., Brandao-Burch, A., Colston, K., Grubb, B.R., Burnstock, G. and Arnett, T.R. (2007). Extracellular nucleotides block bone mineralisation in vitro: evidence for dual inhibitory mechanisms involving both P2Y2 receptors and pyrophosphate. *Endocrinology*, 148(9), pp.4208-4216.

Osman, L., Chester, A.H., Amrani, M., Yacoub, M.H. and Smolenski, R.T. (2006). A novel role of extracellular nucleotides in valve calcification a potential target for atorvastatin. *Circulation*, 114(1 Suppl), I566-572.

Oyama, Y., Hashiguchi, T., Taniguchi, N., Tancharoen, S., Uchimura, T., Biswas, K.K., Kawahara, K., Nitanda, T., Umekita, Y., Lotz, M. and Maruyama, I. (2010). High-mobility group box-1 protein promotes granulomatous nephritis in adenine-induced nephropathy. *Laboratory Investigation*, 90(6), pp.853-866.

Pai, A., Leaf, E.M., El-Abbadi, M. and Giachelli, C.M. (2011). Elastin degradation and vascular smooth muscle cell phenotype change precede cell loss and arterial medial calcification in a uremic mouse model of chronic kidney disease. *The American Journal of Pathology*, 178(2), pp.764-773.

Pai, A.S. and Giachelli, C.M. (2010). Matrix remodeling in vascular calcification associated with chronic kidney disease. *Journal of the American Society of Nephrology*, 21(10), pp.1637-1640.

Palmer, S.C., Navaneethan, S.D., Craig, J.C., Perkovic, V., Johnson, D.W., Nigwekar, S.U., Hegbrant, J. and Strippoli, G.F. (2014). HMG CoA reductase inhibitors (statins) for kidney transplant recipients. *Cochrane Database*

Systematic Reviews, 1, CD005019.

Pan, W., Ciociola, E., Saraf, M., Tumurbaatar, B., Tuvdendorj, D., Prasad, S., Chandalia, M. and Abate, N. (2011). Metabolic consequences of ENPP1 overexpression in adipose tissue. *American Journal of Physiology-Endocrinology and Metabolism*, 301(5), E901-911.

Panupinthu, N., Rogers, J.T., Zhao, L., Solano-Flores, L.P., Possmayer, F., Sims, S.M. and Dixon, S.J. (2008). P2X7 receptors on osteoblasts couple to production of lysophosphatidic acid: a signaling axis promoting osteogenesis. *The Journal of Cell Biology*, 181(5), pp.859-871.

Parfitt, A.M. (1969). Soft-tissue calcification in uremia. *Archives of Internal Medicine*, 124(5), pp.544-556.

Pelegrin, P. (2011). Many ways to dilate the P2X7 receptor pore. *British Journal of Pharmacology*, 163(5), pp.908-911.

Pellegatti, P., Falzoni, S., Donvito, G., Lemaire, I. and Di Virgilio, F. (2011). P2X7 receptor drives osteoclast fusion by increasing the extracellular adenosine concentration. *The FASEB Journal*, 25(4), pp.1264-1274.

Perazella, M.A. and Markowitz, G.S. (2008). Bisphosphonate nephrotoxicity. *Kidney International*, 74(11), pp.1385-1393.

Persy, V. and D'Haese, P. (2009). Vascular calcification and bone disease: the calcification paradox. *Trends in Molecular Medicine*, 15(9), pp.405-416.

Persy, V.P. and McKee, M.D. (2011). Prevention of vascular calcification: is pyrophosphate therapy a solution? *Kidney International*, 79(5), pp.490-493.

Philips, F.S., Thiersch, J.B. and Bendich, A. (1952). Adenine intoxication in relation to in vivo formation and deposition of 2, 8-dioxyadenine in renal tubules. *Journal of Pharmacology and Experimental Therapeutics*, 104(1), pp.20-30.

Piscopiello, M., Sessa, M., Anzalone, N., Castellano, R., Maisano, F., Ferrero, E., Chiesa, R., Alfieri, O., Comi, G., Ferrero, M.E. and Foglieni, C. (2013). P2X7 receptor is expressed in human vessels and might play a role in atherosclerosis.

International Journal of Cardiology, 168(3), pp.2863-2866.

Ponnusamy, M., Liu, N., Gong, R., Yan, H. and Zhuang, S. (2011). ERK pathway mediates P2X7 expression and cell death in renal interstitial fibroblasts exposed to necrotic renal epithelial cells. *American Journal of Physiology-Renal Physiology*, 301(3), F650-659.

Price, P.A., Faus, S.A. and Williamson, M.K. (1998). Warfarin causes rapid calcification of the elastic lamellae in rat arteries and heart valves. *Arteriosclerosis, Thrombosis, and Vascular Biology*, 18(9), pp.1400-1407.

Price, P.A., Roublick, A.M. and Williamson, M.K. (2006). Artery calcification in uremic rats is increased by a low protein diet and prevented by treatment with ibandronate. *Kidney International*, 70(9), pp.1577-1583.

Prosdocimo, D.A., Wyler, S.C., Romani, A.M., O'Neill, W.C. and Dubyak, G.R. (2010). Regulation of vascular smooth muscle cell calcification by extracellular pyrophosphate homeostasis: synergistic modulation by cyclic AMP and hyperphosphatemia. *American Journal of Physiology-Cell Physiology*, 298(3), C702-713.

Proudfoot, D. and Shanahan, C. (2012). Human vascular smooth muscle cell culture. *Methods in Molecular Biology*, 806, pp.251-263.

Proudfoot, D., Skepper, J.N., Hegyi, L., Bennett, M.R., Shanahan, C.M. and Weissberg, P.L. (2000). Apoptosis regulates human vascular calcification in vitro evidence for initiation of vascular calcification by apoptotic bodies. *Circulation Research*, 87(11), pp.1055-1062.

Proudfoot, D., Skepper, J.N., Shanahan, C.M. and Weissberg, P.L. (1998). Calcification of human vascular cells in vitro is correlated with high levels of matrix Gla protein and low levels of osteopontin expression. *Arteriosclerosis, Thrombosis, and Vascular Biology*, 18(3), pp.379-388.

Pruthi, R., Steenkamp, R. and Feest, T. (2014). UK Renal Registry 16th Annual Report: Chapter 8 Survival and cause of death of UK adult patients on renal replacement therapy in 2012: national and centre-specific analyses. *Nephron*

Clinical Practice, 125(1-4), pp.139-169.

Puchtler, H., Meloan, S.N. and Terry, M.S. (1969). On the history and mechanism of alizarin and alizarin red S stains for calcium. *Journal of Histochemistry & Cytochemistry*, 17(2), pp.110-124.

Quarles, L.D., Sherrard, D.J., Adler, S., Rosansky, S.J., McCary, L.C., Liu, W., Turner, S.A. and Bushinsky, D.A. (2003). The calcimimetic AMG 073 as a potential treatment for secondary hyperparathyroidism of end-stage renal disease. *Journal of the American Society of Nephrology*, 14(3), pp.575-583.

Raggi, P., Chertow, G.M., Torres, P.U., Csiky, B., Naso, A., Nossuli, K., Moustafa, M., Goodman, W.G., Lopez, N., Downey, G., Dehmel, B. and Floege, J. (2011). The ADVANCE study: a randomized study to evaluate the effects of cinacalcet plus low-dose vitamin D on vascular calcification in patients on hemodialysis. *Nephrology Dialysis Transplantation*, 26(4), pp.1327-1339.

Rensen, S.S., Doevendans, P.A. and van Eys, G.J. (2007). Regulation and characteristics of vascular smooth muscle cell phenotypic diversity. *Netherlands Heart Journal*, 15(3), pp.100-108.

Reynolds, J.L., Joannides, A.J., Skepper, J.N., McNair, R., Schurgers, L.J., Proudfoot, D., Jahnen-Dechent, W., Weissberg, P.L. and Shanahan, C.M. (2004). Human vascular smooth muscle cells undergo vesicle-mediated calcification in response to changes in extracellular calcium and phosphate concentrations: a potential mechanism for accelerated vascular calcification in ESRD. *Journal of the American Society of Nephrology*, 15(11), pp.2857-2867.

Reynolds, J.L., Skepper, J.N., McNair, R., Kasama, T., Gupta, K., Weissberg, P.L., Jahnen-Dechent, W. and Shanahan, C.M. (2005). Multifunctional roles for serum protein fetuin-a in inhibition of human vascular smooth muscle cell calcification. *Journal of the American Society of Nephrology*, 16(10), pp.2920-2930.

Riser, B.L., Barreto, F.C., Rezg, R., Valaitis, P.W., Cook, C.S., White, J.A., Gass, J.H., Maizel, J., Louvet, L., Drueke, T.B., Holmes, C.J. and Massy, Z.A. (2011). Daily peritoneal administration of sodium pyrophosphate in a dialysis solution

prevents the development of vascular calcification in a mouse model of uraemia. *Nephrology Dialysis Transplantation*, 26(10), pp.3349-3357.

Riteau, N., Gasse, P., Fauconnier, L., Gombault, A., Couegnat, M., Fick, L., Kanellopoulos, J., Quesniaux, V.F., Marchand-Adam, S., Crestani, B., Ryffel, B. and Couillin, I. (2010). Extracellular ATP is a danger signal activating P2X7 receptor in lung inflammation and fibrosis. *American Journal of Respiratory and Critical Care Medicine*, 182(6), pp.774-783.

Robson, S.C. (2012). Role of CD73 and extracellular adenosine in disease: Presented by Maria P. Abbracchio. *Purinergic Signalling*, 7(4), pp.367-372.

Robson, S.C., Sevigny, J. and Zimmermann, H. (2006). The E-NTPDase family of ectonucleotidases: structure function relationships and pathophysiological significance. *Purinergic Signalling*, 2(2), pp.409-430.

Robson, S.C., Wu, Y., Sun, X., Knosalla, C., Dwyer, K. and Enjyoji, K. (2005). Ectonucleotidases of CD39 family modulate vascular inflammation and thrombosis in transplantation. *Seminars in Thrombosis and Hemostasis*, 31(2), pp.217-233.

Rozenfeld, P. and M Neumann, P.M. (2011). Treatment of Fabry disease: current and emerging strategies. *Current Pharmaceutical Biotechnology*, 12(6), pp.916-922.

Russell, R.G., Bisaz, S., Donath, A., Morgan, D.B. and Fleisch, H. (1971). Inorganic pyrophosphate in plasma in normal persons and in patients with hypophosphatasia, osteogenesis imperfecta, and other disorders of bone. *Journal of Clinical Investigation*, 50(5), pp.961-969.

Russo, D., Miranda, I., Ruocco, C., Battaglia, Y., Buonanno, E., Manzi, S., Russo, L., Scafarto, A. and Andreucci, V.E. (2007). The progression of coronary artery calcification in predialysis patients on calcium carbonate or sevelamer. *Kidney International*, 72(10), pp.1255-1261.

Rutsch, F., Boyer, P., Nitschke, Y., Ruf, N., Lorenz-Depierieux, B., Wittkampf, T., Weissen-Plenz, G., Fischer, R.J., Mughal, Z., Gregory, J.W., Davies, J.H., Loirat,

C., Strom, T.M., Schnabel, D., Nurnberg, P. and Terkeltaub, R. (2008). Hypophosphatemia, hyperphosphaturia, and bisphosphonate treatment are associated with survival beyond infancy in generalized arterial calcification of infancy. *Circulation Cardiovascular Genetics*, 1(2), pp.133-140.

Rutsch, F., Ruf, N., Vaingankar, S., Toliat, M.R., Suk, A., Hohne, W., Schauer, G., Lehmann, M., Roscioli, T., Schnabel, D., Epplen, J.T., Knisely, A., Superti-Furga, A., McGill, J., Filippone, M., Sinaiko, A.R., Vallance, H., Hinrichs, B., Smith, W., Ferre, M., Terkeltaub, R. and Nurnberg, P. (2003). Mutations in ENPP1 are associated with 'idiopathic' infantile arterial calcification. *Nature Genetics*, 34(4), pp.379-381.

Sabatine, M.S., Cannon, C.P., Gibson, C.M., Lopez-Sendon, J.L., Montalescot, G., Theroux, P., Claeys, M.J., Cools, F., Hill, K.A., Skene, A.M., McCabe, C.H. and Braunwald, E. (2005). Addition of clopidogrel to aspirin and fibrinolytic therapy for myocardial infarction with ST-segment elevation. *New England Journal of Medicine*, 352(12), pp.1179-1189.

Sage, A.P., Lu, J., Tintut, Y. and Demer, L.L. (2010). Hyperphosphatemia-induced nanocrystals upregulate the expression of bone morphogenetic protein-2 and osteopontin genes in mouse smooth muscle cells in vitro. *Kidney International*, 79(4), pp.414-422.

Sakamoto, M., Hosoda, Y., Kojimahara, K., Yamazaki, T. and Yoshimura, Y. (1994). Arthritis and ankylosis in twy mice with hereditary multiple osteochondral lesions: with special reference to calcium deposition. *Pathology International*, 44(6), pp.420-427.

Salati, L.M., Gross, C.J., Henderson, L.M. and Savaiano, D.A. (1984). Absorption and metabolism of adenine, adenosine-5'-monophosphate, adenosine and hypoxanthine by the isolated vascularly perfused rat small intestine. *The Journal of Nutrition*, 114(4), pp.753-760.

Sali A, Favaloro J, Terkeltaub R, Goding J. (1999). Germline deletion of the nucleoside triphosphate pyrophosphohydrolase (NTPPPH) plasma cellmembrane glycoprotein-1 (PC-1) produces abnormal calcification of periarticular tissues. In:

Vanduffel L, Lemmems R, editors. *Ecto-ATPases and Related Ectoenzymes.* Shaker Publishing, pp.267-282.

Santana, A.C., Degaspari, S., Catanozi, S., Delle, H., de Sa Lima, L., Silva, C., Blanco, P., Solez, K., Scavone, C. and Noronha, I.L. (2013). Thalidomide suppresses inflammation in adenine-induced CKD with uraemia in mice. *Nephrology Dialysis Transplantation*, 28(5), pp.1140-1149.

Sarkar, B.C. and Chauhan, U.P. (1967). A new method for determining micro quantities of calcium in biological materials. *Analytical Biochemistry*, 20(1), pp.155-166.

Schafer, C., Heiss, A., Schwarz, A., Westenfeld, R., Ketteler, M., Floege, J., Muller-Esterl, W., Schinke, T. and Jahnen-Dechent, W. (2003). The serum protein alpha 2-Heremans-Schmid glycoprotein/fetuin-A is a systemically acting inhibitor of ectopic calcification. *The Journal of Clinical Investigation*, 112(3), pp.357-366.

Schiavi, S.C., Tang, W., Bracken, C., O'Brien, S.P., Song, W., Boulanger, J., Ryan, S., Phillips, L., Liu, S., Arbeeny, C., Ledbetter, S. and Sabbaqh, Y. (2012). Npt2b deletion attenuates hyperphosphatemia associated with CKD. *Journal of the American Society of Nephrology*, 23(10), pp.1691-1700.

Schibler, D., Russell, R.G. and Fleisch, H. (1968). Inhibition by pyrophosphate and polyphosphate of aortic calcification induced by vitamin D3 in rats. *Clinical Science*, 35(2), pp.363-372.

Schild, H.O. (1947). pA, a new scale for the measurement of drug antagonism. *British Journal of Pharmacology and Chemotherapy*, 2(3), pp.189-206.

Schlieper, G. (2014). Vascular calcification in chronic kidney disease: not all arteries are created equal. *Kidney International*, 85(3), pp.501-503.

Schlieper, G., Aretz, A., Verberckmoes, S.C., Kruger, T., Behets, G.J., Ghadimi, R., Weirich, T.E., Rohrmann, D., Langer, S., Tordoir, J.H., Amann, K., Westenfeld, R., Brandenburg, V.M., D'Haese, P.C., Mayer, J., Ketteler, M., McKee, M.D. and Floege, J. (2010). Ultrastructural analysis of vascular calcifications in uremia. *Journal of the American Society of Nephrology*, 21(4), pp.689-696.

Schneeberger, C., Speiser, P., Kury, F. and Zeillinger, R. (1995). Quantitative detection of reverse transcriptase-PCR products by means of a novel and sensitive DNA stain. *PCR Methods and Applications*, 4(4), pp.234-238.

Schuchardt, M., Prufer, J., Prufer, N., Wiedon, A., Huang, T., Chebli, M., Jankowski, V., Jankowski, J., Schafer-Korting, M., Zidek, W., van der Giet, M. and Tolle, M. (2011). The endothelium-derived contracting factor uridine adenosine tetraphosphate induces P2Y2-mediated pro-inflammatory signaling by monocyte chemoattractant protein-1 formation. *Journal of Molecular Medicine (Berlin, Germany)*, 89(8), pp.799-810.

Schuchardt, M., Tolle, M., Prufer, J., Prufer, N., Huang, T., Jankowski, V., Jankowski, J., Zidek, W. and van der Giet, M. (2012). Uridine adenosine tetraphosphate activation of the purinergic receptor P2Y enhances in vitro vascular calcification. *Kidney International*, 81(3), pp.256-265.

Scialla, J.J., Lau, W.L., Reilly, M.P., Isakova, T., Yang, H.Y., Crouthamel, M.H., Chavkin, N.W., Rahman, M., Wahl, P., Amaral, A.P., Hamano, T., Master, S.R., Nessel, L., Chai, B., Xie, D., Kallem, R.R., Chen, J., Lash, J.P., Kusek, J.W., Budoff, M.J., Giachelli, C.M. and Wolf, M. (2013). Fibroblast growth factor 23 is not associated with and does not induce arterial calcification. *Kidney International*, 83(6), pp.1159-1168.

Shalhoub, V., Shatzen, E.M., Ward, S.C., Young, J.I., Boedigheimer, M., Twehues, L., McNinch, J., Scully, S., Twomey, B., Baker, D., Kiaei, P., Damore, M.A., Pan, Z., Haas, K. and Martin, D. (2010). Chondro/osteoblastic and cardiovascular gene modulation in human artery smooth muscle cells that calcify in the presence of phosphate and calcitriol or paricalcitol. *Journal of Cellular Biochemistry*, 111(4), pp.911-921.

Shanahan, C.M. (2013). Mechanisms of vascular calcification in CKD-evidence for premature ageing?. *Nature Reviews Nephrology*, 9(11), pp.661-670.

Shanahan, C.M., Cary, N.R., Salisbury, J.R., Proudfoot, D., Weissberg, P.L. and Edmonds, M.E. (1999). Medial Localisation of Mineralisation-Regulating Proteins in Association With Monckeberg's Sclerosis Evidence for Smooth

Muscle Cell-Mediated Vascular Calcification. *Circulation*, 100(21), pp.2168-2176.

Shanahan, C.M., Crouthamel, M.H., Kapustin, A. and Giachelli, C.M. (2011). Arterial calcification in chronic kidney disease: key roles for calcium and phosphate. *Circulation Research*, 109(6), pp.697-711.

Shobeiri, N., Adams, M.A. and Holden, R.M. (2010). Vascular Calcification in Animal Models of CKD: A Review. *American Journal of Nephrology*, 31(6), pp.471-481.

Shobeiri, N., Pang, J., Adams, M.A. and Holden, R.M. (2013). Cardiovascular disease in an adenine-induced model of chronic kidney disease: the temporal link between vascular calcification and haemodynamic consequences. *Journal of Hypertension*, 31(1), pp.160-168.

Shroff, R., Long, D.A. and Shanahan, C. (2013). Mechanistic insights into vascular calcification in CKD. *Journal of the American Society of Nephrology*, 24(2), pp.179-189.

Shroff, R.C., McNair, R., Figg, N., Skepper, J.N., Schurgers, L., Gupta, A., Hiorns, M., Donald, A.E., Deanfield, J., Rees, L. and Shanahan, C.M. (2008). Dialysis accelerates medial vascular calcification in part by triggering smooth muscle cell apoptosis. *Circulation*, 118(17), pp.1748-1757.

Shroff, R.C., McNair, R., Skepper, J.N., Figg, N., Schurgers, L.J., Deanfield, J., Rees, L. and Shanahan, C.M. (2010). Chronic mineral dysregulation promotes vascular smooth muscle cell adaptation and extracellular matrix calcification. *Journal of the American Society of Nephrology*, 21(1), pp.103-112.

Si, H., Banga, R.S., Kapitsinou, P., Ramaiah, M., Lawrence, J., Kambhampati, G., Gruenwald, A., Bottinger, E., Glicklich, D., Tellis, V., Greenstein, S., Thomas, D.B., Pullman, J., Fazzari, M. and Susztak, K. (2009). Human and murine kidneys show gender-and species-specific gene expression differences in response to injury. *PLoS One*, 4(3), e4802.

Sigrist, M.K., Taal, M.W., Bungay, P. and McIntyre, C.W. (2007). Progressive

vascular calcification over 2 years is associated with arterial stiffening and increased mortality in patients with stages 4 and 5 chronic kidney disease. *Clinical Journal of the American Society of Nephrology*, 2(6), pp.1241-1248.

Sim, J.A., Young, M.T., Sung, H.Y., North, R.A. and Surprenant, A. (2004). Reanalysis of P2X7 receptor expression in rodent brain. *The Journal of Neuroscience*, 24(28), pp.6307-6314.

Simionescu, A., Philips, K. and Vyavahare, N. (2005). Elastin-derived peptides and TGF-beta1 induce osteogenic responses in smooth muscle cells. *Biochemical and Biophysical Research Communications*, 334(2), pp.524-532.

Sims, S.M., Panupinthu, N., Lapierre, D.M., Pereverzev, A. and Dixon, S.J. (2013). Lysophosphatidic acid: A potential mediator of osteoblast-osteoclast signaling in bone. *Biochimica et Biophysica Acta*, 1831(1), pp.109-116.

Slee, A.D. (2012). Exploring metabolic dysfunction in chronic kidney disease. *Nutrition and Metabolism (London)*, 9(1), p.36.

Snyder, F.F., Hershfield, M.S. and Seegmiller, J.E. (1978). Cytotoxic and metabolic effects of adenosine and adenine on human lymphoblasts. *Cancer Research*, 38(8), pp.2357-2362.

Solle, M., Labasi, J., Perregaux, D.G., Stam, E., Petrushova, N., Koller, B.H., Griffiths, R.J. and Gabel, C.A. (2001). Altered Cytokine Production in Mice Lacking P2X7Receptors. *Journal of Biological Chemistry*, 276(1), pp.125-132.

Son, B.K., Kozaki, K., Iijima, K., Eto, M., Kojima, T., Ota, H., Senda, Y., Maemura, K., Nakano, T., Akishita, M. and Ouchi, Y. (2006). Statins protect human aortic smooth muscle cells from inorganic phosphate-induced calcification by restoring Gas6-Axl survival pathway. *Circulation Research*, 98(8), pp.1024-1031.

Speer, M.Y., Yang, H.Y., Brabb, T., Leaf, E., Look, A., Lin, W.L, Frutkin, A., Dichek, D. and Giachelli, C.M. (2009). Smooth muscle cells give rise to osteochondrogenic precursors and chondrocytes in calcifying arteries. *Circulation Research*, 104(6), pp.733-741.

St Hilaire, C, Ziegler, S.G., Markello, T.C., Brusco, A., Groden, C., Gill, F., Carlson-Donohoe, H., Lederman, R.J., Chen, M.Y., Yang, D., Siegenthaler, M.P., Arduino, C., Mancini, C., Freudenthal, B., Stanescu, H.C., Zdebik, A.A., Chaganti, R.K., Nussbaum, R.L., Kleta, R., Gahl, W.A. and Boehm, M. (2011). NT5E mutations and arterial calcifications. *New England Journal of Medicine*, 364(5), pp.432-442.

Stechman, M.J., Ahmad, B.N., Loh, N.Y., Reed, A.A., Stewart, M., Wells, S., Hough, T., Bentley, L., Cox, R.D., Brown, S.D. and Thakker, R.V. (2010). Establishing normal plasma and 24-hour urinary biochemistry ranges in C3H, BALB/c and C57BL/6J mice following acclimatisation in metabolic cages. *Laboratory Animals*, 44(3), pp.218-225.

Stenvinkel, P., Carrero, J.J., Axelsson, J., Lindholm, B., Heimburger, O. and Massy, Z. (2008). Emerging biomarkers for evaluating cardiovascular risk in the chronic kidney disease patient: how do new pieces fit into the uremic puzzle? *Clinical Journal of the American Society of Nephrology*, 3(2), pp.505-521.

Stock, T.C., Bloom, B.J., Wei, N., Ishaq, S., Park, W., Wang, X., Gupta, P. and Mebus, C.A. (2012). Efficacy and safety of CE-224,535, an antagonist of P2X7 receptor, in treatment of patients with rheumatoid arthritis inadequately controlled by methotrexate. *The Journal of Rheumatology*, 39(4), pp.720-727.

Sun, C.C., Vaja, V., Chen, S., Theurl, I., Stepanek, A., Brown, D.E., Cappellini, M.D., Weiss, G., Hong, C.C., Lin, H.Y. and Babitt, J.L. (2013). A hepcidin lowering agent mobilizes iron for incorporation into red blood cells in an adenine-induced kidney disease model of anemia in rats. *Nephrology Dialysis Transplantation*, 28(7), pp.1733-1743.

Sun, S., Xia, S., Ji, Y., Kersten, S. and Qi, L. (2012). The ATP-P2X7 signaling axis is dispensable for obesity-associated inflammasome activation in adipose tissue. *Diabetes*, 61(6), pp.1471-1478.

Surprenant, A., Rassendren, F., Kawashima, E., North, R.A. and Buell, G. (1996). The cytolytic P2Z receptor for extracellular ATP identified as a P2X receptor (P2X7). *Science*, 272(5262), pp.735-738.

Sutliff, R.L., Walp, E.R., El-Ali, A.M., Elkhatib, S., Lomashvili, K.A. and O'Neill, W.C. (2011). Effect of medial calcification on vascular function in uremia. *American Journal of Physiology-Renal Physiology*, 301(1), F78-83.

Tamagaki, K., Yuan, Q., Ohkawa, H., Imazeki, I., Moriguchi, Y., Imai, N., Sasaki, S., Takeda, K. and Fukagawa, M. (2006). Severe hyperparathyroidism with bone abnormalities and metastatic calcification in rats with adenine-induced uraemia. *Nephrology Dialysis Transplantation*, 21(3), pp.651-659.

Tamura, M., Aizawa, R., Hori, M. and Ozaki, H. (2009). Progressive renal dysfunction and macrophage infiltration in interstitial fibrosis in an adenine-induced tubulointerstitial nephritis mouse model. *Histochemistry and Cell Biology*, 131(4), pp.483-490.

Tanaka, T., Doi, K., Maeda-Mamiya, R., Negishi, K., Portilla, D., Sugaya, T., Fujita, T. and Noiri, E. (2009). Urinary L-type fatty acid-binding protein can reflect renal tubulointerstitial injury. *The American Journal of Pathology*, 174(4), pp.1203-1211.

Taylor, S.R., Turner, C.M., Elliott, J.I., McDaid, J., Hewitt, R., Smith, J., Pickering, M.C., Whitehouse, D.L., Cook, H.T., Burnstock, G., Pusey, C.D, Unwin, R.J. and Tam, F.W. (2009a). P2X7 deficiency attenuates renal injury in experimental glomerulonephritis. *Journal of the American Society of Nephrology*, 20(6), pp.1275-1281.

Taylor, S.R., Gonzalez-Begne, M., Sojka, D.K., Richardson, J.C., Sheardown, S.A., Harrison, S.M., Pusey, C.D., Tam, F.W. and Elliott, J.I. (2009b). Lymphocytes from P2X7-deficient mice exhibit enhanced P2X7 responses. *Journal of Leukocyte Biology*, 85(6), pp.978-986.

Terai, K., Nara, H., Takakura, K., Mizukami, K., Sanagi, M., Fukushima, S., Fujimori, A., Itoh, H. and Okada, M. (2009). Vascular calcification and secondary hyperparathyroidism of severe chronic kidney disease and its relation to serum phosphate and calcium levels. *British Journal of Pharmacology*, 156(8), pp.1267-1278.

Terkeltaub, R. (2006). Physiologic and pathologic functions of the NPP nucleotide pyrophosphatase/phosphodiesterase family focusing on NPP1 in calcification. *Purinergic Signalling*, 2(2), pp.371-377.

Terkeltaub, R.A. (2001). Inorganic pyrophosphate generation and disposition in pathophysiology. *American Journal of Physiology-Cell Physiology*, 281(1), C1-11.

Tintut, Y., Patel, J., Parhami, F. and Demer, L.L. (2000). Tumor necrosis factor-alpha promotes in vitro calcification of vascular cells via the cAMP pathway. *Circulation*, 102(21), pp.2636-2642.

Tomiyama, C., Carvalho, A.B., Higa, A., Jorgetti, V., Draibe, S.A. and Canziani, M.E. (2010). Coronary calcification is associated with lower bone formation rate in CKD patients not yet in dialysis treatment. *Journal of Bone and Mineral Research*, 25(3), pp.499-504.

Tonelli, M., Wiebe, N., Culleton, B., House, A., Rabbat, C., Fok, M., McAlister, F. and Garg, A.X. (2006). Chronic kidney disease and mortality risk: a systematic review. *Journal of the American Society of Nephrology*, 17(7), pp.2034-2047.

Tripathi, S., Suzuki, N. and Srivastav, A.K. (2013). Response of serum minerals (calcium, phosphate, and magnesium) and endocrine glands (calcitonin cells and parathyroid gland) of wistar rat after chlorpyrifos administration. *Microscopy Research and Technique*, 76(7), pp.673-678.

Truett, G.E., Heeger, P., Mynatt, R.L., Truett, A.A., Walker, J.A. and Warman, M.L. (2000). Preparation of PCR-quality mouse genomic DNA with hot sodium hydroxide and tris (HotSHOT). *Biotechniques*, 29(1), pp.52-54.

Turner, C.M., Tam, F.W., Lai, P.C., Tarzi, R.M., Burnstock, G., Pusey, C.D., Cook, H.T. and Unwin, R.J. (2007). Increased expression of the pro-apoptotic ATP-sensitive P2X7 receptor in experimental and human glomerulonephritis. *Nephrology Dialysis Transplantation*, 22(2), pp.386-395.

Underwood, P.A., Bean, P.A. and Whitelock, J.M. (1998). Inhibition of endothelial cell adhesion and proliferation by extracellular matrix from vascular smooth

muscle cells: role of type V collagen. *Atherosclerosis*, 141(1), pp.141-152.

Urry, D.W. (1971). Neutral sites for calcium ion binding to elastin and collagen: a charge neutralisation theory for calcification and its relationship to atherosclerosis. *Proceedings of the National Academy of Sciences of the United States of America*, 68(4), pp.810-814.

Vandesompele, J., De Preter, K., Pattyn, F., Poppe, B., Van Roy, N., De Paepe, A. and Speleman, F. (2002). Accurate normalisation of real-time quantitative RT-PCR data by geometric averaging of multiple internal control genes. *Genome Biology*, 3(7), RESEARCH0034.

Vezzoli, G., Rubinacci, A., Lazzaroni, M. and Soldati, L. (2014). It's time for a practical method quantifying vascular calcification. *Journal of Translational Medicine*, 12(1), pp.172.

Villa-Bellosta, R. and Sorribas, V. (2013). Prevention of vascular calcification by polyphosphates and nucleotides-role of ATP. *Circulation Journal*, 77(8), pp.2145-2151.

Villa-Bellosta, R., Wang, X., Millan, J.L., Dubyak, G.R. and O'Neill, W.C. (2011a). Extracellular pyrophosphate metabolism and calcification in vascular smooth muscle. *American Journal of Physiology-Heart and Circulatory Physiology*, 301(1), H61-68.

Villa-Bellosta, R., Millan, A. and Sorribas, V. (2011b). Role of calcium-phosphate deposition in vascular smooth muscle cell calcification. *American Journal of Physiology-Cell Physiology*, 300(1), C210-220.

von Albertini, M., Palmetshofer, A., Kaczmarek, E., Koziak, K., Stroka, D., Grey, S., Stuhlmeier, K.M. and Robson, S.C. (1998). Extracellular ATP and ADP activate transcription factor NF-kappaB and induce endothelial cell apoptosis. *Biochemical and Biophysical Research Communications*, 248(3), pp.822-829.

von Kossa, J. (1901). Ueber die im Organismus kunstlich erzeugbaren Verkalkungen. *Ziegler's Beitr path Anat*, 29, pp.163-202.

Vonend, O., Turner, C.M., Chan, C.M., Loesch, A., Dell'Anna, G.C., Srai, K.S., Burnstock, G. and Unwin, R.J. (2004). Glomerular expression of the ATP-sensitive P2X7 receptor in diabetic and hypertensive rat models. *Kidney International*, 66(1), pp.157-166.

Wang, L., Andersson, M., Karlsson, L., Watson, M.A., Cousens, D.J., Jern, S. and Erlinge, D. (2003). Increased mitogenic and decreased contractile P2 receptors in smooth muscle cells by shear stress in human vessels with intact endothelium. *Arteriosclerosis, Thrombosis, and Vascular Biology*, 23(8), pp.1370-1376.

Wang, L., Karlsson, L., Moses, S., Hultgaardh-Nilsson, A., Andersson, M., Borna, C., Gudbjartsson, T., Jern, S. and Erlinge, D. (2002). P2 receptor expression profiles in human vascular smooth muscle and endothelial cells. *Journal of Cardiovascular Pharmacology*, 40(6), pp.841-853.

Wanner, C., Krane, V., Marz, W., Olschewski, M., Mann, J.F., Ruf, G. and Ritz, E. (2005). Atorvastatin in patients with type 2 diabetes mellitus undergoing hemodialysis. *New England Journal of Medicine*, 353(3), pp.238-248.

Weber, C. and Noels, H. (2011). Atherosclerosis: current pathogenesis and therapeutic options. *Nature Medicine*, 17(11), pp.1410-1422.

Weiner, D.E., Tighiouart, H., Elsayed, E.F., Griffith, J.L., Salem, D.N., Levey, A.S. and Sarnak, M.J. (2007). The Framingham predictive instrument in chronic kidney disease. *Journal of the American College of Cardiology*, 50(3), pp.217-224.

Wen, C., Yang, X., Yan, Z., Zhao, M., Yue, X., Cheng, X., Zheng, Z., Guan, K., Dou, J., Xu, T., Zhang, Y., Song, T., Wei, C. and Zhong, H. (2013). Nalp3 inflammasome is activated and required for vascular smooth muscle cell calcification. *International Journal of cardiology*, 168(3), pp.2242-2247.

White, K.E., Evans, W.E., O'Riordan, J.L.H., Speer, M.C., Econs, M.J., Lorenz-Depiereux, B., Grabowski, M., Meitinger, T. and Strom, T.M. (2000). Autosomal dominant hypophosphataemic rickets is associated with mutations in FGF23. *Nature Genetics*, 26(3), pp.345-348.

Wiley, J.S., Sluyter, R., Gu, B.J., Stokes, L. and Fuller, S.J. (2011). The human P2X7 receptor and its role in innate immunity. *Tissue Antigens*, 78(5), pp.321-332.

Williams, C.J., Zhang, Y., Timms, A., Bonavita, G., Caeiro, F., Broxholme, J., Cuthbertson, J., Jones, Y., Marchegiani, R., Reginato, A., Russell, R.G., Wordsworth, B.P., Carr, A.J. and Brown, M.A. (2002). Autosomal dominant familial calcium pyrophosphate dihydrate deposition disease is caused by mutation in the transmembrane protein ANKH. *The American Journal of Human Genetics*, 71(4), pp.985-991.

Wilson, H.L., Varcoe, R.W., Stokes, L., Holland, K.L., Francis, S.E., Dower, S.K., Surprenant, A. and Crossman, D.C. (2007). P2X receptor characterisation and IL-1/IL-1Ra release from human endothelial cells. *British Journal of Pharmacology*, 151(1), pp.115-127..

Yan, Z., Khadra, A., Li, S., Tomi'c, M., Sherman, A. and Stojilkovic, S.S. (2010). Experimental characterisation and mathematical modeling of P2X7 receptor channel gating. *The Journal of Neuroscience*, 30(42), pp.14213-14224.

Yokozawa, T., Zheng, P.D., Oura, H. and Koizumi, F. (1986). Animal model of adenine-induced chronic renal failure in rats. *Nephron*, 44(3), pp.230-234.

Zeidan, A., Nordstrom, I., Dreja, K., Malmqvist, U. and Hellstrand, P. (2000). Stretch-dependent modulation of contractility and growth in smooth muscle of rat portal vein. *Circulation Research*, 87(3), pp.228-234.

Zhao, G., Xu, M.J., Zhao, M.M., Dai, X.Y., Kong, W., Wilson, G.M., Guan, Y., Wang, C.Y. and Wang, X. (2012). Activation of nuclear factor-kappa B accelerates vascular calcification by inhibiting ankylosis protein homolog expression. *Kidney International*, 82(1), pp.34-44.

Zhao, M.M., Xu, M.J., Cai, Y., Zhao, G., Guan, Y., Kong, W., Tang, C. and Wang, X. (2011). Mitochondrial reactive oxygen species promote p65 nuclear translocation mediating high phosphate-induced vascular calcification in vitro and in vivo. *Kidney International*, 79(10), pp.1071-1079.

Zheng, L.M., Zychlinsky, A., Liu, C.C., Ojcius, D.M. and Young, J.D. (1991). Extracellular ATP as a trigger for apoptosis or programmed cell death. *The Journal of Cell Biology*, 112(2), pp.279-288.

Zhu, D., Mackenzie, N.C., Millan, J.L., Farquharson, C. and MacRae, V.E. (2011). The appearance and modulation of osteocyte marker expression during calcification of vascular smooth muscle cells. *PLoS One*, 6(5), e19595.

Zimmermann, H., Zebisch, M. and Strater, N. (2012). Cellular function and molecular structure of ecto-nucleotidases. *Purinergic Signalling*, 8(3), pp.437-502.